# A STUDY OF EXCITATION CONTRACTION COUPLING IN RABBIT CARDIOMYOCYTES

BY

STEWART L.W. MILLER.

Submitted July 2004 in fulfilment of the degree of Doctor of Philosophy to the Faculty of Biomedical and Life Sciences, University of Glasgow, U.K.

Research carried out within the Faculty of Biomedical and Life Sciences, University of Glasgow, U.K.



ProQuest LLC.
789 East Eisenhower Parkway
P.O. Box 1346
Ann Arbor, MI 48106 – 1346

## Declaration

The material contained within this thesis is my own work, except where stated. This material has not been submitted for the fulfilment of any other degree.

Some of the results obtained have been published in paper and abstract form and are detailed below.

Loughrey, C. M., Seidler, T., Miller, S. L., Prestle, J., MacEachern, K. E., Reynolds, D. F., Hasenfuss, G., & Smith, G. L. (2004). Over-expression of FK506-binding protein FKBP12.6 alters excitation-contraction coupling in adult rabbit cardiomyocytes. *J.Physiol.* **556,** 919-934.

Miller, S. L. W., Currie, S., Reynolds, D. F., Seidler, T., Hasenfuss, G., & Smith, G. L. (2003). Effects of calsequestrin overexpression on excitation contraction coupling in isolated rabbit cardiomyocytes. *J.Physiol.* **552P**, C42.

Miller, S. L. W., Reynolds, D. F., Currie, S., Seidler, T., Hasenfuss, G., & Smith, G. L. (2004). *Biophys.J.* **86(1)** Supplement, 248-Pos.

Seidler, T., Miller, S. L., Loughrey, C. M., Kania, A., Burow, A., Kettlewell, S., Teucher, N., Wagner, S., Kogler, H., Meyers, M. B., Hasenfuss, G., & Smith, G. L. (2003). Effects of adenovirus-mediated sorcin overexpression on excitation-contraction coupling in isolated rabbit cardiomyocytes. *Circ.Res.* **93,** 132-139.

## Abstract

Excitation-Contraction coupling is the process that links the depolarisation of the myocardium to its contraction. We have utilised an adenoviral-mediated strategy to overexpress sorcin, calsequestrin (CSQ), FKBP 12.6 and the sodium/calcium exchanger (NCX) in isolated rabbit cardiomyocytes over a period of 24hrs in cell culture. The effects of overexpression of the above-mentioned proteins on excitation-contraction coupling were subsequently investigated using whole cell voltage clamp. The loading of cardiomyocytes with FURA-2 enabled simultaneous measurement of intracellular calcium concentration. Cardiomyocytes transfected with an adenovirus that caused overexpression of the enzyme β-galactosidase were employed as a control.

Sorcin overexpression was found to significantly reduce both the amplitude of the intracellular $Ca^{2+}$ transient and the size of the SR $Ca^{2+}$ load under conditions of whole cell voltage clamp when compared to control. It had no effect on the L-type $Ca^{2+}$ current but significantly enhanced the activity of the sodium/calcium exchanger. Subsequently, overexpression of NCX was shown to affect excitation contraction coupling in a similar manner to sorcin overexpression.

CSQ overexpression was shown to significantly increase the size of L-type $Ca^{2+}$ current, the intracellular $Ca^{2+}$ transient amplitude and the SR $Ca^{2+}$ load under conditions of whole cell voltage clamp when compared to control. When the L-type $Ca^{2+}$ current in the CSQ overexpressing

cardiomyocytes was normalised using nifedipine the SR $Ca^{2+}$ load remained increased while the amplitude of the intracellular $Ca^{2+}$ transient was similar to that observed in control cardiomyocytes.

Finally, FKBP 12.6 overexpression significantly increased both the amplitude of the intracellular $Ca^{2+}$ transient and the size of the SR $Ca^{2+}$ load under conditions of whole cell voltage clamp when compared to control. It had no effect on the L-type $Ca^{2+}$ current. Over expression of an FKBP 12.6 mutant that lacked a calcineurin binding site had little effect on the size of the intracellular $Ca^{2+}$ transient but still significantly increased the SR $Ca^{2+}$ load under conditions of whole cell voltage clamp when compared to control.

Experiments previously carried out in the laboratory using confocal microscopy have demonstrated that both sorcin and FKBP 12.6 overexpression alter the occurrence of spontaneous $Ca^{2+}$ sparks in permeabilised cardiomyocytes. Conversely, CSQ overexpression was shown to have no effect on the occurrence of $Ca^{2+}$ sparks.

## Acknowledgements

The following people deserve special mention for their continual friendship, support and encouragement over the past 3 years:

Prof. Godfrey Smith, who has provided me with fantastic supervision.

Francis, Dave, Susan, Debbie, Russell, Sarah, Niall, Chris, Margaret-Anne, Elspeth & Nicki.

Ann Ward and Aileen Rankin for their technical expertise.

Our German collaborators - Tim Seidler, Jurgen Prestle, and Gerd Hasenfuss, (University of Goettingen).

Finally, I would like to thank my family and in particular my wife Helen for always being there.

The work presented in this thesis was possible only because of the financial support provided by the British Heart Foundation.

## Contents

## Figures

# Abbreviations

| | |
|---|---|
| Ad-LacZ | adenovirus transfected cardiomyocytes with β-galactosidase DNA sequence |
| Ad-CSQ | adenovirus transfected cardiomyocytes with calsequestrin DNA sequence |
| Ad-FKBP12.6 | adenovirus transfected cardiomyocytes with FKBP12.6 DNA sequence |
| Ad-NCX | adenovirus transfected cardiomyocytes with NCX DNA sequence |
| Ad-Sorcin | adenovirus transfected cardiomyocytes with sorcin DNA sequence |
| AM | acetoxymethyl ester |
| ATP | adenosine 5' triphosphate |
| ATPase | adenosine triphosphatase |
| $Ba^{2+}$ | barium ion |
| $BaCl_2$ | barium chloride |
| BAPTA | 1,2-bis(2-aminophenoxy)ethane N,N,N'N'-tetraacetic acid |
| BSA | bovine serum albumin |
| $Ca^{2+}$ | calcium ion |
| $Ca^{2+}$-ATPase | calcium pump |
| $[Ca^{2+}]$ | calcium ion concentration |
| $[Ca^{2+}]_i$ | intracellular calcium ion concentration |
| $[Ca^{2+}]_{ic}$ | intracellular calcium ion concentration |
| $[Ca^{2+}]_{EC}$ | extracellular calcium ion concentration |
| cAMP | adenosine 3':5'-cyclicmonophosphate |
| cADPR | adenosine 3';5'-cyclicdiphosphate ribose |
| CCCP | Carbonyl cyanide *m*-chlorophenolhydrazone |
| $Cd^{2+}$ | cadmium ion |
| CICR | calcium-induced calcium release |
| $Cl^-$ | chloride ion |
| cm | centimetre, length |
| $Cs^+$ | caesium ion |
| CSQ | calsequestrin |
| DHP | dihydropyridine |
| DHPR | dihydropyridine receptor |
| DMSO | dimethylsulphoxide |
| E-C | excitation-contraction |
| EDTA | ethylenediaminetetraacetic acid |
| EGTA | ethylene glycol bis(β-aminoethyl ether)-N,N,N',N'-tetraacetic acid |
| $E_m$ | membrane potential |
| Fluo-3 | fluorescent indicator (calcium sensitive) |
| Fluo-5F | fluorescent indicator (calcium sensitive) |

| | |
|---|---|
| $F_{max}$ | fluorescence measured at saturatingly high calcium |
| $F_{min}$ | fluorescence measured at very low calcium |
| Fura-2 | fluorescent indicator (calcium sensitive) |
| g | gram, weight |
| *g* | acceleration due to gravity |
| GFP | green fluorescent protein |
| HCl | hydrochloric acid |
| HEPES | N-2-hydroxyethylpiperazine-N'-2-ethanosulphonic acid |
| Hz | Hertz, frequency |
| $I_{Ca}$ | calcium current |
| Ins(1,4,5)$P_3$ | inositol (1,4,5)-triphosphate |
| $K^+$ | potassium ion |
| $K_d$ | dissociation constant |
| $K_i$ | inhibitory equilibrium constant |
| KOH | potassium hydroxide |
| l | litre, volume |
| LASER | light amplification by stimulated emission of radiation |
| LSCM | laser-scanning confocal microscopy |
| M | molar, concentration |
| $Mg^{2+}$ | magnesium ion |
| mg | milligram, weight |
| $MgCl_2$ | magnesium chloride |
| min | minute, time |
| ml | milliliter, volume |
| mm | millimeter, length |
| mM | millimolar, concentration |
| mol | mole, quantity |
| MOI | multiplicity of infection |
| ms | millisecond |
| mV | millivolt, electrical voltage |
| *n* | sample size |
| $Na^+$ | sodium ion |
| NADH | β-nicotinamide adenine dinucleotide phosphate (reduced) |
| $NaH_2PO_4$ | sodium dihydrogen orthophosphate |
| NaOH | sodium hydroxide |
| NCX | sodium-calcium exchanger |
| nm | nanometer, length |
| nM | nanomolar, concentration |
| *p* | probability |

| | |
|---|---|
| PLB | phospholamban |
| PMT | photomultiplier tube |
| PRO | proline |
| RyR | ryanodine receptor |
| s | second, time |
| SEM | standard error of the mean |
| SER | serine |
| SERCA | sarco(endo)plasmic reticulum calcium ATPase |
| SR | sarcoplasmic reticulum |
| U | unit of activity |
| V | volt, electrical charge |
| µg | microgram, weight |
| µl | microlitre, volume |
| µM | micromolar, concentration |
| °C | degrees celsius, temperature |

# Chapter 1 – Introduction

The complex process that links the depolarisation of the myocardium to its contraction, thus allowing blood to be pumped around the body, is inextricably coupled to the $Ca^{2+}$ ion. This basic tenet of cardiac function was first reported by Ringer, 1883 who demonstrated that the frog heart would not contract if $Ca^{2+}$ were removed from the extracellular solution. Hence, if we are to fully understand the physiology of myocardial contraction then it is imperative that we gain insight into both the structure of the cardiomyocyte and the cellular mechanisms that control intracellular $[Ca^{2+}]$ ($[Ca^{2+}]_i$) on a beat to beat basis.

It is generally agreed that the cardiac action potential and the concomitant depolarisation of the sarcolemma and t-tubules allow $Ca^{2+}$ to enter the myocyte from the extracellular space via L-type $Ca^{2+}$ channels. The small rise in $[Ca^{2+}]_i$ subsequently triggers further $Ca^{2+}$ release from the sarcoplasmic reticulum (SR). This $Ca^{2+}$ binds to regulatory proteins located on the actin filaments (troponin-tropomyosin complexes). In binding to troponin there is a structural change elicited in tropomyosin, which ultimately allows myosin cross bridges to interact with actin and thus myocardial contraction to occur. For myocardial relaxation to occur then $[Ca^{2+}]_i$ must decline and this is achieved by removal of $Ca^{2+}$ from the cytosol by a number of routes. See figure 1-1 below.

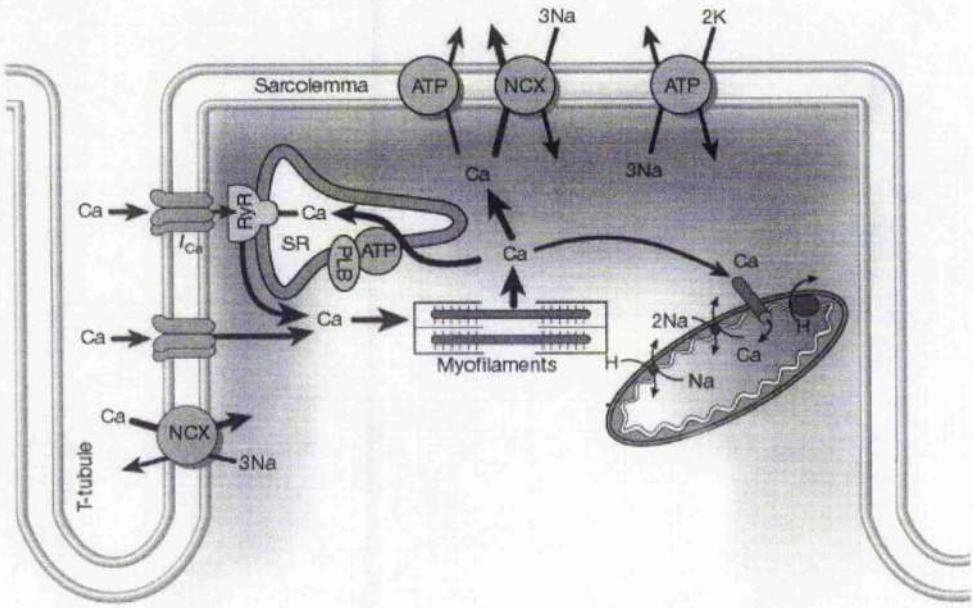


**Figure 1-1. Schematic diagram depicting the various routes for the entry and removal of calcium from the cardiomyocyte during E-C coupling.**

**From Bers, 2002. Of the proteins overexpressed in this study CSQ is located within the sarcoplasmic reticulum while NCX is present in the sarcolemma. Depending on $[Ca^{2+}]_i$, sorcin may be found either in the cytoplasm or associated with membrane bound targets. Similarly FKBP 12.6 may be found either in the cytoplasm or bound to RyR.**

It is the aim of this introduction to outline the molecular mechanisms that are involved in the $Ca^{2+}$ handling process and thus underpin the above description of E-C coupling.

## 1.1 Calcium induced calcium release.

Fabiato, 1983, and Fabiato, 1985a demonstrated that rapid application of $Ca^{2+}$ to mechanically skinned single cardiac myocytes caused the SR to release $Ca^{2+}$, an event that corresponded with the development of tension within the cell. The amount of SR $Ca^{2+}$ release was graded with the amount of trigger $Ca^{2+}$ and furthermore, supra-optimal concentrations of trigger $Ca^{2+}$ (10μM) could inhibit SR $Ca^{2+}$ release. However, using flash photolysis of caged $Ca^{2+}$, Nabauer & Morad, 1990, were unable to observe the inhibition of SR $Ca^{2+}$ release at high $[Ca^{2+}]_i$ in intact ventricular myocytes.

Calcium induced calcium release (CICR) is therefore a positive feedback process and if one considers a "common-pool" model of E-C coupling as described by Stern, 1992 (where both trigger $Ca^{2+}$ and $Ca^{2+}$ released from the SR pass through a common cytosolic pool), then only all or none $Ca^{2+}$ releases should be possible. This model of E-C coupling is difficult to reconcile with Fabiato's experimental findings which demonstrated that graded SR $Ca^{2+}$ release was possible. Stern circumvented this problem by suggesting that $Ca^{2+}$ release from the clusters of RyRs might be "discreet" or "non-propagating" and hence larger $Ca^{2+}$ triggers simply recruited greater numbers of RyR clusters to give the graded response.

## 1.2 Potential triggers for SR $Ca^{2+}$ release.

### 1.2.1 $Ca^{2+}$ entry via the L-type Calcium Channel ($I_{Ca}$).

It is generally accepted that the major source of trigger $Ca^{2+}$ for CICR enters the cardiomyocyte through voltage gated L-type $Ca^{2+}$ channels. This stems from the observation that the $E_m$ dependencies of both intracellular $Ca^{2+}$ transients and muscle contraction are strikingly similar to the bell shape of the I-V relationship for the L-type $Ca^{2+}$ current, see figure 1–2 below from Beuckelmann & Wier, 1988.

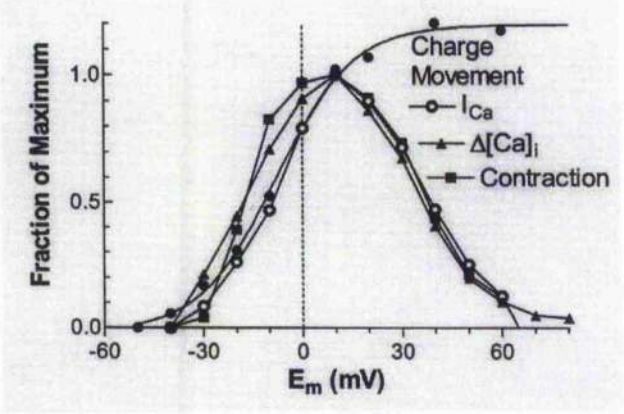


**Figure 1 - 2. Voltage dependence of charge movement, $I_{Ca}$, intracellular $Ca^{2+}$ transients and contraction in guinea-pig ventricular myocytes.**

The observation of $I_{Ca}$ "tail transients" also supports the idea that $Ca^{2+}$ entry on the L-type $Ca^{2+}$ current triggers SR $Ca^{2+}$ release. These have been observed in voltage clamped cardiomyocytes that have been depolarised to positive membrane potentials (+100mV) and then repolarised back to –50mV. At +100mV the L-type $Ca^{2+}$ channels open, but no inward $I_{Ca}$ is

detected and no $Ca^{2+}$ transient is observed. Upon repolarisation to –50mV the $Ca^{2+}$ channels deactivate and as they do so a brief but large $Ca^{2+}$ current flows through, inducing a $Ca^{2+}$ transient and contraction (Cannell *et al.*, 1987).

The structure of the cardiac L-type $Ca^{2+}$ channel is shown in figure 1–3 below.

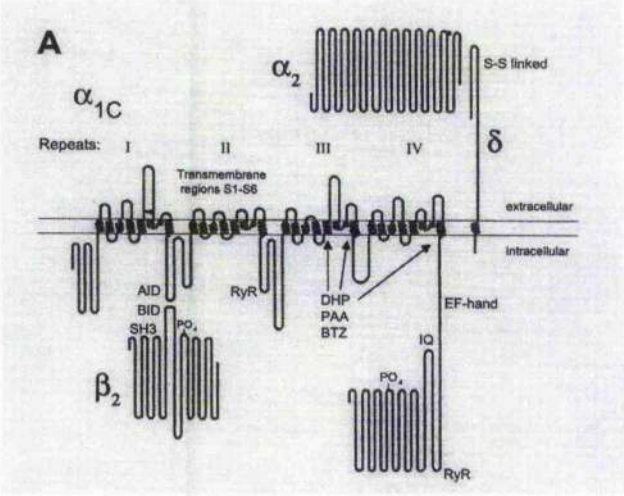


**Figure 1 - 3. Subunit structure of the cardiac L-type $Ca^{2+}$ channel.**

**With putative site for interaction with the ryanodine receptor (RyR) and potential phosphorylation sites ($PO_4$). Adapted from Bers, 2001.**

The channel is made up of an $\alpha_1$ subunit with four domains (I-IV), each containing 6 transmembrane spans ($S_1$-$S_6$). Possible interaction sites between the $\alpha_1$ subunit and the ryanodine receptor (RyR) are indicated, along with potentially important phosphorylation sites ($PO_4$), an EF-hand region and an IQ motif where calmodulin binds. The $\beta_2$ subunit is cytosolic and can also be phosphorylated. In addition there is also an $\alpha_2$ subunit and a $\delta$ subunit that are connected by sulfhydryl bridges.

Measuring specific DHP binding to homogenates from rabbit ventricular myocytes, the density of L-type $Ca^{2+}$ channels has been estimated at ~20 channels/$\mu m^3$ (Bers & Stiffel, 1993). Alternatively, channel density can also be estimated based on whole cell and single channel currents using the following relationship:

$$N = I_{Ca}/(i_{Ca} \times p_o)$$

Here N represents $Ca^{2+}$ channel density, $I_{Ca}$ represents L-type $Ca^{2+}$ current density, $i_{Ca}$ represents single channel current and $p_o$ represents the channel open probability. A similar L-type $Ca^{2+}$ channel density of 18/$\mu m^3$ has been calculated in rabbit ventricular myocytes using this technique (Lew *et al.*, 1991).

$I_{Ca}$ is rapidly activated by depolarisation, reaching a peak in ~2-7ms and depends primarily on temperature and $E_m$. The I-V relationship for $I_{Ca}$ is shown in figure 1–4 below.

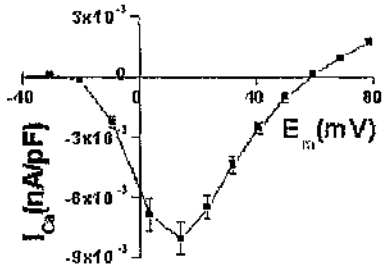


**Figure 1 - 4. I-V relationship for $I_{Ca}$, measured in isolated rabbit cardiomyocytes at room temperature.**

Inactivation of $I_{Ca}$ is time, $E_m$ and $[Ca^{2+}]_i$ –dependent. In voltage clamped guinea pig ventricular myocytes, depolarising to and then holding at 0mV,

the L-type $Ca^{2+}$ current decayed with a $t_{1/2+}$ of 17ms. Repeating the manoeuvre with 10mM EGTA in the pipette, which abolished the intracellular $Ca^{2+}$ transients, inactivation was even slower with a $t_{1/2}$ of 37ms, indicating the $Ca^{2+}$ dependency of inactivation (Hadley & Hume, 1987). Figure 1-5 below, taken from the same study, demonstrates the $E_m$ dependency of $I_{Ca}$.

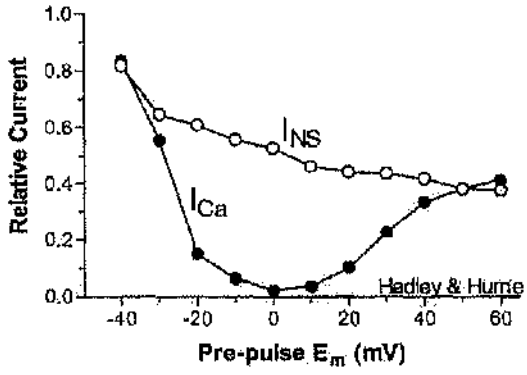


**Figure 1 - 5. $E_m$ dependency of $I_{Ca}$ in guinea-pig ventricular myocytes.**

**$I_{NS}$ represents the amplitude of the currents observed through $I_{Ca}$ when $Na^+$ was used as the charge carrier (Hadley & Hume, 1987).**

The amplitudes of the currents observed through the L-type $Ca^{2+}$ channels are compared at –10mV after 500ms pulses to the indicated $E_m$, using either $Na^+$ ($I_{NS}$) or $Ca^{2+}$ ($I_{Ca}$) as the charge carrier. The additional inactivation with $Ca^{2+}$ is again representative of $Ca^{2+}$-dependent inactivation, which is assumed to act as a negative feedback control to limit further $Ca^{2+}$ entry. A $Ca^{2+}$-binding EF-hand region in the $\alpha_{1C}$ subunit of the cardiac L-type $Ca^{2+}$ channel may underlie the property of $Ca^{2+}$ dependent inactivation. Insertion of this region into a neuronal $Ca^{2+}$ channel conferred $Ca^{2+}$ dependent inactivation that was not exhibited previously (de Leon *et al.*, 1995). It is also possible that calmodulin may have a role in $Ca^{2+}$

dependent inactivation of the cardiac L-type $Ca^{2+}$ channel. It has been suggested that at rest, one $Ca^{2+}$ ion may allow calmodulin to bind to the IQ motif of the $\alpha_{1C}$ subunit. When the channel subsequently opens and $[Ca^{2+}]_i$ rises, more $Ca^{2+}$ may bind to calmodulin, leading to a stronger interaction with the IQ motif and channel inactivation (Zuhlke *et al.*, 1999).

L-type $Ca^{2+}$ channels are typically sensitive to a class of drugs called dihydropyridines (DHPs), e.g. nifedipine, nisoldepine and Bay K 8644. Most DHPs reduce $I_{Ca}$ and hence act as channel antagonists, however Bay K 8644 greatly increases $I_{Ca}$ by increasing the duration of single channel openings, without significantly altering single channel conductance. It has been suggested that it does so by switching the channel to a state named "mode 2" in which long stable openings occur. The normal state is defined as "mode 1" where openings are shorter, whilst "mode 0" describes the state in which the channel is unable to open, e.g. in the presence of nifedipine (Hess *et al.*, 1984). The cardiac L-type $Ca^{2+}$ current can be further modulated by β - adrenergic stimulation. This occurs mainly via protein kinase A (PKA) phosphorylation and has been mimicked using forskolin in voltage clamped isolated ferret ventricular myocytes, causing a 2-fold increase in basal $I_{Ca}$, with maximal $I_{Ca}$ occurring at a more negative $E_m$ (Yuan & Bers, 1995). PKA phosphorylation does not seem to affect single channel conductance, but rather reduces the number of blank sweeps (without any openings) and increases open times (Cachelin *et al.*, 1983).

### 1.2.2 $Ca^{2+}$ entry via the sodium-calcium exchanger.

Work carried out on voltage clamped guinea-pig ventricular myocytes has demonstrated that at membrane potentials less than 20mV, both phasic contraction and $I_{Ca}$ have a similar $E_m$ dependence. However, above 20mV $I_{Ca}$ declined relatively faster than phasic contraction, implying that at these more positive membrane potentials calcium was entering the myocyte via another mechanism. Switching to a $Na^+$ free solution 50ms before depolarisation increased phasic contraction without any increase in L-type $Ca^{2+}$ current. Thus it was inferred that the imposed gradient for removal of $Na^+$ from the myocyte enhanced depolarisation induced entry of $Ca^{2+}$ on NCX and increased the trigger for SR $Ca^{2+}$ release (Levi *et al.*, 1994). This non-linearity between $I_{Ca}$ and cell shortening at positive membrane potentials has also been observed in voltage clamped rabbit cardiac myocytes and was shown to be a function of the amount of sodium present in the pipette. In the presence of nifedipine shortening was reduced, but still observed, however the nifedipine-insensitive shortening could not be elicited in the presence of ryanodine and thapsigargin (Litwin *et al.*, 1998). Hence it seems that reverse sodium calcium exchange is capable of triggering SR $Ca^{2+}$ release, particularly at positive membrane potentials. Interestingly it has been shown that $Ca^{2+}$entry via $I_{Ca}$ is both faster and more efficient than $Ca^{2+}$ entry via reverse mode NCX as a trigger for SR $Ca^{2+}$ release in voltage clamped guinea pig ventricular myocytes (Sipido *et al.*, 1997). Furthermore, with both $I_{Ca}$ and reverse mode NCX present, $Ca^{2+}$ release was triggered solely by $I_{Ca}$ and a contribution of reverse mode

NCX to the trigger could not be detected at membrane potentials below +60mV, even with 20mM $Na^+$ present in the pipette solution.

Working with voltage clamped guinea pig cardiomyocytes Leblanc & Hume, 1990, demonstrated a TTX-sensitive component of contraction and thus postulated that rapid entry of sodium into the myocyte during depolarisation via $I_{Na}$ was able to raise local $[Na^+]_i$ to levels that would support sufficient $Ca^{2+}$ entry via reverse mode NCX to trigger further SR $Ca^{2+}$ release. In the same cell type it has been shown that the sodium current produced by depolarising from –90mV to –50mV was able to elicit a calcium transient only slightly smaller than that triggered by $I_{Ca}$ upon depolarising from –50mV to +5mV. The sodium-dependent transient was unaffected by the inclusion of verapamil, and when ryanodine was also added, only a very small residual transient was observed. When extracellular $Na^+$ was substituted for $Li^+$ a transient could no longer be elicited. Taken together, these observations implied that a substantial $Ca^{2+}$ transient could be generated by a rise in $[Na^+]_i$ and subsequent $Ca^{2+}$ entry via reverse mode NCX triggering further SR $Ca^{2+}$ release (Lipp & Niggli, 1994). It is interesting that Sipido *et al.*, 1995, have shown that DHP antagonists do not provide full block of $I_{Ca}$ in voltage clamped guinea pig cardiomyocytes. In addition calcium transients observed during voltage steps from –90mV to –50mV were blocked by both TTX, but not affected when external sodium was replaced with lithium. These results indicate that the findings of Lipp & Niggli, 1994, may be due to a loss of voltage control combined with an incomplete block of $I_{Ca}$, thus allowing a small amount of $Ca^{2+}$ to enter via L-type $Ca^{2+}$ channels and trigger SR $Ca^{2+}$ release. They also suggest that

increased $[Na^+]_i$ and thus calcium entry via reverse mode NCX is not a likely trigger for SR $Ca^{2+}$ release.

### 1.2.3 $Ca^{2+}$ entry via the T-type $Ca^{2+}$ channel ($I_{Ca,T}$).

Another potential source of trans-sarcolemmal $Ca^{2+}$ entry into the cardiomyocyte is via T-type $Ca^{2+}$ current. $I_{Ca,T}$ activates at more negative membrane potentials than $I_{Ca}$, is significant in Purkinje and some atrial cells and is undetectable in most ventricular myocyte types except for the guinea-pig, where it is small in comparison to $I_{Ca}$. T-type $Ca^{2+}$ currents have been shown to elicit small $Ca^{2+}$ transients in guinea pig ventricular myocytes with large SR $Ca^{2+}$ loads (Sipido *et al.*, 1998). $Ca^{2+}$ influx via T-type channels was also much less efficient in triggering SR $Ca^{2+}$ release when compared to influx via L-type channels.

### 1.2.4 $Ca^{2+}$ entry via sodium channels.

A TTX-sensitive $Ca^{2+}$ current ($I_{Ca\ TTX}$) has been demonstrated in voltage clamped rat ventricular myocytes and has been attributed to a distinct subtype of $Na^+$ channels (Aggarwal *et al.*, 1997). The experiments were carried out in the absence of extracellular $Na^+$ and whilst $I_{Ca\ TTX}$ may be able to trigger CICR it is not likely that any significant $Ca^{2+}$ entry occurs at physiological sodium concentrations. Another study by Santana *et al.*, 1998, also in rat ventricular myocytes, showed that activation of the β-adrenergic receptor or protein kinase A activation altered the selectivity of

the $Na^+$ channel, such that permeation of $Ca^{2+}$ ions occurred to the same extent as $Na^+$. This phenomenon was termed "slip-mode conductance" and was postulated to represent a novel mechanism to explain the inotropic effects of β-adrenergic stimulation, however the observation has not yet been substantiated by research from other groups.

### 1.2.5 Voltage-Dependent $Ca^{2+}$ release.

In contrast to cardiac muscle, skeletal muscle does not require the entry of $Ca^{2+}$ from the extracellular space in order to trigger further SR $Ca^{2+}$ release. In skeletal muscle, the L-type $Ca^{2+}$ channels and the RYRs are linked to form bridging structures between the t-tubules and the SR which have been termed "junctional feet". It has been suggested that charge movement in the t-tubules during depolarisation causes these junctional feet to move via an electrostatic effect (Chandler *et al.*, 1976a & Chandler *et al.*, 1976b). This movement may simply unplug the $Ca^{2+}$ channel in the RyR, allowing the SR to release its store of $Ca^{2+}$ (Rios & Pizarro, 1991). There is some controversy as to whether a voltage-dependent mechanism also exists in cardiac muscle.

Working in voltage clamped guinea pig ventricular myocytes, it has been shown that depolarisation from –65mV to –40mV produced a sizeable intracellular $Ca^{2+}$ transient in the absence of any measurable inward $Ca^{2+}$ current (sodium currents were blocked with 100μM lidocaine). This intracellular $Ca^{2+}$ transient was abolished with the addition of 30nM

ryanodine, implying it was dependent on SR $Ca^{2+}$ release. With further depolarisation from –40mV to 0mV there was a significant L-type $Ca^{2+}$ current which also gave rise to an intracellular $Ca^{2+}$ transient that was not affected by the addition of ryanodine (Ferrier & Howlett, 1995). Thus it was implied that $I_{Ca}$ did not trigger SR $Ca^{2+}$ release, contradicting previous studies (e.g Beuckelmann & Wier, 1988), but rather that a voltage sensitive mechanism was involved. Additional work suggested that this voltage sensitive mechanism may require the presence of cAMP (Ferrier *et al.*, 1998). A major criticism of this work is that the putative voltage dependent mechanism required the presence of extracellular $Ca^{2+}$ to function. Thus an undetectably small inward $Ca^{2+}$ current, especially in circumstances where cAMP may have elevated SR $Ca^{2+}$ load and phosphorylated RYRs, may be responsible for triggering SR $Ca^{2+}$ release upon depolarisation from –65mV to –40mV, particularly if there was any loss in voltage control about –40mV.

Indeed a recent study using voltage clamped rat ventricular myocytes by Trafford & Eisner, 2003, has found no evidence for voltage sensitive $Ca^{2+}$ release in cardiac muscle. With voltage pulses from –80mV to 0mV, addition of 500μM $Cd^{2+}$ (blocking $I_{Ca}$) reduced the rate of rise of the intracellular $Ca^{2+}$ transient to 2.8% of control, demonstrating that the bulk of the $Ca^{2+}$ transient was not due to a voltage dependent mechanism. With sodium free solutions in the pipette, $Cd^{2+}$ entirely abolished the $Ca^{2+}$ transient, implying that the residual $Ca^{2+}$ transient previously observed was triggered by $Ca^{2+}$ entry via NCX. Further contradicting the work of Ferrier et al, who also claimed that the putative voltage sensitive mechanism was insensitive to $Ni^{2+}$, the addition of 5mM $Ni^{2+}$ completely abolished the $Ca^{2+}$

transient observed upon depolarisation from –80mV to 0mV, despite prior incubation with isoprenaline. Hence it seems unlikely that voltage dependent $Ca^{2+}$ release is responsible for any component of the intracellular $Ca^{2+}$ transient observed in cardiac myocytes.

### 1.3 SR $Ca^{2+}$ release channel or Ryanodine Receptor.

While the source of trigger $Ca^{2+}$ for the process of CICR has been the subject of considerable debate, there is little doubt that the RyR represents the SR $Ca^{2+}$ release channel. The ryanodine receptor exists in 3 different isoforms. RyR1 is found in skeletal muscle, RyR3 is found in the brain while RyR2 is considered the cardiac isoform. *In vivo*, RyR2 is thought to exist as a 2260kDa homotetramer which spans the SR membrane providing a channel for $Ca^{2+}$ release (Saito *et al.*, 1988). It has a very high single channel conductance with a relatively low Ca selectivity ($P_{Ca}/P_K$ ~ 6 *vs.* 3000 for the sarcolemmal L-type $Ca^{2+}$ channel).

Evidence that RyRs are capable of discreet $Ca^{2+}$ release is provided in the form of $Ca^{2+}$ sparks. These were first identified using Laser Scanning Confocal Microscopy (LSCM) to study cardiac myocytes loaded with a fluorescent $Ca^{2+}$ indicator and were manifest as spontaneous, transient local increases in fluorescence that occurred in close proximity to the t-tubules (Cheng *et al.*, 1993). Thus it seems likely that the global $Ca^{2+}$ transient that occurs just preceding contraction in cardiomyocytes is the product of the temporal and spatial summation of many $Ca^{2+}$ spark events

synchronised by the action potential and the subsequent entry of trigger $Ca^{2+}$.

Typical $Ca^{2+}$ sparks reach a peak [$Ca^{2+}$] of 200-300nM in ~ 10ms and have a spatial spread of ~2μM (full width half-maximum) while the $Ca^{2+}$ flux associated with a single $Ca^{2+}$ spark has been estimated at 40fC (Cheng *et al.*, 1993). The $Ca^{2+}$ current through RyR2 has been estimated at 0.3pA (Mejia-Alvarez *et al.*, 1999) with a typical open time of ~3ms (Tinker & Williams, 1993) and this would correspond to a flux of ~ 1fC. Hence it seems likely that $Ca^{2+}$ flux through at least 40 RyRs would contribute to a single $Ca^{2+}$ spark. Indeed clusters of 50-200 RyRs have been observed at dyadic junctions in cardiac myocytes (Franzini-Armstrong *et al.*, 1999).

Sparks can also be triggered by electrical depolarisation, as illustrated by Cannell *et al.*, 1995. Working with rat ventricular cardiomyocytes, they demonstrated that depolarisation from –40mV to +10mV and activation of the L-type $Ca^{2+}$ current for a very short period of 3ms, followed by further depolarisation to +80mV for 80ms, caused the initial SR $Ca^{2+}$ release to be abruptly terminated. Repolarising the cardiomyocyte to –90mV then produced a tail current and a more uniform release of SR $Ca^{2+}$. When this initial SR $Ca^{2+}$ release was visualised using confocal microscopy, it was seen to occur at discreet sites along the length of the myocyte. These discreet SR $Ca^{2+}$ release events were identical in morphology to spontaneous $Ca^{2+}$ sparks. Thus, it was postulated that these isolated SR $Ca^{2+}$ release events were infact $Ca^{2+}$ sparks that had been triggered by an abbreviated L-type $Ca^{2+}$ current. An increased L-type $Ca^{2+}$ current would

simply trigger larger numbers of $Ca^{2+}$ sparks which are summed both temporally and spatially to produce the intracellular $Ca^{2+}$ transient.

Lipid bilayer studies of RyR2, in which the channels are not in their normal physiological environment have shown that $Ca^{2+}$ activation and an increase in $P_O$ begins at submicromolar cytosolic [$Ca^{2+}$], peaks around 100μM and decreases thereafter (Xu *et al.*, 1998). ATP may activate RyR2 if [$Ca^{2+}$] is sufficiently high (Rousseau *et al.*, 1986) whereas $Mg^{2+}$ inhibits RyR2 in the mM range (Rousseau & Meissner, 1989). Elevating luminal [$Ca^{2+}$] intrinsically enhances RyR2 channel activity by increasing both the frequency of channel openings (Gyorke & Gyorke, 1998) and the open probability ($P_O$) (Ching *et al.*, 2000). It has been suggested that this may be due to more $Ca^{2+}$ passing through the channel and acting at the cytoplasmic activating site (Tripathy & Meissner, 1996). This seems unlikely as Gyorke & Gyorke, 1998, demonstrated that the effect of increasing luminal $Ca^{2+}$ was independent of the driving voltage direction and was unaffected by high cytosolic concentrations of a fast $Ca^{2+}$ chelator. Furthermore, when the luminal portion of RyR2 is exposed to trypsin digestion, subsequent elevation of luminal $Ca^{2+}$ reduces $P_O$, suggesting that trypsin selectively damages luminal $Ca^{2+}$ activation sites, thus revealing luminal $Ca^{2+}$ inactivation sites (Ching *et al.*, 2000).

It has been elegantly demonstrated using co-immunoprecipitation that RYR2 is infact a megacomplex composed of a number of different proteins (Marx *et al.*, 2000). These include:

- FK-binding protein 12.6 (FKBP 12.6). FKBP 12.6 is a member of a highly conserved family of proteins known as immunophilins and was initially found to be tightly associated with RyR2 from canine cardiac SR (Timerman *et al.*, 1994). Experimental interventions that dissociate FKBP 12.6 from RyR2 have been shown to increase the open probability of the channel, but also induce subconductance states (Kaftan *et al.*, 1996 & Xiao *et al.*, 1997). In addition it has been suggested that FKBP 12.6 may play a role in the functional coupling of RyRs (Marx *et al.*, 2001).

- Muscle A kinase anchoring protein (mAKAP). mAKAP binds protein kinase A and targets it to substrates.

- RII. RII is a protein kinase A regulatory subunit.

- Protein kinase A (PKA). Phosphorylation of RyR2 by PKA occurs at serine-2809 (Marx *et al.*, 2000). Studying canine RyR2 reconstituted in planar lipid bilayers it has been shown that PKA phosphorylation reduces basal $P_O$ at 100nM $[Ca^{2+}]_i$, greatly increases $P_O$ when $[Ca^{2+}]_i$ is raised and accelerates the subsequent decline in $P_O$ (Valdivia *et al.*, 1995). In contrast, when $Ca^{2+}$ spark frequency and SR $Ca^{2+}$ load were measured following PKA phosphorylation in both wild-type and phospholamban knock-out permeabilised mouse ventricular myocytes,

increases in both parameters were only observed in the former. Hence it was inferred that the increased $Ca^{2+}$ spark frequency in the wild-type myocytes was entirely attributable to phospholamban phosphorylation, increased SERCA activity and ultimately the enhanced SR $Ca^{2+}$ load (Nabauer & Morad, 1990).

- Protein phosphatases PP1 and PP2A. PP1 and PP2A act to de-phosphorylate RyR2 and have been shown to decrease the gain of E-C coupling via a reduction in RyR2 channel activity in voltage clamped rat ventricular myocytes (duBell *et al.*, 1996). However, a recent study has demonstrated that addition of PP1 and PP2A to permeabilised rat ventricular myocytes caused a dramatic increase in the frequency of spontaneous $Ca^{2+}$ sparks, implying a stimulatory effect on RyR2 (Terentyev *et al.*, 2003a).

- Protein phosphatase PP2B or calcineurin is also found in cardiac muscle. Whilst Marx *et al.*, 2000, found that it did not co-immunoprecipitate with RyR2, a physical interaction between calcineurin and RyR2, dependent on the presence of $Ca^{2+}$ and FKBP 12.6, has been demonstrated in membrane fractions in rat cardiac tissue (Bandyopadhyay *et al.*, 2000). The same study demonstrated that the addition of calcineurin inhibitors to neonatal rat cardiomyocytes caused an increase in the rate of $Ca^{2+}$ oscillations, providing evidence that it may modulate $Ca^{2+}$ release in the heart.

- Calsequestrin (CSQ). CSQ is the main calcium binding protein inside the SR and it has been demonstrated that two linker proteins, junctin and triadin, both highly concentrated in the SR membrane, bind tightly not just to each other but also luminally to both RyR2 and CSQ (Zhang *et al.*, 1997). The occurrence of spontaneous $Ca^{2+}$ sparks was markedly reduced in transgenic CSQ-overexpressing mouse cardiomyocytes when compared to control (Wang *et al.*, 2000), while adenoviral mediated over-expression of CSQ in rat ventricular myocytes increased the amplitude but had no effect on the frequency of spontaneous $Ca^{2+}$ sparks (Terentyev *et al.*, 2003b).

In addition to the above proteins that together form the RyR2 megacomplex, a number of cytoplasmic proteins are also thought to modulate the SR $Ca^{2+}$ release channel.

- $Ca^{2+}$- Calmodulin dependent protein kinase (CaMKII). CaMKII also phosphorylates RyR2 at serine-2809 (Witcher *et al.*, 1991) with bilayer studies demonstrating both increased (Witcher *et al.*, 1991) and decreased (Lokuta *et al.*, 1995) channel $P_O$ as a result. In voltage clamped cardiomyocytes it has been demonstrated that CaMKII inhibition prevented a $[Ca^{2+}]_i$ – dependent increase in fractional SR $Ca^{2+}$ release, implying that repeated $Ca^{2+}$ transients may activate CaMKII, phosphorylate RyR2 and thus improve the efficiency of E-C coupling (Eisner *et al.*, 1989).

- Calmodulin (CaM). CaM is also known to assert independent effects on RyR2. Studying canine RyRs in SR vesicles it has been demonstrated that at $[Ca^{2+}]$ > 100nM, CaM inhibits $Ca^{2+}$ - induced, caffeine-induced and AMP-induced Ca release (Meissner & Henderson, 1987).

- Sorcin. Sorcin is a 22kDa $Ca^{2+}$-binding protein that belongs to the penta EF-hand (PEF) protein family and is also associated with RyR2 in the heart. Addition of sorcin to the cytoplasmic side of RyR2 causes a significant reduction in its open probability ($IC_{50}$ ~ 480nM), whilst PKA-mediated phosphorylation of sorcin significantly reduces its ability to modulate RYR function (Lokuta *et al.*, 1997). Sorcin also decreased the frequency and duration of spontaneous $Ca^{2+}$ sparks in permeabilised cardiomyocytes and rapid injection of sorcin onto the cytosolic face of RyRs reconstituted in lipid bilayers caused complete inhibition of the channel in <20ms (Farrell *et al.*, 2003).

## 1.4 Removal of $Ca^{2+}$ from the cytoplasm.

The increase in $[Ca^{2+}]_i$ brought about by CICR ultimately enables myocardial contraction to occur. Thus, for myocardial relaxation to occur $[Ca^{2+}]_i$ must decline and this is achieved by removal of $Ca^{2+}$ from the cytosol by a number of routes. In order for SR $Ca^{2+}$ load to remain constant and for the cardiomyocyte to remain in the steady state, $Ca^{2+}$ released by the SR during E-C coupling must be pumped back into the SR during relaxation. In addition the trigger $Ca^{2+}$ that entered the cardiomyocyte from the extracellular space must be also removed from the cytosol at the sarcolemma.

There are 4 main $Ca^{2+}$ transport systems that compete for cytoplasmic $Ca^{2+}$ during relaxation in cardiac muscle: the SR $Ca^{2+}$ pump, the sarcolemmal $Ca^{2+}$ ATPase, the sodium-calcium exchanger and finally the mitochondrial $Ca^{2+}$ uniport system. The extent to which each of these separate systems contribute to relaxation has been investigated in rabbit ventricular myocytes and is illustrated in figure 1 - 6 below. Under normal circumstances the SR $Ca^{2+}$ pump contributes 68.5% of total $Ca^{2+}$ removal flux, with NCX, sarcolemmal $Ca^{2+}$-ATPase and the mitochondrial $Ca^{2+}$ uniporter contributing 30%, 0.86% and 0.62% respectively (Bers, 2001).

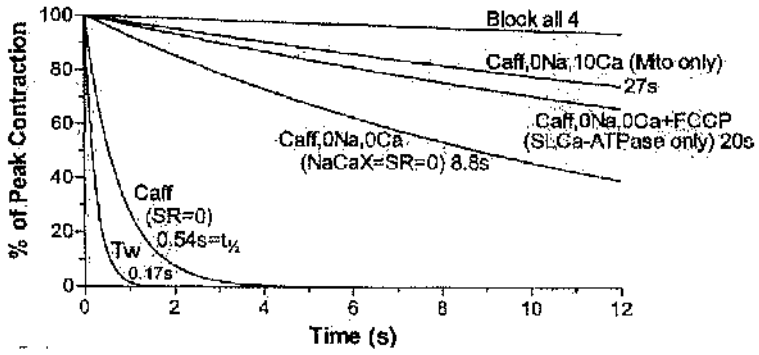


**Figure 1 - 6. Rate of removal of $Ca^{2+}$ from the cytoplasm of a rabbit cardiomyocyte depending on the $Ca^{2+}$ transport systems employed.**

**With all $Ca^{2+}$ transport systems functioning during a normal twitch the $t_{1/2}$ for relaxation was 0.17s. Addition of 10mM caffeine to prevent SR $Ca^{2+}$ uptake increased the $t_{1/2}$ for relaxation to 0.54s. When a twitch was carried out in a solution in a zero $Na^+$ and zero $Ca^{2+}$ solution containing caffeine (to inhibit both SR $Ca^{2+}$ uptake and NCX activity) the $t_{1/2}$ for relaxation was 8.8s. Subsequent addition of FCCP (to also inhibit the mitochondrial $Ca^{2+}$ uniport system) further increased the $t_{1/2}$ for relaxation to 20s. Finally, with mitochondria as the only means of lowering cytosolic $Ca^{2+}$ the $t_{1/2}$ for relaxation was 27s (Bassani *et al.*, 1992).**

A more detailed description of each of these $Ca^{2+}$ transport mechanisms follows below.

### 1.4.1 SR $Ca^{2+}$ pump.

The re-uptake of SR $Ca^{2+}$ is achieved by the action of the sarco(endo)plasmic reticulum $Ca^{2+}$-ATPase (SERCA) pump, which removes 2 $Ca^{2+}$ ions from the cytosol and in doing so consumes 1 molecule of ATP.

SERCA exists in a number of different isoforms. SERCA1a predominates in adult fast twitch skeletal muscle, whereas SERCA1b is present in the foetal and neonatal stages. SERCA2a is the cardiac isoform, with SERCA2b and SERCA3 found in the endoplasmic reticulum of non-muscle cells. In cardiac myocytes, SERCA2a is thought to be located mainly in the longitudinal SR (corresponding to the light fraction of SR vesicles) with a little located in the terminal cisternae along with the $Ca^{2+}$ release channels (corresponding to the heavy fraction of SR vesicles).

The structure of SERCA can be seen in figure 1-7 below, taken from MacLennan *et al.*, 1992, with ~ 70% of the protein located on the cytoplasmic side of the SR membrane.

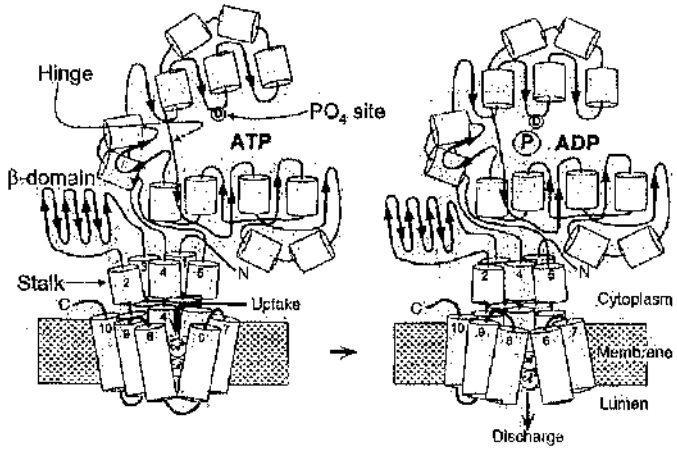


**Figure 1 - 7. Schematic of SERCA structure.**

**Indicating an ATP binding domain, a phosphorylation site (Asp-351) and 10 membrane spanning domains ($M_1$-$M_{10}$), with $M_1$-$M_5$ each having an additional stalk region on the cytoplasmic side.**

SERCA2a is regulated by the endogenous 22KDa protein, phospholamban, which markedly decreases $Ca^{2+}$ transport and $Ca^{2+}$-ATPase activity, particularly at low $[Ca^{2+}]_i$, by increasing the $K_m$(Ca) for the pump to ~300nM. However, phospholamban can be phosphorylated by protein kinase A at Ser-16, reducing the $K_m$(Ca) for the pump to ~100nM, thus increasing SERCA2a activity (Colyer, 1998). Phosphorylation of phospholamban at Thr-17 by CaMKII has also been reported to produce a similar lowering of $K_m$(Ca) for the pump (Simmerman *et al.*, 1986). Hence *in vivo*, β-adrenergic stimulation would be expected to bias the competition to remove $Ca^{2+}$ from the cytosol between SERCA2a and NCX in the favour of the former, leading to an increased SR $Ca^{2+}$ content available for release. In addition SERCA2a activity is further modulated by cellular pH. SR $Ca^{2+}$ uptake in mechanically skinned cardiomyocytes was steadily reduced as pH was decreased from 7.4 (Fabiato, 1985b). Finally, SERCA activity may be completely inhibited by drugs such as cyclopiazonic acid (Goeger *et al.*, 1988), 2,5-di(tert-butyl)-1,4-benzohydroquinone or TBQ (Nakamura *et al.*, 1992) and thapsigargin (Sagara & Inesi, 1991).

### 1.4.2 Sarcolemmal Calcium pump.

$Ca^{2+}$ may be removed from the cytosol and into the extracellular space by the action of the 138kDa sarcolemmal $Ca^{2+}$-ATPase which is similar in structure to SERCA. 10 transmembrane domains (TM1-10) make up 20% of the protein, while the cytosolic domains make up the remaining 80%.

One $Ca^{2+}$ ion is transported per ATP hydrolysed and $Ca^{2+}$ extrusion is coupled to proton influx (1Ca: 1H).

During intracellular $Ca^{2+}$ transients in rabbit ventricular myocytes the $Ca^{2+}$ extrusion rate by the sarcolemmal $Ca^{2+}$-ATPase is thought to be ~ 1μM/sec which is slow compared to that via the sodium-calcium exchanger, ~ 30μM/sec (Bers, 2001). In the absence of SR $Ca^{2+}$ uptake, the sarcolemmal $Ca^{2+}$-ATPase has been shown to account for ~6% of $Ca^{2+}$ removal from rabbit cardiomyocytes (Bassani *et al.*, 1994).

It has been demonstrated using sarcolemmal vesicles from cardiomyocytes that the sarcolemmal $Ca^{2+}$-ATPase can be stimulated (via an increase in $V_{max}$ and a reduction in $K_m$(Ca)) by protein kinase A and to a greater extent by calmodulin (Dixon & Haynes, 1989). Frustratingly, there are no highly selective inhibitors of the sarcolemmal $Ca^{2+}$-ATPase.

1.4.3 Sodium-Calcium Exchanger.

The second route for removal of $Ca^{2+}$ from the cytosol and into the extracellular space at the sarcolemma involves the sodium-calcium exchanger (NCX). Reuter & Seitz, 1968, were the first report the existence of a $Na^+/Ca^{2+}$ countertransport system in the heart. Work using isolated cardiac sarcolemmal vesicles was later to reinforce this observation. Vesicles were loaded with 140mM $Na^+$ and then placed in a solution containing 140mM KCl & radiolabelled $^{45}Ca^{2+}$. The $^{45}Ca^{2+}$ was

subsequently taken up by the vesicles in exchange for $Na^+$. Later, re-introduction of 50mM $Na^+$ to the bathing solution then caused the vesicles to release $^{45}Ca^{2+}$, indicating the reversibility of NCX (Reeves & Sutko, 1980).

The stoichiometry of NCX was elegantly determined, again using sarcolemmal vesicles by Reeves & Hale, 1984. They described the relationship between the membrane potential and the other components of the thermodynamic driving force for NCX as follows:

$$\Delta\mu_{Na\text{-}Ca} = n\Delta\mu_{Na} - \Delta\mu_{Ca} = (n-2)E_m - nE_{Na} + 2E_{Ca} \quad (1)$$

[$\Delta\mu_{Na\text{-}Ca}$ represents the overall driving force for NCX, $E_m$ is the membrane potential, n is the stoichiometry for the exchange process, $E_{Na}$ and $E_{Ca}$ are the equilibrium potentials for $Na^+$ and $Ca^{2+}$ respectively, $\Delta\mu_{Na} = E_m - E_{Na}$ and $\Delta\mu_{Ca} = 2(E_m - E_{Ca})$]

By varying extracellular $K^+$ concentration they were able to impose either a positive or a negative $E_m$ on the vesicles. Manipulation of the $Na^+$ gradients across the vesicles allowed them to oppose the effects of $E_m$, to a point where the driving force for NCX was zero and there was no net movement of $Ca^{2+}$. The above equation could then be re-written:

$$(n-2)E_m = nE_{Na} + 2E_{Ca} \quad (2)$$

They found that there was no net $Ca^{2+}$ movement with $E_m = 31mV$ and $E_{Na} = -10mV$. $[Ca^{2+}]$ was the same on both sides of the vesicles, thus $E_{Ca} = 0$. If we substitute these values into equation 2, then n, the stoichiometry for the exchanger works out to be almost exactly 3 $Na^+$ ions exchanged for

every $Ca^{2+}$ ion. Interestingly Fujioka *et al.*, 2000, have carried out studies in large inside-out patches excised from guinea pig ventricular myocytes that implied a different stoichiometry for NCX. Given that at the reversal potential, the driving force for NCX is zero then equation 1 above can be re-written thus:

$$\mathbf{0 = (n-2)E_m - nE_{Na} + 2E_{Ca}} \quad \mathbf{(3)}$$

$$\mathbf{\Rightarrow E_m = nE_{Na} - 2E_{Ca} / (n-2)} \quad \mathbf{(4)}$$

Knowledge of the reversal potential along with extracellular and intracellular $Na^+$ and $Ca^{2+}$ concentrations then allowed calculation of the stoichiometry for NCX, suggesting 4 $Na^+$ ions for every $Ca^{2+}$ ion transported. In addition it was suggested that this stoichiometry may vary depending on extracellular and intracellular $Na^+$ and $Ca^{2+}$ concentrations.

NCX was has a molecular weight of 108kDa and consists of 970 amino acids (Nicoll *et al.*, 1990). The structure of NCX can be seen in figure 1-8 below.

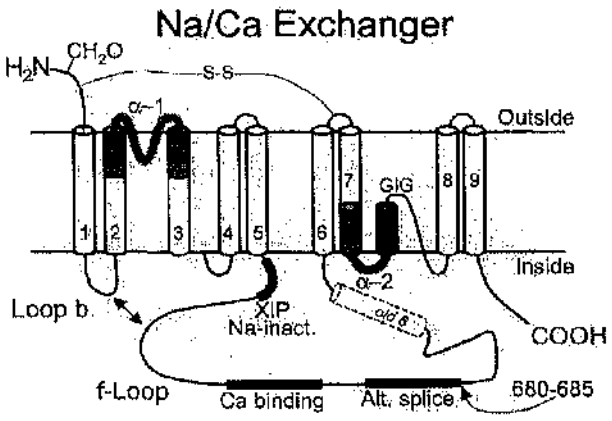


**Figure 1 - 8. Structure of the sodium/calcium exchanger.**

**Revealing 5 transmembrane domains on the amino part of the protein, a cytoplasmic f-loop and 4 more transmembrane domains on the carboxy end. Adapted from Bers, 2001.**

It has been postulated that the second transmembrane domain along with the 2 $\alpha$ repeats may contribute to the ion translocation pathway (Nicoll *et al.*, 1996) and deletion of the intracellular f-loop has been shown to abolish the allosteric regulation of exchanger by $[Ca^{2+}]_i$ and $[Na^+]_i$ (Matsuoka *et al.*, 1993). In addition, there is a charged segment composing of 20 residues at the amino end of the f-loop (XIP) which resembles a calmodulin binding domain and may be autoinhibitory.

Using whole cell voltage clamp, Kimura *et al.*, 1987, carried out an electrophysiological study to better characterise NCX current in intact guinea pig ventricular myocytes. With all other known currents blocked, they were able to dialyse the myocytes with solutions containing various amounts of $Na^+$ and $Ca^{2+}$. With $[Ca^{2+}]_i$ nominally zero there was no inward current activated in the presence of 140mM extracellular $Na^+$. When $[Ca^{2+}]_i$

was increased to 430nM, application of 140mM extracellular $Na^+$ activated an $E_m$-dependent current.

More recently, allosteric regulation of NCX by cytosolic $Ca^{2+}$ ($K_{mCaAct}$ = 125nM) has been demonstrated in voltage clamped ferret cardiomyocytes, as shown in figure 1-9 below.

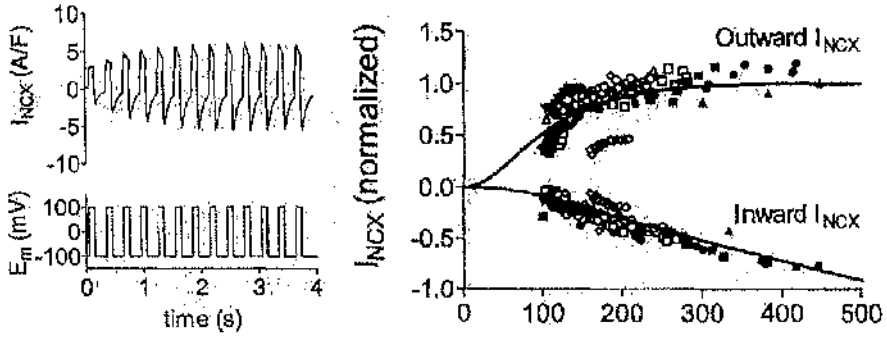


**Figure 1 - 9. Inward and outward NCX currents over a range of $[Ca2+]_i$.**

**$E_m$ alternated between -100mV and +100mV. All other known currents were blocked (Weber *et al.*, 2001).**

The electrochemical effect of increasing $[Ca^{2+}]_i$ would be to increase $Ca^{2+}$ efflux (↑ inward $I_{NCX}$), whilst decreasing $Ca^{2+}$ influx (↓ outward $I_{NCX}$). Thus, any increase in outward $I_{NCX}$ would have to be due to the allosteric stimulation of $I_{NCX}$ by $[Ca^{2+}]_i$. This $Ca^{2+}$-dependent activation may serve to stimulate $Ca^{2+}$ extrusion by $I_{NCX}$ when $[Ca^{2+}]_i$ is high and turn off the exchanger as $[Ca^{2+}]_i$ falls to diastolic levels. Interestingly, work using giant excised patches from Xenopus oocytes overexpressing NCX has also shown that $[Na^+]_i$ may also have a role in modulating the exchanger's

activity. With high [Ca] in the pipette ($[Ca]_o$), and 1μM $Ca^{2+}$ on the intracellular side of the patch, application of 100nM $Na^+$ to the inside surface activated outward $I_{NCX}$. However, sustained exposure to high $[Na^+]_i$ produced a $Na^+$-dependent inactivation of $I_{NCX}$ (Philipson & Nicoll, 2000). The physiological role of this $Na^+$-dependent inactivation is unclear as it is only observed if $[Na^+]_i$ > 30mM, though it may serve to prevent excess $Ca^{2+}$ influx and $Ca^{2+}$ overload under conditions of high $[Na^+]_i$.

NCX may also be further modulated by a host of other factors. The exchanger is markedly affected by alteration of the lipid bilayer. Activity is increased by reconstitution with acidic phospholipids, addition of exogenous negatively charged amphiphiles and cleavage of native phospholipids to yield negatively charged membrane lipids (Philipson & Nicoll, 2000). Bers *et al.*, 1985 have demonstrated that NCX activity is virtually unaffected by changes in surface charge, thus it appears that these amphiphiles and phospholipids do not act by simply concentrating $Ca^{2+}$ near the exchanger. Alkalosis stimulates the exchanger while acidosis inhibits activity (Philipson *et al.*, 1982). Intriguingly, treatment with chymotrypsin, which removes the cytosolic f-loop of the exchanger, abolishes this pH-dependence (Doering & Lederer, 1993 & Doering & Lederer, 1994). Finally, there is some controversy whether PKA-dependent phosphorylation of cardiac NCX affects its activity. Working in guinea pig myocytes treated with isoproterenol, Wei *et al.*, 2003, have reported a 500% increase in NCX activity. In addition, Schulze *et al.*, 2003, have demonstrated in vitro phosphorylation of NCX by PKA and the existence of an NCX macromolecular complex including both the catalytic and regulatory

subunits of PKA, protein kinase C, the serine/threonine phosphatases PP1 & PP2A and the protein kinase A-anchoring protein (mAKAP). However Ginsburg, 2004, would suggest that isoproterenol does not enhance NCX activity.

### 1.4.4 Mitochondrial calcium influx pathways

It has become apparent that the mitochondria within the cardiomyocyte subtly affect $[Ca^{2+}]_i$. There are thought to be two main pathways via which $Ca^{2+}$ can move from the cytosol into the mitochondria, the $Ca^{2+}$ uniporter and the rapid influx pathway. $Ca^{2+}$ flux through the uniporter is downhill and exceeds 10000 ions per second (greater than that of the fastest known pumps and exchangers), depending directly upon mitochondrial membrane potential (Babcock & Hille, 1998). The uniporter in inhibited by ruthenium red and protonophores such as Carbonyl Cyanide *m*-Chlorophenolhydrazone (CCCP) and may be activated by spermine and taurine. The rapid influx pathway for $Ca^{2+}$ entry into the mitochondria lasts only a fraction of a second and is also inhibited by ruthenium red, though the concentration required to do so is 100 fold greater than that required to inhibit the uniporter. Hence it has been speculated that the rapid influx pathway may represent an alternative conformation of the uniporter. It should be noted that mitochondrial $Ca^{2+}$ uptake rate is near zero when cytosolic $Ca^{2+}$ is less than ~300nM (Gunter *et al.*, 2000). Hence it is unlikely to have a significant effect on the decay of a typical intracellular $Ca^{2+}$ transient.

## 1.5 Conclusions and Aims

To conclude with is it apparent that a collusion between many different channels, pumps, exchangers and modulatory factors is required for efficient E-C coupling. However in many cases the contributions that specific individual proteins make towards the process of E-C coupling require further clarification.

Thus it is the intention of this thesis to investigate the effects of overexpressing sorcin, calsequestrin, FKBP 12.6 and NCX on excitation-contraction coupling in voltage clamped rabbit cardiomyocytes. Overexpression will take place over a period of 24hrs in cell culture using adenovirus-mediated transfer of the cDNA coding for the protein of interest.

# Chapter 2 – Methods & Preparatory Studies

## 2.1 – Cardiomyocyte isolation and adenoviral transfection.

### 2.1.1 - Dissociation of Adult Rabbit Cardiac Myocytes.

Male White New Zealand rabbits were anaesthetised with an injection of 100 mg/kg Sodium Pentobarbitone containing 500 U Heparin via the left marginal ear vein. Animals were assumed terminally anaesthetised when both the corneal and the hind limb flexion withdrawal reflexes were absent. All solutions were filter sterilised and prepared with sterile water and all glassware used was autoclaved.

The thoracic cavity was opened and the heart rapidly excised and placed into a beaker containing ice-cold Krebs' solution (120mM NaCl, 20mM HEPES, 5.4mM KCl, 0.52mM $NaH_2PO_4$, 3.5mM $MgCl_2.6H_20$, 20mM Taurine, 10mM Creatine, 11.1mM Glucose, pH 7.4).

The heart was then mounted onto the cannula of a Langendorff retrograde perfusion system via the aorta. Any fatty or connective tissues were trimmed away and 150ml of $Ca^{2+}$ free Krebs' solution at 37°C was perfused through the heart at a rate of 25ml/min to wash away any residual blood and $Ca^{2+}$. The heart was then perfused with an enzyme solution (75ml $Ca^{2+}$ free, sterile Krebs' solution containing 3mg Protease and 50mg Collagenase). The enzyme solution was collected having passed through the heart and then re-circulated. After 2-3 minutes $CaCl_2$ (to 0.05mM) was added to the enzyme solution to activate the Collagenase. After 5-6

minutes, when the myocardium felt softened to the touch, the enzyme solution was washed out of the heart by perfusion with 100ml Sterile Krebs' solution containing 1% (w/v) Bovine Serum Albumin.

The left ventricle was removed from the heart and placed in Krebs' solution containing 0.125mM $CaCl_2$. The tissue was then finely chopped using autoclaved instruments in a laminar flow hood. The chopped tissue was placed in tissue culture grade sterile flasks and then mechanically shaken for 1hr at room temperature to encourage dissociation of single myocytes, after which the cells were allowed to sediment by gravity. Again, in a laminar flow hood and using aseptic technique, the supernatant was removed and the myocytes were subsequently re-suspended in Krebs' solution containing 0.25mM $CaCl_2$. This process was repeated twice more with myocytes re-suspended in 0.5mM and finally 1mM $CaCl_2$.

2.1.2 - Adenoviral over-expression of specific proteins in isolated adult cardiomyocytes.

Viruses exist by virtue of their ability to transfer genetic information into potential host cells. Advances in recombinant DNA technology over the past 20 years have made it possible to exploit this characteristic and thus create efficient gene transfer vectors that cause over-expression of specific proteins which may be of functional significance.

The earliest prototypes of such transfer vectors appeared in the early 1980's. Initially retroviral vectors, that reverse transcribe their RNA genome to proviral DNA that then integrates into the host genomic DNA, were the mode of choice for gene transfer into mammalian cells. However, such integration enhances the risk of cellular transformation caused by insertional mutagenesis or activation of oncogenes (Becker *et al.*, 1994). Furthermore, efficient integration only occurs in dividing cells as the process requires certain host cellular factors that are only present during mitosis (Varmus, 1988). It is generally accepted that adult cardiac tissue is terminally differentiated and thus incapable of mitotic cell division. Hence the absence of significant regeneration via proliferation following myocardial injury (Pasumarthi & Field, 2002). Thus retroviral-mediated gene transfer in tissues such as cardiac muscle, which are thought incapable of mitosis, is not achievable.

DNA viruses have therefore become plausible gene transfer vectors in such tissues. They provide a fast and efficient method of gene delivery to non-

replicating primary cells. Of all the available DNA virus vectors, the adenovirus, of which there are 40 serotypes, is the best studied and thought to be the most useful for the generation of recombinants. It has the capacity to express relatively large DNA inserts at favourable levels and a high infectivity in a broad range of mammalian cell types, with little effect on cell viability. In addition it is relatively easy to propagate high-titre viral stocks .

The structure of the wild-type adenovirus (serotype 5) along with a map of its genome are shown in figures 2-1 and 2-2 below. It is icosahedral in shape and roughly 75nm in diameter with a dense core containing the viral genome.

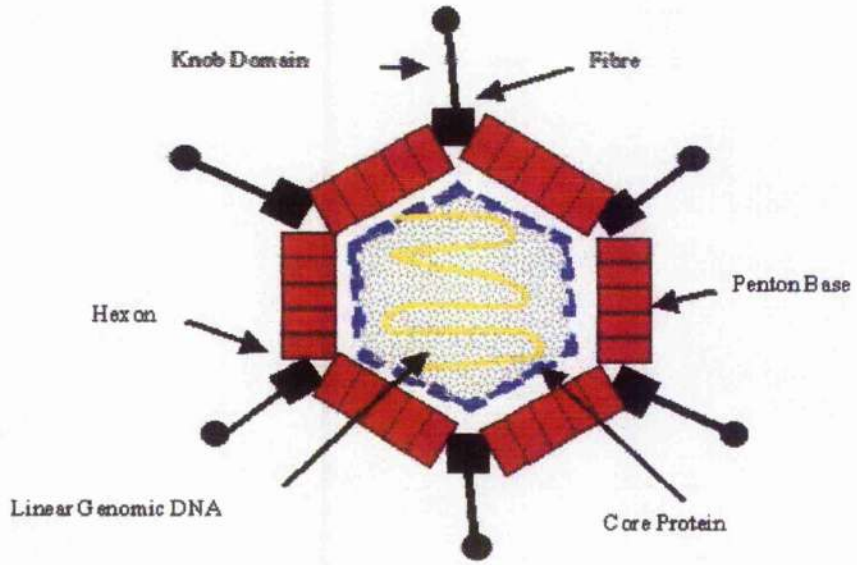


**Figure 2 - 1. Schematic of the structure of the wild-type adenovirus (serotype 5).**

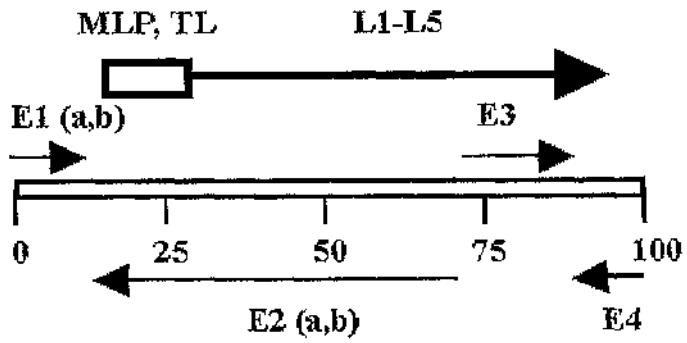


**Figure 2 - 2. Structure of the wild-type adenoviral genome.**

The wild-type adenoviral genome, shown in figure 2-2 above is 36kb in size and can be divided into 100 map units of 360bp each. There are nine major transcription units divided into early (E1-E4) and late (L1-L5). It can accommodate up to 2kb of foreign DNA, however, portions of the E1 or E3 regions of the viral genome, or both, can be deleted to make for an extra 5kb of foreign DNA.

The construction and propagation of the adenoviral vectors required for this study was carried out by Dr. Tim Siedler & Dr. Jurgen Prestle (University of Goettingham) and Dr. Debbie Reynolds (University of Glasgow). The molecular techniques employed to construct these vectors are beyond the remit of this thesis, which is concerned with the functional consequences of their subsequent transfection into cardiomyocytes.

Briefly, constructs containing the cDNA's coding for the following genes of interest (Sorcin, CSQ, FK506-binding-protein or FKBP 12.6, FKBP 12.6 mutant lacking the calicneurin binding site, NCX & β-galactosidase) and the shuttle vector pACCMV.pLpA were combined via restriction digestion with *Eco*RI and *Hind*III. Subsequently the pACCMV.pLpA – cDNA of interest constructs and pJM17 plasmids were used to transfect HEK 293 cells. This co-transfection allowed homologous recombination of the construct with the plasmid to generate a functional adenovirus with the cDNA of interest incorporated.

2.1.3 - Transfection of isolated rabbit cardiomyocytes with adenoviral vectors.

Freshly dissociated rabbit cardiomyocytes were counted using a haemocytometer, subjected to gentle centrifugation and the pellet then re-suspended in M199 medium (supplemented with 312.5mg Taurine, 500mg D, L Carnitine, 327.5mg creatine, 5ml penicillen/streptomycin per 500ml) to a concentration of 1X $10^5$ cells/ml. The various adenoviral overexpression vectors described above were then added to the culture medium containing the cardiomyocytes at an MOI of 100. The cells were then placed in an incubator at 37°C for 24hrs to allow time for transfection and subsequent overexpression of the protein of interest to occur.

2.1.4 - Measurements of protein expression levels using western blots.

Sorcin Study – Measurements by Dr. Susan Currie (University of Glasgow). Sorcin was detected using polyclonal Mouse anti-Sorcin antibodies (1:2000, Zymed laboratories Inc., San Francisco, USA). NCX was detected using MA3-926 antibody (Affinity Bioreagents) in 1:5000 and goat-anti mouse IgM (31440, Pierce) as secondary antibody in 1:10000. Both Sorcin and NCX were normalised to CSQ, detected using and rabbit anti-calsequestrin (1:2000, PA1-913, Affinity Bioreagents).

CSQ Study – Measurements by Dr. Susan Currie (University of Glasgow). CSQ in cell lysates from Ad-LacZ and Ad-CSQ transfected cells was detected with mouse monoclonal anti-calsequestrin at 1:200 dilution (gift from Prof. J.M. East, University of Southampton). CSQ protein was normalised to a standard Ad-Lac Z transfected lysate preparation and quantified using Quantity one software (BioRad).

FKBP Study – Measurements by Dr. Jurgen Prestle (Georg-August-University). Western immunoblot analysis was performed with a polyclonal anti FKBP 12 (C-19) antibody (Santa Cruz Biotechnology) and an enhanced chemoluminescence detection system (Amersham) according to the manufacturer's instructions.

## 2.2 – General Methods.

### 2.2.1 - Solutions used in voltage clamp protocols.

The normal Tyrode's (NT) solution contained (mM): NaCl (140), KCl (4), HEPES (5), $MgCl_2$ (1), $CaCl_2$ (1.8), glucose (11.1), pH 7.4 with NaOH. This solution was modified as appropriate for each experimental protocol.

For E-C coupling and NCX activity studies, the superfusate contained added 4-aminopyridine (5mM, to block $K^+$ currents) and Niflumic acid (0.1mM, to block $Ca^{2+}$-activated $Cl^-$ currents). The pipette solution contained (mM): KCl (20), K aspartate (100), tetraethylammonium chloride (TEACl, 20), HEPES (10), $MgCl_2$ (4.5, calculated free $Mg^{2+} \approx 0.9$mM), disodium ATP (4), disodium creatine phosphate (1), EGTA (0.01), pH 7.25 with KOH.

For NCX current density studies the superfusate was also $K^+$-free, KCl was replaced by CsCl, with added strophanthidin (0.01 mM) and nifedipine (0.01 mM). The pipette solution contained (mM): CsCl (45), EGTA/$Ca^{2+}$EGTA ($Cs^+$ 100, EGTA 50, $Ca^{2+}$ 25), HEPES (20), $MgCl_2$ (11, calculated free $Mg^{2+}$ ≈1.2mM), $Na_2ATP$ (10); pH 7.25. This pipette solution was designed to heavily buffer $[Ca^{2+}]i$ to ~250nM.

For NCX allosteric regulation studies the superfusate was again $K^+$-free, KCl was replaced by CsCl, with added strophanthidin (0.01mM), nifedipine

(0.01mM), niflumic acid (0.1mM) and with or without nickel (10mM). The pipette solution was identical to that used for NCX activity studies.

2.2.2 - Voltage clamp and intracellular [$Ca^{2+}$] measurements in rabbit cardiomyocytes.

After 24hrs incubation with the virus, isolated cardiomyocytes were superfused with a HEPES-based Krebs-Henseleit solution at 20-21°C in a chamber mounted on the stage of an inverted microscope. Voltage clamp was achieved using whole cell ruptured patch technique using an Axoclamp 2A amplifier (Axon Instruments, Foster City, CA, USA) in discontinuous (switch clamp) mode. Pipette resistance was 7-10 MΩ. Membrane potential was voltage clamped at –80mV and then stepped to –70mV for 100ms before returning to –80mV and the membrane capacitance was calculated by integration of the current spikes at either end of this voltage step. Cytosolic loading of Fura-2 was achieved by incubating cardiomyocytes with 5 μM Fura-2-AM at room temperature for 12 min.

2.2.3 - Calibration of the Fura-2 fluorescence signal.

The minimum fluorescence ratio (Rmin) was estimated from the Fura-2 fluorescence ratio measured in quiescent cardiomyocytes prior to stimulation. Separate measurements of Fura-2 ratio before and after intracellular dialysis with a pipette solution containing 10mM EGTA (<1nM

$Ca^{2+}$) established that cardiomyocytes quiescent for >24hrs in culture achieved a low intracellular [$Ca^{2+}$] that was reflected in a Fura-2 fluorescence ration that was indistinguishable from that measured after dialysis in 10mM EGTA. The maximum fluorescence ratio (Rmax) was determined by measuring the Fura-2 fluorescence ratio immediately after impaling the cardiomyocyte at the end of each experiment. The values of Rmin and Rmax were not significantly different in any of the experimental groups. The intracellular [$Ca^{2+}$] ([$Ca^{2+}$]i) was calculated as previously described by Eisner *et al.*, 1989, assuming a dissociation constant (Kd x β) of 1.2μM, a value determined by dialyzing cardiomyocytes with a range of buffered [$Ca^{2+}$].

2.2.4 - Electrophysiology protocols.

E-C coupling protocol: Isolated rabbit cardiomyocytes were held at -80 mV and the voltage stepped to -40 mV for 50 ms in the presence of 5μM TTX to inactivate the inward Na+ current, before stepping to 0 mV for 150 ms. This protocol was repeated at 0.5Hz for 80s to achieve steady-state $Ca^{2+}$ transients. SR $Ca^{2+}$ content and NCX activity were then estimated by rapidly switching to a solution containing 10mM caffeine (to cause SR $Ca^{2+}$ release) and 10mM BDM (to prevent myocardial contraction). In the continued presence of caffeine the SR is unable to re-accumulate $Ca^{2+}$ and elimination of $Ca^{2+}$ is mainly due to NCX. The contribution of non-NCX $Ca^{2+}$ removal mechanisms was estimated from the $Ca^{2+}$ decay obtained by

rapidly switching to 10mM caffeine / 10mM BDM in the presence of 10mM $NiCl_2$ (Diaz *et al.*, 1997).

Determination of $Ca^{2+}$ buffering capacity in cardiomyocytes: This was calculated using a method previously published by Trafford *et al.*, 1999. Under conditions of whole cell voltage clamp, the rapid application of 10mM caffeine causes the SR to release its store of $Ca^{2+}$ and there is a transient increase in the free $[Ca^{2+}]_i$. In the continued presence of caffeine, the subsequent reduction in free $[Ca^{2+}]_i$ occurs because of removal of $Ca^{2+}$ from the cytoplasm at the sarcolemma by the action of both NCX and the sarcolemmal $Ca^{2+}$-ATPase (see figure 3-5). The activity of NCX generates a transient inward current that can be integrated to obtain the time-course of the change of total $Ca^{2+}$ within the cell. With correction for non-NCX removal mechanisms, this integral can then be plotted against the simultaneous changes in free $[Ca^{2+}]_i$ to construct a buffer curve of the type seen in figure 3-7A. Over a limited range of $[Ca^{2+}]_i$ the buffer curve is linear and it is the gradient of this portion of the curve, corrected for cell capacitance, that represents the buffer capacity of the cell.

L-type $Ca^{2+}$ current: (i) I-V relationship (ii) inactivation kinetics: (i) Cardiomyocytes were held at –80mV and the voltage stepped to –40mV for 200ms in the presence of 5μM TTX. This was then repeated at a frequency of 1Hz, each time with a step to –40mV (50ms) and then a cumulative additional depolarisation of 10mV (150ms) until a holding voltage of +80mV was achieved. (ii) Cardiomyocytes were held at –80mV and the voltage stepped to –40mV (50ms) in the presence of 5μM TTX, before stepping to

0mV for 150ms. This was then repeated at a frequency of 1Hz, the initial voltage step increasing by 10mV each time until a value of +20mV was achieved. Both protocols were then carried out in the presence of 1mM $Cd^{2+}$ to obtain the background current that was then subtracted in order to obtain the current attributable to $I_{Ca}$.

NCX current density: After achieving the whole-cell configuration, a period of 4-5 minutes was allowed for dialysis of the pipette solution into the cell. Currents were then measured in response to a 3s ramp from -120 mV to +80 mV from a holding potential of -80 mV. An ascending ramp was chosen since this has been shown to cause less perturbation of subsarcolemmal $[Ca^{2+}]$ than a descending ramp, and the resulting currents are closer to those obtained using a voltage step protocol (Convery & Hancox, 1999). The ramp protocol was performed at 0.1 Hz until steady-state currents were achieved, whereupon data from five ramps was averaged. The protocol was repeated in the presence of 5mM $NiCl_2$ to obtain the background current, and this was subtracted to obtain the current attributable to NCX (nickel sensitive current).

NCX allosteric regulation. Myocytes were pre-treated with 1μM thapsigargin and 10mM caffeine in order to empty the SR of any stored $Ca^{2+}$ and to prevent any further $Ca^{2+}$ uptake. Voltage steps to +100mV of either 100 or 200 msec duration were applied from a resting potential of -100mV at frequencies of either 5Hz or 3.3Hz in order to obtain an adequate rise in intracellular $Ca^{2+}$. For each step the mean current and the mean $[Ca^{2+}]_i$ were obtained.

2.2.5 - $Ca^{2+}$ spark measurements in permeabilised cardiomyocytes.

These measurements were performed by Dr. Chris Loughrey, University of Glasgow.

Isolated cardiomyocytes were placed on coverslip at the bottom of a small bath and perfused with a mock intracellular solution with the following composition (mM): 100 KCl, 5 $Na_2ATP$, 10 $Na_2$Creatine Phosphate, 5.5 $MgCl_2$, 25 HEPES, 0.05 $K_2EGTA$, 0.01 Fluo-3 free acid (Molecular Probes), pH 7.0 (20-21°C). The $[Ca^{2+}]$ in the solution was typically 150nM. Perfusion was terminated and β-escin 0.1mg/ml (Sigma) added to the cell suspension. When cardiomyocytes were permeabilised (ascertained by confocal imaging, 0.5-1min) the β-escin was removed by re-perfusion of the bath.

$Ca^{2+}$ sparks were recorded for 1 minute using laser scanning confocal microscopy, after which time 10mM caffeine was rapidly applied in order to assess SR $Ca^{2+}$ content. Line-scan images were recorded using a BioRad Radiance 2000 confocal system. Iris diameter was set at 1.9mm providing an axial (z) resolution of about 0.9μm and X-Y resolution of about 0.5μm based on full width half maximal amplitude measurements of images of 0.1μm fluorescent beads (Molecular probes). Data was acquired in line-scan mode at 2msec/line; pixel dimension was 0.3μm (512 pixels/scan; zoom=1.4). The scanning laser line was oriented parallel with the long axis of the cell and placed approximately equidistant between the outer edge of

the cell and the nucleus/nuclei, to ensure the nuclear area was not included in the scan line (see figure 2-3).

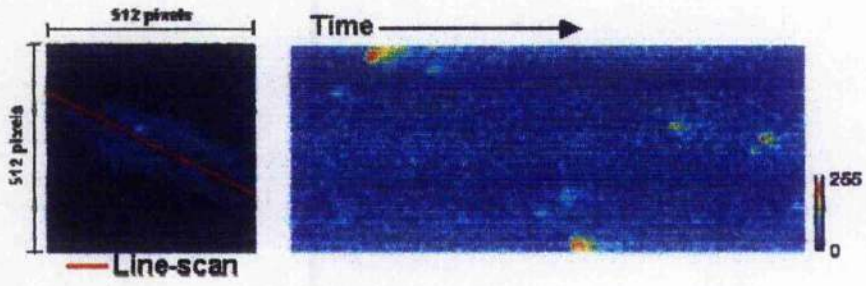


**Figure 2- 1. Line-scan confocal imaging.**

**Left panel shows a 512x512 pixel image of a permeabilised cardiomyocyte and the positioning of the line-scan. By repeatedly scanning this line an image is formed as in the right panel where by distance across the cell is expressed on the vertical axis and time on the horizontal. The extracellular signal has been cropped from the image.**

The LaserScan (BioRad) software saved the data as a series of image files each containing 30,000 line scans (i.e. 1 min of continuous recording). An experimental record typically comprised 2-3 line-scan image files; these were reviewed off-line.

The [Ca2+] in the solution used to generate Ca2+ sparks was measured by ensuring the line-scan covered a significant region of extracellular space as well as the entire cell length. Under these conditions the fluorescence signal recorded from the line-scan contains signals from both intracellular and extracellular compartments. To enable traces to be converted to [Ca2+] a series of calibration solutions were used at the end of each period of spark measurement. The cardiomyocyte was superfused sequentially with

the following solutions: (i) a solution containing nominally ~400nM; (ii) a solution containing < 1nM $Ca^{2+}$ to give an $F_{min}$ (iii) a solution containing 33$\mu$M $Ca^{2+}$ to give an $F_{max}$ (all calibration solutions contained 10mM total [EGTA]). See figure 2-4. Using these values for $F_{min}$ and $F_{max}$ the $[Ca^{2+}]$ at a given fluorescence can then be calculated using the following equation.

$$[Ca^{2+}] = K_D(F - F_{min}) / (F_{max} - (F - F_{min}))$$

Since in the steady state, extracellular $[Ca^{2+}]$ will equal intracellular $[Ca^{2+}]$ in the permeabilised cell, the $[Ca^{2+}]$ in the experimental solution can be calculated (using an apparent affinity constant of Fluo-3 for $Ca^{2+}$ of 558nM). In all experiments included in the analysis, the $[Ca^{2+}]$ in the test solution was 145-165nM. $Ca^{2+}$ sparks were quantified using an automatic detection and measurement algorithm adapted from a previously published method (Cheng *et al.*, 1999). All $Ca^{2+}$ spark measurements were made within 5mins of cell permeabilisation, this time was standardized to minimize loss of soluble proteins.

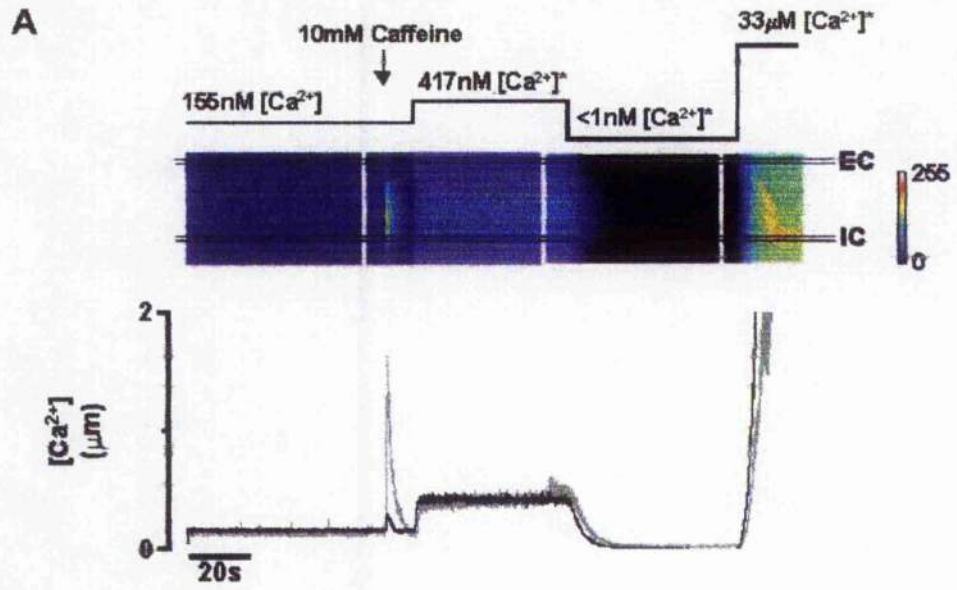


**Figure 2- 1. Calibration of $[Ca^{2+}]$ using confocal microscopy.**

***Sequential fluorescence confocal line-scan images (512x30000 pixels) from a*** **permeabilised cardiomyocyte exposed to experimental and calibration solutions. The calculated $[Ca^{2+}]$ in the perfusion solution is shown above the images, experimental solutions contained a total [EGTA] of 50μM and 10μM Fluo-3. $[Ca^{2+}]$ marked by * indicates solutions containing a total [EGTA] of 10mM. Addition of 10mM caffeine is indicated by the arrow. $[Ca^{2+}]$ was calculated from the mean fluorescence signal of a 20-pixel region from the intracellular and extracellular compartments. The $[Ca^{2+}]$ was calculated on the basis of the fluorescence signals in 417nM, <1nM $Ca^{2+}$ and 30μM (buffered with 10mM total EGTA).**

2.2.6 – Statistics.

Data is expressed as means±SEM. For ion currents and $Ca^{2+}$ transients, comparisons were performed by using the unpaired Student's t-test, unless otherwise stated, and differences were considered significant when $P<0.05$.

## 2.3 - Preparatory Studies.

### 2.3.1 - Isolation of the L-type $Ca^{2+}$ current.

E-C coupling in cardiomyocytes occurs via the process of CICR. During depolarisation, $Ca^{2+}$ enters the cell via L-type $Ca^{2+}$ channels and subsequently triggers further $Ca^{2+}$ release from the SR. The amplitude and integral of $I_{Ca}$ are therefore of paramount importance in studies of E-C coupling.

A glance through the literature reveals that there are differences in the methods used for measuring peak $I_{Ca}$ using voltage clamp. Perhaps the most common method is to clamp the cell at a membrane potential of –40mV and then step to 0mV for a given time period, before returning to the holding potential of –40mV (e.g. Naqvi *et al.*, 2001). While allowing measurement of $I_{Ca}$, the cell is voltage clamped at an unphysiological membrane potential of –40mV for extended periods of time (resting membrane potential is normally –80mV). Other investigators have held the membrane potential at –70mV, ramped to –50mV to inactivate $I_{Na}$, and then further depolarised to isolate $I_{Ca}$ (Bassani *et al.*, 1995). We tried using a similar ramp protocol to investigate E-C coupling. Freshly dissociated cardiomyocytes were voltage clamped at a membrane potential of –80mV and the voltage ramped to –40mV over a period of 50ms. Myocytes were held at –40mV for a further 50ms and then stepped to 0mV for 150ms, before returning to –80mV. However, as figure 2-5 below demonstrates

there was still obvious loss of voltage control due to $I_{Na}$, an overshoot of ~20mV, which we feared may affect the subsequent activation of $I_{Ca}$.

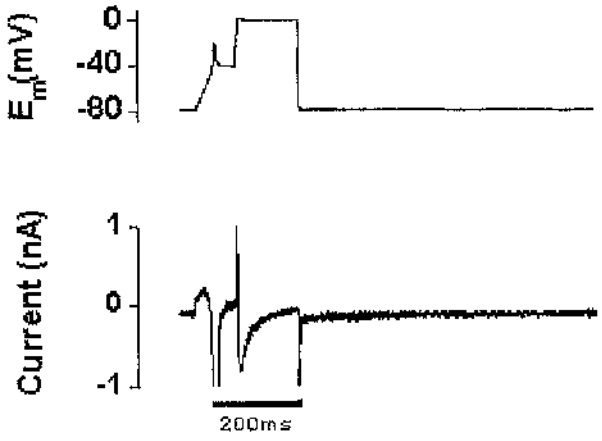


**Figure 2- 5. Depolarising voltage clamp protocol, incorporating a ramp from -80mV to –40mV and the resultant current trace.**

**Data from freshly dissociated rabbit cardiomyocyte at room temperature.**

It was therefore decided to compare the ramp protocol in figure 2-5 above, with a prepulse protocol in which the cardiomyocyte was voltage clamped at a membrane potential of -80 mV, stepped to -40 mV for 50 ms and then to 0mV for a further 150ms before returning to –80mV. Each protocol was carried out both in the absence, and then in the presence of 5µM TTX to block $I_{Na}$ and thus improve voltage control. Figure 2-6 below shows typical voltage and current traces for both protocols in the presence of TTX.

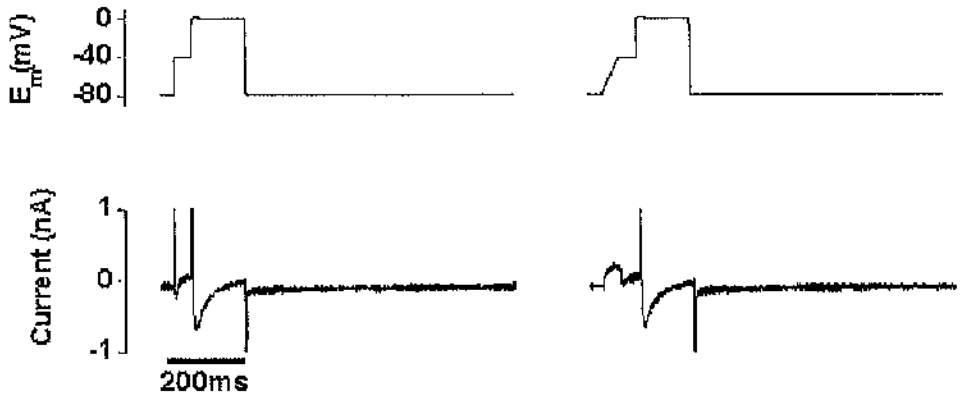


**Figure 2- 6. Depolarising voltage clamp protocols, incorporating either step (prepulse) or a ramp from -80mV to –40mV and the resultant current traces.**

**Data from freshly dissociated rabbit cardiomyocytes at room temperature.**

As is evident from figure 2-6, the inclusion of 5μM TTX completely blocked $I_{Na}$ and thus improved voltage control in both protocols. Interestingly, the inclusion of TTX in the perfusate also significantly affected the amplitude of $I_{Ca}$ recorded using both the prepulse and the ramp protocols as shown in figure 2-7 below. Mean $I_{Ca}$ amplitudes recorded using both the prepulse protocol ($9.99X10^{-3} \pm 1.15X10^{-3}$ nA/pF v $7.24X10^{-3} \pm 9.31X10^{-4}$ nA/pF, n=6, $p < 0.001$) and the ramp protocol ($1.04X10^{-2} \pm 1.35X10^{-3}$ nA/pF v $7.7X10^{-3} \pm 9.08X10^{-4}$ nA/pF, n=6, $p < 0.01$) were significantly reduced upon addition of 5μM TTX to the perfusate. There was no significant difference in the size of $I_{Ca}$ when the prepulse protocol was compared with the ramp protocol, both in the absence of, and in the presence of TTX. (2-tailed, paired Student's t-test was used for comparisons).

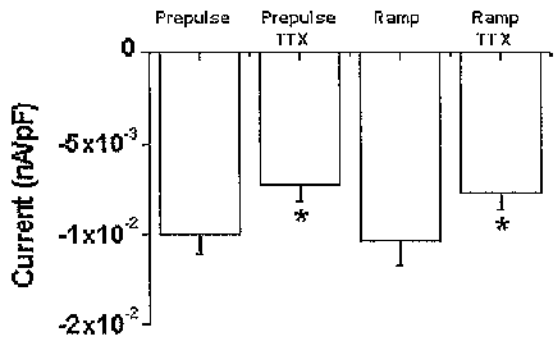


**Figure 2- 7. Comparison of mean L-type $Ca^{2+}$ current amplitudes using prepulse and ramp voltage clamp protocols, both in the absence and presence of TTX.**

**Data from freshly dissociated rabbit cardiomyocytes at room temperature.**

It was thus decided to use the prepulse protocol in combination with TTX as our standard method for the investigation of E-C coupling. The possibility that TTX was partially inhibiting the L-type $Ca^{2+}$ current was eliminated by studying current traces obtained using the prepulse protocol in a zero sodium solution. As shown in figure 2-8 below, there was no significant difference in the L-type $Ca^{2+}$ current recorded when the prepulse protocol in the presence of TTX was compared to the prepulse protocol in zero sodium ($-4.65X10^{-3} \pm 5.22x10^{-4}$ nA/pF, n=20 v $-4.39X10^{-3} \pm 7.38X10^{-4}$ nA/pF, n=7, $p > 0.05$). In addition figure 2-8 illustrates that the prepulse protocol in combination with TTX produces a significantly larger L-type $Ca^{2+}$ current when compared to voltage clamping at –40mV and stepping to 0mV ($-4.65X10^{-3} \pm 5.22x10^{-4}$ nA/pF, n=20 v $-3.09X10^{-3} \pm 2.54X10^{-4}$ nA/pF, n=26, $p < 0.01$).

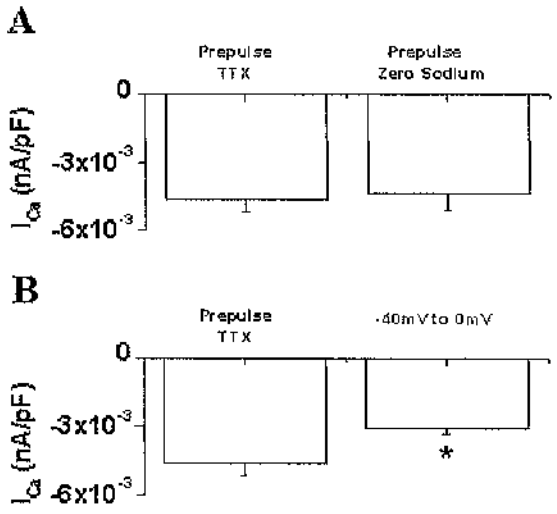


**Figure 2- 8. $I_{Ca}$ amplitude under various conditions.**

**(A) Comparison of mean L-type $Ca^{2+}$ current amplitudes using the prepulse voltage clamp protocol with either TTX or under conditions of zero sodium. (B) Comparison of mean L-type $Ca^{2+}$ current amplitudes using both the prepulse voltage clamp protocol with TTX and a depolarising step from –40mV to 0mV.**

The average values for peak $I_{Ca}$, obtained using the prepulse protocol (4.6pA/pF), are in good agreement with those already reported in the literature despite species differences. Clamping membrane potential at –40mV and then stepping to 0mV, Naqvi *et al.*, 2001, reported an average $I_{Ca}$ current density of 2.6pA/pF in isolated rabbit cardiomyocytes at room temperature. Alternatively, holding the membrane potential at –70mV, ramping to –50mV to inactivate $I_{Na}$, and then further depolarising to 0mV, Bassani *et al.*, 1995, have reported an average $I_{Ca}$ current density ~ 5.5pA/pF in isolated ferret cardiomyocytes at 22°C.

2.3.2 - Manipulation of L-type $Ca^{2+}$ current in Freshly Dissociated and 1 Day Culture Cardiomyocytes.

Freshly dissociated and 1 day culture cardiomyocytes were held at -80 mV and the voltage stepped to -40 mV for 50 ms in the presence of 5μM TTX to inactivate the inward $Na^+$ current, before stepping to 0 mV for 150 ms. Holding potential was then returned to –80mV (see figure 2-9). This protocol enabled excellent resolution of $I_{Ca}$ and was repeated at 0.5Hz for 80s to achieve steady-state $Ca^{2+}$ transients. In addition either 0.05, 0.1, 0.15, 0.2, 0.5, 1 or 3μM nifedipine was added to the superfusate to achieve a reduction in $I_{Ca}$ amplitude.

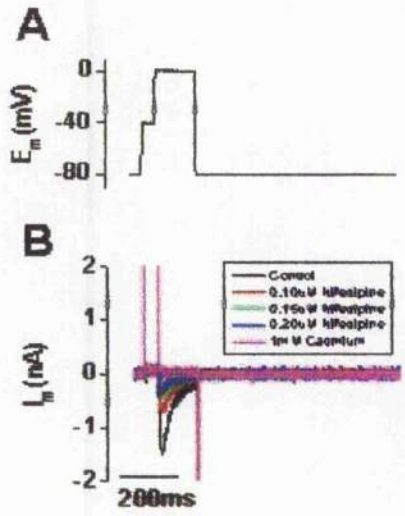


**Figure 2- 1. Effect of nifedipine on $I_{Ca}$. (A) Voltage and (B) Current traces in a freshly dissociated rabbit cardiomyocyte at room temperature.**

The dose response curve for the effect of nifedipine on $I_{Ca}$ depending on the cell type studied can be see below in figure 2-10. The $I_{Ca}$ at each [nifedipine] was corrected for cell capacitance and expressed as a

percentage of the $I_{Ca}$ observed in the absence of nifedipine. Sigmoidal curves were fitted to the data using a Bolztmann distribution. It is apparent from figure 2-10 that freshly dissociated cardiomyocytes exhibit a significantly increased sensitivity to nifedipine when compared to 1-day culture cardiomyocytes. At a concentration of 0.2μM nifedipine, $I_{Ca}$ was on average 25% of control in freshly dissociated cells (n=8), compared to 57% of control in 1-day culture cells (n=7), $p < 0.001$.

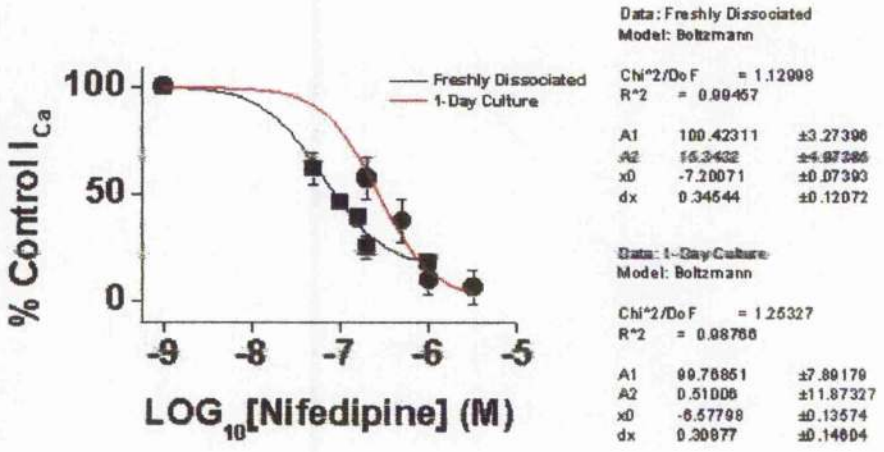


**Figure 2- 1. The effect of nifedipine on $I_{Ca}$ amplitude in freshly dissociated and 1-day cultured rabbit cardiomyocytes at room temperature.**

This phenomenon has also been observed when comparing nifedipine sensitivity in freshly dissociated and cultured rat ventricular cardiomyocytes (Pignier *et al.*, 2002). Additionally, the data presented in figure 2-8 above may suggest that a proportion of the L-type $Ca^{2+}$ current in freshly dissociated cardiomyocytes is resistant to nifedipine. Minimum $I_{Ca}$ in the freshly dissociated cardiomyocytes in the presence of nifedipine was ~15% of maximum according to the Boltzmann fit. In the 1-day culture cardiomyocytes it was possible to reduce the current to 0.5% of maximum

(i.e. almost complete inhibition). However, the errors on these predicted minimum values are large and further investigation of the effects of high concentrations of nifedipine (i.e. 1μM & 3μM) on L-type $Ca^{2+}$ current in both cell types would be required to confirm this possibility.

In conclusion, it was noted that a concentration of ~ 0.1μM nifedipine would be sufficient to reduce the L-type $Ca^{2+}$ current by 50% in freshly dissociated cardiomyocytes, whereas 0.5μM nifedipine would be required to be assured of a similar reduction in the 1-day culture cardiomyocytes.

2.3.3 - Investigating the "gain" of E-C coupling.

The "gain" of E-C coupling can be described as the amplification factor of CICR and this may become altered following adenoviral overexpression of specific proteins in the cardiomyocyte. It can be calculated, in its most literal sense, by taking the total amount of calcium released from the SR and dividing it by the integrated triggering $I_{Ca}$. Furthermore, one can also correct for the contribution of $I_{Ca}$ to the calcium transient (Bers, 2001).

Therefore, Gain = $(\Delta[Ca]_{tot} - \int I_{Ca}dt / \int I_{Ca}dt)$.

An alternative way of studying gain is to plot the average relationship between SR $Ca^{2+}$ content and the steady state $Ca^{2+}$ transient amplitude for a particular cell type. SR content may be increased or decreased using

experimental interventions. Provided these interventions do not affect $I_{Ca}$ current density, a simplified gain curve may be constructed.

If the normal relationship between SR $Ca^{2+}$ load and calcium transient amplitude for a given cell type is altered by the adenoviral overexpression of another protein, providing L-type $Ca^{2+}$ current density is unchanged, then a change in the "gain" of E-C coupling must have occurred.

Methods for increasing SR $Ca^{2+}$ content in 1-day cultured rabbit cardiomyocytes.

(i) Cardiomyocytes were held at -80 mV and the voltage stepped to -40 mV for 50 ms in the presence of 5μM TTX to inactivate the inward $Na^{+}$ current, before stepping to 0 mV for 150 ms. Holding voltage was then returned to –80mV. The protocol was repeated at 1Hz for 80s to achieve steady-state $Ca^{2+}$ transients. SR $Ca^{2+}$ load was then assessed by rapid application of 10mM caffeine. Stimulating the myocyte at 1Hz v. normal stimulation rate of 0.5Hz would be expected to reduce the time for diastolic extrusion of $Ca^{2+}$ from the myocyte and thus increase SR $Ca^{2+}$ load.

(ii) Cardiomyocytes were held at -60 mV and the voltage stepped to -40 mV for 50 ms in the presence of 5μM TTX to inactivate the inward Na+ current, before stepping to 0 mV for 150 ms. Holding voltage was then returned to –60mV. The protocol was repeated at 0.5Hz for 80s to achieve steady-state $Ca^{2+}$ transients and 10mM caffeine

was applied to assess SR $Ca^{2+}$ load. Holding the membrane potential at –60mV should reduce the extrusion of $Ca^{2+}$ from the myocyte via NCX and thus increase SR $Ca^{2+}$ load.

(iii) Cardiomyocytes were held at -80 mV and the voltage stepped to -40 mV for 50 ms in the presence of 5μM TTX to inactivate the inward $Na^{+}$ current, before stepping to 0 mV for 150 ms. Holding voltage was then returned to –80mV. 20mM citrate was added to the standard pipette solution (Terentyev *et al.*, 2002). The protocol was repeated at 0.5Hz for 80s to achieve steady state $Ca^{2+}$ transients and SR $Ca^{2+}$ content was assessed by rapid application of 10mM caffeine. Addition of citrate to the pipette solution should increase SR buffer capacity and thus increase SR $Ca^{2+}$ content.

Methods for decreasing SR $Ca^{2+}$ content in 1-day cultured rabbit cardiomyocytes.

(i) Cardiomyocytes were held at -80 mV and the voltage stepped to -40 mV for 50 ms in the presence of 5μM TTX to inactivate the inward $Na^{+}$ current, before stepping to 0 mV for 150 ms. Holding voltage was then returned to –80mV. The protocol was repeated until steady state $Ca^{2+}$ transients were observed. 5μM thapsigargin was washed on to the cardiomyocytes for either 40 or 100s to reduce SR $Ca^{2+}$ load via inhibition of the SERCA pump.

The effects of these manoeuvres on SR $Ca^{2+}$ content and $Ca^{2+}$ transient amplitude are shown in figures 2-11 & 2-12 below.

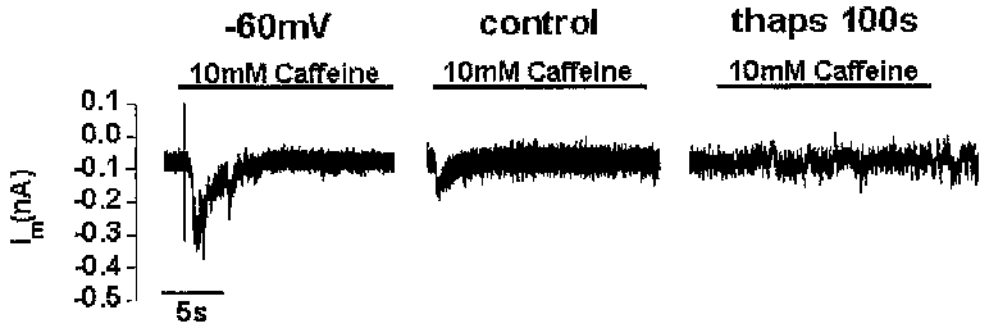


**Figure 2- 11. Transient inward current upon rapid application of 10mM caffeine in 1-day cultured, Ad-LacZ transfected cardiomyocytes.**

**Integral of the transient inward current gives a measure of SR $Ca^{2+}$ load when resting membrane potential is held at −60mV, under control conditions and after application of 5μM thapsigargin for 100s.**

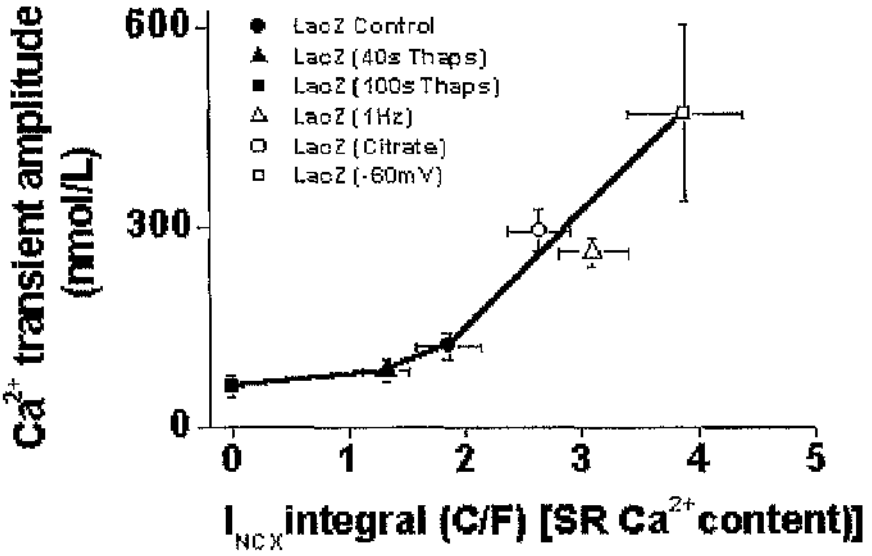


**Figure 2- 12. Relationship between SR $Ca^{2+}$ load and $Ca^{2+}$ transient amplitude in 1-day cultured, Ad-LacZ transfected cardiomyocytes.**

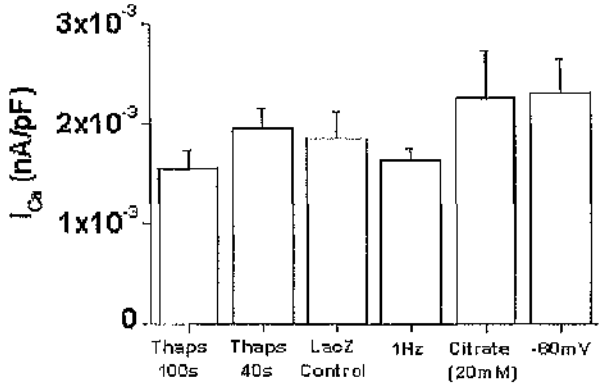


**Figure 2- 13. L-type $Ca^{2+}$ current density under different conditions of SR $Ca^{2+}$ load in 1-day cultured, Ad-LacZ transfected cardiomyocytes.**

As is evident from figure 2-13 above, none of the experimental manoeuvres used to construct what is in effect a "gain curve" for 1 day cultured Ad-LacZ transfected cardiomyocytes significantly altered L-type $Ca^{2+}$ current density when compared either with control or each other, $p > 0.05$. L-type $Ca^{2+}$ current densities were as follows: LacZ Control ($1.85X10^{-3} \pm 2.68X10^{-4}$nA/pF, n=17), Thapsigargin 40s ($1.94X10^{-3} \pm 2.07E^{-4}$nA/pF, n=17), Thapsigargin 100s ($1.54X10^{-3} \pm 1.91X10^{-4}$nA/pF, n=12), 1Hz stimulation rate ($1.63X10^{-3} \pm 1.04X10^{-4}$nA/pF, n=37), 20mM Citrate in patch pipette ($2.25X10^{-3} \pm 4.66X10^{-4}$ nA/pF, n=13), -60mV holding potential ($2.30X10^{-3} \pm 3.36X10^{-4}$nA/pF, n=9).

If adenoviral overexpression of a specific protein increases $I_{Ca}$, then it may be possible to reduce it to control levels with the use of nifedipine. This would then allow valid "gain" comparisons to be made.

2.3.4 - Background and introduction to the use of 2, 3 - butane – dione monoxime.

In studies of cardiac E-C coupling it is often necessary to quantify SR $Ca^{2+}$ content. The standard procedure for this measurement involves whole cell voltage clamp. Cardiomyocytes are electrically stimulated until the intracellular $Ca^{2+}$ transient has reached a steady state. The myocyte is then clamped at a membrane potential of –80mV and 10mM caffeine is rapidly applied. The SR releases its store of $Ca^{2+}$, which can be quantified, and the huge rise in intracellular $Ca^{2+}$ causes the myocyte to contract. Frequently, when using cultured cardiomyocytes that appear to be more fragile than freshly dissociated cardiomyocytes, this large release of SR $Ca^{2+}$ causes the cell to irreversibly hyper-contract, the clamp is lost and no information on SR load can be obtained from the cell.

2, 3 – butane - dione monoxime (BDM) is a potent inhibitor of the myofibrillar ATPase (Blanchard *et al.*, 1990) and thus prevents myocardial contraction despite an increase in intracellular $Ca^{2+}$ concentration. BDM therefore appeared to be an appropriate agent to include along with caffeine and thus increase the success rate when assessing SR $Ca^{2+}$ load in voltage clamped myocytes.

However, there is much evidence to suggest that the effects of BDM are not solely confined to its inhibition of the myofibrillar ATPase. Murine whole heart studies have shown that 15mM BDM reduced conduction velocity (Verrecchia & Herve, 1997) and doubled action potential duration (Baker *et*

*al.*, 2000), while a porcine whole heart study (Lee *et al.*, 2001) has demonstrated that 5-20mM BDM reduced the $APD_{90}$ in a dose dependent manner. In addition, in whole hearts, it has been shown to flatten the electrical restitution curve in pigs (Lee *et al.*, 2001), dogs (Riccio *et al.*, 1999) and rabbits (Banville & Gray, 2002).

In isolated guinea pig cardiac myocytes BDM reduces $I_{Ca}$ (Gwathmey *et al.*, 1991), promotes voltage dependent inactivation of the current (Ferreira *et al.*, 1997) and also significantly affects SR $Ca^{2+}$ release (Gwathmey *et al.*, 1991). In rat ventricular myocytes, Adams *et al.*, 1998, have demonstrated that 10mM BDM caused a transient increase in the size of the intracellular $Ca^{2+}$ transient and a reduction in the steady state SR $Ca^{2+}$ load. Working with saponin-treated rat cardiac trabeculae, Steele & Smith, 1993, have demonstrated that 5-30mM BDM decreased the amount of calcium released from the SR in response to caffeine. In addition 2.4mM BDM is reported to have caused a 50% reduction in NCX activity, again in guinea pig cardiomyocytes (Watanabe *et al.*, 2001).

In light of these reports it was decided to investigate the effects of 10mM BDM on various aspects of E-C coupling and the determination of SR $Ca^{2+}$ content in freshly dissociated cardiomyocytes.

Effect of 10mM BDM on E-C coupling: Freshly dissociated cardiomyocytes were held at -80 mV and the voltage stepped to -40 mV for 50 ms in the presence of 5μM TTX to inactivate the inward $Na^+$ current, before stepping to 0 mV for 150 ms. Holding potential was then returned to –80mV. This protocol enabled excellent resolution of the L-type $Ca^{2+}$ current and was repeated at 0.5Hz for 120s. After 1 minute 10mM BDM was added to the perfusate for a 30s period. The typical effect of this manoeuvre on the intracellular $Ca^{2+}$ transient amplitude can be seen in figure 2-14 below.

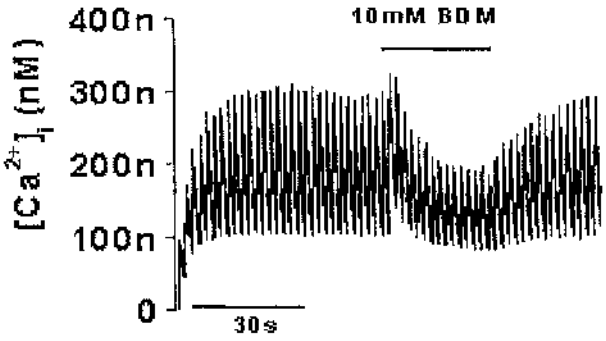


**Figure 2- 14. Effect of 10mM BDM on the steady state intracellular $Ca^{2+}$ transient in a freshly dissociated rabbit cardiomyocyte.**

10mM BDM significantly reduced both average diastolic $[Ca^{2+}]_i$ (133nM v 152nM, n=6, $p<0.05$) and average systolic $[Ca^{2+}]_i$ (245nM v 387nM, n=6, $p<0.05$) when compared to control. Thus, there was also a significant reduction in $Ca^{2+}$ transient amplitude (113nM v 231nM, n=6, $p<0.01$) upon addition of 10mM BDM. In addition $I_{Ca}$ amplitude was significantly reduced in the presence of 10mM BDM ($-2.74X10^{-3}$ v $-4.66X10^{-3}$ nA/pF, n=6, $p<0.01$) when compared to control. Interestingly after washout of 10mM BDM average diastolic $[Ca^{2+}]_i$ was significantly increased (172nM v 152nM,

n=6, p<0.05) when compared to control with no prolonged effects observed on either systolic $[Ca^{2+}]_i$ or $Ca^{2+}$ transient amplitude. In addition $I_{Ca}$ amplitude was significantly increased ($-5.48X10^{-3}$ v $-4.66X10^{-3}$ nA/pF, n=6, p<0.05) after washout of BDM when compared to control. (2-tailed paired students t-test was used for comparisons). These results are shown in figure 2-15 below.

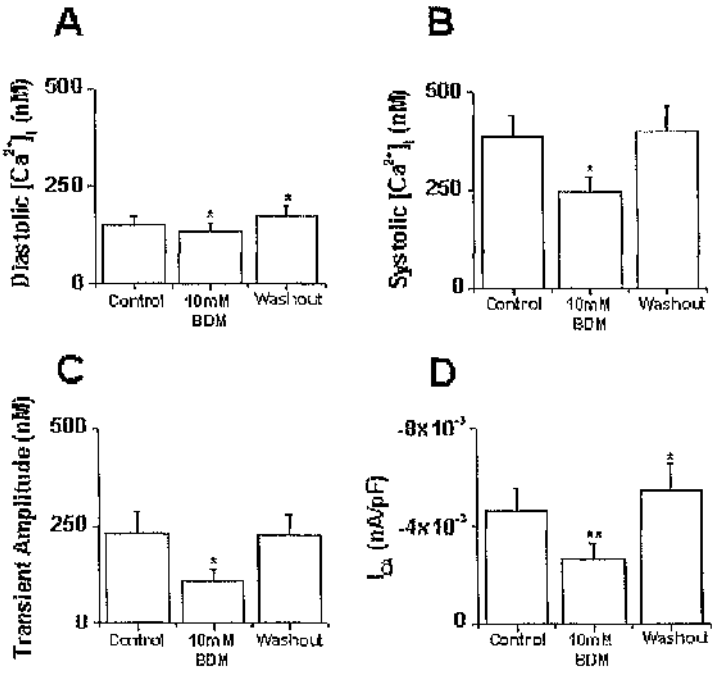


**Figure 2- 15. BDM and EC-coupling.**

**The effects of 10mM BDM on average (A) diastolic $[Ca^{2+}]$, (B) systolic $[Ca^{2+}]$, (C) transient amplitude and (D) $I_{Ca}$ current density in freshly dissociated rabbit cardiomyocytes.**

Effect of 10mM BDM on estimation of SR $Ca^{2+}$ content, NCX activity and sarcolemmal $Ca^{2+}$-ATPase activity: Freshly dissociated cardiomyocytes were held at -80 mV and the voltage stepped to -40 mV for 50 ms in the presence of 5μM TTX to inactivate the inward $Na^{+}$ current, before stepping to 0 mV for 150 ms. Holding potential was then returned to –80mV. This protocol was repeated at 0.5Hz for 80s to achieve steady-state $Ca^{2+}$ transients. SR $Ca^{2+}$ content and NCX activity were then estimated by rapidly switching to a solution containing 10mmol/L caffeine. The above voltage clamp protocol was then repeated and instead 10mmol/L caffeine and 10mmol/L BDM was rapidly applied to cause SR $Ca^{2+}$ release. In the continued presence of caffeine the SR is unable to re-accumulate $Ca^{2+}$ and elimination of $Ca^{2+}$ is mainly due to NCX. This removal of $Ca^{2+}$ from the cell by NCX manifests itself as a transient inward current ($I_{NCX}$). The rate of decay of both the caffeine induced $Ca^{2+}$ transient and $I_{NCX}$ provide a measure of NCX activity whilst the integral of $I_{NCX}$ provides a measure of SR calcium content. If caffeine is applied in the presence of 10mmol/L $Ni^{2+}$ the SR releases its store of $Ca^{2+}$ but is unable to re-accumulate $Ca^{2+}$. Elimination of $Ca^{2+}$ from the cell by NCX is blocked by the presence of $Ni^{2+}$ and under these circumstances elimination of $Ca^{2+}$ is mainly due to sarcolemmal $Ca^{2+}$ ATPase activity. Application of caffeine in the presence of $Ni^{2+}$ was compared to application of caffeine in the presence of $Ni^{2+}$ and 10mM BDM.

The average rates of decay of the caffeine induced current $Ca^{2+}$ transient ($0.68s^{-1}$ v $0.75s^{-1}$(in BDM), n=11, $p>0.05$) and $I_{NCX}$ ($0.92s^{-1}$ v $1.14s^{-1}$(in BDM), n=8, $p>0.05$) were not significantly altered by the presence of 10mM

BDM in the perfusate. In addition, the average SR $Ca^{2+}$ load (1.94C/F v 1.92C/F, n=7, p>0.05) was unaltered by BDM. These results can be seen in figure 2-16 below.

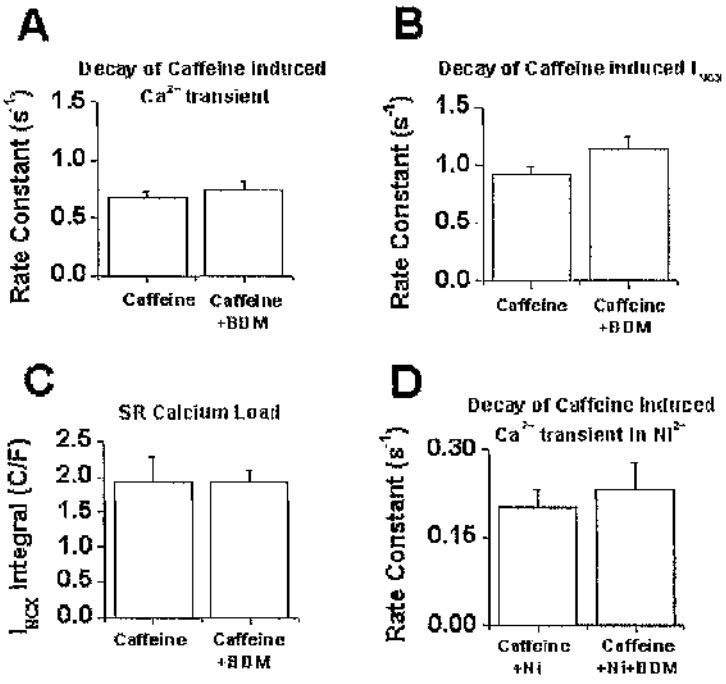


**Figure 2- 16. BDM and the assessment of SR $Ca^{2+}$ content.**

**Effect on 10mM BDM on (A) the rate of decay of the caffeine induced $Ca^{2+}$ transient, (B) the rate of decay of the transient inward current, (C) SR $Ca^{2+}$ load and (D) the rate of decay of the caffeine induced $Ca^{2+}$ transient in $Ni^{2+}$ in freshly dissociated rabbit cardiomyocytes. 2-tailed paired students t-test was used for comparisons.**

The rate of decay of the caffeine induced current $Ca^{2+}$ transient in the presence of $Ni^{2+}$ ($0.20s^{-1}$ v $0.23s^{-1}$(in BDM), n=8, p>0.05), as seen in figure 2-16 above, was not significantly altered by the presence of 10mM BDM in the perfusate.

Given that 10mM BDM had prolonged effects on both $I_{Ca}$ and the intracellular $Ca^{2+}$ transient, its presence in the perfusate during voltage clamp protocols that investigate E-C coupling would not be tolerable. However 10mM BDM had no significant effects on the decay of the caffeine induced $Ca^{2+}$ transient, the decay or integral of the caffeine induced $I_{NCX}$ or the decay of the caffeine induced $Ca^{2+}$ transient in the presence of $Ni^{2+}$. Hence, if one were to routinely include 10mM BDM along with 10mM caffeine in order to assess steady state SR $Ca^{2+}$ load or sarcolemmal $Ca^{2+}$-ATPase activity, it would be necessary to thoroughly change/wash the perfusion bath before running any more voltage clamp protocols that investigate E-C coupling.

2.3.5 – Determination of the relationship between cell volume and cell capacitance for 1-day cultured rabbit cardiomyocytes.

Exact knowledge of cell volume allows direct correlation of ionic current measurements with simultaneous measurements of ion concentrations in individual cells (Satoh *et al.*, 1996). Given that the "specific capacitance" of cell membranes is fairly consistent when different muscle cell types and species are compared, ~1μF/cm$^2$ (Hille, 1992), membrane capacitance measurements are often used to estimate the surface membrane area of cells and indirectly as an index of cell volume. However, surface membrane area cannot always be related exactly to cell volume, especially in cells such as ventricular cardiomyocytes where there is an abundance of membrane invaginations in the form of a complex t-tubular system. The exact relationship between cell volume and membrane capacitance has already been established for freshly dissociated rabbit cardiomyocytes using a combination of whole cell voltage clamp and laser scanning confocal microscopy (Satoh *et al.*, 1996). LSCM can detect fluorescent signals from uniformly thin optical sections of dye loaded cells with high spatial and temporal resolution. Therefore a series of Z-sections through a myocyte can be combined and analysed to give an accurate measurement of cell volume.

However, in this study E-C coupling is studied in 1-day cultured cardiomyocytes. Cell culture techniques have been shown reduce t-tubule density in cultured cardiomyocytes by up to 57% after 6 days (Mitcheson *et al.*, 1996), a structural alteration that would alter the relationship between

cell volume and membrane capacitance. The exact relationship between cell volume and membrane capacitance for both freshly dissociated and 1-day cultured rabbit ventricular cardiomyocytes was determined using whole cell voltage clamp and LSCM.

Measurement of membrane capacitance: Isolated cardiomyocytes (either freshly dissociated or 1-day cultured) were loaded with a cytoplasmic fluorescent marker by incubation with 5μM calcein at room temperature for 30 minutes. Myocytes were then washed and then re-suspended in a HEPES-based Krebs-Henseleit solution at 20-21°C and placed in a chamber mounted on the stage of an inverted microscope. Voltage clamp was achieved using whole cell ruptured patch technique using an Axoclamp 2A amplifier (Axon Instruments, Foster City, CA, USA) in continuous mode. Pipette resistance was 3-5MΩ. Cell capacitance was estimated using the current spikes seen at either end of a voltage step. Membrane potential was voltage clamped at –80mV and then stepped to –70mV for 100ms before returning to –80mV. Membrane capacitance was assessed by integrating both capacitance spikes and then taking an average to represent the charge movement during a spike. Membrane capacitance was then calculated by dividing the average charge movement by the size of the voltage step.

Measurement of cell volume: Calcein fluorescence imaging to calculate cell volume was performed using a Bio-Rad Radiance 2000 confocal system. Calcein was excited at 488nm (Kr laser) and measured > 515nm with the use of the epifluorescence optics of an inverted microscope with a water-

immersion objective lens (magnification X60, numerical aperture 1.2). A stack of images through the myocyte was obtained by moving the objective in the axial direction (z-plane) using a computer controlled stepping motor. Depending on myocyte thickness, approx. 40 sections at 0.5μM steps were required to image the entire myocyte. At each optical plane the cell was scanned 4 times and an average fluorescent image (using Kalman averaging) of 512 by 512 pixels was obtained. With a X60 objective and a zoom factor of 1.4 for the LSCM, pixel size was ~ $0.1\mu M^2$. Photobleaching of calcein was kept to a minimum by choosing the lowest possible laser power.

Image analysis: To determine cell volume accurately from the optical sections of cellular fluorescence it is necessary to eliminate any out-of-focus or background fluorescence, image noise and non-cellular volume elements from the images obtained using the LSCM. This was achieved using photometric thresholding, the level of which was determined as follows. A 2D image through each myocyte was compiled using IDL™ software, from which the maximal boundaries of the myocyte could be easily denoted, as seen in figure 2-17 below.

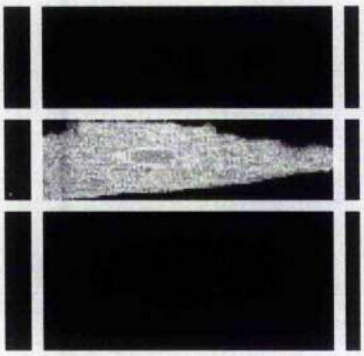

**Figure 2- 17. 2-D confocal section through a calcein loaded 1-day cultured rabbit cardiomyocyte.**

This area, containing only the image of the myocyte, was then excised from all of the optical sections for that cell. A frequency histogram for fluorescence intensity was constructed from all of the excised sections, an example of which is shown in figure 2-18 below. Each frequency histogram exhibited a clear peak at a fluorescence intensity value of around 225. Any fluorescence intensities less than one third of this peak value were arbitrarily designated as background and thus disregarded from the excised sections.

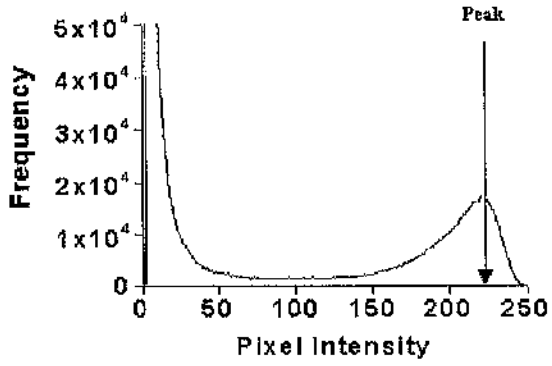


**Figure 2- 18. Frequency histogram of pixel intensities from the image of a 1-day cultured rabbit cardiomyocyte loaded with calcein.**

Thus the surface area of each section was determined by multiplying the number of cellular pixels above the chosen threshold value with the size of an individual pixel. A raw value for cell volume (in pL) was then calculated by multiplying the area of all the significant pixels by the Z-interval between the optical sections (0.5μM).

Calculation of correction factor for volume distortions due to spherical aberration: Spherical aberration occurs partly because of the point spread function of the objective lens and partly because of the mismatch in refractive index between the lens immersion medium / mounting medium (both water) and the objective lens / coverslip (both glass). It causes mainly the z-plane of the specimen to be over estimated and thus can lead to errors in volume calculations of up to 50% (Majlof & Forsgren, 1993).

The spherical aberration in our confocal system was calculated by optically sectioning fluorescent objects of known geometry and dimensions

(microspheres, 15μM diameter, Molecular Probes). The volume of the microspheres was determined using exactly the same method as described for cardiomyocytes above. The actual volume of the microspheres was 1766$\mu M^3$ compared to a calculated value of 1686$\mu M^3$ using LSCM. Therefore our calculated cell volumes were multiplied by a factor of 1.05 by way of correction.

The linear relationships between cell volume and membrane capacitance for both freshly dissociated and 1-day cultured cardiomyocytes are shown in figure 2-19 below.

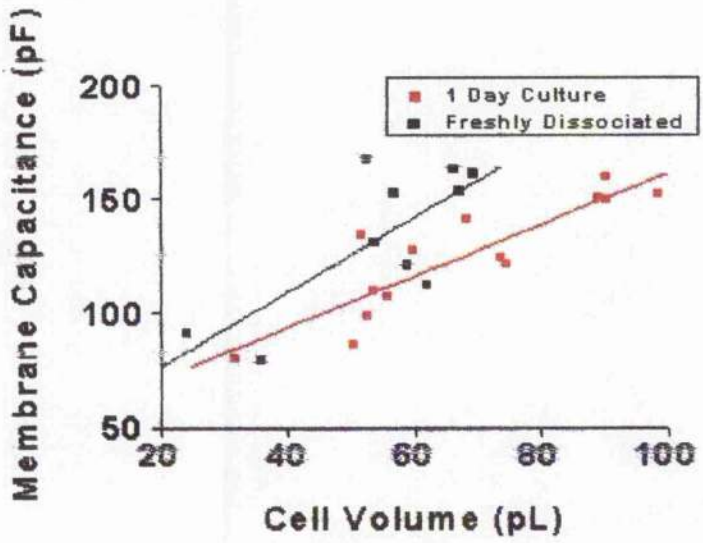


**Figure 2- 1. Relationship between cell volume and membrane capacitance for freshly dissociated and 1-day cultured rabbit cardiomyocytes.**

The capacitance-volume ratios were significantly increased when freshly dissociated were compared to 1-day culture cardiomyocytes (2.52 ± 0.18 pF/pL, n=10, v 1.92 ± 0.09 pF/pL, n=14, $p < 0.01$). Capacitance-volume ratios have previously been reported for freshly dissociated rabbit (4.58 ±

0.45 pF/pL), ferret (5.39 ± 0.57 pF/pL) and rat (8.44 ± 1.35 pF/pL) cardiomyocytes (Satoh *et al.*, 1996). Thus, in our hands, the capacitance-volume ratio for freshly dissociated rabbit cardiomyocytes is roughly half of what would have been predicted based on previous work. The reason for this difference is unknown and given this discrepancy, a more detailed investigation of this relationship would be recommended.

# Chapter 3- Sorcin overexpression and E-C coupling in isolated rabbit cardiomyocytes.

## 3.1 An introduction to sorcin

### 3.1.1 Sorcin and the ryanodine receptor

Sorcin (**so**luble **r**esistance-related **c**alcium-binding prote**in**) is a 22kDa $Ca^{2+}$-binding protein and was first discovered in the cytoplasm of multi-drug resistant cells (Meyers *et al.*, 1985). The crystal structure of $Ca^{2+}$ free human sorcin has been determined (Xie *et al.*, 2001), and belongs to the penta EF-hand (PEF) protein family. It was shown to be distributed widely in rodent tissues including the liver, small intestine, brain, lung, skeletal muscle, spleen, kidney and perhaps most interestingly, the heart, where it appeared to be associated with the ryanodine receptor complex (Meyers *et al.*, 1995a). In addition, the same study demonstrated that forced expression of sorcin in lung fibroblasts led to the unexpected expression of ryanodine receptor protein which could be co-precipitated using antibodies against sorcin. Exposure of these cells to caffeine caused a rapid and transient rise in intracellular $Ca^{2+}$, suggesting that functional calcium release channels were present.

Further insight into the functionality of sorcin was gained when it was demonstrated that the binding of $Ca^{2+}$ to recombinant sorcin caused the protein to undergo a conformational change that rendered it insoluble in detergent, thus prompting speculation that lipids were the targets of sorcin on cellular membranes (Meyers *et al.*, 1995b). Hence, the association of sorcin with the ryanodine receptor complex and this calcium-dependant

conformational change prompted speculation that it may have a role in $Ca^{2+}$ homeostasis in cardiac myocytes. Using preparations of cardiac SR microsomes to make single channel recordings of RyRs it was shown that the addition of sorcin to the cytoplasmic side of the calcium release channel caused a significant reduction in its open probability ($IC_{50}$ ~ 480nM) (Lokuta *et al.*, 1997). Interestingly, this study also demonstrated that caffeine activated RYRs could also be inhibited by sorcin at low $[Ca^{2+}]_i$ (suggesting that $Ca^{2+}$ is not an obligatory factor for sorcin functionality) and that protein kinase A phosphorylation of sorcin significantly reduced its ability to modulate RYR function.

Information regarding the most important functional domains of the sorcin molecule has been gained by studying either sub-fragments or mutant variants of the protein. Western blots have demonstrated that the sorcin calcium binding domain (SCBD), amino acid residues 33-198, was able to undergo a translocation from the cytosol to associate with RyRs located in membrane fractions under physiological calcium concentrations. However a different sub fragment, made up of amino acid residues 90-198 and unable to bind $Ca^{2+}$, was unable to undergo a similar translocation (Zamparelli *et al.*, 2000). Work by Mella *et al.*, 2003, has demonstrated that sorcin has 2 $Ca^{2+}$ binding sites, with dissociation constants of 0.42 X $10^{-6}$M and 6.3 X $10^{-6}$M respectively. Of the five EF-hand motifs within the sorcin molecule only 3 (EF1, EF2 & EF3) are potentially able to bind $Ca^{2+}$. In order to identify the functional pair the same group introduced point mutations into the hand motifs EF1, EF2 & EF3 to yield E53Q, E94A & E124A respectively. The affinity for $Ca^{2+}$ and 2 sorcin targets , annexin VII

and RyR followed the order wild-type > E53Q > E94A > E124A, indicating that disruption of EF3, followed by EF2 had the largest functional impact.

### 3.1.2 Sorcin and the L-type $Ca^{2+}$ channel

Subsequently it was also demonstrated that the $\alpha_1$-subunit of the cardiac voltage-dependant L-type $Ca^{2+}$ channel could be immunoprecipitated using antibodies for sorcin. Shortened forms of the $\alpha_1$-subunit, cleaved at the C terminus could not be immunoprecipitated using the anti-sorcin antibody, implying that distal C-terminal regions may be involved in the stabilisation of the sorcin/$\alpha_1$-subunit interaction (Meyers *et al.*, 1998). Hence, the possibility that sorcin may also be involved in the modulation of $Ca^{2+}$ entry into the cardiomyocyte during excitation-contraction coupling.

### 3.1.3 Effects of exogenous sorcin on intact cardiomyocytes

A preliminary study reported that 1μM recombinant sorcin increased both the L-type $Ca^{2+}$ current and the intracellular $Ca^{2+}$ transient in voltage clamped cardiomyocytes. Sorcin also decreased the frequency and duration of spontaneous $Ca^{2+}$ sparks in permeabilised cardiomyocytes (Farrell, 2002). The authors speculated that sorcin acted by inhibiting $Ca^{2+}$ leak via the RYR, thus gradually increasing SR $Ca^{2+}$ load, and in combination with its action on the L-type $Ca^{2+}$ current, caused an increase in the gain of CICR. However, a more comprehensive study by the same group confirmed the inhibitory effect of sorcin on the occurrence of

spontaneous $Ca^{2+}$ sparks but in contradiction to their previous work demonstrated a reduced intracellular $Ca^{2+}$ transient with no effect on either the amplitude or kinetics of the L-type $Ca^{2+}$ current (Farrell *et al.*, 2003). Given the effect of endogenous sorcin on the occurrence of spontaneous $Ca^{2+}$ sparks, one could infer that the only action of sorcin revealed in this study was an inhibition of the RyR. It is surprising that this effect alone could account for the reduction in the intracellular $Ca^{2+}$ transient observed. It is thought that interventions which affect only RyR open probability and hence SR $Ca^{2+}$ release during E-C coupling, have only short-term effects on the size of the intracellular $Ca^{2+}$ transient, with compensatory changes in SR load occurring to preserve normal transient size (Trafford *et al.*, 2000). It is possible that sorcin's reduction of RyR $P_O$ could act to reduce diastolic $Ca^{2+}$ leak from the SR and thus increase its $Ca^{2+}$ load. In this situation however, with no effect of sorcin on the L-type $Ca^{2+}$ current, one might expect to see increased, not decreased intracellular $Ca^{2+}$ transients in cardiomyocytes exposed to sorcin. It is therefore disappointing that this study did not report the effects of exogenous sorcin on SR $Ca^{2+}$ load. The study also demonstrated that a very high $[Ca^{2+}]_i$ ($ED_{50}$ = ~200μM) was required to produce a conformational change in sorcin and thus cause its translocation between the cytoplasmic and membranous compartments. Mathematical models predict that $[Ca^{2+}]$ may transiently rise to such levels in the dyadic spaces during E-C coupling (Peskoff & Langer, 1998;Greenstein & Winslow, 2002).

### 3.1.4 Effects of virus mediated sorcin overexpression on intact cardiomyocytes

Zhu, 2003, have reported that Herpes Simplex Virus mediated overexpression of sorcin has time dependent effects on E-C coupling in normal and failing rat cardiomyocytes. 12hrs after transfection, $Ca^{2+}$ transient size was reduced when compared to control, however after 36hrs, $Ca^{2+}$ transient size was increased. The difference between the results of the group's previous study (which showed that 3μM sorcin in the patch pipette immediately reduced $Ca^{2+}$ transient size) and the increases in $Ca^{2+}$ transient size observed after 36hrs with HSV-mediated sorcin overexpression are intriguing and merit further investigation. Unfortunately, once again, SR $Ca^{2+}$ loads were not reported in this study.

Suarez *et al.*, 2004 have used adenovirus to mediate sorcin overexpression in both mouse hearts *in vivo* and isolated rat cardiomyocytes. A 274% sorcin overexpression had profound effects on the cardiac contractility of subsequently isolated mouse hearts. A 40% increase in left ventricular pressure, a 54% increase in max dP/dt and a 72% increase in min dP/dt were observed when the sorcin overexpressing cohort were compared with control. The mechanism for these improvements in contractility was inferred from overexpressing sorcin over a period of 48hrs in single rat cardiomyocytes. When field stimulated, these sorcin-overexpressing myocytes exhibited significantly larger $Ca^{2+}$ transients when compared to control. In addition, rapid application of 10mM caffeine also revealed a significantly increased SR $Ca^{2+}$ content in the sorcin over-expressing

myocytes. The SR rich fractions of the sorcin overexpressing myocytes revealed a 71% increase in RyR protein expression, a 3 fold increase in SERCA2a expression and a 66% increase in phospholamban expression when compared to control. This up-regulation of SERCA2a may explain the increase SR $Ca^{2+}$ load and the increased $Ca^{2+}$ transients in the sorcin overexpressing myocytes.

### 3.1.5 Transgenic overexpression of sorcin in the heart

Transgenic mice, in which sorcin was over-expressed twenty-fold in the heart, are reported to have contractile abnormalities and significant depression intracellular $Ca^{2+}$ transient (Meyers *et al.*, 2003). There were no changes in the expression of other calcium regulatory proteins, $I_{Ca}$ current density or $I_{Ca}$ time course of activation, however the rapid component of $I_{Ca}$ inactivation was significantly accelerated. These effects of sorcin on $I_{Ca}$ were then confirmed using *Xenopus* oocyte expression studies. Given the faster inactivation of $I_{Ca}$ in the transgenic mice, one would assume that less $Ca^{2+}$ entered the myocyte during excitation. This reduced trigger for CICR may well be the cause for the observed reduction in intracellular $Ca^{2+}$ transient, however in the absence of essential data on SR $Ca^{2+}$ load, such speculation is not helpful.

### 3.1.6 Additional sorcin interactions and sorcin mutants

Sorcin has been shown to co-localise with NMDA receptors (Gracy *et al.*, 1999) and presenilin 2 (Pack-Chung *et al.*, 2000) in the brain. In the presence of $Ca^{2+}$, sorcin is also capable of binding to the N-terminal domain of annexin VII, a member of a protein family characterised by their ability to bind to phospholipid membranes in a $Ca^{2+}$-dependent manner. It has thus been suggested that the interaction of sorcin and annexin VII may serve to modulate the functions of proteins on membrane surfaces in a $Ca^{2+}$ dependent manner (Brownawell & Creutz, 1997). Surface plasmon resonance experiments have also shown that sorcin and annexin VII form an increasingly stable complex between 3 and 6μM calcium. However SCBD (residues 33-198) did not form a complex with annexin VII under the same conditions, again implying that the N-terminal domain of sorcin (amino acid residues 1-32) binds to annexin VII (Verzili *et al.*, 2000). Interestingly, cardiomyocytes from annexin VII double knockout mice exhibit reduced rates of cell shortening when stimulated at high frequencies (Herr *et al.*, 2001).

Finally, the translocation of sorcin from cytosol to cell membranes requires the binding of 2 $Ca^{2+}$ ions per sorcin monomer. Sorcin contains 3 EF-hand motifs, EF1, EF2 and EF3, that are able to bind $Ca^{2+}$ at μM concentrations. In order to determine the functional pair, the conserved bidentate-Z glutamate in these EF-hands was mutated to yield E53Q (in EF1), E94A (in EF2) and E124A (in EF3). The affinity for $Ca^{2+}$, RyR and annexin VII followed the order wild-type > E53Q > E94A > E124A, indicating that

disruption of EF3 and EF2 had the greatest functional impact. Thus it was inferred that the functional EF-hand motifs were EF3 and EF2 (Mella *et al.*, 2003).

### 3.1.7 Aims

To evaluate the effect of sorcin on cardiac E-C coupling, adult rabbit ventricular myocytes were transfected with a recombinant adenovirus coding for human sorcin (Ad-sorcin). A β-galactosidase virus was used as a control (Ad-LacZ). Viruses were constructed by Dr. Tim Seidler, Georg-August-Universitat, Goettingen, Germany.

It was proposed that after 24 hrs in culture the virus-transfected cells would be loaded with fura-2 and E-C coupling studied using whole cell voltage clamp. This was to enable the effects of sorcin overexpression on the L-type $Ca^{2+}$ current, the intracellular $Ca^{2+}$ transient, SR $Ca^{2+}$ load, NCX activity and sarcolemmal $Ca^{2+}$ ATPase activity to be determined. In addition, the effects of acute overexpression of sorcin on $Ca^{2+}$ spark characteristics were obtained using laser scanning confocal microscopy.

The effect of recombinant sorcin on NCX activity was studied in freshly dissociated adult rabbit cardiomyocytes. Additionally, the effects of the sorcin fragment SCBD and the sorcin mutants W99G and W105G on NCX activity were also investigated. Recombinant sorcin, SCBD and the sorcin mutants W99G and W105G were supplied by Dr. Emilia Chiancone, University of Rome La Sapienza, Rome, Italy. Finally, the effect of

adenoviral mediated overexpression of the sorcin mutant, E124A (again constructed by Dr. Tim Seidler), on NCX activity was also investigated.

### 3.2 Methods & Results

#### 3.2.1 Measurement of sorcin mRNA and protein expression levels

The levels of sorcin mRNA and protein overexpression at various MOI's were kindly determined using real time PCR and Western blot technique and can be seen in figure 3-1.

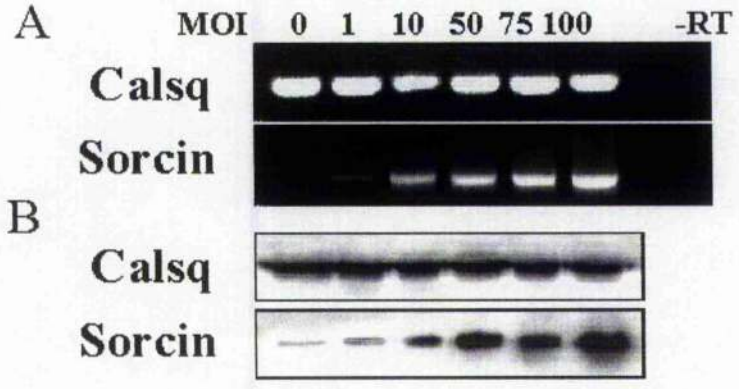


**Figure 3 - 1. Sorcin mRNA and protein expression.**

**Verification of sorcin mRNA (A) and protein overexpression (B) in isolated rabbit cardiomyocytes, 48hrs after transfection with Ad-sorcin at various MOI's. Calsequestrin levels were used a standard in both RT-PCR and Western blots. Measurements by Dr Tim Seidler (Georg-August-Universitat, Goettingen)**

At MOI 100 (i.e. 100 virus particles per cardiomyocyte), sorcin levels were 4-6 time greater than in Ad-LacZ control. Sorcin overexpression did not affect calsequestrin expression.

3.2.2 Effect of sorcin overexpression on the L-type $Ca^{2+}$ current and intracellular $Ca^{2+}$ transient.

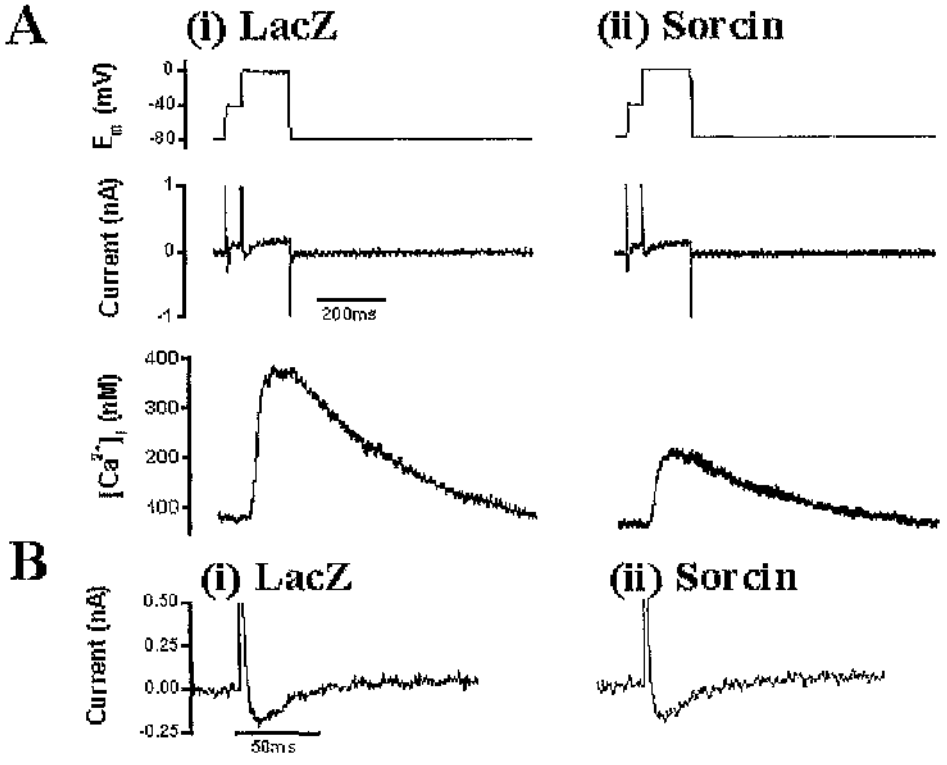


**Figure 3 - 2. Depolarisation-induced L-type $Ca^{2+}$ currents and intracellular $Ca^{2+}$ transients in voltage clamped Ad-LacZ (I) and Ad-sorcin (Ii) transfected cardiomyocytes.**

**A, Typical traces of membrane potential ($E_m$), membrane current and $[Ca^{2+}]_i$ from single cardiomyocytes (average of 10 sweeps). B, Membrane current recorded upon voltage step from –40mV to 0mV for 150ms, illustrating the time course and the amplitude of $I_{Ca}$.**

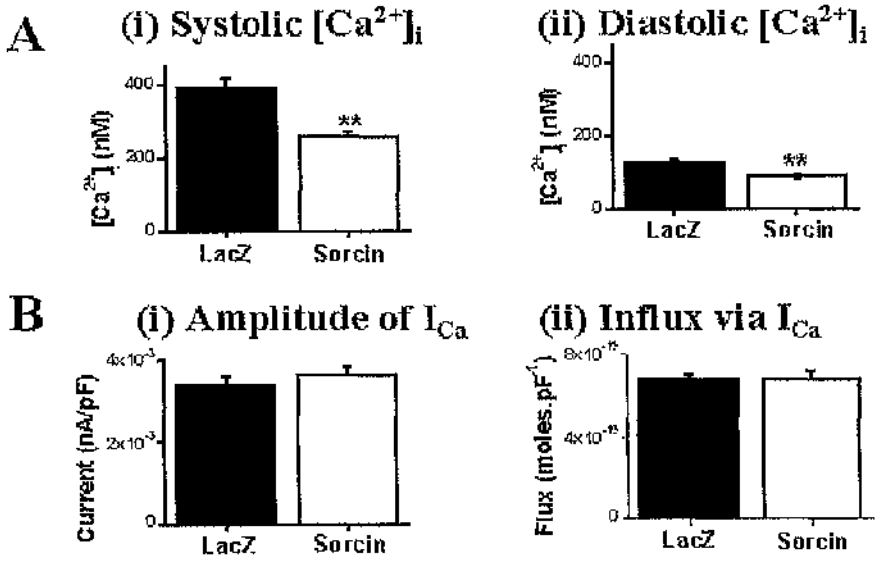


**Figure 3 - 3. EC-coupling in Ad-LacZ and Ad-sorcin transfected cardiomyocytes.**

**A, Mean ± SEM values of peak systolic (i) and end diastolic (ii) $[Ca^{2+}]_i$ and B, Mean ± SEM values of peak $I_{Ca}$ (i) and $Ca^{2+}$ influx via $I_{Ca}$ in Ad-LacZ (n=38) and Ad-sorcin (n=42) transfected cardiomyocytes.**

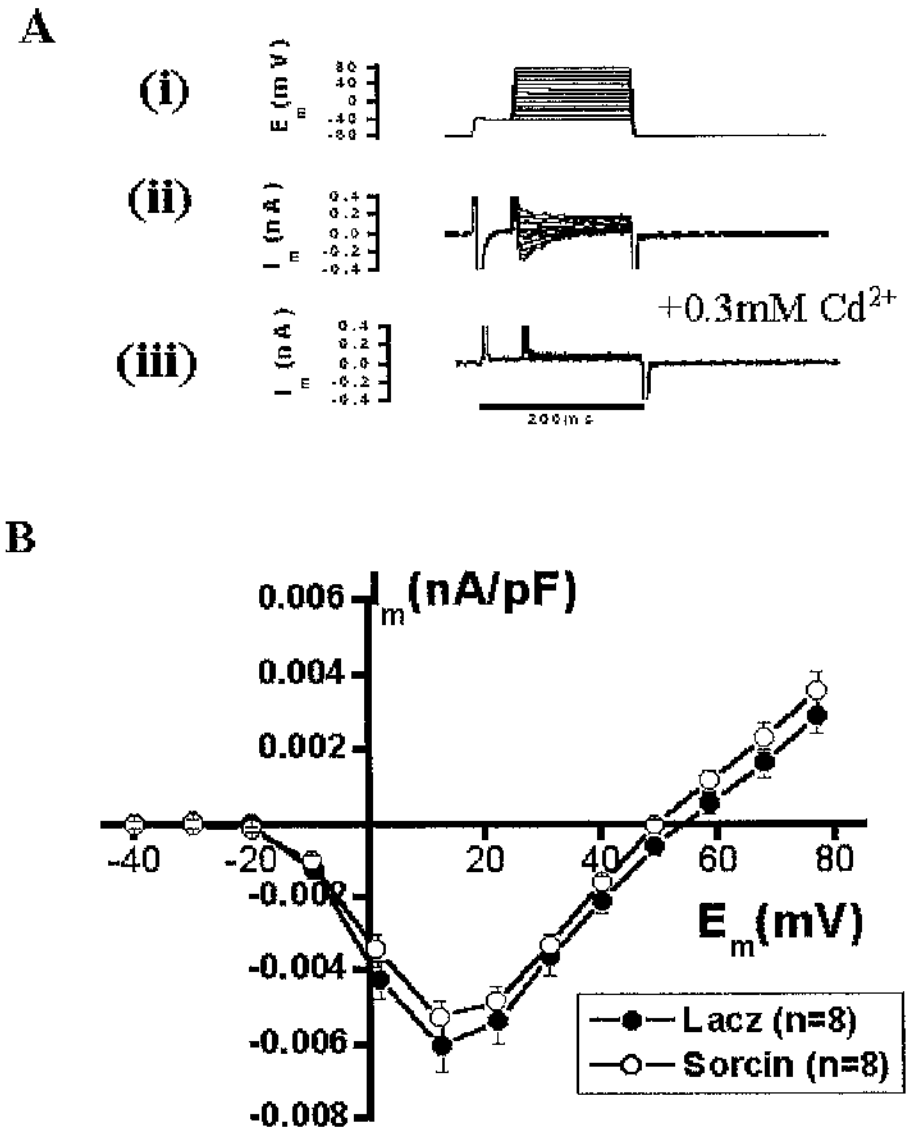


**Figure 3 - 4. I-V relationship for $I_{Ca}$ in Ad-sorcin and Ad-LacZ transfected cardiomyocytes.**

**Voltage clamp protocol (i) used to investigate the i-V relationship for $I_{Ca}$ in Ad-sorcin and Ad-LacZ transfected cardiomyocytes. Current traces obtained in the absence (ii) and in the presence of $Cd^{2+}$ (iii). B, I-V relationship for $I_{Ca}$ (points represent mean ± SEM values).**

Figure 3-3A demonstrates that Ad-sorcin transfection significantly decreased both peak systolic and end diastolic $[Ca^{2+}]_i$ in voltage clamped rabbit cardiomyocytes, causing a reduced $Ca^{2+}$ transient amplitude. Figure 3-3B shows that neither the amplitude nor the time integral of $I_{Ca}$ (which can be converted to a $Ca^{2+}$ influx) are significantly altered by sorcin overexpression. This observation was confirmed via investigation of the I-V relationship for $I_{Ca}$. Figure 3-4 clearly shows that Ad-sorcin transfection had no significant effect on $I_{Ca}$ amplitude over a range of membrane potentials.

3.2.3 Effect of sorcin overexpression on SR $Ca^{2+}$ content (assessed by rapid application of 10mM caffeine).

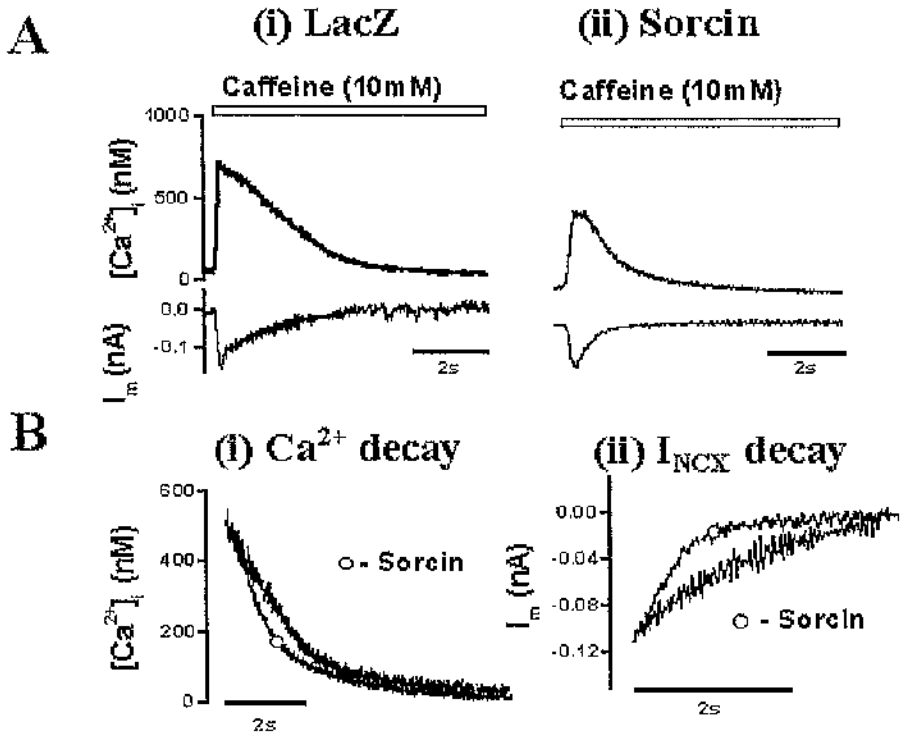

Figure 3 - 5. SR $Ca^{2+}$ content in typical Ad-LacZ and Ad-sorcin transfected cardiomyocytes.

A, SR $Ca^{2+}$ release and corresponding membrane currents recorded upon rapid application of 10mM caffeine in typical Ad-LacZ (i) and Ad-sorcin (ii) transfected cardiomyocytes. B, Superimposed declines of $[Ca^{2+}]_i$ (i) and $I_{NCX}$ (ii) in typical control and experimental cardiomyocytes.

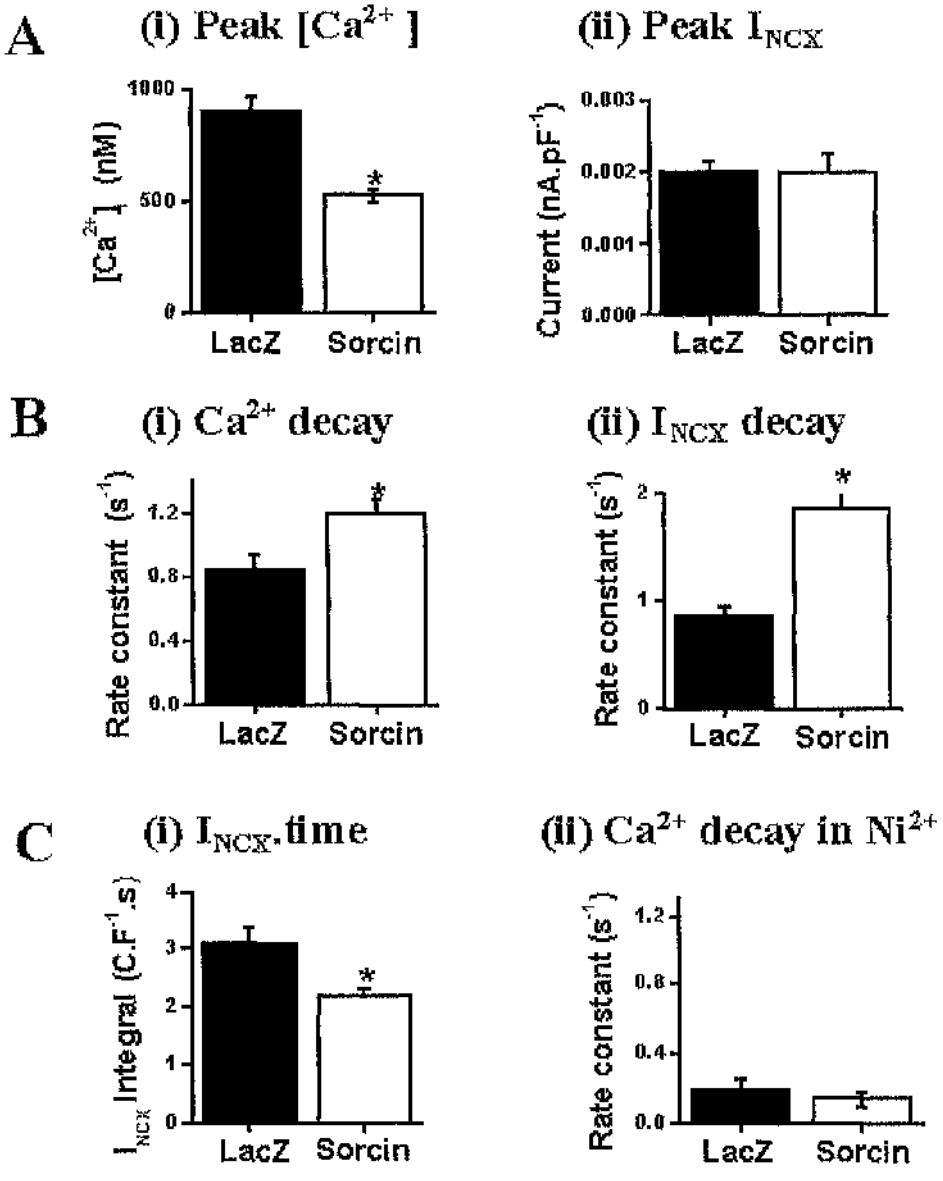

**Figure 3 - 1. Sorcin overexpression and SR $Ca^{2+}$ content.**

**A *(i)* Mean ± *SEM values for peak* $[Ca^{2+}]_i$ *in the presence of 10mM caffeine in Ad-LacZ (n=21) and Ad-sorcin (n=17) groups, (ii) peak* $I_{NCX}$ (LacZ, n=18 v Sorcin, n=13). B (i) Mean ± SEM values for rate constant of $[Ca^{2+}]_i$ decay (LacZ, n=17 v Sorcin, n=12), (ii) rate constant of $I_{NCX}$ decay (LacZ, n=11 v Sorcin, n=8). C (i) Mean ± SEM values for $I_{NCX}$.time integral (LacZ, n=18, v Sorcin, n=13), (ii) and rate constant of $[Ca^{2+}]_i$ in $Ni^{2+}$ (LacZ, n=5 V Sorcin, n=4).**

## 3.2.4 Effect of sorcin overexpression on $Ca^{2+}$ buffering capacity

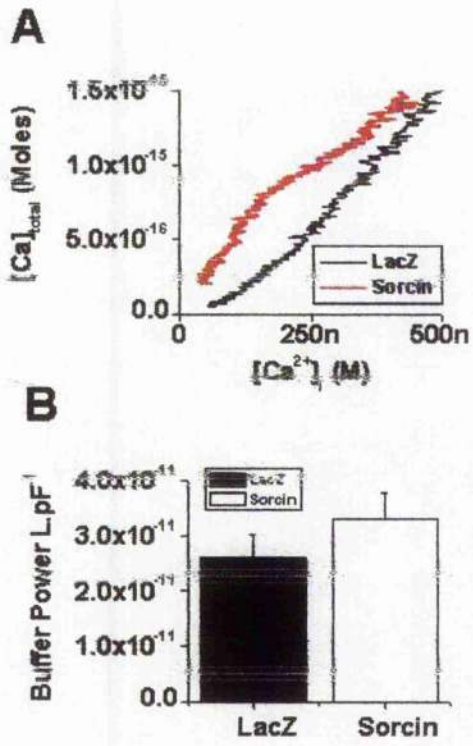


**Figure 3 - 2. Sorcin overexpression and $Ca^{2+}$ buffering capacity.**

***(A) Relationship between free*** $[Ca^{2+}]_i$ ***and the total amount of*** $Ca^{2+}$ ***extruded from*** typical Ad-LacZ and Ad-Sorcin transfected cardiomyocytes during the rapid

**application of 10mM caffeine. (B) Mean ± SEM buffer power for Ad-LacZ (n=17) and Ad-sorcin (n=13) transfected cardiomyocytes, $p > 0.05$.**

Rapid application of 10mM caffeine was applied to cardiomyocytes contracting in the steady state. Caffeine causes the SR to release its store of $Ca^{2+}$ into the cytoplasm. In the continued presence of caffeine, reduction of $[Ca^{2+}]_i$ occurs mainly via extrusion at the sarcolemma by the action of NCX. The extrusion of $Ca^{2+}$ from the cytosol via NCX generates a transient inward current ($I_{NCX}$), the integral of which, along with the size of caffeine-induced $Ca^{2+}$ transient give a measure of SR $Ca^{2+}$ load. Figures 3-6 A (i) and C (i) clearly demonstrate that both the caffeine-induced $Ca^{2+}$ transient and the integral of $I_{NCX}$ with respect to time are significantly reduced in the Ad-sorcin transfected cardiomyocytes when compared to control. These results indicate that sorcin overexpression significantly reduces SR $Ca^{2+}$ content.

While figure 3-6 A (ii) shows that the peak of the transient inward current was unaffected by sorcin overexpression, figure 3-6 B (ii) shows that its rate constant of decay, calculated by fitting with a single exponential, is significantly increased in Ad-sorcin transfected cardiomyocytes when compared to Ad-LacZ. Similarly, the rate constant for the decay of the caffeine-induced $Ca^{2+}$ transient (see figure 3-6 B (i)) was also significantly increased in the Ad-sorcin transfected myocytes. These increased rate constants suggest that the rate of extrusion of $Ca^{2+}$ from the cytosol at the sarcolemma via NCX has been significantly increased by sorcin overexpression. If caffeine is applied in the presence of $Ni^{2+}$, the SR

releases its store of $Ca^{2+}$; however, under these circumstances $Ni^{2+}$ acts to block the action of NCX. Removal of $Ca^{2+}$ from the cytosol occurs at a much slower rate, by the action of either the sarcolemmal $Ca^{2+}$-ATPase or via mitochondrial $Ca^{2+}$ uptake. Figure 3-6 C (ii) demonstrates that when caffeine was applied with $Ni^{2+}$, the rate constant for the decay of the corresponding $Ca^{2+}$ transient was similar in both experimental groups. Indication that sorcin overexpression does not affect these alternative $Ca^{2+}$ removal mechanisms. Figure 3-7 demonstrates that sorcin overexpression did not significantly alter $Ca^{2+}$ buffer capacity.

3.2.5 Effect of sorcin overexpression on NCX activity.

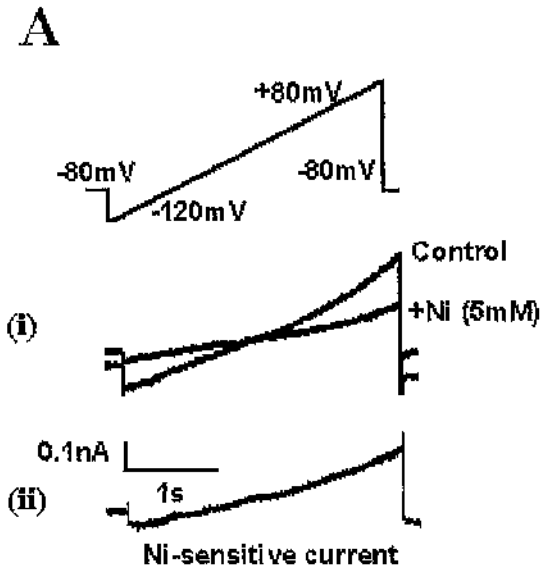

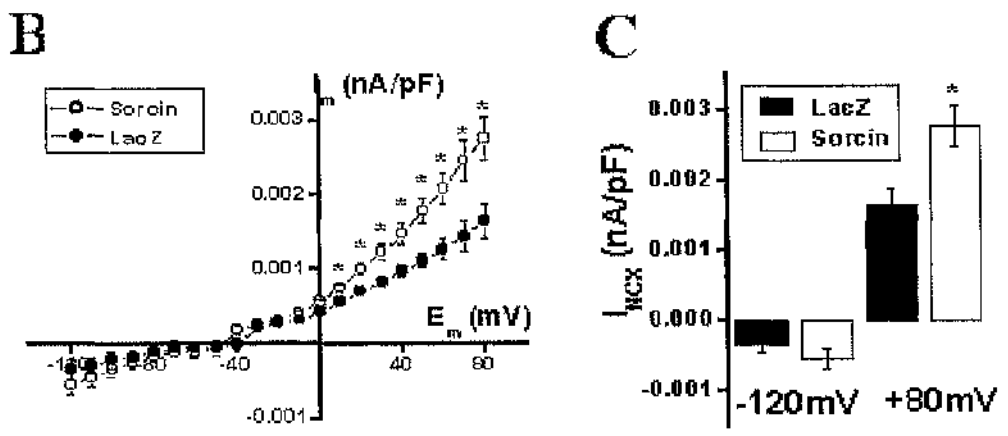


**Figure 3 - 8. The I-V relationship for the $Ni^{2+}$-sensitive NCX current.**

**A, Voltage clamp protocol used to determine the I-V relationship under control conditions and in the presence of 5mM $Ni^{2+}$ (i) and the difference current attributable to NCX (ii). B, Average I-V relationship in Ad-LacZ (n=7) and Ad-sorcin (n=20) transfected cardiomyocytes. C, Average currents measured at membrane potentials of -120mV and +80mV in both experimental groups.**

The effect of sorcin overexpression on NCX activity was further investigated by determining the $Ni^{2+}$-sensitive NCX current measured whilst slowly ramping the membrane potential from –120mV to +80mV (Figure 3-8, A). With $[Ca^{2+}]_i$ buffered at 250nM using 50mM EGTA in the patch pipette solution and $[Na^+]_i$ at 20mM, NCX currents were larger in Ad-sorcin transfected cardiomyocytes when compared to Ad-LacZ control. This increase was significant at membrane potentials between +10mV and +80mV, with a trend towards larger currents at –120mV (Figures 3-8, B & C).

3.2.6 Effect of sorcin overexpression on spontaneous $Ca^{2+}$ spark activity and SR $Ca^{2+}$ load in permeabilised rabbit cardiomyocytes.

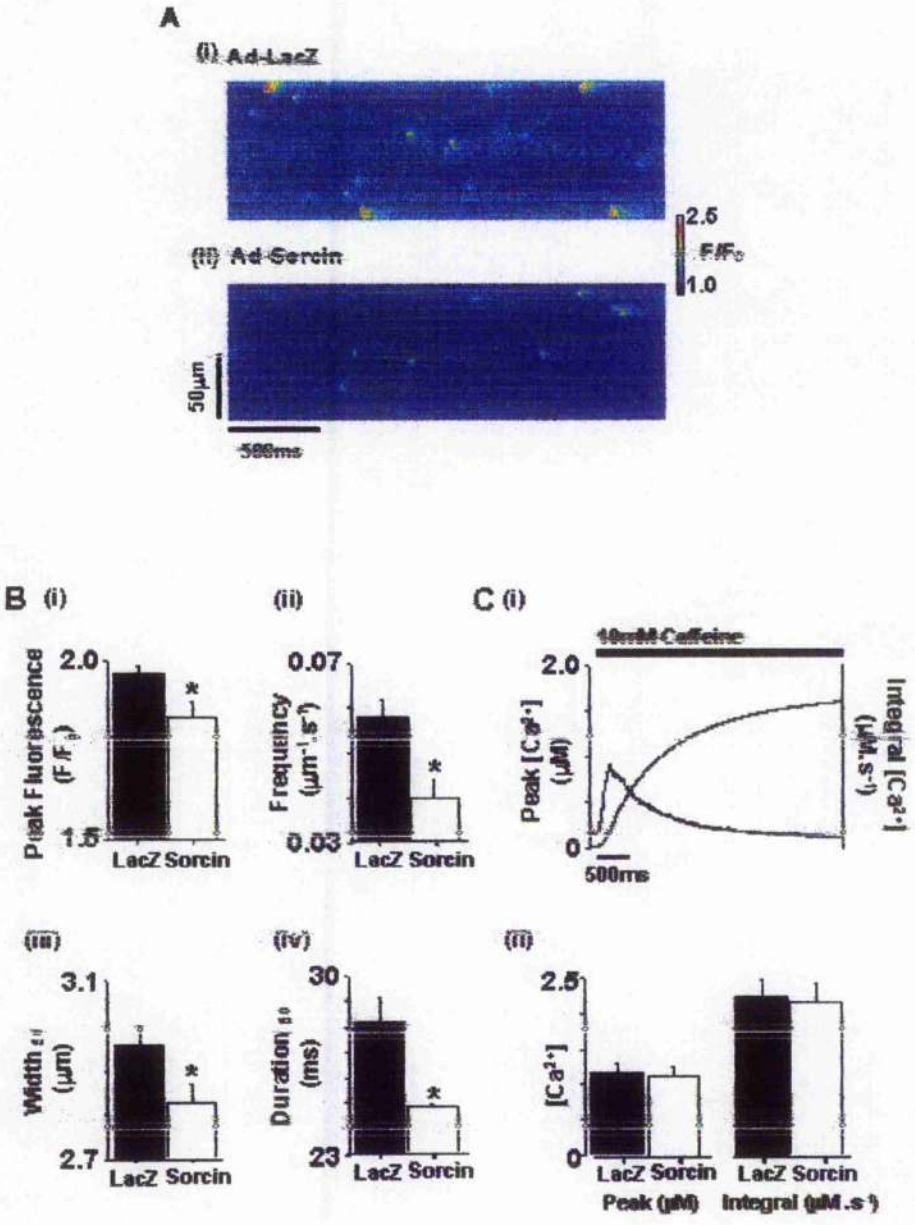

**Figure 3 - 9. Spontaneous $Ca^{2+}$ sparks in permeabilised cardiomyocytes transfected with Ad-LacZ and Ad-sorcin.**

**A, Pseudo colour line scan epifluorescence image from single cardiomyocytes in each experimental group. B, Mean ± SEM values for peak $F/F_0$ (I), spark frequency (ii), spark width (iii) and spark duration (iv). Results compiled from 1844 events from 21 Ad-LacZ transfected cells and 739 events from 11 Ad-sorcin transfected cells. * $P<0.01$. C, Caffeine-induced $[Ca^{2+}]_i$ signal calculated from the mean fluorescence of a 20-pixel intracellular region, with accompanying integral (i) and mean values of peak $[Ca^{2+}]_i$ and integral signals in response to caffeine in both experimental groups. Measurements were performed by Dr. Chris Loughrey, University of Glasgow.**

The direct effects of sorcin overexpression on SR function were investigated in β-escin permeabilised cardiomyocytes. Permeabilisation provided a route with which to functionally bypass the effects of sorcin on NCX activity, which would have indirectly reduced SR $Ca^{2+}$ load and thus complicated $Ca^{2+}$ spark analysis. Single cardiomyocytes were superfused with a standard solution containing nominally 150nM $Ca^{2+}$, pH 7.0 with ATP and creatine phosphate added to preserve SR function. Inclusion of 10μM fluo-3 allowed spontaneous $Ca^{2+}$ sparks to be visualised using laser-scanning confocal microscopy. Figures 3-9 A (i) & (ii) show typical line scan traces and $Ca^{2+}$ sparks from cardiomyocytes transfected with Ad-LacZ and Ad-sorcin respectively. The $Ca^{2+}$ sparks recorded in the Ad-sorcin transfected cells were typically smaller and less frequent than those observed in Ad-LacZ transfected cells. Figure 3-9 B demonstrates that average $Ca^{2+}$ spark peak, frequency, width and duration were all

significantly reduced in the Ad-sorcin transfected cells (peak F/Fo, 1.96±0.02 vs.1.84 ±0.04 , P<0.05; frequency: 0.058±0.004 vs. 0.040±0.004 $\mu m^{-1}s^{-1}$, P<0.05; width, 2.96±0.05 vs. 2.82±0.06 μm, P<0.05; duration, 28.2±1.0 vs. 24.8±1.2ms, P<0.05; Ad-Laz n=21cells vs. Ad-sorcin n=11cells). After perfusion with 150nM $Ca^{2+}$, 50μM EGTA and 10μM fluo-5, 10mM caffeine was rapidly applied in order to assess SR $Ca^{2+}$ content. Figure 3-9 C demonstrates that both the mean amplitude and time integral of the caffeine-induced $Ca^{2+}$ releases and hence SR $Ca^{2+}$ loads were similar in both experimental groups (peak $[Ca^{2+}]_i$ in caffeine was 1.17±0.14 μM/L for Ad-LacZ [n=12] and 1.15±0.13 μM/L for Ad-sorcin [n=13]).

3.2.7 Relationship between SR $Ca^{2+}$ content and $Ca^{2+}$ transient amplitude in Ad-LacZ and Ad-sorcin transfected cardiomyocytes.

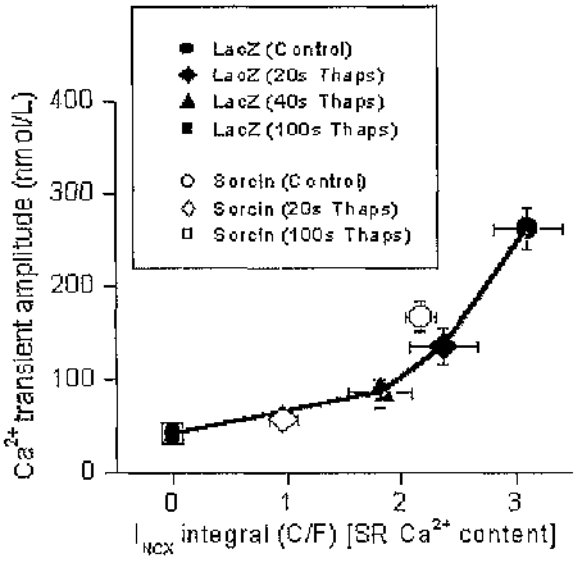

**Figure 3 - 10. Relationship between $I_{NCX}$ integral (an index or SR $Ca^{2+}$ content) and $Ca^{2+}$ transient amplitude for Ad-LacZ and Ad-sorcin transfected cardiomyocytes.**

**Data were obtained in the steady state with lower SR loads were achieved by exposure to 5μM thapsigargin for various times as indicated.**

The reduced $Ca^{2+}$ transient amplitude in the Ad-sorcin transfected cardiomyocytes could be explained solely by the reduced SR $Ca^{2+}$ load. This possibility was investigated by progressively decreasing SR $Ca^{2+}$ content in both experimental groups with the use of thapsigargin and noting the resultant effects on $Ca^{2+}$ transient amplitude. Figure 3-10 demonstrates that the relationship for $Ca^{2+}$ transient amplitude vs. $I_{NCX}$ integral for Ad-LacZ transfected cardiomyocytes is close to hyperbolic. Furthermore, the data for the sorcin group fall very close to the relationship described for the Ad-LacZ group. Hence it is possible that the effects of sorcin overexpression on E-C coupling could be explained by a reduction in SR $Ca^{2+}$ content alone, with no evidence for an effect of sorcin on the gain of E-C coupling.

3.2.8 Effect of sorcin overexpression on the allosteric regulation of NCX.

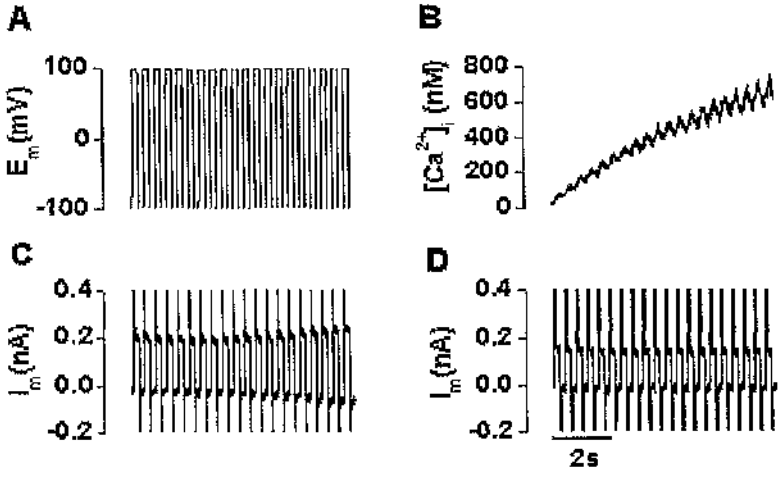


**Figure 3 - 11. Sorcin overexpression and allosteric regulation of NCX.**

**Typical voltage trace (A), with corresponding $[Ca^{2+}]_i$ (B) and current traces in the absence (C) and in the presence of $Ni^{2+}$ (D).**

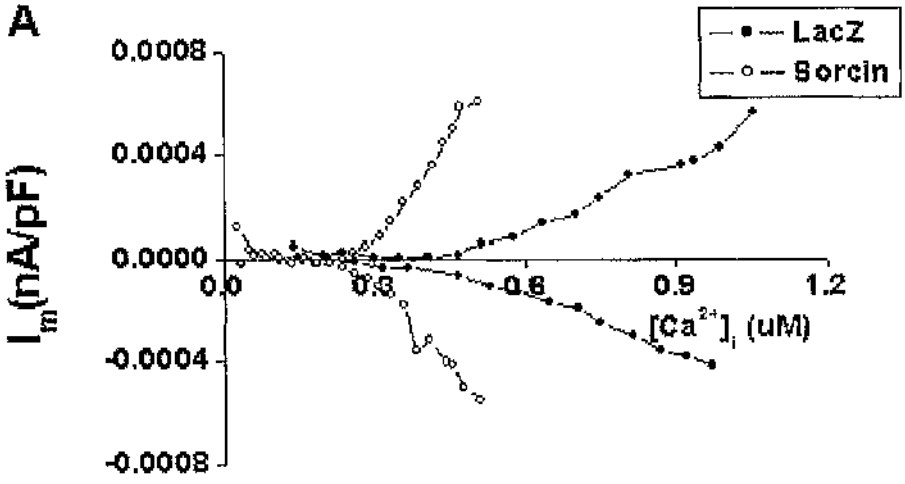


**Figure 3 - 12. Allosteric regulation of NCX in typical Ad-LacZ and Ad-sorcin transfected cardiomyocytes.**

**A, Typical outward and inward $Ni^{2+}$-sensitive ($I_{NCX}$) traces with varying $[Ca^{2+}]_i$ in both cell types.**

In order to investigate the allosteric regulation of NCX in both Ad-LacZ and Ad-sorcin transfected cardiomyocytes, all other known currents were blocked and membrane potential was alternated between –100mV and +100mV, both in the absence and in the presence of $Ni^{2+}$. The $Ni^{2+}$-sensitive current was assumed to represent $I_{NCX}$. The observed rise in $[Ca^{2+}]_i$ would be expected to increase $Ca^{2+}$ efflux ( ↑ inward $I_{NCX}$), whilst decreasing $Ca^{2+}$ influx ( ↓ outward $I_{NCX}$). Hence any increase in outward $I_{NCX}$ would be due to the allosteric stimulation of $I_{NCX}$ by $[Ca^{2+}]_i$. Figure 3-11 shows that as $[Ca^{2+}]_i$ increased, so did outward $I_{NCX}$, indicating that allosteric regulation of NCX was operating in our cultured cardiomyocytes. Figure 3-12 demonstrates that the characteristics of this allosteric regulation appear to have been altered by sorcin overexpression. It would suggest that the kd for both the inward and the outward $I_{NCX}$ currents was reduced in Ad-sorcin transfected cardiomyocytes when compared to Ad-LacZ. It was not possible to determine whether sorcin overexpression affected $V_{max}$, as in the majority of cardiomyocytes studied, neither inward nor outward $I_{NCX}$ currents reached a plateau at increased $[Ca^{2+}]_i$.

3.2.9 Effect of exogenous sorcin on NCX activity in freshly dissociated adult rabbit cardiomyocytes.

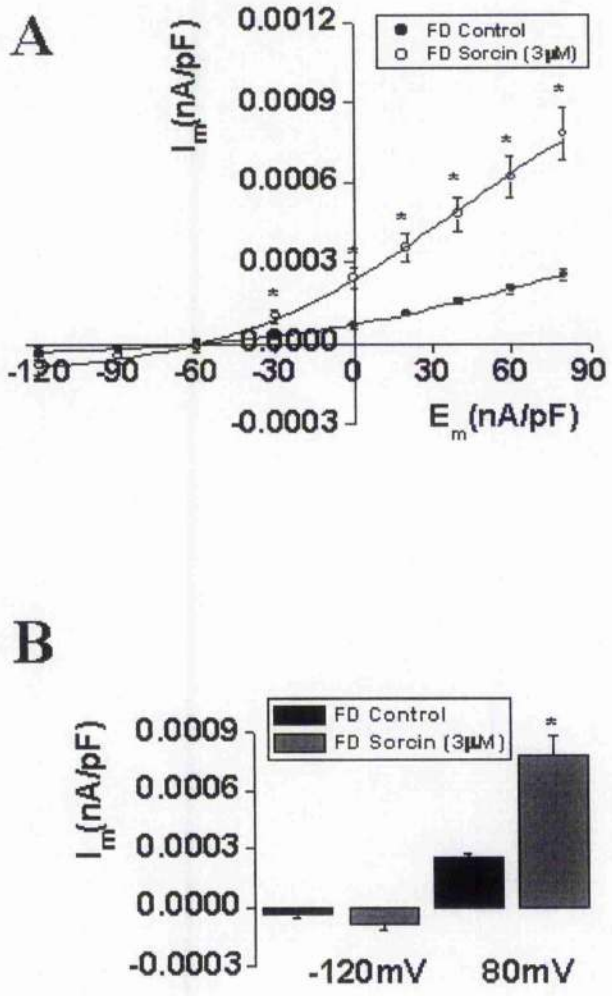


**Figure 3 - 13. The effect of exogenous sorcin on the I-V relationship for the $Ni^{2+}$-sensitive NCX current in freshly dissociated rabbit cardiomyocytes.**

**A, Average I-V relationship in freshly dissociated cardiomyocytes (n=11) and with 3μM sorcin in patch pipette (n=11). B, Average currents measured at membrane potentials of -120mV and +80mV in both experimental groups.**

The effect of exogenous sorcin on NCX activity in freshly dissociated cardiomyocytes was investigated by determining the $Ni^{2+}$-sensitive NCX current measured whilst ramping the membrane potential from –120mV to +80mV (Figure 3-13, A). With $[Ca^{2+}]_i$ buffered at 250nM using 50mM EGTA in the patch pipette solution and $[Na^+]_i$ at 20mM, NCX currents were increased with the addition of 3μM sorcin to the patch pipette. This increase was significant at membrane potentials between -40mV and +80mV, with a trend towards larger currents at –120mV (Figures 3-13, B ).

3.2.10 Effect of exogenous sorcin on NCX activity in freshly dissociated adult rabbit cardiomyocytes using nominally $Ca^{2+}$ free (i.e. <1nM) extracellular solution.

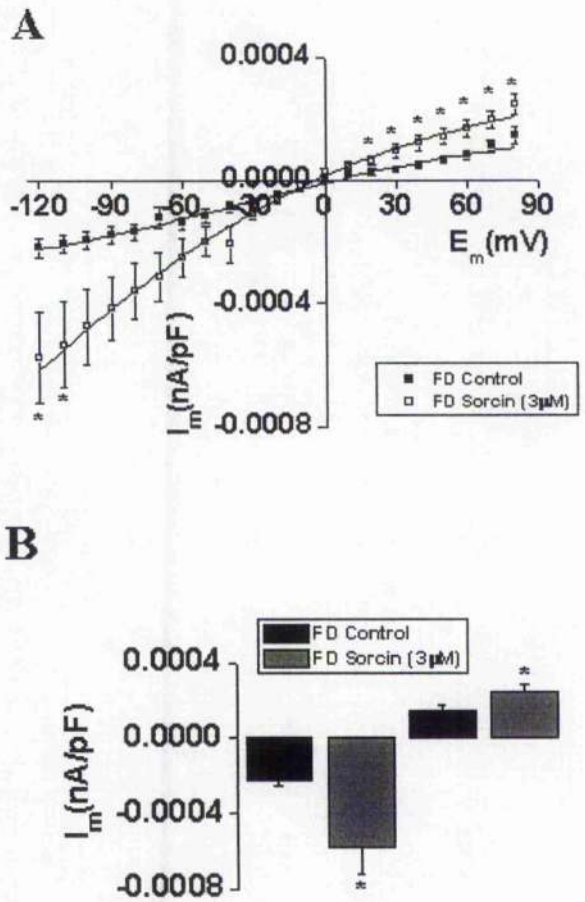


**Figure 3 - 14. The effect of exogenous sorcin on the I-V relationship for the $Ni^{2+}$-sensitive NCX current in freshly dissociated rabbit cardiomyocytes under conditions of low extracellular calcium.**

**A, Average I-V relationship in freshly dissociated cardiomyocytes (n=16) and with 3μM sorcin in patch pipette (n=9). B, Average currents measured at membrane potentials of -120mV and +80mV each experimental group.**

The effect of exogenous sorcin on NCX activity in freshly dissociated cardiomyocytes under conditions "nominally zero" extracellular $Ca^{2+}$ was investigated by determining the $Ni^{2+}$-sensitive NCX current measured whilst ramping the membrane potential from –120mV to +80mV (Figure 3-14, A). It would be predicted that a reduced extracellular $[Ca^{2+}]$ would enhance $Ca^{2+}$ extrusion via NCX at membrane potentials negative to the reversal potential. Thus under these conditions it may be possible to resolve a significantly increased inward NCX current in the presence of exogenous sorcin. Indeed with $[Ca^{2+}]_i$ buffered at 250nM using 50mM EGTA in the patch pipette solution and $[Na^+]_i$ at 20mM, NCX currents were increased with the addition of 3μM sorcin to the patch pipette. This increase was significant at both negative (-120mV & -110mV) and positive membrane (+20mV to +80mV) potentials.

3.2.11 Effect of exogenous sorcin mutants on NCX activity in freshly dissociated adult rabbit cardiomyocytes.

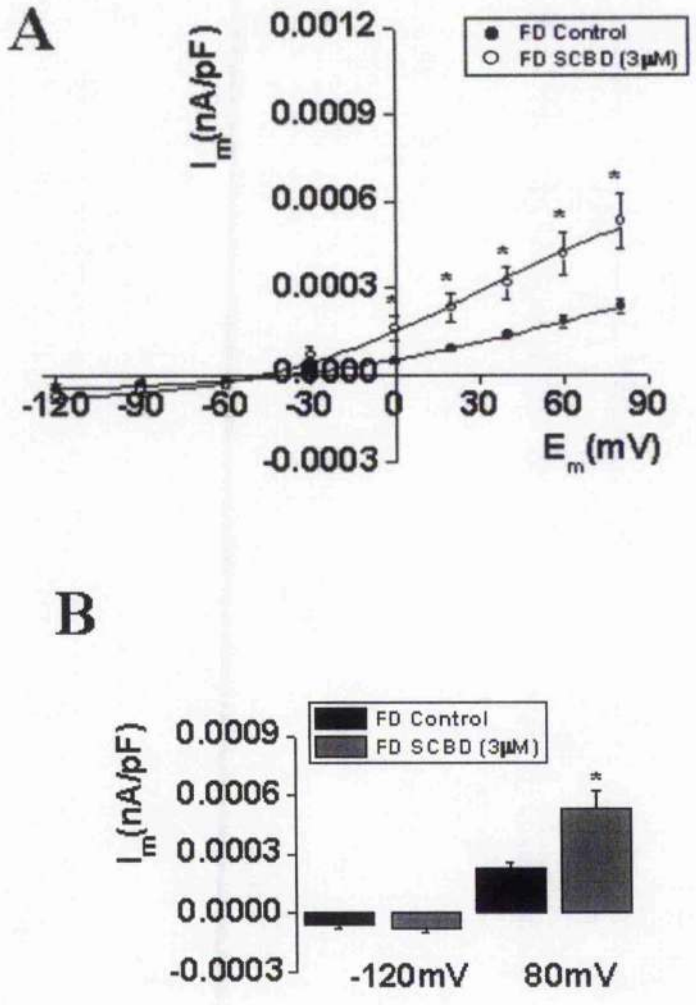


**Figure 3 - 15. The effect of exogenous sorcin mutant (SCBD) on the I-V relationship for the $Ni^{2+}$-sensitive NCX current in freshly dissociated rabbit cardiomyocytes.**

**A, Average I-V relationship in freshly dissociated cardiomyocytes (n=11) and with 3μM SCBD in patch pipette (n=8). B, Average currents measured at membrane potentials of -120mV and +80mV each experimental group.**

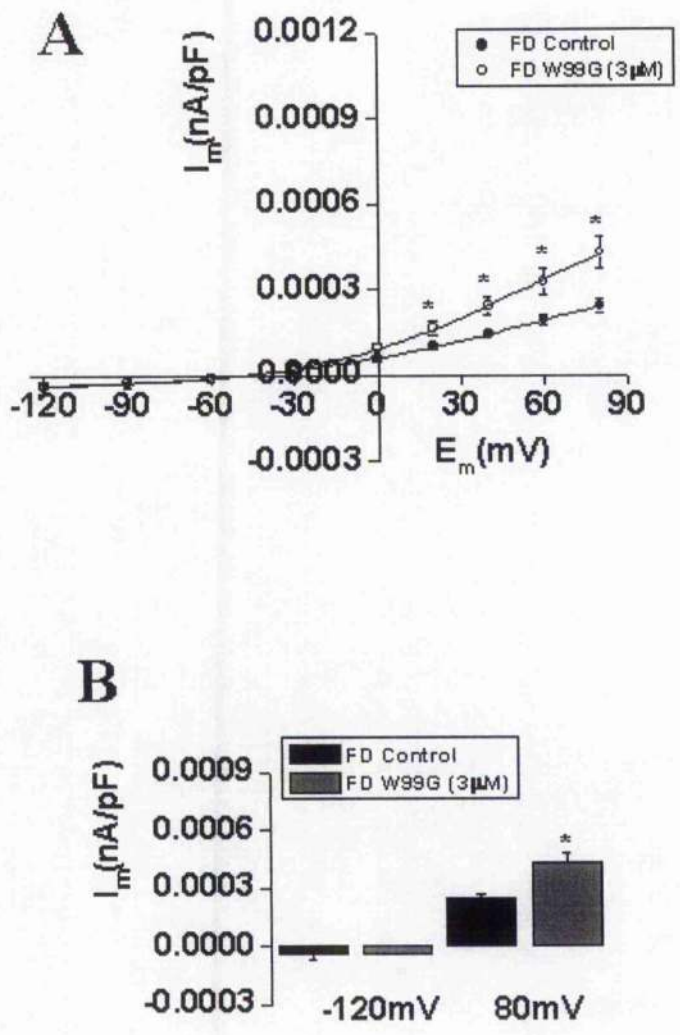


**Figure 3 - 16. The effect of exogenous sorcin mutant (W99G) on the I-V relationship for the $Ni^{2+}$-sensitive NCX current in freshly dissociated rabbit cardiomyocytes.**

**A, Average I-V relationship in freshly dissociated cardiomyocytes (n=11) and with 3μM W99G in patch pipette (n=8). B, Average currents measured at membrane potentials of -120mV and +80mV each experimental group.**

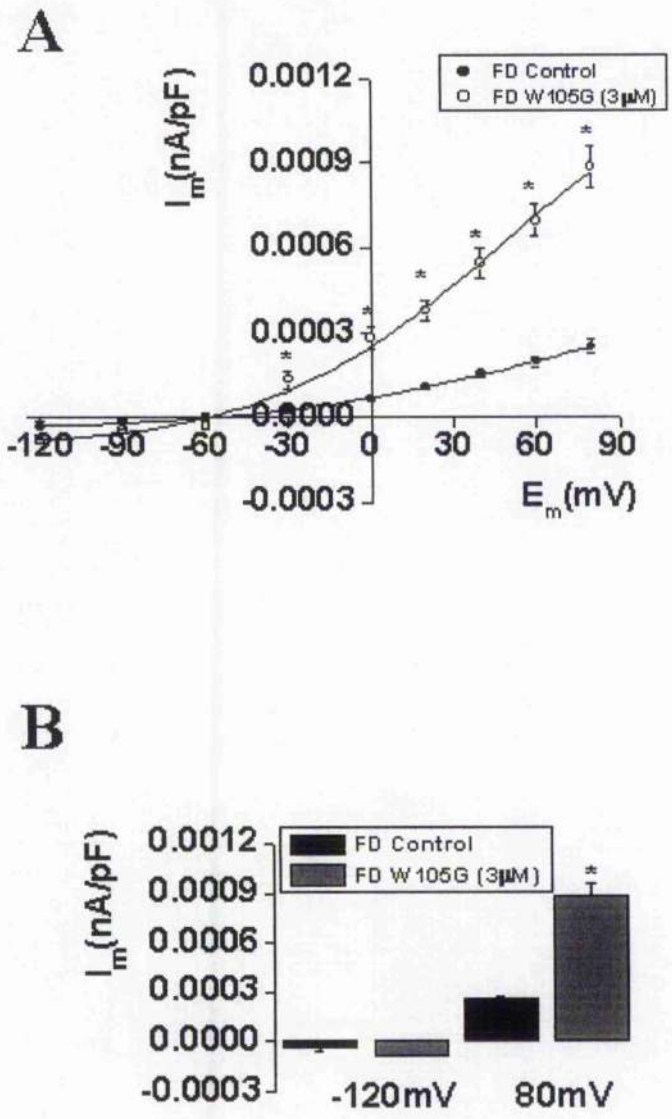


**Figure 3 - 17. The effect of exogenous sorcin mutant (W105G) on the I-V relationship for the $Ni^{2+}$-sensitive NCX current in freshly dissociated rabbit cardiomyocytes.**

**A, Average I-V relationship in freshly dissociated cardiomyocytes (n=11) and with 3μM W105G in patch pipette (n=8). B, Average currents measured at membrane potentials of -120mV and +80mV each experimental group.**

The effect of exogenous sorcin mutants SCBD, W99G and W105G on NCX activity in freshly dissociated cardiomyocytes was investigated by determining the $Ni^{2+}$-sensitive NCX current measured whilst ramping the membrane potential from −120mV to +80mV. With $[Ca^{2+}]_i$ buffered at 250nM using 50mM EGTA in the patch pipette solution and $[Na^+]_i$ at 20mM, NCX currents were significantly increased at positive membrane potentials by the addition of each of the sorcin mutants to the patch pipette. (Figures 3-15 – 3-17). Addition of SCBD to the patch pipette was less effective in increasing NCX current when compared to wild type sorcin. SCBD lacks the N-terminus of the wild type sorcin peptide and therefore one might speculate that this part of the molecule is required for sorcin to exert at least some of its effects on NCX. The W105G and the W99G mutations are located in the d-helix of the sorcin peptide and thus have the potential to prevent exposure of sorcin's N-terminus subsequent to $Ca^{2+}$ binding. The W105G mutant increased NCX current to the same extent as wild type sorcin, whereas the W99G mutant was much less effective in this respect, implying that this mutation reduced exposure of sorcin's N-terminus to a much greater extent. Figure 3-18 below demonstrates that adenoviral-mediated overexpression of the sorcin mutant E124A had no affect on NCX activity in 1-day cultured rabbit cardiomyocytes. This would be predicted given the E124A mutation destroys the $Ca^{2+}$ binding site on sorcin's EF3 hand motif.

3.2.12 Effect of adenoviral overexpression of sorcin mutant E124A (EF-3 site mutant) on NCX activity in 1-day cultured adult rabbit cardiomyocytes.

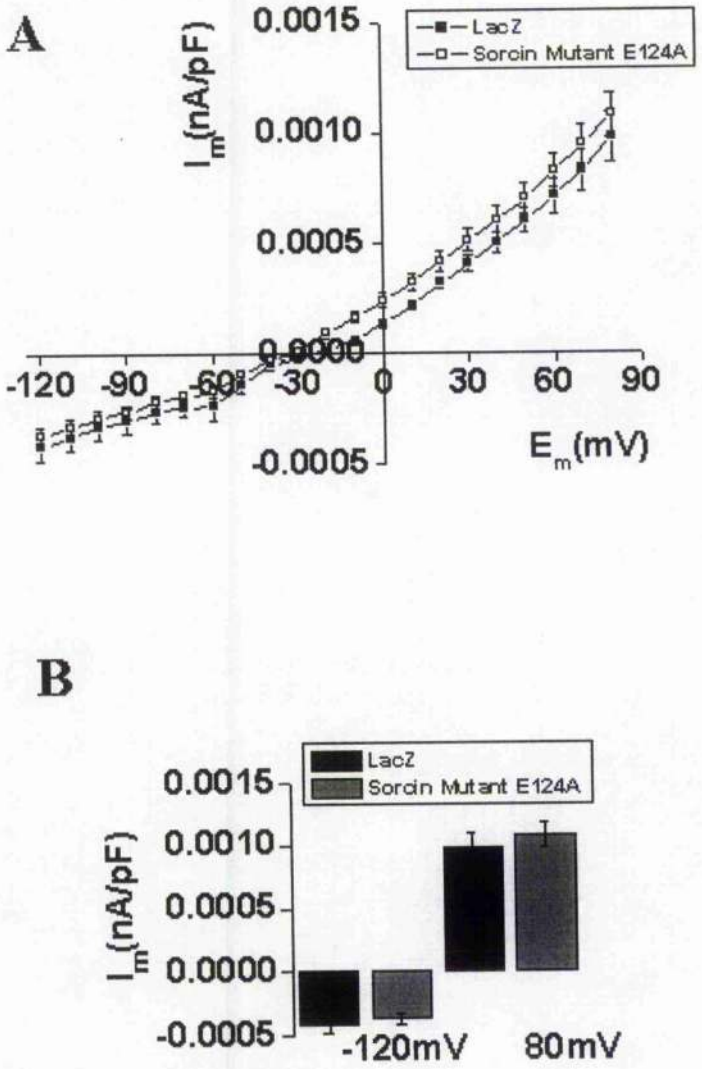


**Figure 3 - 18. The effect of adenoviral overexpression of sorcin mutant (E124A) on the I-V relationship for the $Ni^{2+}$-sensitive NCX current in 1-day cultured rabbit cardiomyocytes.**

**A, Average I-V relationship in Ad-LacZ (n=22) and Ad-sorcin (E124A) (n=13) transfected cardiomyocytes. B, Average currents measured at membrane potentials of -120mV and +80mV each experimental group.**

## 3.3 Discussion

This chapter has studied the effects of adenoviral mediated sorcin overexpression on cardiac E-C coupling in cultured rabbit cardiomyocytes. Recombinant sorcin, along with several mutant variants of the wild type protein were also employed in freshly dissociated rabbit cardiomyocytes in order to further investigate particular aspects of sorcin's actions.

### 3.3.1 The effect of sorcin on sarcolemmal $Ca^{2+}$ entry.

It has been demonstrated that sorcin is capable of binding to the $\alpha_1$-subunit of the L-type $Ca^{2+}$ channel (Meyers *et al.*, 1998), raising the possibility that sorcin may be able to modulate $Ca^{2+}$ entry into the cardiomyocyte during E-C coupling. This study has demonstrated that acute adenoviral-mediated sorcin overexpression in cultured rabbit cardiomyocytes has no effect on the amplitude, time course or I-V relationship of the L-type $Ca^{2+}$ current. This observation is in agreement with a study carried out by Farrell *et al.*, 2003, which demonstrated that exogenous sorcin (3μM) had no effect on either the amplitude or the kinetics of the L-type $Ca^{2+}$ current. Transgenic overexpression of sorcin in mice has been reported to accelerate the rapid component of $I_{Ca}$ inactivation, an effect that would reduce the size of the trigger for CICR (Meyers *et al.*, 2003). However, a reduction in the size of the trigger for CICR cannot explain the reduction in the size of the intracellular $Ca^{2+}$ transient we observe in the Ad-sorcin transfected cardiomyocytes. The lack of effect of sorcin on $I_{Ca}$ in our study might be

explained by the observed reduction in both diastolic and systolic $[Ca^{2+}]_i$, which may have adversely affected sorcin's ability to translocate between the cytosol and potential membrane bound targets.

### 3.3.2 The effect of sorcin on sarcolemmal $Ca^{2+}$ extrusion.

This study has revealed a novel effect of sorcin on sarcolemmal $Ca^{2+}$ extrusion with Ad-sorcin transfected cardiomyocytes exhibiting enhanced NCX activity when compared to Ad-LacZ control. The increase in NCX activity was manifest as a faster rate of decay of the caffeine-induced calcium transient, a faster rate of decay of the transient inward current ($I_{NCX}$) in response to caffeine and increased $Ni^{2+}$-sensitive outward currents at membrane voltages positive to the reversal potential for $I_{NCX}$. Furthermore, end diastolic $[Ca^{2+}]_i$ was also significantly reduced in Ad-sorcin transfected cardiomyocytes, again indicative of enhanced $Ca^{2+}$ extrusion via NCX. However, the rate of decay of the caffeine-induced calcium release in the presence of $Ni^{2+}$ was unaffected by sorcin overexpression, illustrating that $Ca^{2+}$ extrusion from the cardiomyocytes via $Ni^{2+}$ insensitive mechanisms, such as the sarcolemmal $Ca^{2+}$-ATPase, is unaltered by sorcin.

This effect of sorcin on NCX activity was also demonstrated using whole cell voltage clamp in freshly dissociated rabbit cardiomyocytes with the addition of 3μM exogenous sorcin to the patch pipette. Under these conditions voltage ramps from −120mV to +80mV again revealed

significantly increased $Ni^{2+}$-sensitive outward currents at membrane potentials positive to the reversal potential for NCX. At membrane potentials negative to the reversal potential for NCX there was a trend towards increased $Ni^{2+}$-sensitive inward currents, although this increase did not reach significance. Better definition of the $Ni^{2+}$-sensitive inward currents was achieved by bathing the myocytes in a solution containing nominally zero $Ca^{2+}$. Such conditions make inward NCX current more favourable, and indeed, under these circumstances addition of 3μM sorcin to the patch pipette revealed a significantly increased $Ni^{2+}$-sensitive inward current during voltage ramps.

The cellular mechanism under-lying the sorcin-induced increase in NCX activity is unknown and was further investigated by adding either fragments or mutant variants of the sorcin molecule to the patch pipette under conditions of whole cell voltage clamp. The amino acid sequence of sorcin is shown in figure 3-19 below.


**Figure 3-19. The amino acid sequence of the sorcin peptide.**

Addition of the sorcin calcium binding domain (SCBD), residues 33-198, to the patch pipette significantly increased the outward $Ni^{2+}$-sensitive current when compared to control at membrane potentials positive to the reversal potential for NCX during voltage ramps, but not to the extent of wild-type sorcin. SCBD lacks the N-terminal domain of the wild-type sorcin protein, a part of the molecule that has previously been shown to bind to annexin VII (Brownawell & Creutz, 1997). Thus one might speculate that sorcin must bind to annexin VII, or some other as yet unknown cytosolic target, in order to exert some of its effects on NCX.

Similarly, sorcin mutants W99G and W105G were also added to the patch pipette during voltage ramps. These point mutations are located in a part of the sorcin molecule known as the D helix which links the EF3 hand motif to the EF2 hand motif. It has been proposed that binding of $Ca^{2+}$ to the EF3

motif causes a conformational change that is transferred to the EF2 motif via the D helix. The pairing of the EF2 motif and the EF1 motif facilitates transfer of the information that $Ca^{2+}$ is bound to the latter site and from there, onto the N-terminus of the protein (Mella *et al.*, 2003). The N-terminus, which is hydrophobic and therefore normally inaccessible, becomes exposed and may go on to bind to potential sorcin targets. If, as suggested previously, the N-terminal domain of sorcin must bind to annexin VII or another cytosolic target in order to exert some of its effects on NCX, then we might expect these mutants to be less effective in increasing NCX activity when compared to wild-type sorcin. Indeed, our results demonstrate that whilst the W105G mutant increases NCX activity to a similar extent as wild-type sorcin, the W99G mutant is much less effective in doing so.

Hence, both SCBD and W99G have a reduced capability to stimulate NCX and both are disabled with regard to their N-terminal domains. It is therefore plausible that that this part of the sorcin molecule, under normal circumstances, must bind to a cytosolic target such as annexin VII in order to exert some of its effects on NCX. However, it is noteworthy that both SCBD and W99G still significantly increase NCX activity when compared to control. Thus sorcin must also be able to regulate the exchanger via a pathway that is independent of its N-terminal domain.

In addition, the effect of adenoviral overexpression of a sorcin mutant, E124A, on NCX activity in cultured rabbit cardiomyocytes was investigated, again using voltage ramps. The E124A mutation is located in the EF3 hand motif of the sorcin molecule and has previously been shown to cause

severe functional disruption in terms of sorcin's affinity for $Ca^{2+}$, RyR and annexin VII (Mella *et al.*, 2003). In agreement with these observations, our results demonstrate that the E124A sorcin mutant has no effect on NCX activity.

3.3.3 The effect of sorcin on E-C coupling in voltage clamped adult rabbit cardiomyocytes.

Whole cell voltage clamp studies revealed that both the intracellular calcium transient amplitude and the SR calcium content were significantly reduced in the Ad-sorcin transfected cardiomyocytes. Given that both the peak amplitude and integral of the L-type $Ca^{2+}$ current, the trigger for CICR, were unaffected by sorcin overexpression it seemed likely that the reduction in SR $Ca^{2+}$ content could account for the reduction in the size of the intracellular $Ca^{2+}$ transient. In order to determine whether this was the case, the relationship between SR $Ca^{2+}$ load and intracellular calcium transient amplitude for both Ad-LacZ and Ad-sorcin transfected cardiomyocytes was established. Reduction in SR $Ca^{2+}$ load was achieved by perfusing cells with thapsigargin for varying lengths of time. It is clear from figure 3-10, that when the SR $Ca^{2+}$ load of the Ad-LacZ transfected cardiomyocytes was reduced to a level equivalent to that normally observed in the Ad-sorcin transfected cells, the calcium transient amplitudes in both experimental groups did not differ significantly. Furthermore, when the SR $Ca^{2+}$ load in the Ad-sorcin transfected cardiomyocytes was reduced, the amplitude of the $Ca^{2+}$ transient was also very similar to that predicted for

Ad-LacZ transfected cardiomyocytes with a similar SR $Ca^{2+}$ load. Hence, these results indicate that the reduced SR $Ca^{2+}$ content in the Ad-sorcin transfected cardiomyocytes can predominantly account for the reduction in the amplitude of the intracellular $Ca^{2+}$ transient observed. Given we have established that sorcin increases NCX activity, it seems highly likely that increased $Ca^{2+}$ extrusion from the cardiomyocyte via this route may ultimately account for the reduced SR $Ca^{2+}$ load observed in Ad-sorcin transfected cardiomyocytes. A previous study by Schillinger *et al.*, 2000, used adenoviral mediated gene transfer to overexpress NCX in cultured rabbit cardiomyocytes and observed reduced fractional shortening and smaller caffeine contractures, similar to the results reported here. Indeed, the data presented in Chapter 6 of this thesis are also consistent with adenoviral-mediated overexpression of NCX reducing SR $Ca^{2+}$ load and the size of the intracellular $Ca^{2+}$ transient.

### 3.3.4 The effect of sorcin on $Ca^{2+}$ spark characteristics in permeabilised myocytes.

Previous studies have demonstrated that in the presence of increasing [$Ca^{2+}$], sorcin reduces ryanodine binding and hence RyR open probability in cardiac microsomes (Lokuta *et al.*, 1997). Hence, one would expect that sorcin may affect the characteristics of spontaneous $Ca^{2+}$ sparks. In this study spontaneous $Ca^{2+}$ sparks were studied in β-escin permeabilised cardiomyocytes using laser scanning confocal microscopy (LSCM). Permeabilisation of the myocytes enabled circumvention of sorcin's effects

on NCX and also perfusion of the intracellular milieu with a solution that had a tightly controlled [$Ca^{2+}$]. Previous work has established that $Ca^{2+}$ sparks in permeabilised cells are indistinguishable from those observed in intact cells, but with the advantage that intracellular conditions can be standardised (Lukyanenko & Gyorke, 1999).

The data presented here demonstrate that whilst SR $Ca^{2+}$ load was similar in both Ad-LacZ and Ad-sorcin transfected groups, the spontaneous $Ca^{2+}$ sparks observed differed markedly, with spark amplitude, width, duration and frequency all significantly reduced. These results are consistent with previous observations that sorcin prolongs the mean close time of the RyR without modifying single channel conductance (Lokuta *et al.*, 1997) and that sorcin has an inhibitory effect on the occurrence of spontaneous $Ca^{2+}$ sparks (Farrell *et al.*, 2003).

### 3.3.5 Anomalies.

Given sorcin overexpression reduces the $P_O$ of RyR (Lokuta *et al.*, 1997), one would expect to see an effect on the gain of E-C coupling in the Ad-sorcin transfected group. Our data in cultured rabbit cardiomyocytes demonstrates that the relationship between SR $Ca^{2+}$ content and calcium transient amplitude (with L-type $Ca^{2+}$ current unaffected) is the same in both Ad-LacZ and Ad-sorcin transfected myocytes. This would suggest that E-C coupling gain is unaffected by sorcin overexpression. Figure 3-20 below demonstrates the effect of perfusion with 100μM tetracaine on E-C

coupling gain in freshly dissociated rabbit cardiomyocytes. Tetracaine reduces the $Ca^{2+}$ sensitivity of RyR2 and thus reduces its $P_O$ at any given $[Ca^{2+}]_i$.

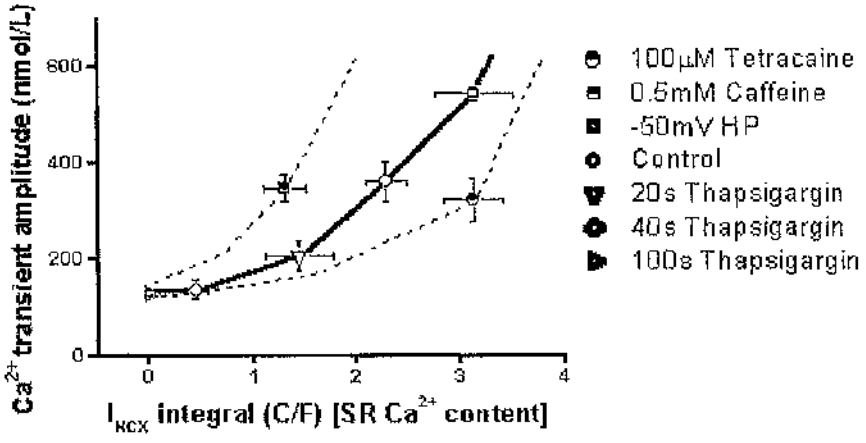


**Figure 3 -20. Relationship between INCX integral (an index of SR content) and Ca2+ transient amplitude for freshly dissociated cardiomyocytes under control conditions and in the presence of both caffeine and tetracaine.**

**Reduced SR loads were achieved by exposure to 5μM thapsigargin for various times. (Diagram kindly supplied by Dr. Sarah Kettlewell, data as yet unpublished).**

Tetracaine clearly reduces the gain of E-C coupling, shifting the normal relationship between SR $Ca^{2+}$ load and calcium transient amplitude to the right. Hence a reduced calcium transient amplitude is expected for any given SR $Ca^{2+}$ load. One might predict that sorcin overexpression (where sorcin also reduces the $P_O$ of RyR) would have a similar effect to tetracaine on the gain of E-C coupling.

However, it should be noted that tetracaine and sorcin have different effects on the occurrence of spontaneous $Ca^{2+}$ sparks. We demonstrate here that

sorcin clearly reduces both the size and frequency of spontaneous $Ca^{2+}$ sparks, without affecting SR $Ca^{2+}$ load. On the other hand, tetracaine has a bi-phasic effect on spontaneous $Ca^{2+}$ sparks. Initially it inhibits $Ca^{2+}$ sparks, reducing both the frequency and magnitude of release events, but with time the SR $Ca^{2+}$ gradually increases, ultimately increasing the frequency and magnitude of $Ca^{2+}$ sparks with respect to control (Gyorke *et al.*, 1997). If we make two assumptions: 1 - that calcium transients are the product of the temporal and spatial summation of individual $Ca^{2+}$ sparks, the release of which are co-ordinated by the L-type $Ca^{2+}$ current. 2- that the calcium released during a spontaneous $Ca^{2+}$ spark is identical to the calcium released when a cluster of RyRs is activated by L-type $Ca^{2+}$ current Cannell *et al.*, 1995, then perhaps it is not surprising that sorcin and tetracaine do not affect the gain of E-C coupling in a similar way. The resolution of this anomaly would require a better investigation of the relationship between $Ca^{2+}$ spark and $Ca^{2+}$ transient amplitude.

# Chapter 4 - Calsequestrin overexpression and E-C coupling in isolated rabbit cardiomyocytes.

## 4.1 An introduction to calsequestrin.

### 4.1.1 Structure and location of Calsequestrin.

Calsequestrin (CSQ) is the main calcium binding protein inside the SR and was first identified in skeletal muscle by MacLennan & Wong, 1971. Campbell *et al.*, 1983, were the first to identify and purify the protein in cardiac muscle. CSQ is made up of 109 amino acid residues and has an approximate molecular mass of 60kDa. A large proportion of these amino acids are acidic and thus permit a single molecule of calsequestrin to bind in the region of 40-50 $Ca^{2+}$ ions (Yano & Zarain-Herzberg, 1994). Franzini-Armstrong *et al.*, 1987 demonstrated using electron microscopy that cardiac calsequestrin aggregates in an area of the SR called the terminal cisternae which are known to contain SR calcium release channels or RyRs. Such observations led to the suggestion that calsequestrin may also have a function in the modulation of the RyR.

### 4.1.2 Calsequestrin and the ryanodine recpetor.

Studies carried out using lipids bilayers have suggested that a combination of luminal [$Ca^{2+}$] and the presence of CSQ may combine to modulate the RyR. Ikemoto *et al.*, 1989, demonstrated that the fluorescence intensity and hence the structure of a junctional face membrane – CSQ molecular complex (from skeletal muscle) was altered when [$Ca^{2+}$] was increased. When CSQ was dissociated from the complex there was no such change in

fluorescence, and hence structure, when [$Ca^{2+}$] was increased. This work suggested that if dissociation of CSQ could affect the structure of a molecular complex containing the RyR, then it may also affect the function of the RyR.

Kawasaki & Kasai, 1994, incorporated the heavy fraction of skeletal muscle SR vesicles into bilayers and demonstrated that the open probability ($P_O$) of the RyR increased slightly when 2mM $Ca^{2+}$ was added to the luminal side of the bilayer. Subsequent addition of 500μM CSQ to the luminal side of the bilayer with stirring then caused a marked increase in RyR channel activity. If $Ca^{2+}$ were absent then such addition of CSQ had no effect on channel activity. In a similar preparation, also using skeletal muscle heavy SR vesicles, Szegedi *et al.*, 1999, have shown that increasing luminal free [$Ca^{2+}$] from 50μM to 1mM caused a decrease in the $P_O$ of the RyR from 0.6 to <0.1. However, if luminal free [$Ca^{2+}$] was fixed at 1mM and dephosphorylated CSQ was added to the luminal side, a dose dependent increase in RyR $P_O$ was observed. Intriguingly this control was highly dependent on the phosphorylation state of CSQ, with phosphorylated CSQ having no effect on the $P_O$ of the RyR.

Beard *et al.*, 2002, have dissociated CSQ from SR junctional face membranes. RYRs from these membrane fractions exhibited a 3-fold increase in relative mean current when compared to control. Adding CSQ back to the luminal side of the channel reversed this increased activity and would suggest that under these circumstances, CSQ served to inhibit RyR activity.

Zhang *et al.*, 1997, provide evidence that CSQ may be involved in the regulation of the cardiac RyR. They demonstrated that two linker proteins, junctin and triadin, both highly concentrated in the SR membrane, bind tightly not just to each other but also luminally to both RyR and CSQ. Such a complex formation would anchor CSQ beside the SR membrane and in close proximity to the RyR. Subsequently, Gyorke *et al.*, 2004, have investigated the effects of different combinations of junctin, triadin and CSQ on the open probability of purified cardiac RyRs in lipid bilayers (see figure 4-1).

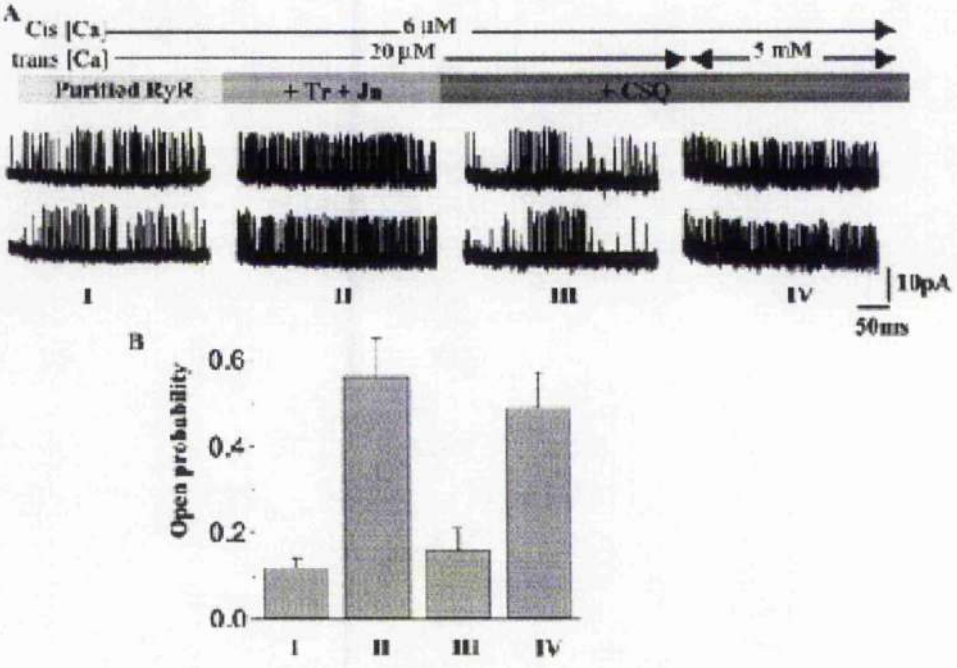


**Figure 4 - 1. Effects of sequential addition of junctin and triadin 1 and calsequestrin on activity of purified RyRs and their ability to respond to luminal Ca.**

**(A) Representative traces of current recordings from a single purified RyR before (I) and after (II) addition of triadin 1 and junctin (5 μg/ml of each) to the trans chamber, after subsequent addition of calsequestrin (III), and after an increase of trans [$Ca^{2+}$]**

**from 20 μM to 5 mM (IV). Data presented as mean ± SE (n = 3) from Gyorke *et al.*, 2004.**

It is clear from figure 4-1 that addition of CSQ to purified RyR, with junctin and triadin already bound, causes a reduction in the open probability of the channel with luminal [$Ca^{2+}$] held constant.

The effects of altering luminal free [$Ca^{2+}$] on cardiac RyR are well documented. Lukyanenko *et al.*, 1996, demonstrated that SR $Ca^{2+}$ overload increased the frequency and amplitude, but not the duration of spontaneous $Ca^{2+}$ sparks in intact ventricular myocytes. Studying single RyRs in lipid bilayers they also showed that elevating luminal $Ca^{2+}$ increased the $P_O$ of the channel. Also using single cardiac RyRs in lipid bilayers, Ching *et al.*, 2000, have shown that increasing luminal $Ca^{2+}$ increased the $P_O$ of the RyR. Again in a cardiac lipid bilayer preparation Gyorke & Gyorke, 1998, have shown that under conditions of low luminal $Ca^{2+}$, elevating cytoplasmic $Ca^{2+}$ from 0.1 to 10μM caused a gradual increase in the $P_O$ of the RyR. Increasing cytoplasmic $Ca^{2+}$ above 100μM caused a gradual decrease in RyR $P_O$. Elevating luminal $Ca^{2+}$ enhanced RyR activity, enhanced the sensitivity of the channel to cytoplasmic $Ca^{2+}$ and reversed the inhibition of the channel by high cytosolic $Ca^{2+}$. These results all suggest that cardiac RyR activity is increased by elevated SR intraluminal $Ca^{2+}$.

### 4.1.3 Transgenic overexpression of calsequestrin in the heart.

Several investigators have employed genetic engineering to generate mice that intrinsically over-express cardiac CSQ. Such models are associated with both cardiac hypertrophy and depressed cardiovascular function, as seen in heart failure.

Sato *et al.*, 1998, have shown that a 20-fold over-expression of CSQ was associated with a 46% reduction in myocyte shortening and a 45% depression of the intracellular $Ca^{2+}$ transient amplitude, despite the observation that SR $Ca^{2+}$ load was increased. In addition they observed a decreased L-type $Ca^{2+}$ current density coupled with a prolongation of the channel's inactivation kinetics, an increase in protein expression of SR $Ca^{2+}$ ATPase, phospholamban and calreticulin, a decrease in expression of FKBP12 whilst expression of RyR, junctin and triadin remained unchanged in the transgenic hearts.

Jones *et al.*, 1998, demonstrated that a 10-fold over-expression of CSQ again caused a significant reduction in CICR. This was despite an unchanged peak $I_{Ca}$, a significantly slower inactivation of $I_{Ca}$ and a 10-fold increase in SR $Ca^{2+}$ content in the CSQ-overexpressing cardiomyocytes. It should be noted that protein expression of RyR, junctin and triadin were reduced, whilst expression of the calcium uptake proteins, SERCA and phospholamban, were unaltered or slightly increased in the transgenic hearts.

Wang *et al.*, 2000, have shown that the occurrence of spontaneous $Ca^{2+}$ sparks is markedly reduced in transgenic CSQ-overexpressing mouse cardiomyocytes when compared to control. The density of $I_{Ca}$ was slightly reduced whilst the inactivation kinetics of the current were greatly reduced. Global $Ca^{2+}$ transients were smaller in amplitude and had a reduced rate of rise in the CSQ-overexpressing myocytes, despite an increased SR $Ca^{2+}$ content.

Knollmann *et al.*, 2000, investigated the remodelling of ionic currents in the failing hearts of transgenic mice overexpressing CSQ. There was a marked reduction in both density and absolute magnitude of the transient outward ($I_{to}$) and inward rectifying ($I_{K1}$) $K^+$ currents, something that has also been demonstrated in human heart failure (Beuckelmann *et al.*, 1993) and has been implicated in the development of ventricular arrhythmias. The density of both basal and isoprenaline stimulated $I_{Ca}$ was almost halved in the CSQ-overexpressing cardiomyocytes, with the inactivation kinetics of $I_{Ca}$ again significantly slowed. Interestingly the density of the $Na^+$-$Ca^{2+}$ exchange current was increased by 35% in the CSQ-overexpressing myocytes.

4.1.5 Adenoviral mediated overexpression of calsequestrin in the heart.

More recently, Terentyev *et al.*, 2003b, have employed an adenoviral gene transfer strategy in order to induce a four fold overexpression of calsequestrin in rat ventricular myocytes. SR $Ca^{2+}$ load, as assessed by

the size of the caffeine-induced calcium transient and the integral of the concomitant transient inward current was doubled when compared to control. Expression of SERCA and PLB was unaltered. CSQ overexpression did not affect the L-type $Ca^{2+}$ current, however it did increase the rise time, the magnitude and the duration of intracellular $Ca^{2+}$ transients measured using whole cell voltage clamp. In addition, the amplitude but not the frequency of spontaneous $Ca^{2+}$ sparks measured in permeabilised myocytes was significantly increased in the CSQ overexpressing group. Interestingly, Viatchenko-Karpinski *et al.*, 2004, have also used adenovirus to overexpress a CSQ mutant ($CSQ^{D307H}$) in rat ventricular cardiomyocytes that has been linked to catecholaminergic polymorphic ventricular tachycardia. Cardiomyocytes transfected with $CSQ^{D307H}$ exhibited a reduced SR $Ca^{2+}$ load, reduced $I_{Ca}$-induced $Ca^{2+}$ transients and smaller spontaneous $Ca^{2+}$ sparks when compared to cardiomyocytes overexpressing wild-type CSQ. The results implied that the mutant form of CSQ impaired both its SR storage and release functions.

Taken together, both of these studies provide strong evidence that CSQ is both a storage and a regulatory protein in the cardiac muscle $Ca^{2+}$ signalling cascade.

### 4.1.6 Aims

To evaluate the effect of CSQ on cardiac E-C coupling, adult rabbit ventricular myocytes were transfected with a recombinant adenovirus coding for human CSQ (Ad-CSQ). A β-galactosidase virus was used as a

control (Ad-LacZ). Viruses were constructed by Dr. Tim Seidler, Georg-August-Universitat, Goettingen, Germany.

It was proposed that after 24 hrs in culture the virus-transfected cells would be loaded with fura-2 and E-C coupling studied using whole cell voltage clamp. This was to enable the effects of CSQ overexpression on the L-type $Ca^{2+}$ current, the intracellular $Ca^{2+}$ transient, SR $Ca^{2+}$ load, NCX activity and sarcolemmal $Ca^{2+}$ ATPase activity to be determined. In addition, the effects of acute overexpression of CSQ on $Ca^{2+}$ spark characteristics were obtained using laser scanning confocal microscopy.

## 4.2 Results

### 4.2.1 Measurement of CSQ mRNA and protein expression levels.

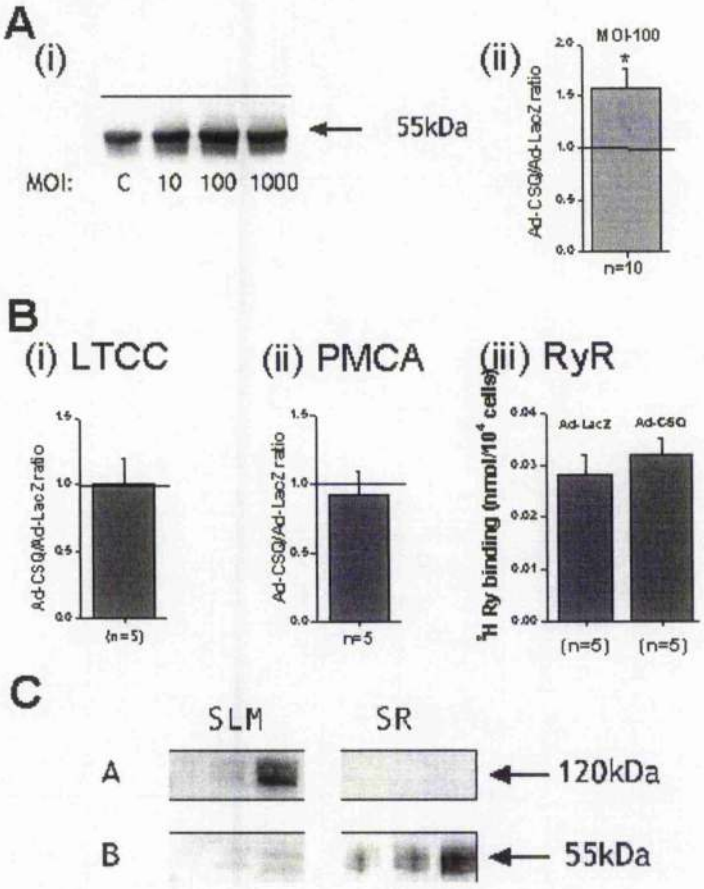


**Figure 4 - 2. Protein expression in Ad-CSQ transfected cardiomyocytes.**

**(A) (i) Verification of CSQ protein over-expression in isolated adult rabbit cardiomyocytes 24h after transfection with various MOI's (ii) CSQ protein overexpression, Ad-LacZ (MOI = 100) vs. Ad-CSQ (MOI = 100). (B) Verification of (i) unaltered L-type $Ca^{2+}$ channel expression (ii) unaltered sarcolemmal $Ca^{2+}$-ATPase expression and (iii) unaltered maximal $^{3}H$ Ryanodine binding when Ad-LacZ transfected cardiomyocytes are compared to Ad-CSQ. (C) Verification that CSQ can only be detected in SR preparations and not in sarcolemmal preparations from Ad-**

**CSQ transfected cardiomyocytes. Measurements by Dr. Susan Currie, University of Glasgow.**

4.2.2 Effect of CSQ overexpression on the L-type $Ca^{2+}$ current and intracellular $Ca^{2+}$ transient.

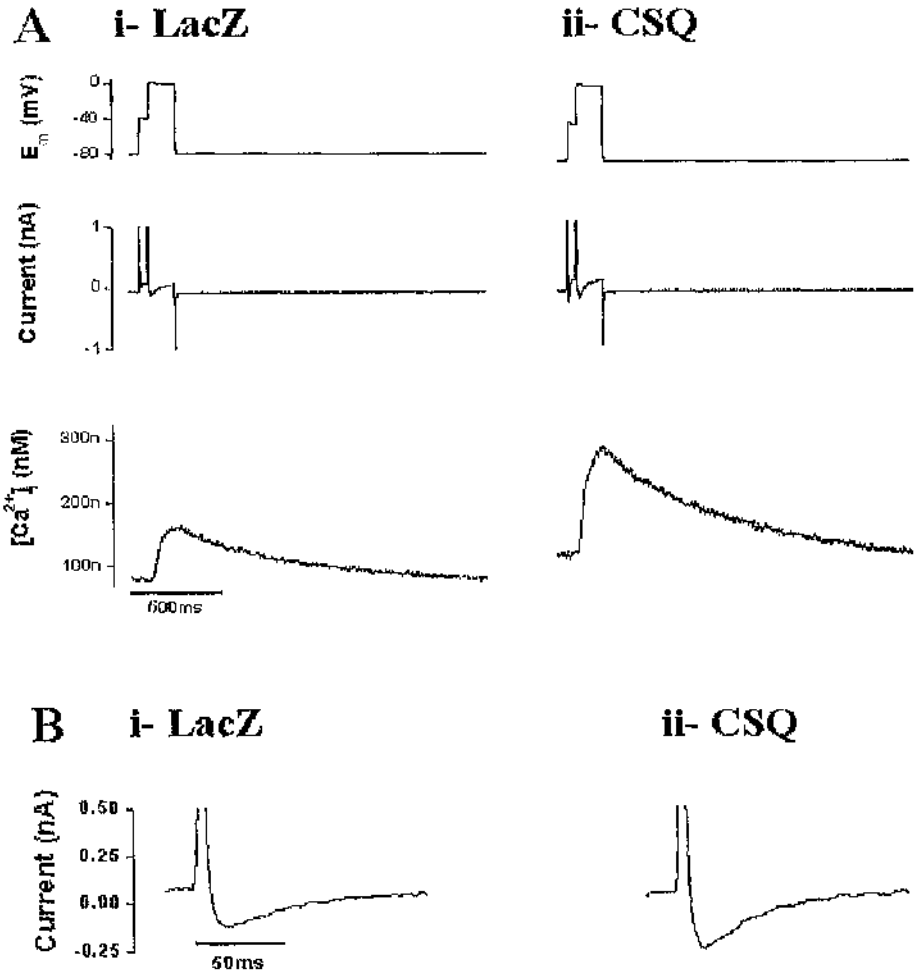


**Figure 4 - 3. Depolarisation-induced L-type $Ca^{2+}$ currents and intracellular $Ca^{2+}$ transients in voltage clamped Ad-LacZ (i) and Ad-CSQ (ii) transfected cardiomyocytes.**

**A, Typical traces of membrane potential ($E_m$), membrane current and $[Ca^{2+}]_i$ from single cardiomyocytes (average of 10 sweeps). B, Membrane current recorded upon**

voltage step from –40mV to 0mV for 150ms, illustrating the time course and the amplitude of $I_{Ca}$.

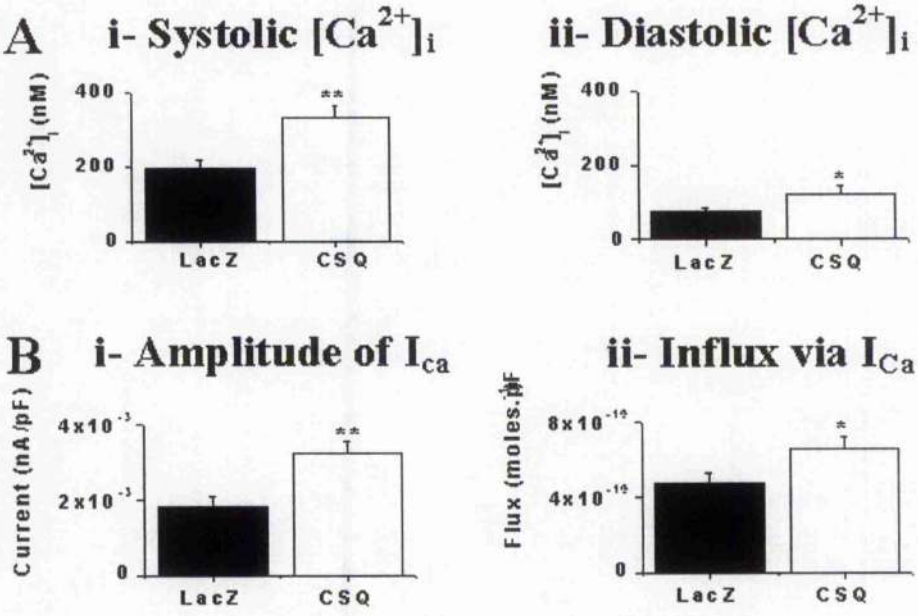


**Figure 4 - 4. EC-coupling in Ad-LacZ and Ad-CSQ transfected cardiomyocytes.**

**A, Mean ± SEM values of peak systolic (i) and end diastolic (ii) $[Ca^{2+}]_i$ and B, Mean ± SEM values of peak $I_{Ca}$ (i) and $Ca^{2+}$ influx via $I_{Ca}$ in Ad-LacZ and Ad-CSQ transfected cardiomyocytes. (Ad-LacZ, n=17 vs. Ad-CSQ, n=23).**

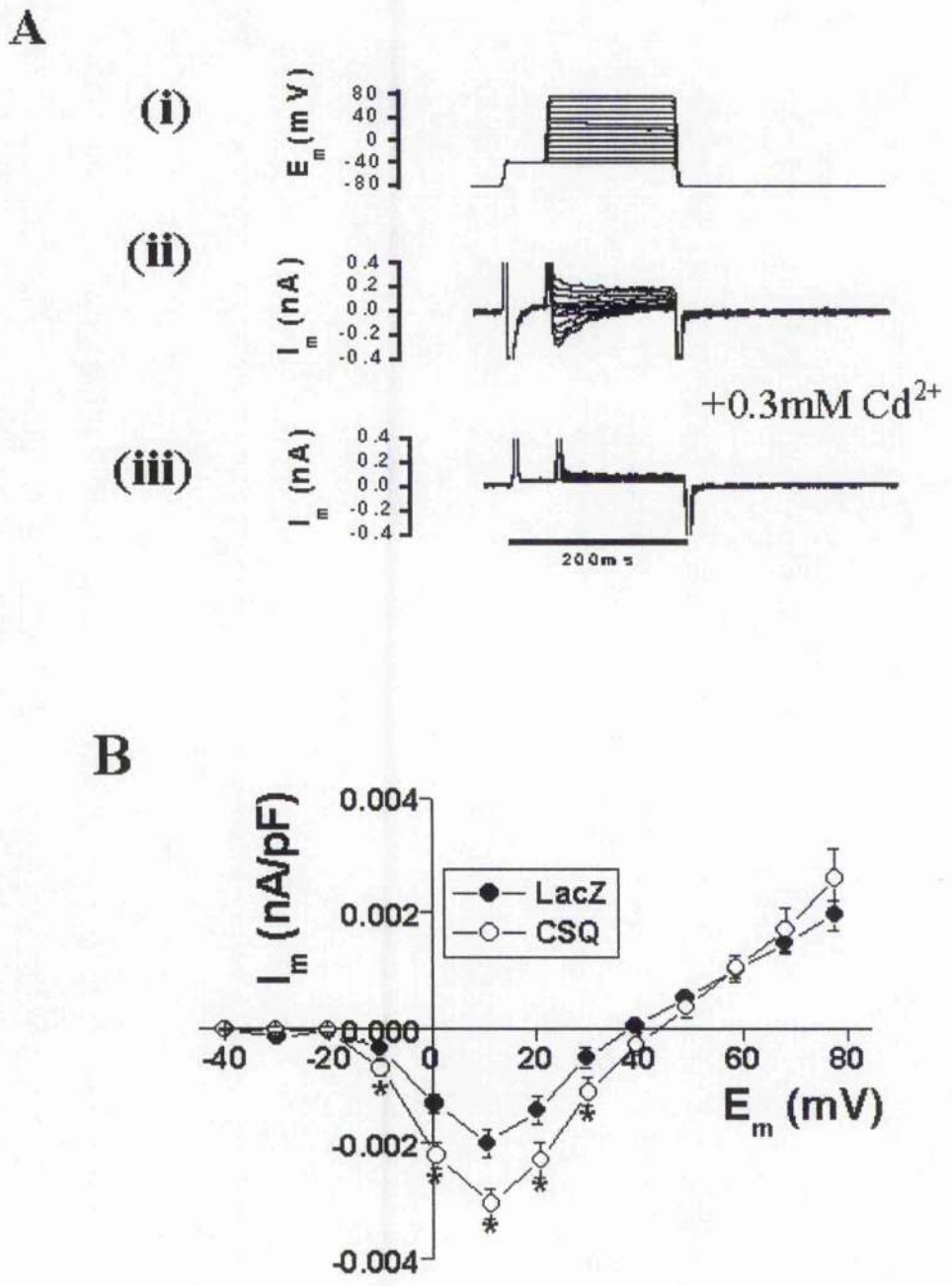


**Figure 4 - 5. I-V relationship for $I_{Ca}$ in Ad-CSQ and Ad-LacZ transfected cardiomyocytes.**

**Voltage clamp protocol (i) used to investigate the I-V relationship for $I_{Ca}$ in Ad-CSQ and Ad-LacZ transfected cardiomyocytes. Current traces obtained in the absence (ii)**

and in the presence of $Cd^{2+}$ (iii). B, I-V relationship for $I_{Ca}$ (points represent mean ± SEM values). (Ad-LacZ, n=9 vs. Ad-CSQ, n=13).

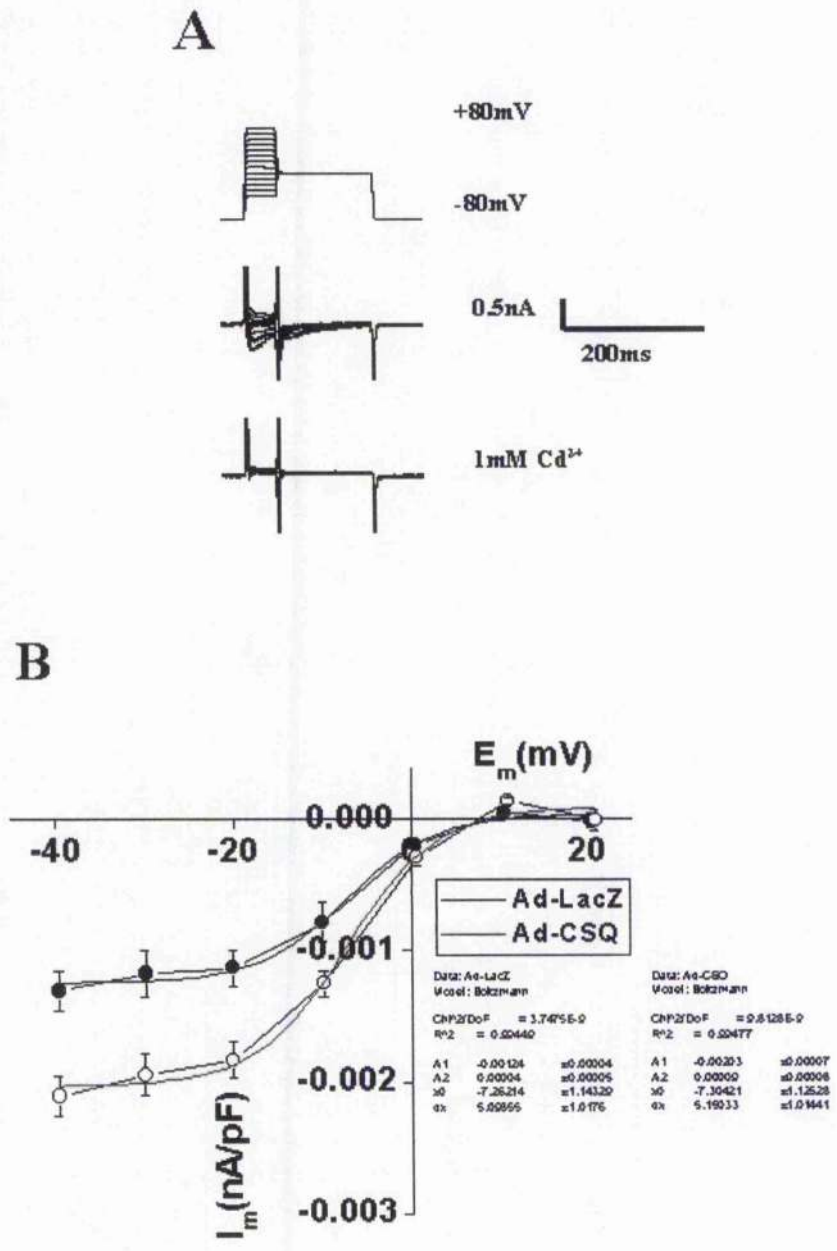


**Figure 4 - 6. (A) Voltage clamp protocol used to determine the inactivation curve of the $Cd^{2+}$ sensitive L-type $Ca^{2+}$ current.**

**Typical current traces under control conditions and in the presence of $Cd^{2+}$. The difference represents the $Cd^{2+}$ sensitive current attributed to $I_{Ca}$. Panel B shows the**

**average I-V relationship of the inactivation of the $Cd^{2+}$ sensitive L-type $Ca^{2+}$ current measured in Ad-LacZ (n=13) and Ad-CSQ (n=11) transfected cardiomyocytes.**

Figure 4-4 A demonstrates that Ad-CSQ transfection significantly increased both peak systolic and end diastolic $[Ca^{2+}]_i$ in voltage clamped rabbit cardiomyocytes. Figure 4-4 B shows that both the amplitude and the time integral of $I_{Ca}$ (which can be converted to a $Ca^{2+}$ influx) are significantly increased by CSQ overexpression. This observation was confirmed via investigation of the I-V relationship for $I_{Ca}$. Figure 4-5 clearly shows that Ad-CSQ transfection significantly increased $I_{Ca}$ amplitude over a range of membrane potentials. Figure 4-6 demonstrates that the inactivation kinetics of $I_{Ca}$ were unaltered by CSQ overexpression, with the membrane potential for half inactivation of the current approximately –7mV in both experimental groups.

4.2.3 Effect of CSQ overexpression on SR $Ca^{2+}$ content (assessed by rapid application of 10mM caffeine).

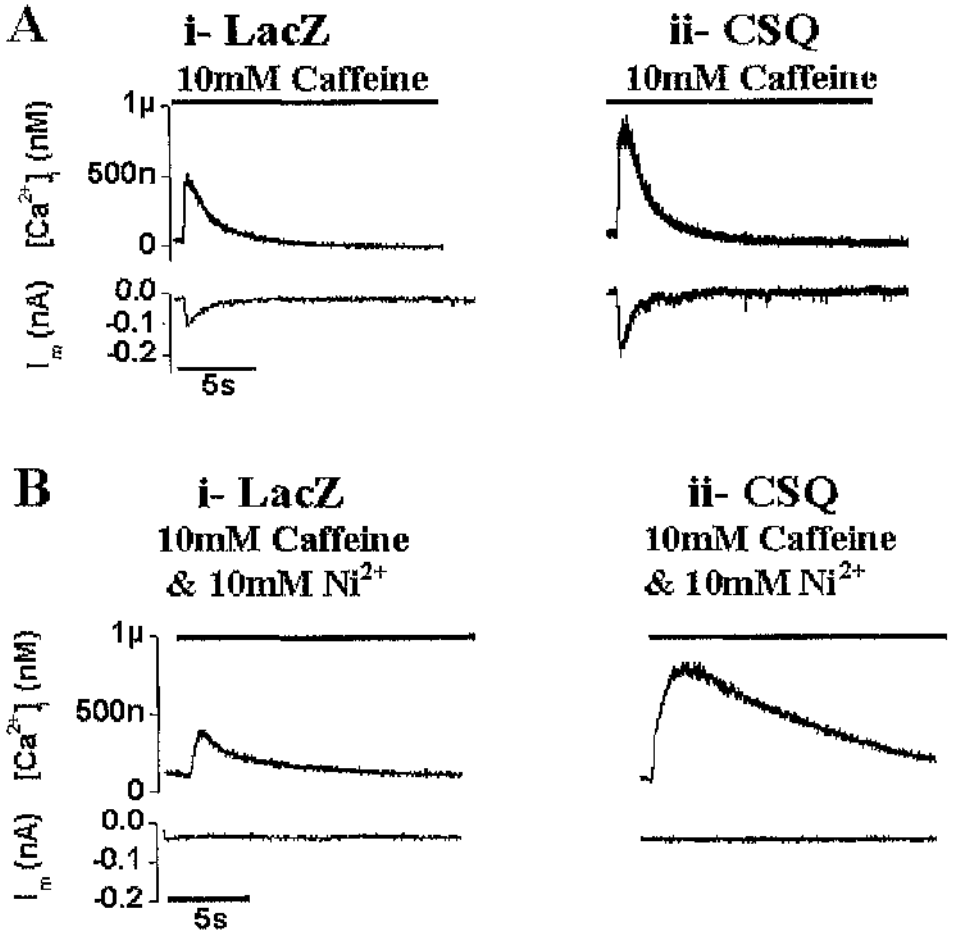


**Figure 4 – 7. CSQ overexpression and SR $Ca^{2+}$ load.**

**A, SR $Ca^{2+}$ release and corresponding membrane currents recorded upon rapid application of 10mM caffeine in typical Ad-LacZ (i) and Ad-CSQ (ii) transfected cardiomyocytes. B, SR $Ca^{2+}$ release and corresponding membrane currents recorded upon rapid application of 10mM caffeine & 10mM $Ni^{2+}$ in typical Ad-LacZ (i) and Ad-CSQ (ii) transfected cardiomyocytes.**

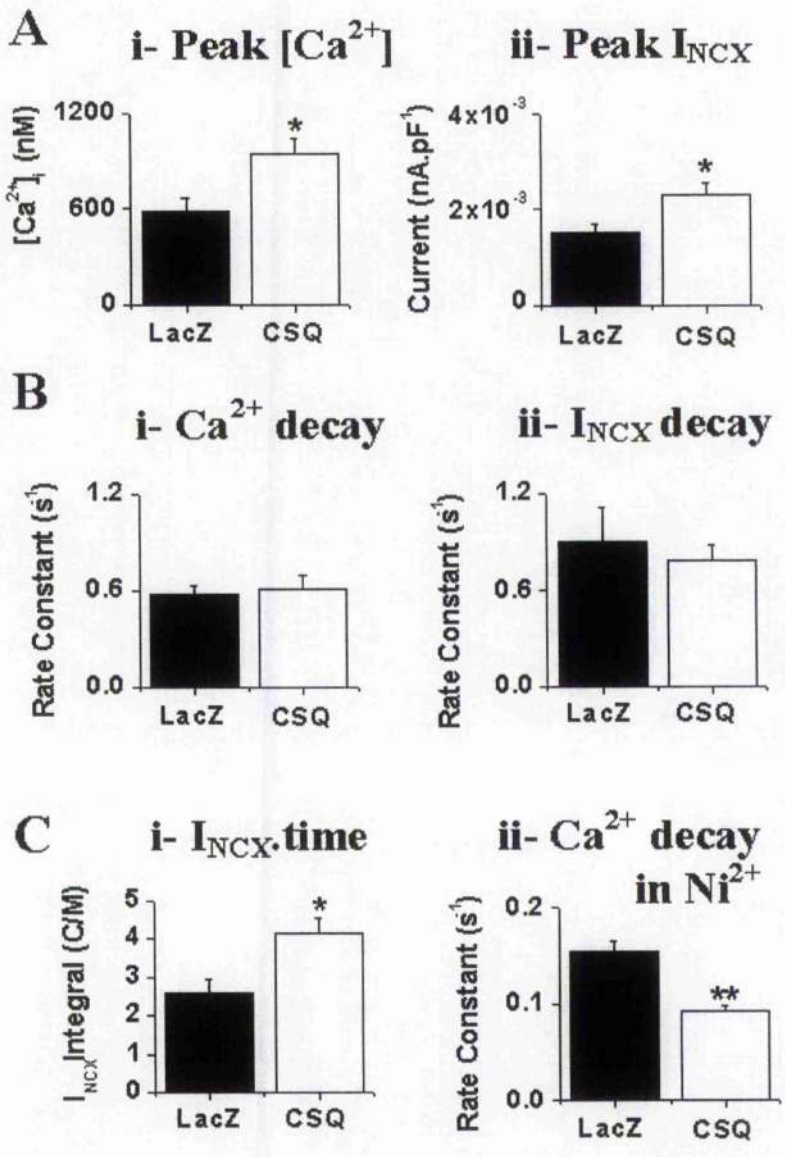


**Figure 4 - 8. SR $Ca^{2+}$ content in Ad-LacZ and Ad-CSQ transfected cardiomyocytes.**

**Panel A (i), Peak $[Ca^{2+}]$ for LacZ (n=17) and CSQ (n=19) groups, P< 0.05); (ii) Peak $I_{NCX}$ for LacZ (n=11) and CSQ (n=12) groups, P< 0.05. Panel B (i), rate constant for the decay of the caffeine induced $Ca^{2+}$ transient for LacZ (n=15) and CSQ (n=11) groups (P = ns); (ii) rate constant for the decay of the transient inward current for LacZ (n=7) and CSQ (n=8) groups (P = ns). Panel C (i), $I_{NCX}$.time integral, LacZ (n=6) and CSQ (n=8) groups (P< 0.05); (ii) rate constant for the decay of the caffeine**

**induced $Ca^{2+}$ transient in the presence of 10mmol/L $Ni^{2+}$ for LacZ (n=6) and CSQ (n=6) groups (P< 0.01);**

Rapid application of 10mM caffeine was again used to determine the SR $Ca^{2+}$ load of cardiomyocytes contracting in the steady state. Figures 4-8 A (i) and C (i) clearly demonstrate that both the caffeine-induced $Ca^{2+}$ transient and the integral of the caffeine-induced transient inward current with respect to time are significantly increased in the Ad-CSQ transfected cardiomyocytes when compared to control. These results indicate that CSQ overexpression significantly reduces SR $Ca^{2+}$ content.

Whilst figure 4-8 A (ii) shows that the peak of the transient inward current was significantly increased by CSQ overexpression, figure 4-8 B (ii) shows that its rate constant of decay, calculated by fitting with a single exponential, was not significantly different when compared to Ad-LacZ control. Similarly, the rate constant for the decay of the caffeine-induced $^{Ca2+}$ transient (see figure 4-8 B (i)) was also unaffected in the Ad-CSQ transfected myocytes. These similar rate constants suggest that the rate of extrusion of $Ca^{2+}$ from the cytosol at the sarcolemma via NCX has not been affected by CSQ overexpression. Figure 4-8 C (ii) demonstrates that when caffeine was applied with $Ni^{2+}$, the rate constant for the decay of the corresponding $Ca^{2+}$ transient was significantly reduced in the Ad-CSQ transfected myocytes when compared to control. This would suggest that CSQ overexpression inhibits the activity of the sarcolemmal $Ca^{2+}$-ATPase. However, Figure 4-9 below suggests that the rate constant for the decay of the caffeine-induced $Ca^{2+}$ transient in the presence of $Ni^{2+}$ is a function of

the size of the $Ca^{2+}$ transient. The larger the caffeine-induced $Ca^{2+}$ transient, the slower its rate of decay. Figure 4-10 demonstrates that CSQ overexpression did not significantly alter $Ca^{2+}$ buffering capacity within the cultured cardiomyocytes.

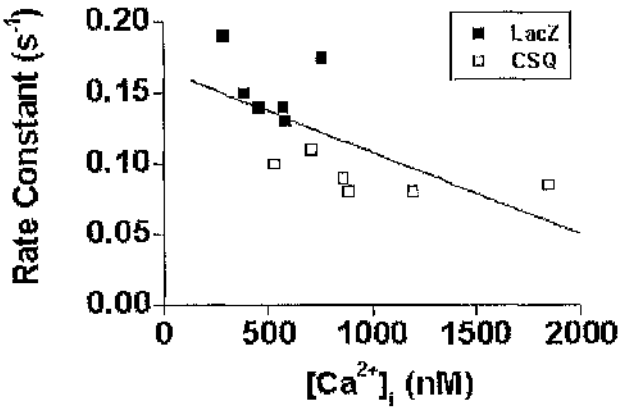


**Figure 4 – 9. Relationship between the peak of the caffeine-induced $Ca^{2+}$ transient and the rate constant of its decay in the presence of $Ni^{2+}$ in both Ad-LacZ and Ad-CSQ transfected cardiomyocytes.**

### 4.2.4 Effect of CSQ overexpression on $Ca^{2+}$ buffering capacity

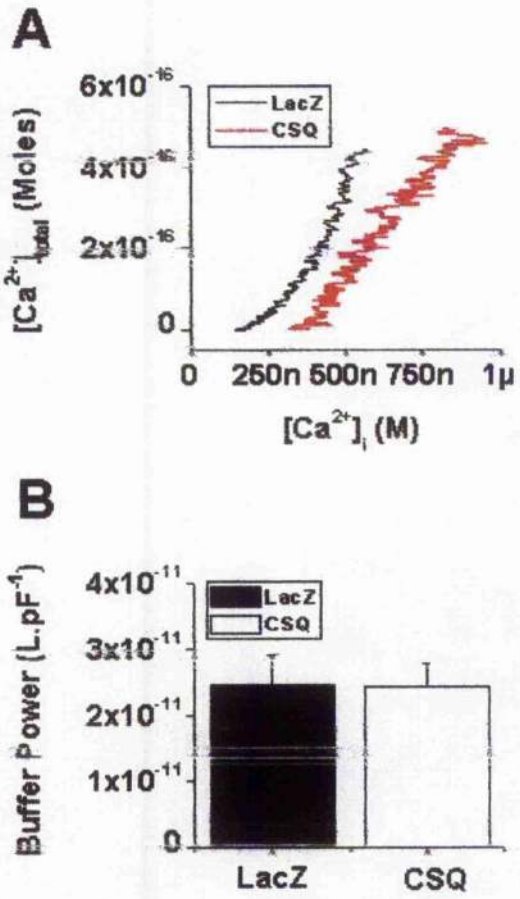


**Figure 4 - 1. CSQ overexpression and $Ca^{2+}$ buffering capacity.**

**(A) Relationship between free $[Ca^{2+}]_i$ and the total amount of $Ca^{2+}$ extruded from typical Ad-LacZ and Ad-CSQ transfected cardiomyocytes during the rapid application of 10mM caffeine. (B) Mean ± SEM buffer power for Ad-LacZ (n=14) and Ad-CSQ (n=14) transfected cardiomyocytes, $p > 0.05$.**

4.2.5 Effect of CSQ overexpression on NCX activity.

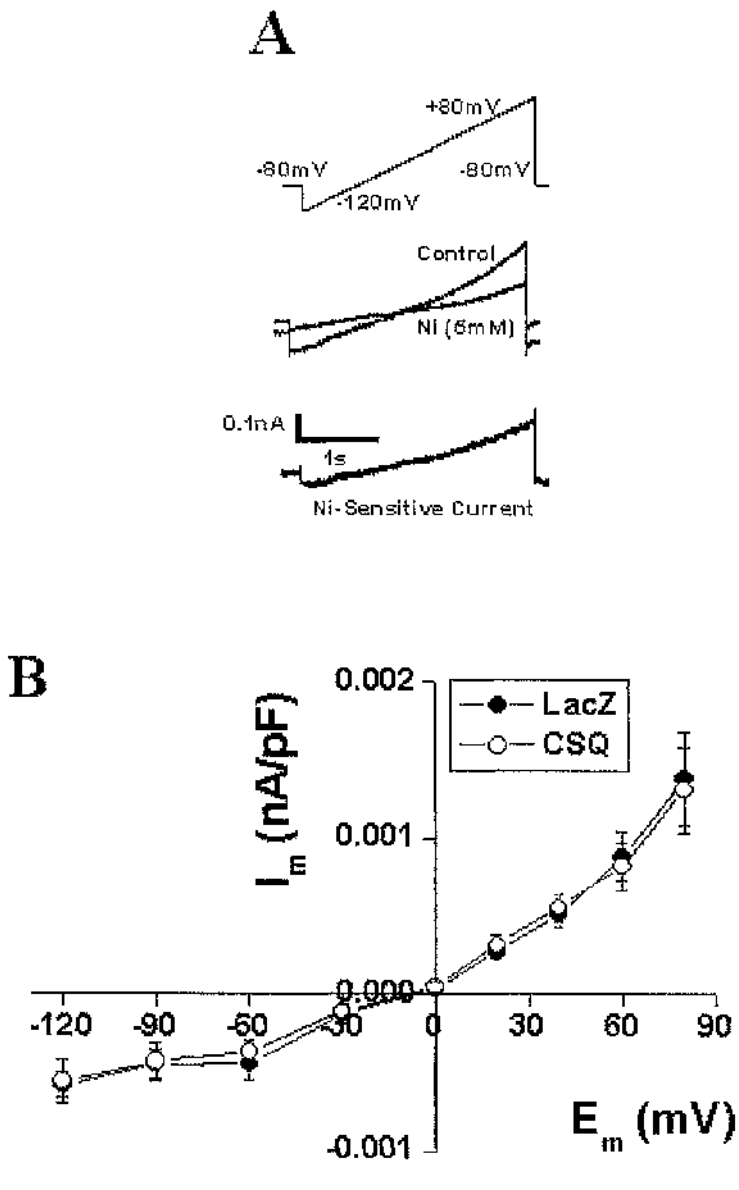


**Figure 4 - 11. The I-V relationship for the $Ni^{2+}$-sensitive NCX current.**

**A, Voltage clamp protocol used to determine the I-V relationship under control conditions and in the presence of 5mM $Ni^{2+}$ along with the difference current, attributable to NCX. B, Average I-V relationship in Ad-LacZ (n=15) and Ad-CSQ (n=15) transfected cardiomyocytes.**

The effect of CSQ overexpression on NCX activity was further investigated by determining the $Ni^{2+}$-sensitive NCX current measured whilst slowly ramping the membrane potential from –120mV to +80mV (Figure 4-11, A). With $[Ca^{2+}]_i$ buffered at 250nM using 50mM EGTA in the patch pipette solution and $[Na^+]_i$ at 20mM, NCX currents were identical in Ad-CSQ transfected cardiomyocytes when compared to Ad-LacZ control (Figure 4-11, B).

4.2.6 Effect of CSQ overexpression on E-C coupling in the presence of nifedipine

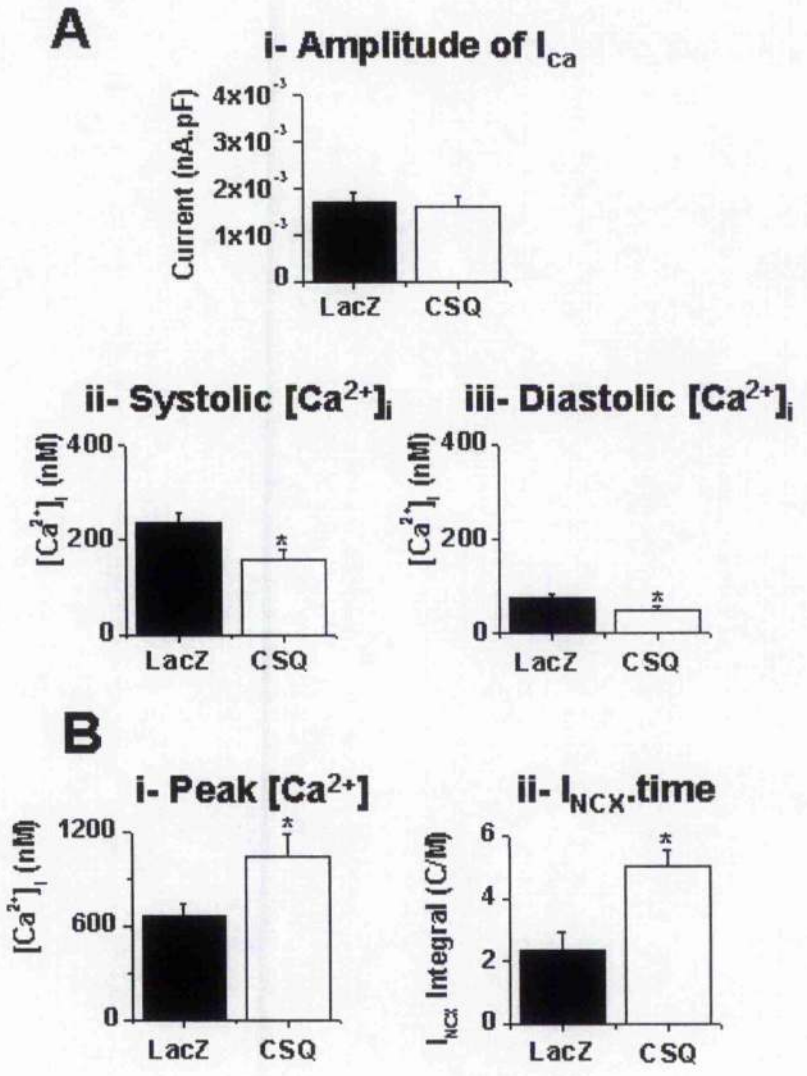


**Figure 4 - 12. Effects of 0.5μM nifedipine on E-C coupling in Ad-CSQ transfected cardiomyocytes.**

**Panel A shows mean +SEM values of: (i) L-type $Ca^{2+}$ current amplitude (ii) peak systolic $[Ca^{2+}]_i$, (iii) end diastolic $[Ca^{2+}]_i$ using the standard E-C coupling voltage clamp protocol for Ad-LacZ, n=10 (no nifedipine present) and Ad-CSQ, n=9 (0.5μM nifedipine present) transfected cells. Panel B shows (i) Peak $[Ca^{2+}]_i$ and (ii) $I_{NCX}$.time integral, recorded on application of 10mmol/L caffeine in LacZ (no nifedipine present) and CSQ (0.5μM nifedipine present) transfected cardiomyocytes.**

L-type $Ca^{2+}$ current amplitude in voltage clamped Ad-CSQ transfected cardiomyocytes was reduced to control levels with the addition of 0.5μM nifedipine to the superfusate (Figure 4-12 A(i)). Under these conditions both peak systolic [$Ca^{2+}$] and end diastolic [$Ca^{2+}$] were significantly lower than in Ad-LacZ transfected cardiomyocytes (Figure 4-12 A(ii)&(iii)). Rapid application of 10mM caffeine revealed a significantly increased peak caffeine-induced $Ca^{2+}$ release (AdLacZ, 664±71nmol/L n=6; Ad-CSQ, 1041±143nmol/L, n=9, $p< 0.05$) and a significantly increased time-integral of the resultant transient inward NCX current (AdLacZ, 2.33±0.58C/M n=4; Ad-CSQ, 5.00±0.53C/M, n=8, $p< 0.05$) in the Ad-CSQ transfected cardiomyocytes, supporting the conclusion that SR $Ca^{2+}$ load was again significantly increased in this cell type (see figure 4-12 B).

4.2.7 Relationship between SR $Ca^{2+}$ content and $Ca^{2+}$ transient amplitude in Ad-LacZ and Ad-CSQ transfected cardiomyocytes

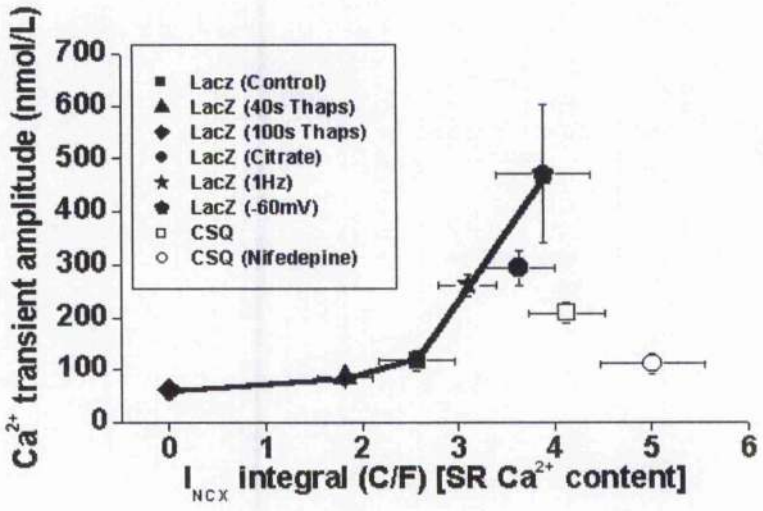


**Figure 4 - 13. CSQ overexpression and the gain of EC-coupling.**

**Relationship between INCX integral (an index of SR $Ca^{2+}$ content) and $Ca^{2+}$ transient amplitude for cardiomyocytes from Ad-LacZ (Control; Thapsigargin 40s exposure; Thapsigargin 100s exposure; Citrate; 1Hz stimulation ; Hold -60mV) and Ad-CSQ (Control; Nifedipine) groups. Measurements were obtained in the steady state; lower SR loads were achieved by exposure to 5μM Thapsigargin for various times, higher SR loads were obtained by adding 20mM Citrate to the pipette solution, by stimulating at a frequency of 1Hz or by holding membrane potential at -60mV between depolarisations.**

The SR $Ca^{2+}$ load of Ad-LacZ transfected cardiomyocytes was increased either by the addition of 20mmol/L citrate to the pipette solution (SR $Ca^{2+}$ load 3.64+/-0.37 C/M and $Ca^{2+}$ transient amplitude 294+/-32 nmol/L), by clamping at –60mV during diastole (SR $Ca^{2+}$ load 3.89 ± 0.49 C/M and $Ca^{2+}$

transient amplitude 471 ± 131 nmol/L) or by stimulating at a frequency of 1Hz (SR $Ca^{2+}$ load 3.10 ± 0.30 C/M and $Ca^{2+}$ transient amplitude 262 ± 21 nmol/L). SR $Ca^{2+}$ load was decreased by the addition of 5μM thapsigargin to the superfusate. After 40s, SR $Ca^{2+}$ load was reduced to 1.82+/-0.28 C/M and the $Ca^{2+}$ transient amplitude to 85+/-15 nmol/L. Exposure for 100s completely emptied the SR of $Ca^{2+}$ and the $Ca^{2+}$ transient amplitude was reduced to 61+/-16 nmol/L. These points allowed determination of the normal relationship between SR $Ca^{2+}$ content and $Ca^{2+}$ transient amplitude (figure 4-13) for 1-day cultured rabbit cardiomyocytes.

4.2.8 Effect of CSQ overexpression on spontaneous $Ca^{2+}$ spark activity and SR $Ca^{2+}$ load in permeabilised rabbit cardiomyocytes

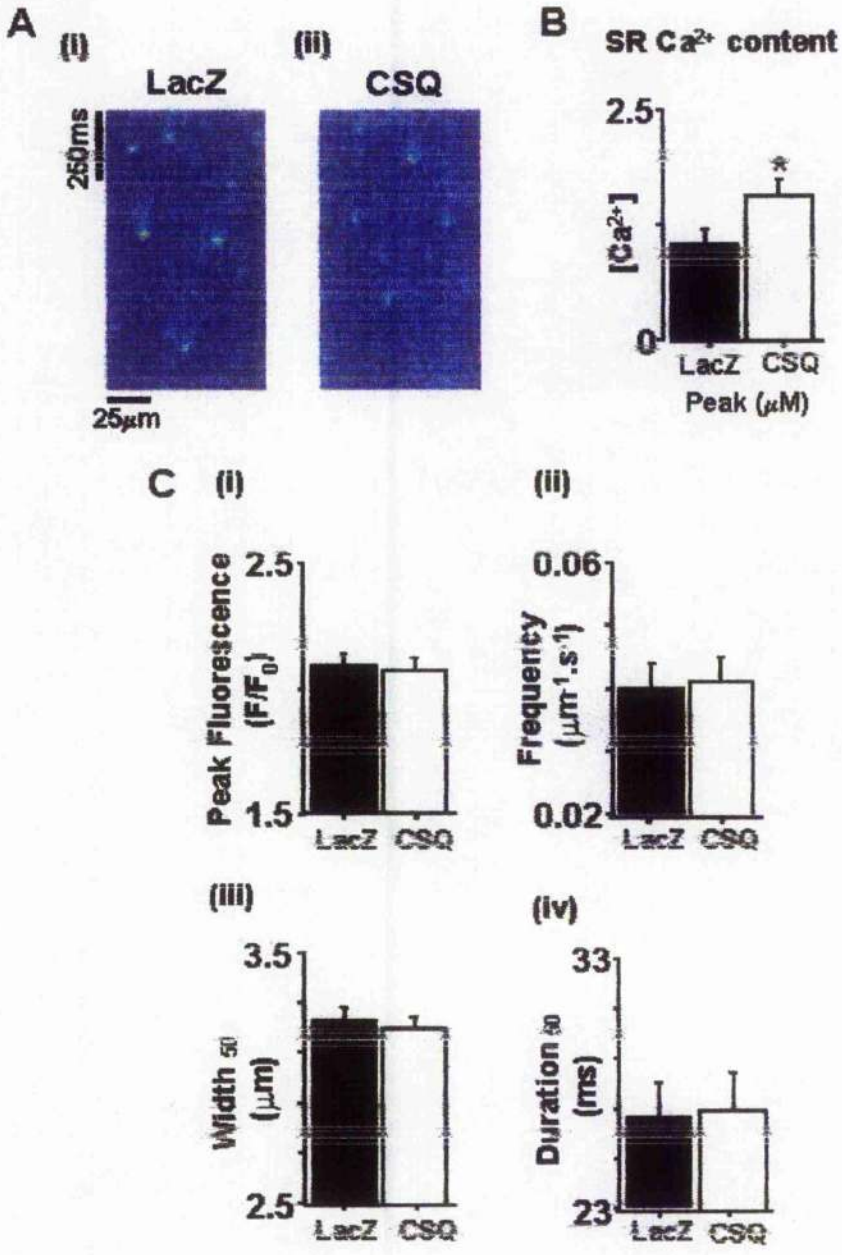

**Figure 4 - 14. Spontaneous $Ca^{2+}$ sparks in permeabilised cardiomyocytes transfected with Ad-LacZ and Ad-CSQ.**

**A, Pseudo colour line scan epifluorescence image from single cardiomyocytes in each experimental group. B, SR $Ca^{2+}$ load in each experimental group as assessed by rapid application of 10mM caffeine. C, Mean ± SEM values for peak $F/F_0$ (i), spark frequency (ii), spark width (iii) and spark duration (iv). Results compiled from n=12 Ad-LacZ and n=17 Ad-CSQ transfected cells. Measurements by Dr. Chris Loughrey.**

The direct effects of CSQ overexpression on SR function were investigated in β-escin permeabilised cardiomyocytes. Single cardiomyocytes were superfused with a standard solution containing nominally 150mM $Ca^{2+}$, pH 7.0 with ATP and creatine phosphate added to preserve SR function. Inclusion of 10μM fluo-3 allowed spontaneous $Ca^{2+}$ sparks to be visualised using laser-scanning confocal microscopy. Figures 4-14 A (i) & (ii) show typical line scan traces and $Ca^{2+}$ sparks from cardiomyocytes transfected with Ad-LacZ and Ad-CSQ respectively. Figure 4-14 C demonstrates that the $Ca^{2+}$ sparks recorded in the Ad-CSQ transfected cells were near identical those observed in Ad-LacZ transfected cells (peak F/Fo, 2.09±0.05 vs. 2.07 ±0.05 , P>0.05; frequency, 0.040±0.004 vs. 0.041±0.004 $\mu m^{-1}s^{-1}$, P>0.05; width, 3.23±0.05 vs. 3.21±0.04 μm, P>0.05; duration, 26.6±1.0 vs. 27.0±1.6ms, P>0.05; Ad-Laz n=12cells vs. Ad-CSQ n=17cells). After perfusion with 150mM $Ca^{2+}$, 50μM EGTA and 10μM fluo-5, 10mM caffeine was rapidly applied in order to assess SR $Ca^{2+}$ content. Figure 4-14 B demonstrates that the mean amplitude of the caffeine-induced $Ca^{2+}$ releases and hence the SR $Ca^{2+}$ load, was significantly increased in the Ad-CSQ transfected cardiomyocytes (peak $[Ca^{2+}]_i$ in

caffeine was 1.05±0.16 μM/L for Ad-LacZ [n=12] and 1.57±0.17 μM/L for Ad-CSQ [n=17]).

4.2.9 Effect of CSQ overexpression on sensitivity to 0.5mM caffeine

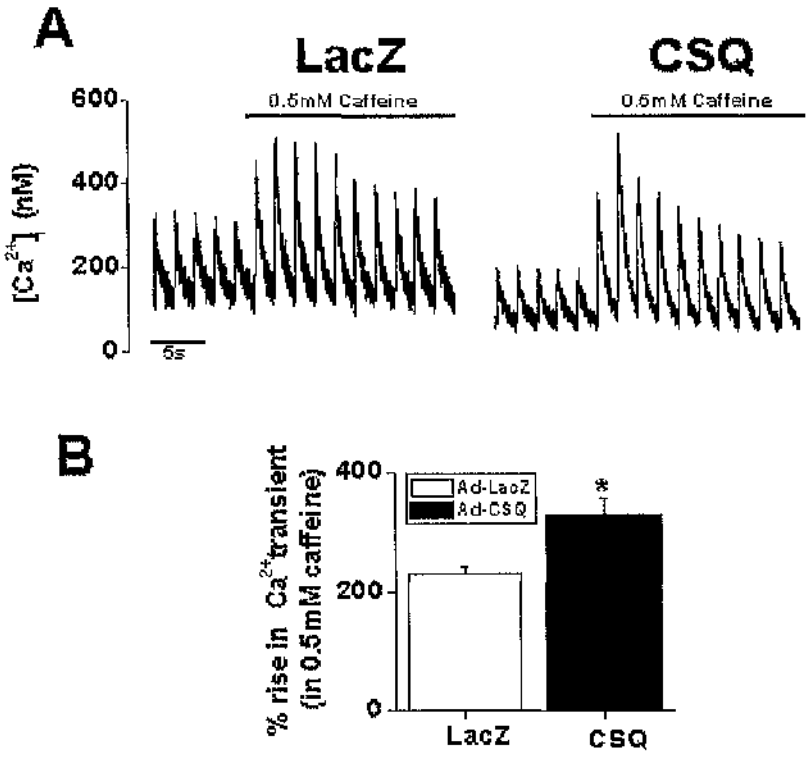


**Figure 4 - 15. CSQ overexpression and the effects of 0.5mM caffeine on EC-coupling.**

**A, Effect of 0.5mM caffeine on the size of the steady state intracellular $Ca^{2+}$ transient in Ad-LacZ and Ad-CSQ (0.5μM nifedipine present) transfected cardiomyocytes. B, Mean ± SEM % rise in $Ca^{2+}$ transient size in both experimental groups (Ad-LacZ n=12, Ad-CSQ n=11).**

It is clear from figure 4-15 that the transient increase in the size of the steady state intracellular $Ca^{2+}$ transient caused by the wash on of 0.5mM caffeine was greater in Ad-CSQ transfected cardiomyocytes when compared to the Ad-LacZ group. The transient increase in $Ca^{2+}$ transient size for Ad-LacZ transfected cardiomyocytes was 230 ± 14% vs. 326 ± 31% in Ad-CSQ transfected cells.

4.2.10 Effect of CSQ overexpression on the relationship between stimulation frequency and peak systolic $Ca^{2+}$

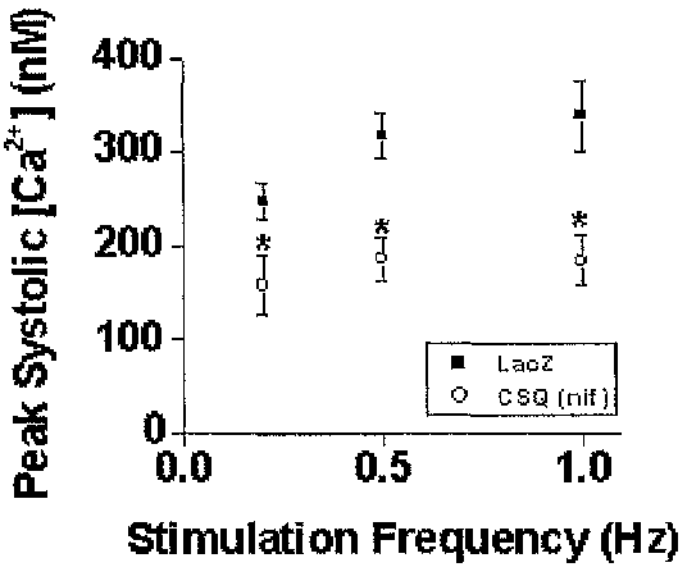


**Figure 4 - 16. Effect of stimulation frequency on peak systolic [$Ca^{2+}$] in Ad-LacZ (n=6) and Ad-CSQ (n=6) transfected cardiomyocytes under conditions of whole cell voltage clamp.**

**Ad-CSQ transfected cardiomyocytes were stimulated in the presence of 0.5μM nifedipine.**

The relationship between stimulation frequency and peak systolic [$Ca^{2+}$] is altered in Ad-CSQ transfected cardiomyocytes with respect to Ad-LacZ control. Figure 4-16 demonstrates that at a stimulation frequency of 1Hz, peak systolic [$Ca^{2+}$] is nearly halved in Ad-CSQ transfected cells.

## 4.3 Discussion.

This chapter suggests that adenoviral mediated CSQ overexpression in cultured rabbit cardiomyocytes causes significant alterations in the regulation of cardiac E-C coupling.

### 4.3.1 The effect of CSQ on sarcolemmal $Ca^{2+}$ entry and extrusion.

This study reveals that CSQ over-expression significantly increases L-type $Ca^{2+}$ current density, without altering the inactivation kinetics of the channel. Western blot analysis (see figure 4-2) demonstrates that there is no change in L-type $Ca^{2+}$ channel protein expression when CSQ over-expressing cardiomyocytes are compared to LacZ controls. Terentyev *et al.*, 2003b also employed adenovirus to overexpress cardiac CSQ but reported no effect on the L-type $Ca^{2+}$ current. In contrast, the transgenic over-expression of CSQ has shown L-type $Ca^{2+}$ current density to be either reduced (Sato *et al.*, 1998, Knollmann *et al.*, 2000 & Wang *et al.*, 2000) or unaltered (Jones *et al.*, 1998). The inactivation of $I_{Ca}$ was slowed in all cases.

NCX activity appears unchanged in CSQ over-expressing cardiomyocytes. The rate constant of $Ca^{2+}$ extrusion in response to caffeine, the rate constant of $I_{NCX}$ decay in response to caffeine and the $Ni^{2+}$-sensitive NCX currents over a voltage range –120mV to +80mV were all similar when compared to LacZ controls. Transgenic over-expression of CSQ has

shown NCX activity to be either increased (Knollmann *et al.*, 2000) or unchanged (Sato *et al.*, 1998).

Notably, the rate constant of $Ca^{2+}$ extrusion in response to caffeine and in the presence of nickel, taken to represent sarcolemmal $Ca^{2+}$ ATPase activity, was significantly reduced in CSQ-overexpressing cardiomyocytes. However this reduction in sarcolemmal $Ca^{2+}$-ATPase activity was subsequently shown to be a function of the size of the caffeine-induced $Ca^{2+}$ transient. It is not clear how this discovery relates to the data presented in the other results chapters in this thesis and a more detailed study of this relationship would be recommended for future study. Furthermore, western blot analysis demonstrated that sarcolemmal $Ca^{2+}$ ATPase protein expression was unaltered in the CSQ-overexpressing cardiomyocytes with respect to LacZ control.

The cellular mechanism underlying the CSQ-induced increase in L-type $Ca^{2+}$ current is unknown. However, over-expression of CSQ in cell culture has recently been shown to inhibit store operated $Ca^{2+}$ entry in mouse skeletal myotubes with depleted SR $Ca^{2+}$ contents (Shin *et al.*, 2003), lending weight to our observation that over-expression of cardiac CSQ also affects sarcolemmal $Ca^{2+}$ fluxes.

### 4.3.2 Effects of CSQ overexpression on SR $Ca^{2+}$ content.

SR $Ca^{2+}$ content is thought to be "autoregulated" (Eisner *et al.*, 2000) and is a function of SR buffer capacity, SR $Ca^{2+}$ leak and $[Ca^{2+}]_i$ , the latter affecting both SERCA activity and sarcolemmal $Ca^{2+}$ influx/efflux. When all of these factors are in balance, a "steady state" is achieved. Overexpression of CSQ increased steady state SR $Ca^{2+}$ content of cardiomyocytes by a factor of 1.61, when compared to LacZ controls. However, in addition to increasing SR buffer capacity, CSQ overexpression also significantly increased L-type $Ca^{2+}$ current. When nifedipine was used to normalise the L-type $Ca^{2+}$ current to control levels, steady state SR calcium content was increased in CSQ over-expressing cells by a factor of 2.15. Western blot analysis shows that adenoviral transfection increased CSQ protein expression by a factor of 1.58 when compared to LacZ control. An increased SR $Ca^{2+}$ load is consistent with the results of other studies that have employed either transgenic or adenoviral-mediated strategies in order to overexpress cardiac CSQ (Sato *et al.*, 1998, Jones *et al.*, 1998 & Terentyev *et al.*, 2003b).

### 4.3.3 Effects of CSQ overexpression on spontaneous $Ca^{2+}$ sparks.

The data presented here indicate that CSQ overexpression had no effect on either the magnitude or the frequency of spontaneous $Ca^{2+}$ sparks in permeabilised cardiomyocytes, despite significantly increasing the SR $Ca^{2+}$ load. Gyorke *et al.*, 2004, also using adenovirus to cause a 4-fold increase in cardiac CSQ expression, observed larger spontaneous $Ca^{2+}$ sparks but

showed no effect on the frequency of release events. Conversely, transgenic overexpression of cardiac CSQ has been demonstrated to significantly reduce the frequency of spontaneous $Ca^{2+}$ sparks in murine cardiomyocytes (Jones *et al.*, 1998, Wang *et al.*, 2000). Typically transgenic overexpression, increases CSQ expression by a much greater extent (10-15 fold) and this increased level of overexpression may contribute to the differences observed in spontaneous $Ca^{2+}$ sparks when comparisons are made with studies employing adenoviral overexpression.

### 4.3.4 Effects of CSQ overexpression on E-C coupling.

Adenoviral CSQ overexpression in cardiomyocytes increased both diastolic $[Ca^{2+}]_i$ and systolic $[Ca^{2+}]_i$ when compared to LacZ control. However, CSQ overexpression also significantly increased the L-type $Ca^{2+}$ current and steady state SR $Ca^{2+}$ load, both of which would contribute to an increased intracellular $Ca^{2+}$ transient. To isolate the effects of CSQ overexpression on SR function, Ad-CSQ myocytes were perfused in a solution containing 0.5μM nifedipine, which reduced $I_{Ca}$ to control levels. Under these conditions, CSQ overexpressing myocytes exhibited reduced diastolic $[Ca^{2+}]_i$, reduced systolic $[Ca^{2+}]_i$, an increased SR $Ca^{2+}$ content and a similar calcium transient amplitude when compared to LacZ control. These results are consistent with CSQ overexpression reducing the open probability of RyR (as observed by Gyorke *et al.*, 2004), where an increased SR $Ca^{2+}$ content with no effect on steady state $Ca^{2+}$ transient amplitude would be expected (Trafford *et al.*, 2000). They also agree with unpublished results

obtained by Dr. Sarah Kettlewell (see discussion, chapter 3), where tetracaine, a drug that reduces the $Ca^{2+}$ sensitivity of RyR2, increased SR $Ca^{2+}$ content but did not affect steady state calcium transient amplitude in voltage clamped rabbit cardiomyocytes. Hence the reduction in the gain of E-C coupling in Ad-CSQ transfected cardiomyocytes illustrated in figure 4-13. Experiments where 0.5mM caffeine was washed on to cardiomyocytes contracting in the steady state revealed a relatively larger temporary increase in intracellular $Ca^{2+}$ transient size when Ad-CSQ transfected cells were compared to the Ad-LacZ control group. These results imply that RyRs in the Ad-CSQ transfected cardiomyocytes were originally subjected to a greater degree of inhibition than those in the Ad-LacZ group and thus also support the conclusion that CSQ reduces RyR open probability.

Lipid bilayer studies using cardiac RyRs (Lukyanenko *et al.*, 1996, Ching *et al.*, 2000 & Gyorke & Gyorke, 1998) suggest that an increase in luminal free $[Ca^{2+}]$ increases the $P_O$ of the RyR. With the proviso that SERCA has adequate time to refill the SR, one would not expect adenoviral-mediated CSQ overexpression to alter the steady state free SR $[Ca^{2+}]$ in a contracting cardiomyocyte. However, CSQ overexpression would increase the $Ca^{2+}$ buffering capacity of the SR, thus increasing the time required to refill the SR to any given free $[Ca^{2+}]$ during diastole. At faster stimulation rates the SR may not have adequate time to refill and free SR $[Ca^{2+}]$ may actually be reduced, which in turn may also reduce the open probability of the RyR. The data presented in figure 4-16 reveal that at a slower stimulation rate (0.2Hz), the peak systolic $[Ca^{2+}]$ is not increased in either cell type despite the longer diastolic interval. Conversely, a faster stimulation rate (1Hz) did

not significantly reduce peak systolic [$Ca^{2+}$] in either cell type despite a shorter diastolic interval. These results would suggest that at the standard stimulation frequency used throughout this study (0.5Hz), the SR has adequate time to refill with $Ca^{2+}$ during diastole.

Transgenic overexpression of cardiac CSQ has generally demonstrated an increased SR $Ca^{2+}$ load along with a reduction in the size of intracellular [$Ca^{2+}$] transient (Sato *et al.*, 1998, Wang *et al.*, 2000 & Jones *et al.*, 1998). However, both Sato *et al.*, 1998, and Wang *et al.*, 2000, also reported a reduction in the size of the L-type $Ca^{2+}$ current. Therefore it is only the study by Jones and colleagues, in which $I_{Ca}$ was unchanged, where we may be able to infer that CSQ overexpression reduced the gain of E-C coupling. Intriguingly, Terentyev *et al.*, 2003b, have reported that a 4-fold adenoviral-mediated overexpression of CSQ increased both the SR $Ca^{2+}$ load and the size of the intracellular $Ca^{2+}$ transient, with no effect on $I_{Ca}$. In these experiments voltage pulses were applied at 1-minute intervals and hence there would be a long period of time for free [$Ca^{2+}$] in the SR to rise between successive stimulations. An increased SR free [$Ca^{2+}$] may infact mask the inhibitory effects of CSQ on RyR open probability, resulting in a net increase in the gain of E-C coupling.

### 4.3.5 Conclusions.

In summary, the present findings seem to indicate that CSQ is both a storage and a signalling protein in the cardiac muscle $Ca^{2+}$ signalling

cascade. Increased CSQ levels increased SR $Ca^{2+}$ load, enhanced L-type $Ca^{2+}$ current and thus caused an increased intracellular $Ca^{2+}$ transient. However, when the enhanced L-type $Ca^{2+}$ current was normalised in the CSQ overexpressing cardiomyocytes, the amplitude of the intracellular $Ca^{2+}$ transient was unaltered, despite an increased SR $Ca^{2+}$ load. A recent study by Gyorke *et al.*, 2004 demonstrated that CSQ reduced the $P_O$ of RyR2 in lipid bilayers. This observation is consistent with data presented here, where CSQ overexpression reduces the gain of E-C coupling.

# Chapter 5 - FKBP 12.6 overexpression and E-C coupling in isolated rabbit cardiomyocytes.

## 5.1 An introduction to FKBP 12.6

### 5.1.1 Immunophilins

Immunophilins are a highly conserved family of proteins that possess the ability to bind the immunosuppressant drugs cyclosporin A, FK506 and rapamycin. The protein family can be further divided into cyclophilins that bind cyclosporin A and **FK**506-**B**inding **P**roteins (FKBP's) that bind FK506 and rapamycin (Marks, 1996). Both cyclophilins and FKBP's exhibit rotamase enzymatic activity which is inhibited by the above-mentioned immunosuppressant drugs. Interestingly the inhibition of rotamase activity does not contribute to the mechanism of immunosuppression. Instead it appears that the immunophilin-drug complexes are the actual immunosuppressive species. They bind to and inhibit calcineurin, a serine-threonine phosphatase required for T-cell activation. Inhibition of calcineurin blocks the nuclear translocation of transcription factors such as NF-κB and NFAT which control the expression of cytokine genes whose products are required for immune response co-ordination (Lam *et al.*, 1995).

### 5.1.2 FKBP isoforms

The FKBP's are named according to their molecular masses which range from 12 to 52kDa. FKBP 12 was found be associated with highly purified RYR1 from rabbit skeletal muscle SR (Jayaraman *et al.*, 1992), whereas

FKBP 12.6 was found to be tightly associated with RyR2 from canine cardiac SR (Timerman *et al.*, 1994). Hence it was thought that FKBP 12 modulated skeletal RyR1 and that FKBP 12.6 modulated cardiac RyR2.

However, It was subsequently demonstrated using $^{35}$S-labelled FKBP 12 and 12.6 that both isoforms could bind to FKBP stripped rabbit skeletal muscle SR and exchange with exogenously bound FKBP 12. In contrast only FKBP 12.6 could rebind to FKBP stripped canine cardiac SR or exchange with exogenously bound FKBP 12.6 (Timerman *et al.*, 1996). FKBP 12.6 differs from FKBP 12 by only 18 of 108 amino acid residues. Xin *et al.*, 1999, have taken various combinations of these 18 residues and mutated them to those found in FKBP 12. The triple mutant Q31E/N32D/F59W of human FKBP 12.6 lacked selective binding to canine cardiac RyR2, comparable to FKBP 12. Hence the residues Gln$^{31}$, Asn$^{32}$ and Phe$^{59}$ of FKBP 12.6 must account for its selective binding to cardiac canine RyR2.

Jeyakumar *et al.*, 2001, have determined the FKBP binding characteristics of cardiac microsomes from a diverse range of vertebrates, again using $^{35}$S-labelled FKBP 12 and 12.6. Cardiac microsomes from the dog were unique in that they were only capable of binding/exchanging FKBP 12.6. Cardiac microsomes from all the other vertebrates studied (human, rabbit, rat, mouse, chicken, frog, fish) were capable of binding/exchanging both FKBP 12 and FKBP 12.6. Both FKBP 12 and FKBP 12.6 bound with an approximate stoichiometry of 4 per RyR2, however FKBP 12.6 was found to have a 7-fold greater affinity for RyR2 when compared to FKBP 12. Given

that the cardiac microsomes from all the vertebrates studied expressed both FKBP 12 and 12.6 and that both FKBP isoforms were able to bind to RyR2 (except in the dog), the idea that FKBP 12 modulates skeletal RyR1 and FKBP 12.6 modulates cardiac RyR2 may be an oversimplification. Furthermore it is noteworthy that double knockout FKBP 12 transgenic mice have normal skeletal muscle, but instead exhibit profound dilated cardiomyopathy (Shou *et al.*, 1998).

### 5.1.3 Isolated cardiac RYR2 and FKBP 12.6

Preparations of cardiac SR vesicles have been employed to determine how FKBP 12.6 modulates RyR2 at the single channel level. Using SR vesicles derived from the dog heart, Kaftan *et al.*, 1996, used 2μM rapamycin to dissociate FKBP 12.6 from RyR2. Similarly, Xiao *et al.*, 1997, have employed FK506 to dissociate FKBP 12.6 from rat cardiac RyR2 in planar lipid bilayers. In both studies these manoeuvres were found to increase the open probability of RyR2, but also reduced the amplitude of the current passing through the channel, thus causing subconductance states. Marx *et al.*, 2000, have established a link between the phosphorylation status of RyR2 and its ability to bind FKBP 12.6. They demonstrated that PKA phosphorylation of RyR2 resulted in a 90% reduction in the amount of FKBP 12.6 co-immunoprecipitating with RyR2. This caused an increase in the open probability of the channel and induced subconductance states.

In addition it has also proved possible to isolate multiple RyR2 under conditions such that they remain physically coupled to one another. The current level recorded through a single canine RyR2 was ~4pA, with current levels of ~8 and 12pA through 2-coupled and 3-coupled channels respectively. Intriguingly, addition of rapamycin and hence dissociation of FKBP 12.6 caused channels that had previously been functionally attached to become uncoupled and then exhibit subconductance states. It was proposed that coupled gating between RyR2s via FKBP 12.6 might permit simultaneous opening during systole and also simultaneous closing during diastole (Marx *et al.*, 2001). In contrast, Barg *et al.*, 1997, and Timerman *et al.*, 1996, have also studied the activity of cardiac RyR2 in planar lipid bilayers and demonstrated that dissociation of FKBP 12.6 from the channel did not modulate its function.

### 5.1.4 $Ca^{2+}$ sparks and FKBP 12.6

Given that drugs which dissociate FKBP 12.6 (FK506 and rapamycin) appear to alter single channel RyR2 activity, one might expect them to affect the characteristics of spontaneous $Ca^{2+}$ sparks in intact cardiomyocytes. Indeed the addition of FK506 to rat ventricular myocytes caused a 4-fold increase in the frequency (McCall *et al.*, 1996) and a 6-fold increase in the duration (Xiao *et al.*, 1997) of spontaneous $Ca^{2+}$ sparks. Cardiomyocytes from FKBP 12.6 knock out mice also exhibit increases in the amplitude and duration of $Ca^{2+}$ sparks (Xin *et al.*, 2002). These results appear consistent with the data from single channel studies where

dissociation of FKBP 12.6 from RyR2 increased the open probability of the channel. One would expect an increased RyR2 open probability to increase the frequency and/or size of spontaneous calcium sparks.

### 5.1.5 intact cells and FKBP 12.6

The effects of removing FKBP 12.6 from RyR2 on E-C coupling have been studied using intact cardiomyocytes. In voltage clamped rat ventricular myocytes the addition of FK506 significantly increased steady state calcium transient amplitude and in most cases also increased SR $Ca^{2+}$ load. FK506 inhibited $Ca^{2+}$ efflux from the cardiomyocytes via NCX and this may account for the increased SR $Ca^{2+}$ load observed. Given that an increased SR $Ca^{2+}$ load would, in itself, be expected to increase the size of the $Ca^{2+}$ transient, it is not possible to separate this effect from that of removing FKBP 12.6 from RyR2 on $Ca^{2+}$ transient amplitude. However, under conditions in which both the SR $Ca^{2+}$ load and the L-type $Ca^{2+}$ current were unaltered, FK506 still significantly increased the intracellular $Ca^{2+}$ transient amplitude (McCall *et al.*, 1996). Hence, removal of FKBP 12.6 from RyR2 may increase the gain of E-C coupling. Also working with voltage clamped rat ventricular myocytes, Xiao *et al.*, 1997, have reported that FK506 increased the size of the intracellular $Ca^{2+}$ transient without affecting the L-type $Ca^{2+}$ current. The observation could again be explained by an inhibition of NCX by FK506 and thus an increased SR $Ca^{2+}$ load.

Su *et al.*, 2003, have compared the actions of FK506 in voltage clamped mouse and rabbit ventricular myocytes. In the mouse cardiomyocytes they observed increased intracellular $Ca^{2+}$ transients with no effect on SR $Ca^{2+}$ load. This result would be largely consistent both with the effects of FK506 on rat cardiomyocytes previously discussed and with the observation that FKBP 12.6 knockout mice also exhibit larger intracellular $Ca^{2+}$ transients (Xin *et al.*, 2002). Conversely, Su *et al.*, demonstrated that in the rabbit cardiomyocytes FK506 caused a decreased intracellular $Ca^{2+}$ transient and a reduced SR $Ca^{2+}$ load. FK506 had no effect on membrane potential, L-type $Ca^{2+}$ current or NCX activity in either species. The authors postulated that the difference may be due to the fact that $[Na^+]_i$ is low in rabbit myocytes and would thus allow increased NCX extrusion of any $Ca^{2+}$ leaked from the SR by FK506-induced dissociation of FKBP 12.6 from RYR2. Prestle *et al.*, 2001, have used adenovirus to overexpress FKBP 12.6 in cultured rabbit cardiomyocytes with transfected myocytes also displaying increased fractional shortening and increased SR $Ca^{2+}$ loads. SR $Ca^{2+}$ uptake in permeabilised cardiomyocytes was faster in FKBP 12.6 transfected cells when compared to control, however in the presence of 5μM ryanodine $Ca^{2+}$ uptake rates were unaltered. Thus it was inferred that FKBP 12.6 stabilised the closed conformational state of RyR2, reducing diastolic SR $Ca^{2+}$ leak and consequently increasing SR $Ca^{2+}$ load and myocyte shortening. Thus the results of both the Su and Prestle rabbit studies are complementary, with FK506 decreasing SR $Ca^{2+}$ load and $Ca^{2+}$ transient size and FKBP 12.6 overexpression increasing SR $Ca^{2+}$ load and transient size. Hence it may be the case that species differences between

the mouse/rat and the rabbit make comparisons between different studies difficult.

Intriguingly, duBell *et al.*, 1997, have also seen an increase in the size of the intracellular $Ca^{2+}$ transient when FK506 was added to rat ventricular cardiomyocytes. However, the increased $Ca^{2+}$ transient was accompanied by an ~3-fold increase in action potential duration. When the depolarising duration was controlled in voltage clamp experiments, addition of FK506 had no effect on the size of the $Ca^{2+}$ transient. Prolongation of the action potential was explained by the observation that FK506 inhibited both the transient outward $K^+$ current ($I_{to}$) and the delayed rectifier $K^+$ current ($I_K$). A longer action potential may secondarily increase $Ca^{2+}$ influx and/or decrease $Ca^{2+}$ efflux, thus increasing SR $Ca^{2+}$ load and also the size of the intracellular $Ca^{2+}$ transient.

Finally, George *et al.*, 2003, have co-expressed human RyR2 and either FKBP 12 or FKBP 12.6 in a CHO cell line. In cells expressing only human RyR2, the magnitude of $Ca^{2+}$ release in response to stimulation by 4-CMC was in proportion to the amount of RyR2 expression. In cells co-expressing RyR2 and FKBP 12.6, triggered $Ca^{2+}$ release was markedly reduced despite the paradoxical observation the ER $Ca^{2+}$ store was "super-filled". Co-expression of RyR2 and FKBP 12 affected neither triggered $Ca^{2+}$ release nor the size of the ER $Ca^{2+}$ store.

### 5.1.6 FKBP 12.6 and Calcineurin

The immunosuppressant drug FK506 has often been used experimentally to dissociate FKBP 12.6 from the ryanodine receptor. However the resultant FK506-FKBP 12.6 complex inhibits calcineurin, a serine/threonine phosphatase that is found in the cytoplasm of many cell types. It has been demonstrated that dissociation of FKBP 12.6 from RyR2 increases the open probability of the channel (Xiao *et al.*, 1997). Complicating matters is the fact that the open probability of RyR2 also varies according to the phosphorylation status of the channel. PKA phosphorylation of canine RyR2 in lipid bilayers greatly increases $P_O$ when $[Ca^{2+}]_i$ is raised (Valdivia *et al.*, 1995) while the addition of protein phosphatases PP1 and PP2A to voltage clamped rat cardiomyocytes decreases the gain of E-C coupling by reducing RyR2 channel activity (duBell *et al.*, 1996). Hence, inhibition of calcineurin by the FK506-FKBP 12.6 complex and a subsequent increase in the phosphorylation of RyR2 may explain the increased open probability of the channel, with the dissociation of FKBP 12.6 functionally irrelevant.

The relative importance of calcineurin inhibition can be inferred from a study by Kaftan *et al.*, 1996. They applied the drug rapamycin to canine RyR2 in lipid bilayers. Rapamycin also dissociates FKBP 12.6 from RyR2, but the resultant rapamycin-FKBP 12.6 complex does not inhibit calcineurin. The observation that rapamycin was still capable of increasing RyR2 open probability would suggest that calcineurin plays no part in the modulation of RyR2 gating and that the dissociation of FKBP 12.6 from RyR2 is much greater functional importance.

In contradiction, a study by Bandyopadhyay *et al.*, 2000, using solubilised rat cardiac SR protein has provided evidence to suggest that calcineurin may be anchored to RyR2 via FKBP 12.6 in a $Ca^{2+}$-depenent manner and that this may be of functional significance. Treatment of neonatal rat cardiomyocytes with various calcineurin inhibitors (20μM deltamethrin, 10μM cyclosporin A, 10μM FK506) caused $Ca^{2+}$ oscillations in previously quiescent cells. Treatment with 10μM rapamycin, which does not inhibit calcineurin, did not cause $Ca^{2+}$ oscillations to occur as frequently. It was suggested that the occurrence of repetitive oscillations due to FK506 were caused by both the dissociation of FKBP 12.6/calcineurin from RyR2 and the inhibition of the phosphatase activity of calcineurin. Deltamethrin and cyclosporin A also evoked $Ca^{2+}$ oscillations and given they do not dissociate FKBP 12.6 from RyR2, it was implied that calcineurin mediated dephosphorylation was involved in the modulation of RyR2 activity. Addition of deltamethrin or cyclosporin A to rapamycin induced oscillations had little effect and it was implied that only calcineurin associated with RyR2 could regulated the channel's activity.

Intriguingly, Cameron *et al.*, 1995, have demonstrated that calcineurin is anchored to the $IP_3$ receptor via FKBP however a different study on human solubilised cardiac protein found that calcineurin was not part of the ryanodine receptor macromolecular complex (Marx *et al.*, 2000).

### 5.1.7 Aims

To evaluate the effect of FKBP 12.6 on cardiac E-C coupling, adult rabbit ventricular myocytes were transfected with a recombinant adenovirus coding for human FKBP 12.6 (Ad-FKBP 12.6). A β-galactosidase virus was used as a control (Ad-LacZ). Viruses were constructed by Dr. Tim Seidler, Georg-August-Universitat, Goettingen, Germany.

It was proposed that after 24 hrs in culture the virus-transfected cells would be loaded with fura-2 and E-C coupling studied using whole cell voltage clamp. This was to enable the effects of FKBP 12.6 overexpression on the L-type $Ca^{2+}$ current, the intracellular $Ca^{2+}$ transient, SR $Ca^{2+}$ load, NCX activity and sarcolemmal $Ca^{2+}$ ATPase activity to be determined. The effects of acute overexpression of FKBP 12.6 on $Ca^{2+}$ spark characteristics were also obtained using laser scanning confocal microscopy.

In addition, a recombinant adenovirus, which over-expressed a mutant form of FKBP 12.6 lacking the calcineurin-binding site (Ad-FKBP 12.6 mut), was also employed to determine the functional significance of this phosphatase with regard to E-C coupling.

## 5.2 Results

### 5.2.1 Measurement of FKBP 12.6 mRNA and protein expression levels.

The levels of FKBP 12.6 mRNA and protein overexpression at various MOI's were determined using real time PCR and Western blot technique.

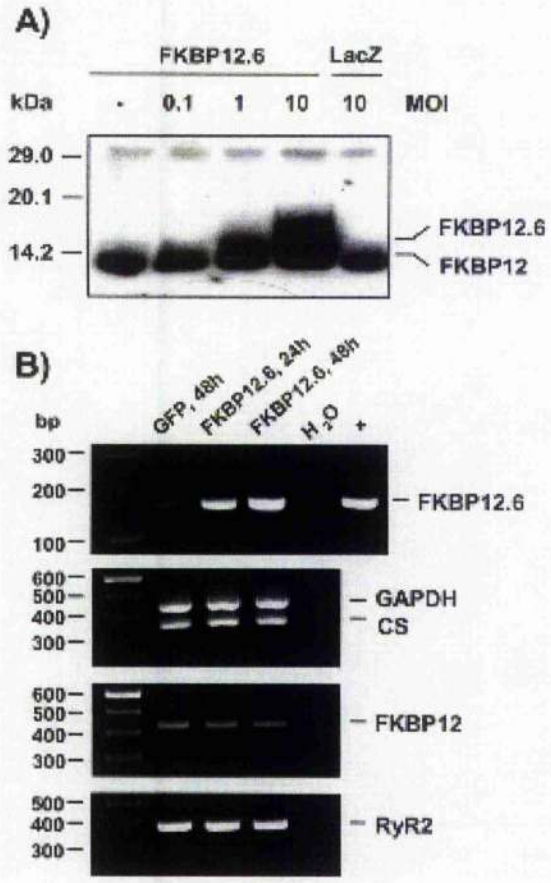


**Figure 5 - 1. Western immunoblot analysis of Ad-LacZ (LacZ)–infected and Ad-FKBP12.6 infected myocytes.**

**Cells were infected with indicated MOI and harvested after 48 hours of culture time. FKBP12.6 protein expression increases with increasing virus titers. FKBP12.6 migrates as a broad band during electrophoresis and could not be clearly separated from endogenous FKBP12. B, RT-PCR analysis of Ad-GFP (GFP)–infected and Ad-FKBP12.6-GFP (FKBP12.6)–infected myocytes. Cells were infected at an MOI of 10 and were harvested for RT-PCR analysis with gene-specific primers after 24 and 48**

**hours of culture time. Size of DNA markers are indicated on the left. + indicates positive control with FKBP12.6 plasmid DNA as template. Duplex RT-PCR with GAPDH- and calsequestrin-specific primers using the same probes indicates equal cDNA load in each PCR. FKBP12.6 mRNA expression in Ad-FKBP12.6-GFP–infected cells increases with culture time, whereas endogenous FKBP12 and RyR2 mRNA expression remains unchanged. Measurements by Dr. Jurgen Prestle (Georg-August-Uiversitat, Goettingen).**

5.2.2 Effect of FKBP 12.6 overexpression on the L-type $Ca^{2+}$ current and intracellular $Ca^{2+}$ transient.

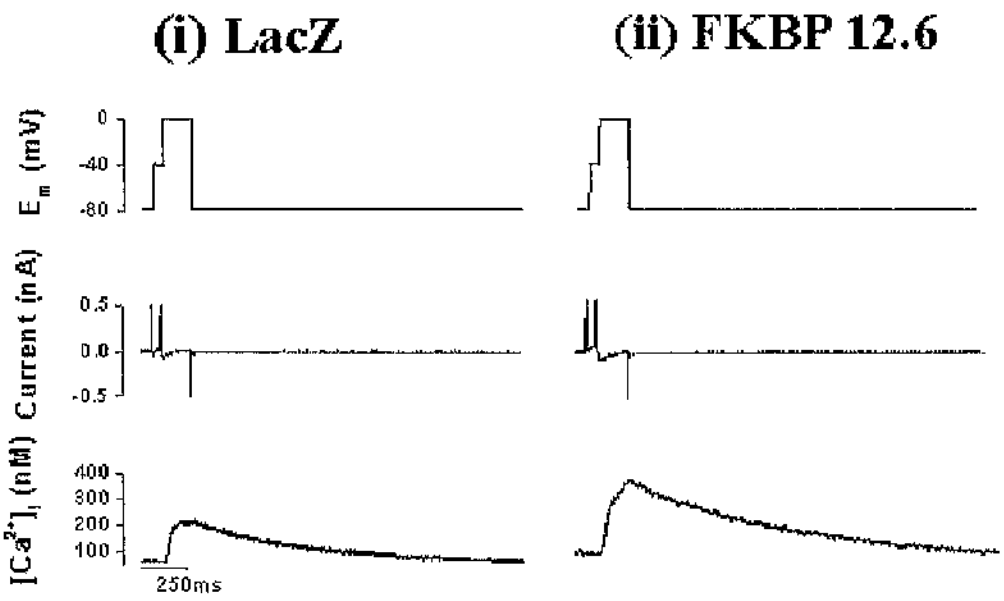

Figure 5 - 2. Depolarisation-induced L-type $Ca^{2+}$ currents and intracellular $Ca^{2+}$ transients in voltage clamped Ad-LacZ (i) and Ad-FKBP 12.6 (ii) transfected cardiomyocytes. A, Typical traces of membrane potential ($E_m$), membrane current and $[Ca^{2+}]_i$ from single cardiomyocytes (average of 10 sweeps).

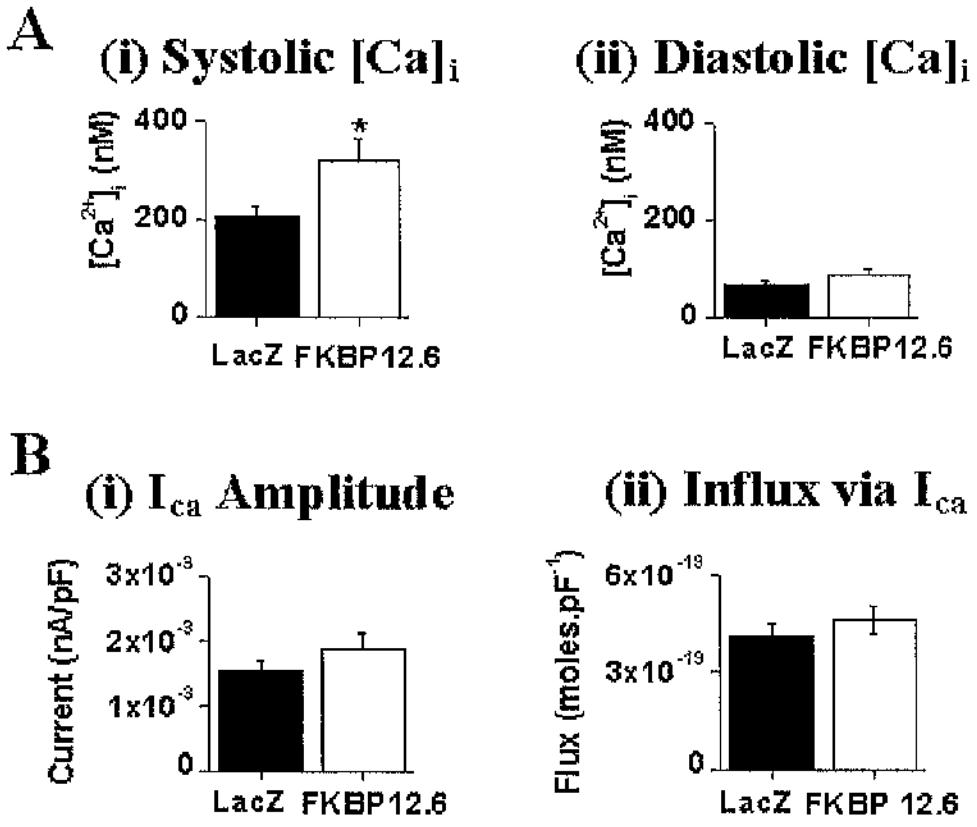


Figure 5 - 3. A, Mean ± SEM values of peak systolic (i) and end diastolic (ii) $[Ca^{2+}]_i$ and B, Mean ± SEM values of peak $I_{Ca}$ (i) and $Ca^{2+}$ influx via $I_{Ca}$ (ii) in Ad-LacZ (n=22) and Ad-FKBP 12.6 (n=18) transfected cardiomyocytes.

Figure 5-3 demonstrates that Ad-FKBP 12.6 transfection significantly increased peak systolic $[Ca^{2+}]_i$ and slightly elevated end diastolic $[Ca^{2+}]_i$ in voltage clamped rabbit cardiomyocytes, causing a increased $Ca^{2+}$ transient amplitude. In addition it shows that neither the amplitude nor the time integral of $I_{Ca}$ (which can be converted to a $Ca^{2+}$ influx) are significantly altered by FKBP 12.6 overexpression.

5.2.3 Effect of FKBP 12.6 overexpression on SR $Ca^{2+}$ content (assessed by rapid application of 10mM caffeine)

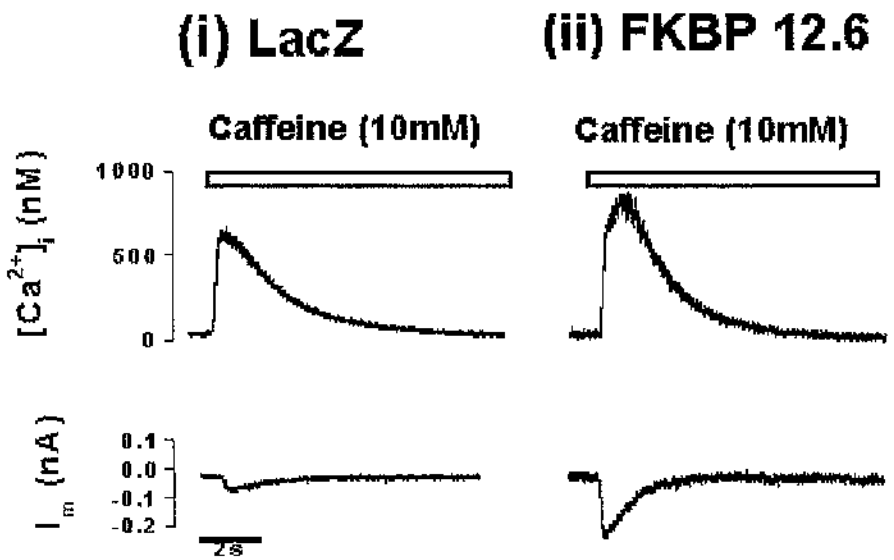


**Figure 5 - 4. FKBP 12.6 overexpression and rapid application of 10mM caffeine.**

**A, SR $Ca^{2+}$ release and corresponding membrane currents recorded upon rapid application of 10mM caffeine in typical Ad-LacZ (i) and Ad-FKBP 12.6 (ii) transfected cardiomyocytes.**

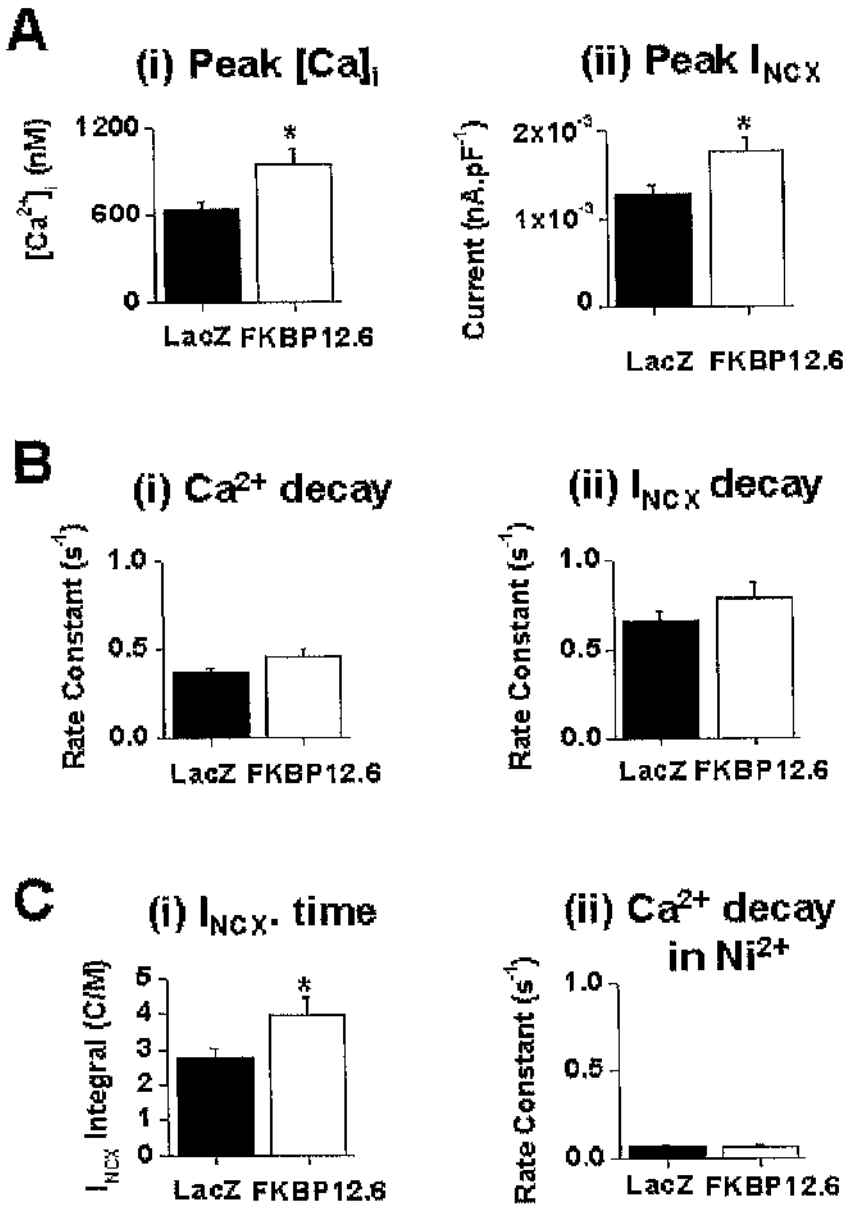


**Figure 5 - 5. FKBP 12.6 overexpression and SR $Ca^{2+}$ load.**

**A, Mean ± SEM values for (i) peak $[Ca^{2+}]_i$ (Ad-LacZ, n=18 vs. Ad-FKBP, n=17) and (ii) and peak $I_{NCX}$ (Ad-LacZ, n=12 vs. Ad-FKBP, n=11). B, Mean ± SEM values for (i) rate constant of $[Ca^{2+}]_i$ decay (Ad-LacZ, n=12 vs. Ad-FKBP, n=13) and (ii) and rate constant of $I_{NCX}$ decay (Ad-LacZ, n=12 vs. Ad-FKBP, n=11). C, Mean ± SEM values for (i) $I_{NCX}$-time integral (Ad-LacZ, n=12 vs. Ad-FKBP, n=11) and (ii) rate constant of $[Ca^{2+}]_i$ decay in $Ni^{2+}$ (Ad-LacZ, n=6 vs. Ad-FKBP, n=5).**

10mM caffeine was rapidly applied to cardiomyocytes contracting in the steady state in order to assess SR $Ca^{2+}$ load. Figures 5-5 A (i) and C (i) clearly demonstrate that both the caffeine-induced $Ca^{2+}$ transient and the integral of the caffeine-induced transient inward current with respect to time are significantly increased in Ad-FKBP 12.6 transfected cardiomyocytes when compared to control. These results indicate that FKBP 12.6 overexpression significantly increases SR $Ca^{2+}$ content.

Figure 5-5 A (ii) shows that the peak of the transient inward current was significantly increased by FKBP 12.6 overexpression, figure 5-5 B (ii) shows that its rate constant of decay, calculated by fitting with a single exponential, is similar in Ad-FKBP 12.6 transfected cardiomyocytes when compared to Ad-LacZ. Likewise, the rate constant for the decay of the caffeine-induced $Ca^{2+}$ transient (see figure 5-5 B (i)) was also unaltered in the Ad-FKBP 12.6 transfected myocytes. These similar rate constants of decay would suggest that FKBP 12.6 overexpression has no effect on the rate of extrusion of $Ca^{2+}$ from the cytosol at the sarcolemma via NCX. Figure 5-5 C (ii) demonstrates that when caffeine was applied with $Ni^{2+}$, the rate constant for the decay of the corresponding $Ca^{2+}$ transient was similar in both experimental groups. Indication that FKBP 12.6 overexpression does not affect sarcolemmal $Ca^{2+}$-ATPase activity.

5.2.4 Effect of FKBP 12.6 overexpression on spontaneous $Ca^{2+}$ spark activity and SR $Ca^{2+}$ load in permeabilised rabbit cardiomyocytes

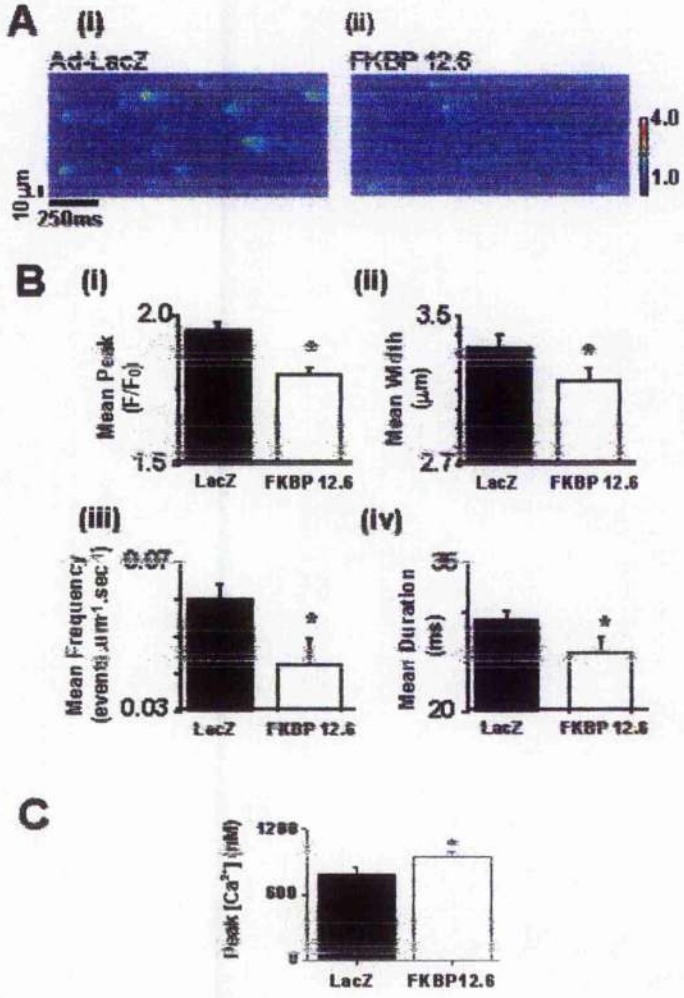


**Figure 5 - 1. Effects of FKBP 12.6 overexpression on spontaneous $Ca^{2+}$ sparks.**

**A, *Pseudo-colour line scan epi-fluorescence image from single permeabilized* cardiomyocytes perfused with the experimental solution containing 155nmol/L $Ca^{2+}$ (i) Ad-LacZ infected cell and (ii) Ad-FKBP12.6 infected cell. B, Mean ±SEM values for: (i) peak F/Fo; (ii) spark width (full width half maximal) (iii) spark frequency; (iv) spark duration (full width half maximal). C, Peak $[Ca^{2+}]_i$ during caffeine induced $Ca^{2+}$ release in permeabilised cardiomyocytes equilibrated in 150nmol/L $Ca^{2+}$. Measurements by Dr. C Loughrey - University of Glasgow.**

5.2.5 Effect of FKBP 12.6 overexpression on the synchronicity of E-C coupling in field stimulated rabbit cardiomyocytes

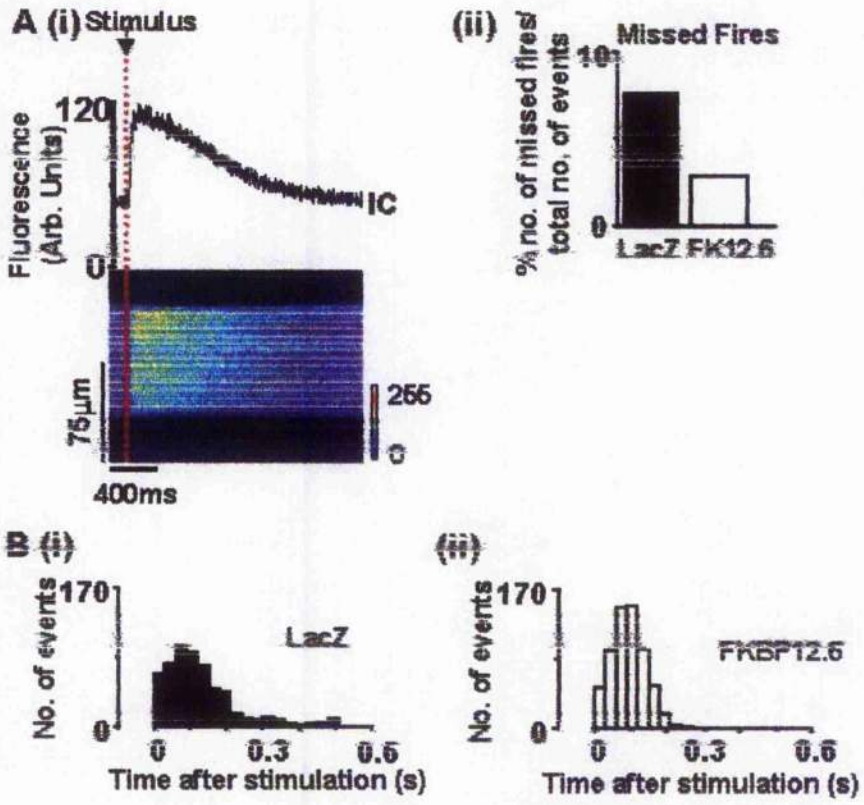


**Figure 5 - 1. FKBP 12.6 overexpression and synchrony of SR $Ca^{2+}$ release.**

**A *(i), Mean cellular fluorescence from a confocal linescan image of a $Ca^{2+}$ transient* recorded from a cultured cardiomyocyte after transfection with Ad-FKBP12.6. The confocal linescan image was split into 12x20pixel sections as indicated in the pseudo-colour image. The mean fluorescence signal in each 20-pixel section was used to measure the time from stimulus to 50% of the transient amplitude ($Time_{50}$). A (ii), % of sites not generating a $Ca^{2+}$ transient (Time50 > 0.5 s) in both experimental groups. B, Distribution histograms of $Time_{50}$ values measured from (i) Ad-LacZ group (n=9 cells) and (ii) Ad-FKBP12.6 group (n=9 cells).**

The effect of FKBP 12.6 overexpression on SR $Ca^{2+}$ release function was investigated by measuring spontaneous $Ca^{2+}$ sparks in β-escin permeabilised cardiomyocytes. Single cardiomyocytes were superfused with a standardised [$Ca^{2+}$] and pH in the presence of ATP and CrP and $Ca^{2+}$ spark activity was monitored for one minute by the inclusion of 10μmol/L Fluo-3 in the perfusing solution. SR $Ca^{2+}$ load was then assessed by the rapid application of 10mM caffeine. Figure 5-6 (i) and (ii) show typical line scan traces and $Ca^{2+}$ sparks from cardiomyocytes transfected with Ad-LacZ and Ad-FKBP 12.6 respectively. Figure 5-6 B demonstrates that $Ca^{2+}$ spark activity was clearly altered by FKBP 12.6 overexpression with spark peak, frequency, width and duration all significantly reduced. (Peak F/Fo (1.80±0.03 vs 1.96±0.02), width (3.15±0.07μm vs 3.33±0.07μm); duration (26.09 ms ± 1.5 vs 29.21±1.0ms) and frequency (0.04±0.007 events.$\mu m^{-1}.s^{-1}$ vs 0.06±0.004events.$\mu m^{-1}.s^{-1}$; Ad-FKBP12.6 n=9 cells v Ad-LacZ n=18 cells). Figure 5-6 C shows that the mean amplitude of caffeine-induced $Ca^{2+}$ release, and hence SR $Ca^{2+}$ load, was significantly increased in the Ad-FKBP 12.6 transfected group.

Cardiomyocytes over-expressing FKBP12.6 appeared to have a more uniform $Ca^{2+}$ release pattern compared to Ad-LacZ transfected cardiomyocytes. Some sites along the length of the Ad-LacZ cardiomyocyte did not respond to field stimulation, others sites responded after a delay. The time from stimulation to 50% of the peak of each transient (Time $_{50}$) was calculated for each of the 12 bands (see Figure 5-7 A(i) on 6 serial steady-state $Ca^{2+}$-transients from each cardiomyocyte. The range of $Time_{50}$ values measured in a number of cardiomyocytes from the two experimental

groups were displayed as histograms (Figure 5-7 B) for: (i) Ad-LacZ cells; (ii) Ad-FKBP12.6; Only the values for $Time_{50}$ less then 0.5s are shown, values greater than 0.5s are considered 'miss-fires' and quantified separately. The distribution of $Time_{50}$ values for the cells infected with FKBP12.6 had a much narrower profile than the control Ad-LacZ cells. FKBP12.6-over-expression significantly reduced the mean $Time_{50}$ by 40% and the range of values for $Time_{50}$ by 62%. As indicated in Figure 5-7 A(ii), the corresponding number of miss-fires was lower in FKBP12.6 infected cells (2.73%) than Ad-LacZ cells (7.5%). In order to determine whether the increased SR $Ca^{2+}$ load in the Ad-FKBP 12.6 transfected cardiomyocytes may explain this increased synchronicity the 4 largest $Ca^{2+}$ transients in the Ad-LacZ group were compared with the 4 smallest $Ca^{2+}$ transients in the Ad-FKBP12.6 group. The SR $Ca^{2+}$ contents of the 4 Ad-LacZ transfected cardiomyocytes were not significantly different from those of the 4 Ad-FKBP 12.6 transfected cells. The mean $Ca^{2+}$ transient peak in these two sub-groups was not significantly different, yet the mean $Time_{50}$ and range of $Time_{50}$ values were still significantly lower in the Ad-FKBP12.6 group (data not included). This would suggest that FKBP12.6 over-expression causes a more rapid and synchronous increase of intracellular $Ca^{2+}$, independent of its effects on SR $Ca^{2+}$ load.

5.2.6 Relationship between SR $Ca^{2+}$ content and $Ca^{2+}$ transient amplitude in Ad-LacZ and Ad-FKBP 12.6 transfected cardiomyocytes.

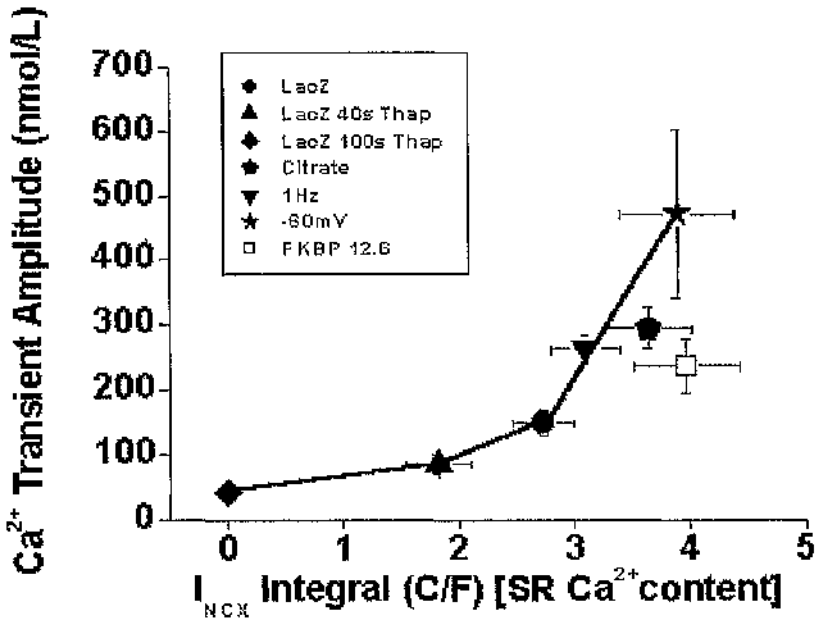


**Figure 5 - 8. FBKP 12.6 overexpression and the gain of EC-coupling.**

**Relationship between $I_{NCX}$ integral (an index of SR $Ca^{2+}$ content) and $Ca^{2+}$ transient amplitude for cardiomyocytes from Ad-LacZ (Control; Thapsigargin 40s exposure; Thapsigargin 100s exposure; Citrate; 1Hz stimulation ; Hold -60mV) and Ad-FKBP 12.6 groups. Measurements were obtained in the steady state; lower SR loads were achieved by exposure to 5μM Thapsigargin for various times, higher SR loads were obtained by adding 20mM Citrate to the pipette solution, by stimulating at a frequency of 1Hz or by holding membrane potential at -60mV between depolarisations.**

The increased $Ca^{2+}$ transient amplitude in the Ad-FKBP 12.6 transfected cardiomyocytes could be explained by the increased SR $Ca^{2+}$ load. This possibility was investigated by using experimental intervention to either increase or decrease SR $Ca^{2+}$ content in Ad-LacZ transfected

cardiomyocytes and noting the resultant effects on $Ca^{2+}$ transient amplitude. Figure 5-8 demonstrates that the relationship for $Ca^{2+}$ transient amplitude vs. $I_{NCX}$ integral for Ad-LacZ transfected cardiomyocytes is close to hyperbolic. The average $Ca^{2+}$ transient amplitude for the FKBP 12.6 group is not significantly different to that observed in Ad-LacZ transfected cardiomyocytes with similar SR loads (SR $Ca^{2+}$ load increased with citrate). Hence there is little evidence for an effect of FKBP 12.6 on the gain of E-C coupling. Thus it is possible that the effects of FKBP 12.6 overexpression on E-C coupling could be explained by an increase in SR $Ca^{2+}$ content alone.

5.2.7 Effect of FKBP 12.6 mutant (lacking the calcineurin binding site) overexpression on the L-type $Ca^{2+}$ current and intracellular $Ca^{2+}$ transient.

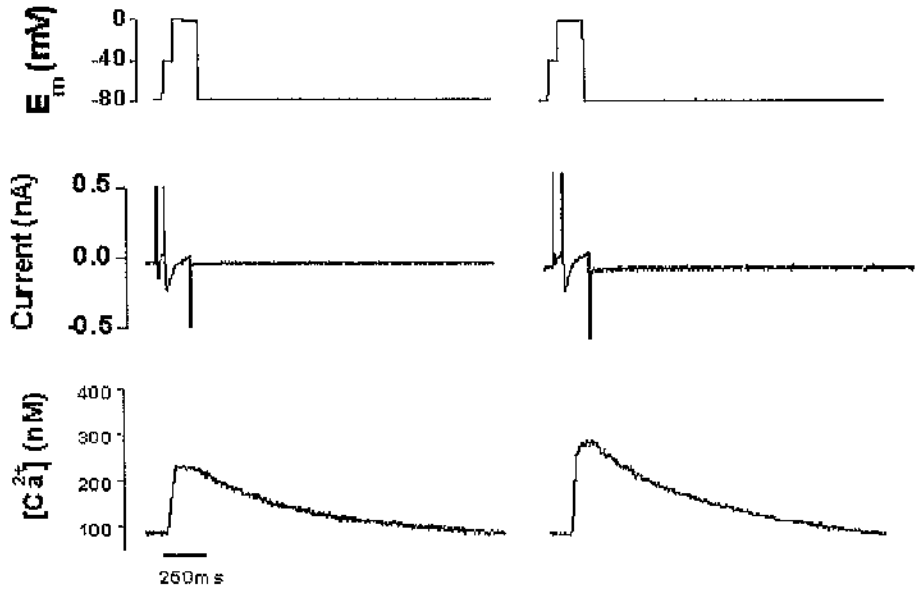


**Figure 5 - 9. FKBP 12.6 mutant overexpression and EC-coupling.**

**Depolarisation-induced L-type $Ca^{2+}$ currents and intracellular $Ca^{2+}$ transients in voltage clamped Ad-LacZ (i) and Ad-FKBP 12.6 mutant (ii) transfected**

**cardiomyocytes. A, Typical traces of membrane potential ($E_m$), membrane current and $[Ca^{2+}]_i$ from single cardiomyocytes (average of 10 sweeps).**

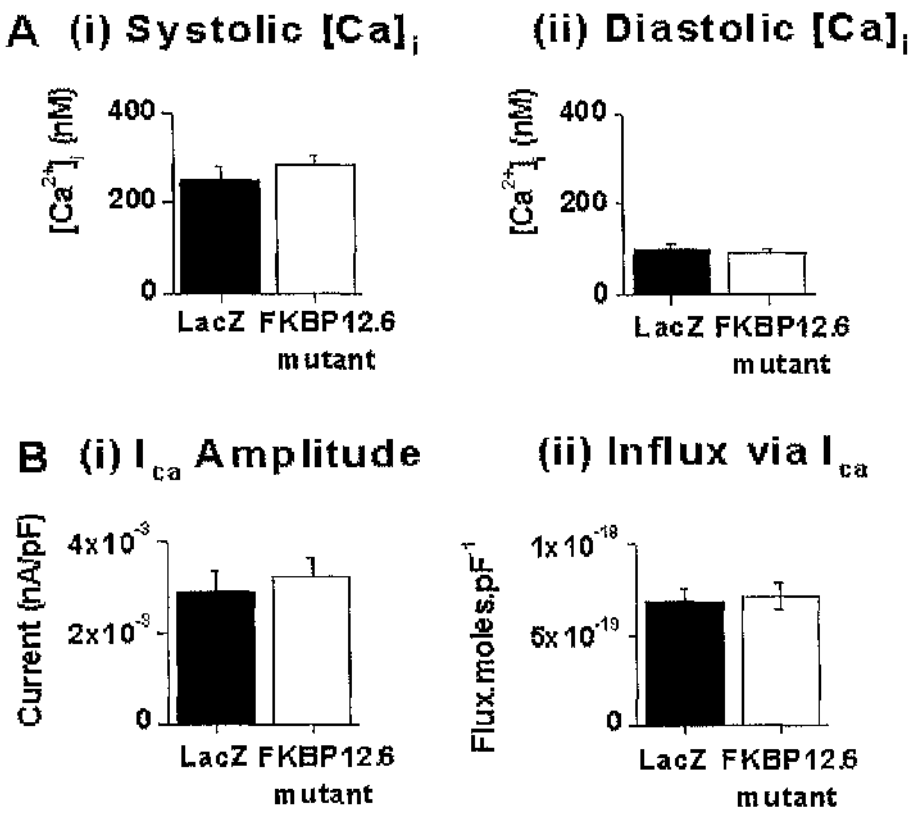


**Figure 5 - 10. A, Mean ± SEM values of peak systolic (i) and end diastolic (ii) $[Ca^{2+}]_i$ and B, Mean ± SEM values of peak $I_{Ca}$ (i) and $Ca^{2+}$ influx via $I_{Ca}$ (ii) in Ad-LacZ (n=20) and Ad-FKBP 12.6 (n=18) mutant transfected cardiomyocytes.**

Figure 5-10 demonstrates that Ad-FKBP 12.6 mutant transfection slightly increased in peak systolic $[Ca^{2+}]_i$ (ns) and slightly decreased end diastolic $[Ca^{2+}]_i$ (ns) in voltage clamped rabbit cardiomyocytes. However FKBP 12.6 mutant overexpression did not cause a significant increase in the size of the $Ca^{2+}$ transient amplitude. It also demonstrates that neither the amplitude

nor the time integral of $I_{Ca}$ (which can be converted to a $Ca^{2+}$ influx) are significantly altered by FKBP 12.6 mutant overexpression.

5.2.8 Effect of FKBP 12.6 mutant overexpression on SR $Ca^{2+}$ content (assessed by rapid application of 10mM caffeine)

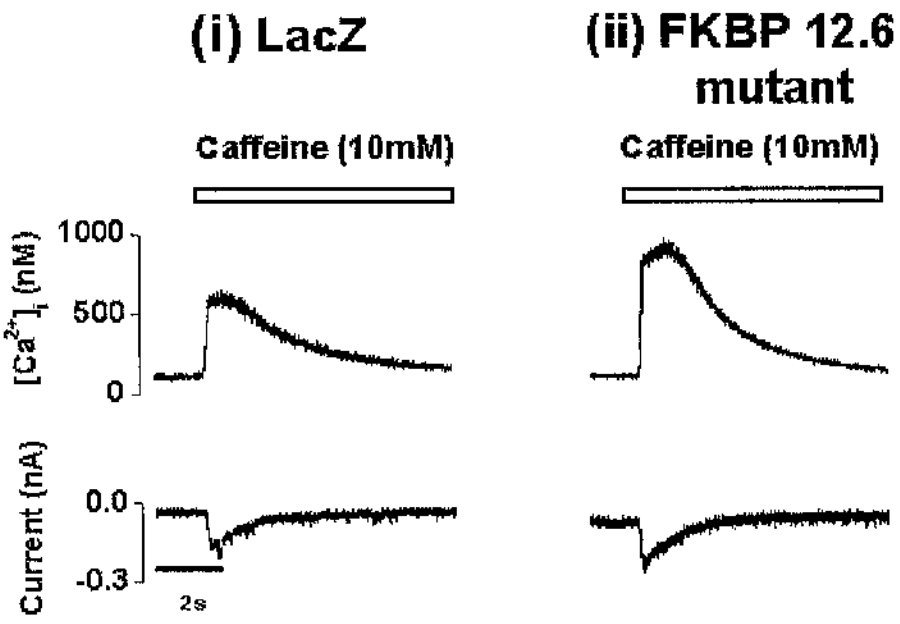


**Figure 5 - 11. FKBP 12.6 mutant overexpression and rapid application of 10mM caffeine.**

**A, SR $Ca^{2+}$ release and corresponding membrane currents recorded upon rapid application of 10mM caffeine in typical Ad-LacZ (i) and Ad-FKBP 12.6 mutant (II) transfected cardiomyocytes.**

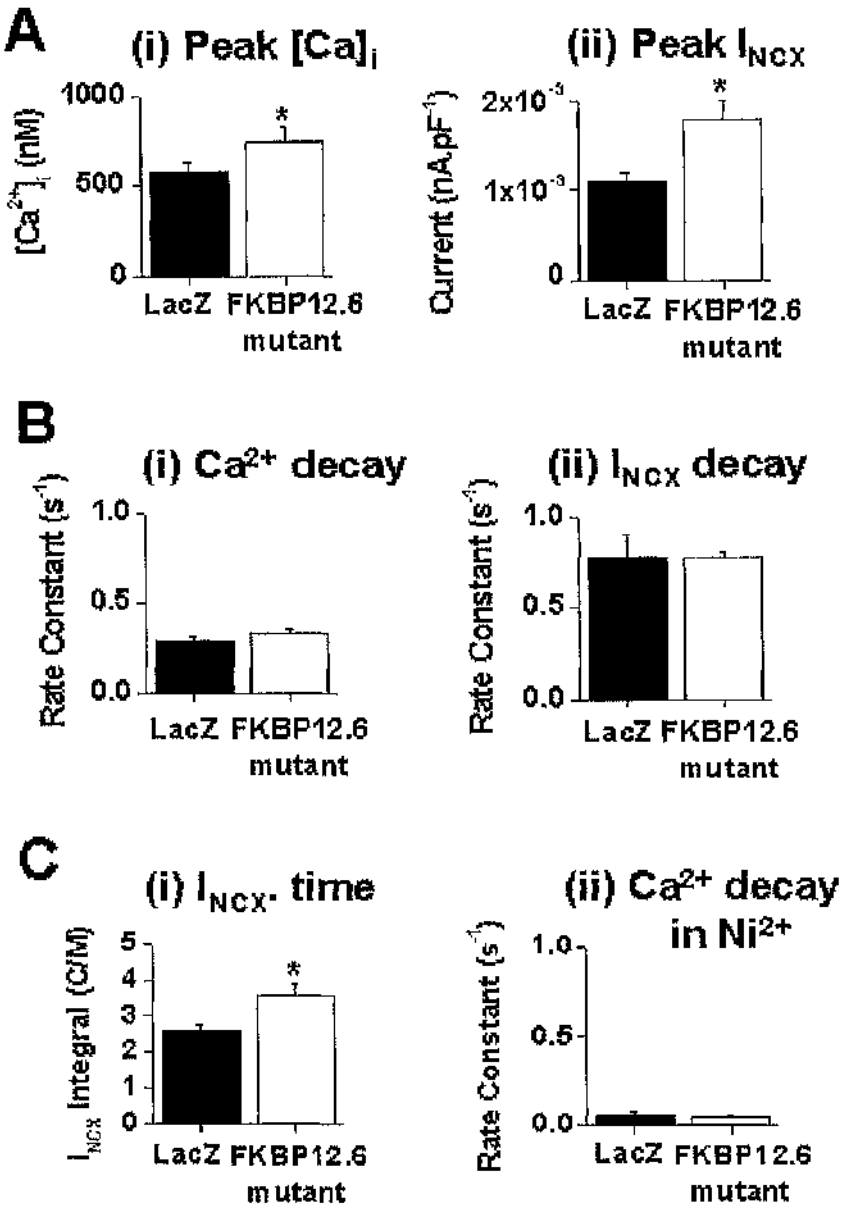


**Figure 5 - 12. FKBP 12.6 mutant overexpression and SR $Ca^{2+}$ load.**

**A, Mean ± SEM values for (I) peak $[Ca^{2+}]_i$ (Ad-LacZ, n=10 vs. Ad-FKBP mut, n=10) and (Ii) and peak $I_{NCX}$ (Ad-LacZ, n=10 vs. Ad-FKBP mut, n=10). B, Mean ± SEM values for (I) rate constant of $[Ca^{2+}]_i$ decay (Ad-LacZ, n=10 vs. Ad-FKBP mut, n=8) and (ii) and rate constant of $I_{NCX}$ decay (Ad-LacZ, n=8 vs. Ad-FKBP mut, n=9). C, Mean ± SEM values for (i) $I_{NCX}$.time integral (Ad-LacZ, n=10 vs. Ad-FKBP mut, n=10) and (ii) rate constant of $[Ca^{2+}]_i$ decay in $Ni^{2+}$ (Ad-LacZ, n=5 vs. Ad-FKBP mut, n=5).**

Once again, 10mM caffeine was rapidly applied to Ad-LacZ and Ad-FKBP 12.6 mutant transfected cardiomyocytes contracting in the steady state, causing the SR to release its store of $Ca^{2+}$ into the cytoplasm. Figures 5-12 A (i) and C (i) clearly demonstrate that both the caffeine-induced $Ca^{2+}$ transient and the integral of the transient inward current with respect to time are significantly increased in Ad-FKBP 12.6 mutant transfected cardiomyocytes when compared to control. These results indicate that FKBP 12.6 mutant overexpression significantly increases SR $Ca^{2+}$ content.

Figure 5-12 A (ii) shows that the peak of the transient inward current was significantly increased by FKBP 12.6 mutant overexpression. Figure 5-12 B (ii) shows that its rate constant of decay, calculated by fitting with a single exponential, is similar in Ad-FKBP 12.6 mutant transfected cardiomyocytes when compared to Ad-LacZ. Likewise, the rate constant for the decay of the caffeine-induced $Ca^{2+}$ transient (see figure 5-12 B (i)) was also unaltered in the Ad-FKBP 12.6 mutant transfected myocytes. These similar rate constants of decay would suggest that FKBP 12.6 mutant overexpression has no effect on the rate of extrusion of $Ca^{2+}$ from the cytosol at the sarcolemma via NCX. Figure 5-12 C (ii) demonstrates that when caffeine was applied with $Ni^{2+}$ (to block NCX), the rate constant for the decay of the corresponding $Ca^{2+}$ transient (either via the action of the sarcolemmal $Ca^{2+}$ ATPase or via mitochondrial $Ca^{2+}$ uptake) was similar in both experimental groups. Indication that FKBP 12.6 mutant overexpression does not affect these alternative $Ca^{2+}$ removal mechanisms.

5.2.9 Effect of FKBP 12.6 mutant overexpression on spontaneous $Ca^{2+}$ spark activity and SR $Ca^{2+}$ load in permeabilised rabbit cardiomyocytes

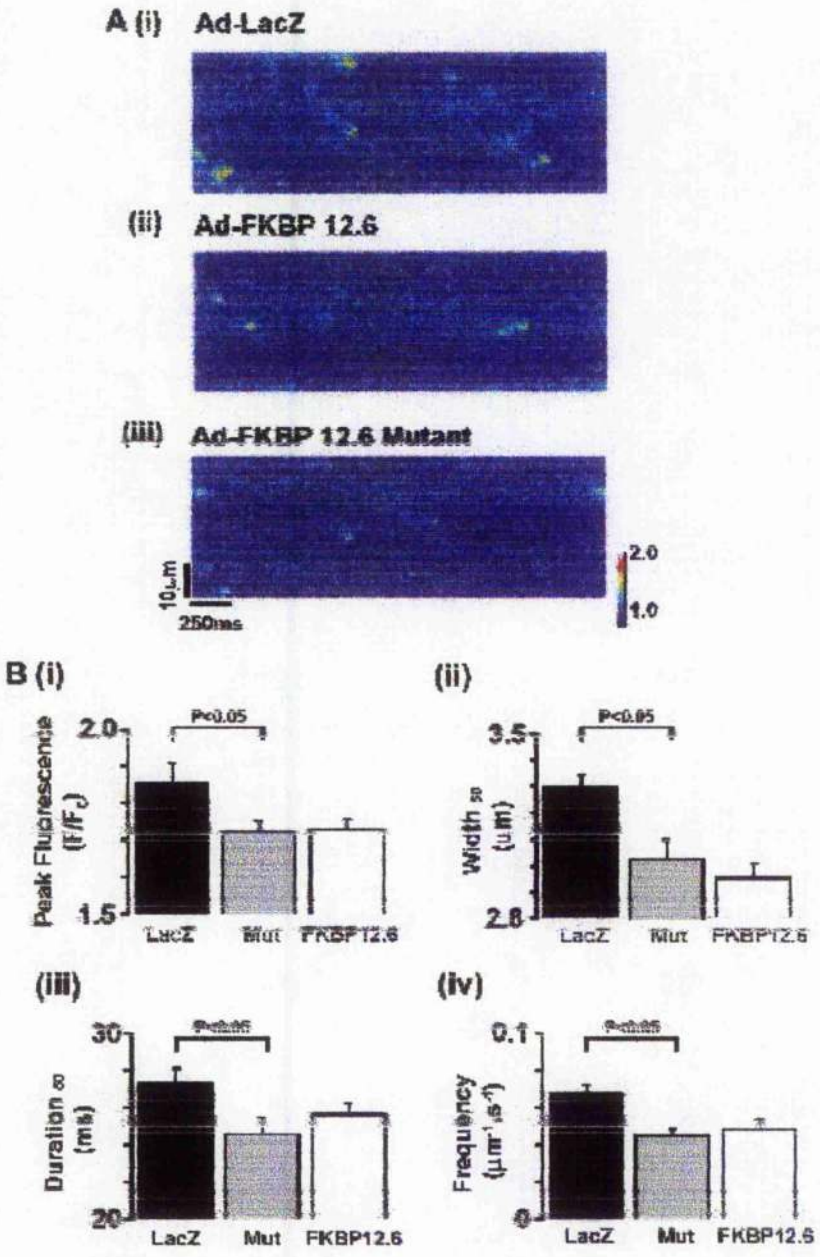

**Figure 5 - 13. Effects of FKBP 12.6 mutant overexpression on spontaneous $Ca^{2+}$ sparks.**

**A(i-iii) shows confocal line-scan images recorded from permeabilised rabbit cardiomyocytes after transfection with (i) Ad-LacZ, (ii) Ad-FKBP12.6, (iii) Ad-FKBP12.6 Mutant respectively on the same day and under the same conditions. Figures XB(i-iv) show average $Ca^{2+}$ spark peak fluorescence, width, duration and frequency for each experimental group. Measurements by Dr. C Loughrey - University of Glasgow.**

$Ca^{2+}$ sparks recorded in FKBP12.6 and FKBP12.6 Mutant transfected cardiomyocytes were smaller and less frequent than the Ad-LacZ control. The average $Ca^{2+}$ spark peak, frequency, width and duration (Figures 5-13 B i–iv) were all significantly reduced in the FKBP12.6 over-expressing cells (peak F/Fo, 1.85±0.06 vs.1.73±0.03, $P<0.05$; frequency, 0.067±0.005 vs. 0.048±0.006 $\mu m^{-1}s^{-1}$, $P<0.05$; width, 3.30±0.05 vs. 3.00±0.06μm, $P<0.05$; duration, 27.30±0.8 vs. 25.4±0.6ms, $P<0.05$; Ad-LacZ n=11cells vs. Ad-FKBP12.6 n=10cells) and were not significantly different from $Ca^{2+}$ sparks in cells over-expressing the Ad-FKBP12.6 mutant (peak F/Fo, 1.72±0.03; frequency, 0.045±0.004$\mu m^{-1}s^{-1}$; width, 3.03±0.08μm; duration, 24.62±0.9ms; Ad-FKBP12.6 Mutant n=12 cells).

5.2.10 Relationship between SR $Ca^{2+}$ content and $Ca^{2+}$ transient amplitude in Ad-LacZ and Ad-FKBP 12.6 mutant transfected cardiomyocytes.

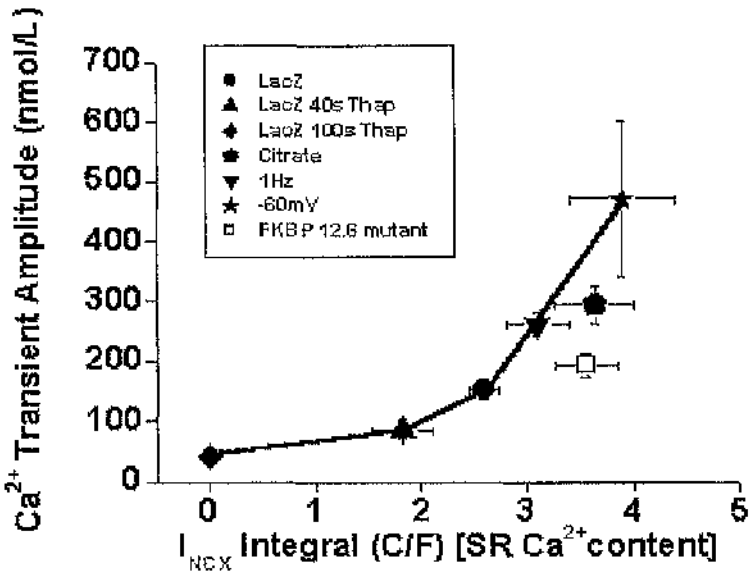


**Figure 5 - 14. FKBP 12.6 mutant overexpression and the gain of EC-coupling.**

**Relationship between $I_{NCX}$ integral (an index of SR $Ca^{2+}$ content) and $Ca^{2+}$ transient amplitude for cardiomyocytes from Ad-LacZ (Control; Thapsigargin 40s exposure; Thapsigargin 100s exposure; Citrate; 1Hz stimulation ; Hold -60mV) and Ad-FKBP 12.6 mutant groups. Measurements were obtained in the steady state; lower SR loads were achieved by exposure to 5μM Thapsigargin for various times, higher SR loads were obtained by adding 20mM Citrate to the pipette solution, by stimulating at a frequency of 1Hz or by holding membrane potential at -60mV between depolarisations.**

The increased SR $Ca^{2+}$ load in the Ad-FKBP 12.6 mutant transfected cardiomyocytes would be expected to significantly increase the size of the calcium transient amplitude. The normal relationship between SR $Ca^{2+}$ load and calcium transient amplitude was determined by experimental intervention in Ad-LacZ transfected cardiomyocytes. The average $Ca^{2+}$

transient amplitude for the FKBP 12.6 mutant group is significantly reduced when compared to Ad-LacZ transfected cardiomyocytes with similar SR loads (SR $Ca^{2+}$ load increased with citrate). Thus the data for the FKBP 12.6 mutant group falls to the right of the relationship described for the Ad-LacZ group, with a much smaller $Ca^{2+}$ transient amplitude than would be predicted for the average SR $Ca^{2+}$ load (see figure 5-14). Hence it seems that FKBP 12.6 mutant overexpression has reduced the gain of E-C coupling.

## 5.3 Discussion

This chapter has investigated the effects of adenoviral mediated FKBP 12.6 overexpression on cardiac E-C coupling in cultured rabbit cardiomyocytes. An adenovirus that over-expressed a mutant form of FKBP 12.6 lacking the calcineurin-binding site (Ad-FKBP 12.6 mutant), was also employed to determine the functional significance of this phosphatase. Figure 5-15 below depicts the amino acid sequence of FKBP 12.6 and also highlights the mutation that prevents calcineurin from binding.

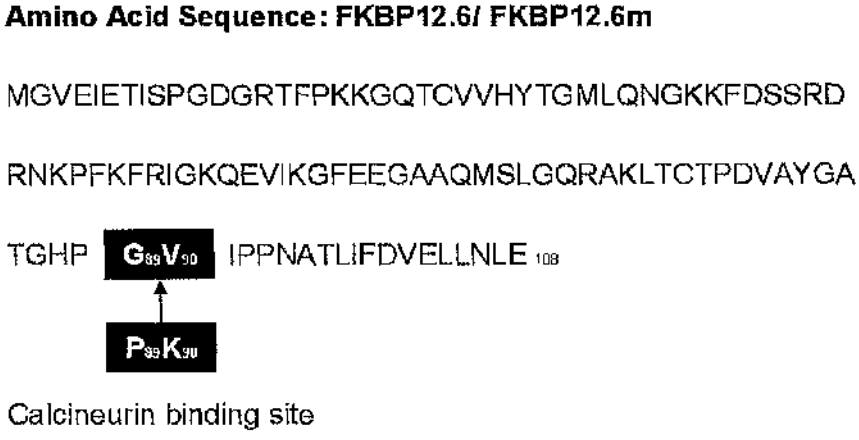


**Figure 5-15. The amino acid sequence of FKBP 12.6 and the FKBP 12.6 mutant lacking the calcineurin binding site.**

### 5.3.1 Can FKBP 12.6 overexpression increase its occupancy of RyR2?

It is thought that under normal conditions, the occupancy of RyR2 with FKBP12.6 is close to maximal i.e. 4FKBP12.6:1RyR2 tetramer (Marx *et al.*,

2000). Hence it could be argued that adenoviral mediated over-expression of FKBP12.6 may not boost FKBP12.6:RyR2 stoichiometry significantly.

The present study was carried out using cultured cardiomyocytes. Prestle *et al.*, 2001 have demonstrated that rapamycin has no effect on RyR2-mediated $Ca^{2+}$ leak in 2 day cultured myocytes, indicating that FKBP 12.6 may already be dissociated from RyR2 in these cells. Additionally, spontaneous $Ca^{2+}$ sparks in 2-day cultured cardiomyocytes are significantly larger when compared to those observed in freshly dissociated myocytes. (Loughrey *et al.*, 2004). Removal of FKBP 12.6 from RyR2 has been shown to increase the frequency, amplitude, width and duration of spontaneous $Ca^{2+}$ sparks (McCall *et al.*, 1996, Xin *et al.*, 2002 & Xiao *et al.*, 1997). Therefore it seems likely that overexpression of FKBP 12.6 in cultured cardiomyocytes will serve to return the FKBP12.6:RyR2 stoichiometry toward normal levels and thus reveal the functional significance of the protein.

### 5.3.2 The effect of FKBP 12.6 and FKBP 12.6 mutant on sarcolemmal $Ca^{2+}$ entry and extrusion

FK-binding proteins are not thought to modulate any of the pathways by which $Ca^{2+}$ might enter or leave the cardiomyocyte. This study has demonstrated that acute adenoviral-mediated FKBP 12.6 overexpression in cultured rabbit cardiomyocytes has no effect on the amplitude or the integral of $I_{Ca}$. Similar observations were made with FKBP 12.6 mutant

overexpression. Hence an increase in the size of the trigger for CICR cannot explain the increased intracellular $Ca^{2+}$ transient in the Ad-FKBP 12.6 transfected myocytes.

NCX activity is unaltered in both FKBP 12.6 and FKBP 12.6 mutant over-expressing cardiomyocytes. The rate constants for the decay of the caffeine-induced $Ca^{2+}$ transient and the corresponding transient inward current were not significantly different when compared to LacZ controls. The rate constant of $Ca^{2+}$ extrusion in response to caffeine and in the presence of nickel, taken to represent sarcolemmal $Ca^{2+}$ ATPase activity, was also unaltered in both FKBP 12.6 and FKBP 12.6 mutant transfected cardiomyocytes. Thus it seems unlikely that any reduction in the rate of $Ca^{2+}$ extrusion from the cardiomyocyte at the sarcolemma could account for the increased SR $Ca^{2+}$ load in both the FKBP 12.6 and FKBP 12.6 mutant transfected cardiomyocytes.

### 5.3.3 The effect of FKBP 12.6 overexpression on $Ca^{2+}$ spark characteristics in permeabilised myocytes

The results presented here indicate that $Ca^{2+}$ sparks occurred less frequently and were smaller in amplitude, width and duration in FKBP12.6 over-expressing cardiomyocytes. These observations are consistent with previous studies which have demonstrated that removal of FKBP 12.6 from RyR2 increases $Ca^{2+}$ spark frequency (McCall *et al.*, 1996), amplitude (Xin *et al.*, 2002) and width/duration (Xiao *et al.*, 1997 & Xin *et al.*, 2002). The

inhibitory effects of FKBP12.6 over-expression on $Ca^{2+}$ spark activity are also consistent with the idea that it stabilses the closed conformational state of RyR2 and thus reduces diastolic SR $Ca^{2+}$ leak (Prestle *et al.*, 2001).

### 5.3.3 The effect of FKBP 12.6 on E-C coupling in voltage clamped adult rabbit cardiomyocytes.

Whole cell voltage clamp studies revealed that both the intracellular calcium transient amplitude and the SR calcium content were significantly increased in the Ad-FKBP 12.6 transfected cardiomyocytes. Both the peak amplitude and integral of $I_{Ca}$, the trigger for CICR, were unaffected by FKBP 12.6 overexpression. Therefore it seemed plausible that the increased SR $Ca^{2+}$ content could explain the larger intracellular $Ca^{2+}$ transient. In order to determine whether this was the case, the relationship between SR $Ca^{2+}$ load and intracellular calcium transient amplitude for Ad-LacZ transfected cardiomyocytes was established. It is clear from figure 5-8, that when the SR $Ca^{2+}$ load of the Ad-LacZ transfected cardiomyocytes was increased to levels observed in Ad-FKBP 12.6 transfected cardiomyocytes, the calcium transient amplitudes in both experimental groups did not differ significantly. Hence overexpression of FKBP 12.6 did not appear to significantly alter the gain of E-C coupling.

Prestle *et al.*, 2001, used the same adenovirus to overexpress FKBP 12.6, again in cultured rabbit cardiomyocytes. They also observed an increased SR $Ca^{2+}$ load, explained by a stabilisation of the closed conformational

state of RyR2 by FKBP 12.6 and thus a reduction in diastolic SR $Ca^{2+}$ leak. Similarly, this mechanism could also account for the increased SR $Ca^{2+}$ content observed in Ad-FKBP 12.6 transfected cells in the present study. It is noteworthy that Su *et al.*, 2003, have demonstrated that in rabbit cardiomyocytes, FK506 caused a decreased intracellular $Ca^{2+}$ transient and a reduced SR $Ca^{2+}$ load. Hence the results presented here are entirely consistent with the results of the Su study, with FK506 decreasing SR $Ca^{2+}$ load and $Ca^{2+}$ transient size and FKBP 12.6 overexpression increasing SR $Ca^{2+}$ load and $Ca^{2+}$ transient size.

### 5.3.4 The effect of FKBP 12.6 overexpression on the synchronicity of E-C coupling

Field stimulation studies combined with confocal microscopy revealed a marked asynchrony of $Ca^{2+}$ release in Ad–LacZ transfected cardiomyocytes when compared to FKBP 12.6 overexpressing cells. This was manifest as an increase in the mean $Time_{50}$ (the time from stimulus to 50% of the transient amplitude) and an increase in the % number of "missed fires".

Asynchronous SR $Ca^{2+}$ release has previously been observed in cultured ventricular myocytes and was attributed to decreased transverse (t) -tubular system density (Lipp *et al.*, 1996). Measurements obtained in our laboratory using the membrane dye Di-8-ANEPPS show that t-tubular system staining is not significantly different when Ad-LacZ transfected cardiomyocytes are compared to FKBP 12.6 overexpressing cells (data not

included). Thus it would appear improbable that the affects of FKBP12.6 over-expression on E-C coupling synchronicity are mediated by changes in t-tubular density.

This increase in E-C coupling synchrony does not appear to be simply due to the higher SR $Ca^{2+}$ content observed in the FKBP12.6 overexpressing myocytes. When $Ca^{2+}$ transients of similar amplitudes (and therefore similar SR $Ca^{2+}$ content) from cardiomyocytes in both experimental groups were compared, the Ad-FKBP12.6 group still retained a lower mean $Time_{50}$ and range of $Time_{50}$ values than the control group. This would suggest that enhanced SR $Ca^{2+}$ content alone cannot account for the increased synchrony of release and that the coupling of L-type $Ca^{2+}$ channel activity to SR $Ca^{2+}$ release is enhanced after FKBP12.6 over-expression.

### 5.3.5 The effect of FKBP 12.6 mutant overexpression on $Ca^{2+}$ spark characteristics in permeabilised myocytes

Spontaneous $Ca^{2+}$ sparks in cardiomyocytes over-expressing a FKBP12.6 mutant unable to bind to calcineurin were identical to sparks from cells over-expressing unaltered FKBP12.6. This suggests that a reduction in $Ca^{2+}$ spark size and frequency can be attributed to the over-expression of FKBP12.6 and not the phosphatase action of calcineurin on RyR2. This spark data complements the study of Marx *et al.*, 2000, who failed to demonstrate an association between calcineurin and the RyR2 macromolecular complex in adult human cardiomyocytes. In contrast,

Bandyopadhyay *et al.*, 2000 have shown a $Ca^{2+}$ dependent association between the two proteins in neonatal rat cardiomyocytes. A possible explanation for these contradictory findings may be the [$Ca^{2+}$] under which the associations were studied. While Marx *et al.*, carried out their experiments at low [$Ca^{2+}$], Bandyopadhyay *et al.*, used 100μM $Ca^{2+}$. While [$Ca^{2+}$] within the sarcolemmal cleft is unknown, it is possible that a [$Ca^{2+}$] of 100μM may be transiently attained, however mean intracellular [$Ca^{2+}$] only rises to approximately 1μM during a transient.

5.3.6 The effect of FKBP 12.6 mutant on E-C coupling in voltage clamped adult rabbit cardiomyocytes

Voltage clamp studies revealed that the SR $Ca^{2+}$ content was significantly increased in the Ad-FKBP 12.6 mutant transfected cardiomyocytes when compared to Ad-LacZ control. Both the peak amplitude and integral of the L-type $Ca^{2+}$ current, the trigger for CICR, were unaffected by FKBP 12.6 mutant overexpression. Counter-intuitively, the intracellular calcium transient amplitude was not significantly increased. Thus the gain of E-C coupling was effectively reduced by overexpression with the FKBP 12.6 mutant.

The increased SR $Ca^{2+}$ load suggests that the FKBP 12.6 mutant retains the ability to stabilise RyR2 in the closed conformational state and thus reduce $Ca^{2+}$ leak from the SR during diastole. Since the intracellular $Ca^{2+}$ transient was not significantly increased, it may be that the FKBP 12.6

mutant reduces the efficacy of the L-type $Ca^{2+}$ current in triggering SR $Ca^{2+}$ release. Whether this is due to its inability to bind calcineurin or because of a subtle structural alteration in the mutant which may adversely affect RyR2 opening remains unclear and would require further investigation. One final possibility is that the FKBP 12.6 mutant may be unable to co-ordinate the type of synchronous SR $Ca^{2+}$ release observed with overexpression of wild-type FKBP 12.6.

### 5.3.7 Anomalies

Previously Kaftan *et al.*, 1996, and Xiao *et al.*, 1997, have used rapamycin and FK506 respectively to dissociate FKBP 12.6 from RyR2 in planar lipid bilayers. These interventions increased the open probability of RyR2. Logic would predict that overexpression of FKBP 12.6 would decrease the open probability of RyR2. Spontaneous $Ca^{2+}$ sparks in FKBP 12.6 overexpressing permeabilised cardiomyocytes were reduced in frequency, amplitude, width and duration when compared to Ad-LacZ control, consistent with a reduced open probability for RyR2. However, SR $Ca^{2+}$ load was also significantly increased in the FKBP 12.6 overexpressing cardiomyocytes. An increased SR $Ca^{2+}$ load has been shown to increase the frequency and size of spontaneous $Ca^{2+}$ sparks (Cheng *et al.*, 1996) and FKBP 12.6 co-ordinates coupled gating and thus allows larger currents through RyR2 (Marx *et al.*, 2001). Hence we may have expected larger $Ca^{2+}$ sparks in the Ad-FKBP 12.6 transfected myocytes. It would therefore appear that a reduced RyR2 open probability over-rides any effect of increased SR $Ca^{2+}$ load or coupled gating and is thus the critical

determinant of $Ca^{2+}$ spark size in FKBP 12.6 overexpressing cardiomyocytes.

Assuming that calcium transients are the product of the temporal and spatial summation of individual $Ca^{2+}$ sparks, the release of which are co-ordinated by the L-type $Ca^{2+}$ current, then we might expect the $Ca^{2+}$ transient amplitude for any given SR $Ca^{2+}$ load to be reduced in FKBP 12.6 overexpressing cardiomyocytes (ie the gain of E-C coupling to be reduced). While the point which describes the relationship between SR $Ca^{2+}$ load and $Ca^{2+}$ transient amplitude for FKBP 12.6 overexpressing cardiomyocytes does lie slightly to the right of the gain curve for Ad-LacZ transfected cells, it is not a significant excursion. It may be possible that any reduction in spark size and thus the gain of E-C coupling in FKBP 12.6 transfected cardiomyocytes is masked by the increase in SR $Ca^{2+}$ release synchronicity also observed.

The characteristics of spontaneous $Ca^{2+}$ sparks observed in FKBP 12.6 and FKBP 12.6 mutant overexpressing cardiomyocytes were similar when compared to each other, but reduced in frequency, amplitude, width and duration when compared to Ad-LacZ control. However whole cell voltage clamp studies revealed that while SR $Ca^{2+}$ load was significantly increased in both FKBP 12.6 and FKBP 12.6 mutant overexpressing cardiomyocytes, calcium transient amplitude was only significantly increased in the former case ($I_{Ca}$ did not differ significantly). Once again, assuming that calcium transients are simply the sum of individual $Ca^{2+}$ sparks, co-ordinated by $I_{Ca}$, then we might also have expected a significantly increased $Ca^{2+}$ transient

amplitude in the FKBP 12.6 mutant overexpressing cardiomyocytes. This difference in intracellular $Ca^{2+}$ transient amplitude may indicate a role for calcineurin in modulating the ability of $I_{Ca}$ to trigger $Ca^{2+}$ release from the SR.

# Chapter 6 – NCX overexpression and E-C coupling in isolated rabbit cardiomyocytes.

## 6.1 An introduction to NCX

### 6.1.1 The role of NCX

The process of E-C coupling brings about an increase in $[Ca^{2+}]_i$ that enables the myocardium to contract. For the heart to function efficiently as a pump it must also be able to relax. This requires a reduction in $[Ca^{2+}]_i$ and removal of $Ca^{2+}$ from the cytosol and is achieved via the actions of the SR $Ca^{2+}$ pump, the sodium-calcium exchanger (NCX), the sarcolemmal $Ca^{2+}$ ATPase and the mitochondrial $Ca^{2+}$ uniport system. The contribution that NCX makes towards this relaxation varies greatly according to the species studied. In the rabbit it is thought to account for 28% of the decline in $[Ca^{2+}]_i$ (Bassani *et al.*, 1992), while in the rat and mouse the estimates are 7% and 9% respectively (Bers, 2001, Li *et al.*, 1998).

It is noteworthy that $Ca^{2+}$ entry into cardiomyocytes via reverse mode NCX may also serve as trigger for CICR. Using rabbit ventricular cardiomyocytes, Litwin *et al.*, 1998, have demonstrated a non-linearity between the size of the L-type $Ca^{2+}$ current and cell shortening at membrane potentials above +20mV that was a function of the amount of sodium present in the patch pipette. Hence it was suggested that positive membrane potentials could cause $Ca^{2+}$ entry via reverse mode sodium-calcium exchange. However, the membrane potential during the voltage clamp protocol used to study EC-coupling in this investigation does not rise above 0mV. Thus it is unlikely that significant $Ca^{2+}$ entry via reverse mode

sodium-calcium exchange should occur during depolarisation in this investigation. In addition it has been postulated that rapid entry of sodium into the myocyte during depolarisation via $I_{Na}$ may raise local $[Na^+]_i$ to levels that would support $Ca^{2+}$ entry via reverse mode NCX sufficient to trigger SR $Ca^{2+}$ release (Leblanc & Hume, 1990). To ensure that this was not a complicating factor in our investigation and to improve voltage control, EC-coupling experiments were carried out in the presence of TTX to block $I_{Na}$. A more thorough treatment of these possibilities along with a detailed description of NCX characteristics may be found in Chapter 1.

### 6.1.2 Manipulation of NCX in the rabbit

Schillinger *et al.*, 2000, were the first to use adenovirus to mediate overexpression of NCX in rabbit cardiomyocytes. Fractional shortening was reduced by 15% in the Ad-NCX overexpressing cardiomyocytes, which also exhibited significantly smaller caffeine contractures, indicative of a reduced SR $Ca^{2+}$ load. In a follow up study they demonstrated that Ad-NCX transfected cardiomyocytes were more susceptible to treatment with oubain when compared to control. Oubain inhibits the $3Na^+/2K^+$-ATPase causing a rise in $[Na^+]_i$ that would be expected to enhance $Ca^{2+}$ entry via NCX during depolarisation and reduce $Ca^{2+}$ extrusion via NCX during diastole. Ad-NCX transfected cardiomyocytes developed irreversible contractures at lower concentrations of oubain when compared to Ad-LacZ control. Additionally, relaxation velocity was reduced by ~50% in Ad-NCX transfected cardiomyocytes treated with oubain when compared to control

cardiomyocytes under the same conditions (Schillinger *et al.*, 2003). Thus a combination of increased NCX activity and reduced $3Na^+/2K^+$-ATPase activity may have the potential to cause significant diastolic dysfunction. Ranu *et al.*, 2002, employed a similar method to overexpress NCX in rabbit cardiomyocytes. Their results were similar to those of the Hasenfuss group in that they observed a reduced contraction amplitude, reduced diastolic and systolic $[Ca^{2+}]_i$ and a depleted SR $Ca^{2+}$ load as assessed by rapid application of caffeine.

### 6.1.3 Manipulation of NCX in the rat and mouse

The adenovirus has also been employed to cause a 2-fold overexpression of NCX in the rat (Zhang *et al.*, 2001). At a physiological extracellular $[Ca^{2+}]$ of 1.8mM there was no significant difference in twitch amplitude when Ad-NCX transfected cardiomyocytes were compared to control. Conversely, Tadros *et al.*, 2002, have down regulated NCX in rat cardiomyocytes using an antisense oligonucleotide to NCX1 that reduced expression by ~66% after 6 days. Again, with an extracellular $[Ca^{2+}]$ of 1.8mM neither contraction nor $Ca^{2+}$ transient amplitude were significantly affected.

A number of groups have developed transgenic mice that overexpress NCX. Terracciano *et al.*, 1998, demonstrated that both diastolic $[Ca^{2+}]_i$ and $Ca^{2+}$ transient amplitude were unaltered in NCX overexpressing mice when compared to control. However, the rates of contraction and relaxation were

both significantly faster in the transgenic myocytes. When rapid cooling contractures were carried out using $Na^+$ and $Ca^{2+}$ free solutions, the rate of relaxation was still faster in NCX overexpressing myocytes, suggesting that SERCA2a activity was faster in these cells. Intriguingly neither SERCA2a nor PLB expression was altered in the transgenic myocytes. SR $Ca^{2+}$ content, as assessed by rapid application of caffeine, was also increased by ~70% and may explain the faster rate of contraction in the NCX overexpressing cardiomyocytes. It is strange that such a marked increase in SR $Ca^{2+}$ content should have no effect on the amplitude of the $Ca^{2+}$ transient. Yao *et al.*, 1998, also found that transgenic overexpression of NCX in murine cardiomyocytes accelerated the rate of decay, but had no effect on the amplitude of the $Ca^{2+}$ transient. In contrast to the findings of Terracciano *et al.*, 1998, SR $Ca^{2+}$ load was unaltered and the time to peak $Ca^{2+}$ during a transient was prolonged. Finally Linck *et al.*, 2000, found that transgenic over expression of NCX in murine cardiomyocytes had no obvious effects on $Ca^{2+}$ handling. Neither the $I_{Ca}$, the $Ca^{2+}$ transient amplitude nor the SR $Ca^{2+}$ load were affected. It is noteworthy that Henderson *et al.*, 2004 have developed a transgenic NCX1 double knockout mouse in which, quite remarkably, there is still functional adult myocardium. NCX1 was completed ablated in 80% of cardiomyocytes with no alterations in the expression of SERCA, PMCA, PLB, DHPR, RyR or CSQ. The L-type $Ca^{2+}$ current was reduced by 50% and the authors have speculated that the cardiomyocytes simply adapt to the absence of NCX by limiting $Ca^{2+}$ influx into the cell via other routes.

### 6.1.4 Aims

To evaluate the effect of NCX on cardiac E-C coupling, adult rabbit ventricular myocytes were transfected with a recombinant adenovirus coding for human NCX (Ad-NCX). A β-galactosidase virus was used as a control (Ad-LacZ). Viruses were constructed by Dr. Tim Seidler, Georg-August-Universitat, Goettingen, Germany.

It was proposed that after 24 hrs in culture the virus-transfected cells would be loaded with fura-2 and E-C coupling studied using whole cell voltage clamp. This was to enable the effects of NCX overexpression on the L-type $Ca^{2+}$ current, the intracellular $Ca^{2+}$ transient, SR $Ca^{2+}$ load, NCX activity and sarcolemmal $Ca^{2+}$ ATPase activity to be determined.

## 6.2 Results

### 6.1.1 Effect of NCX overexpression on NCX activity

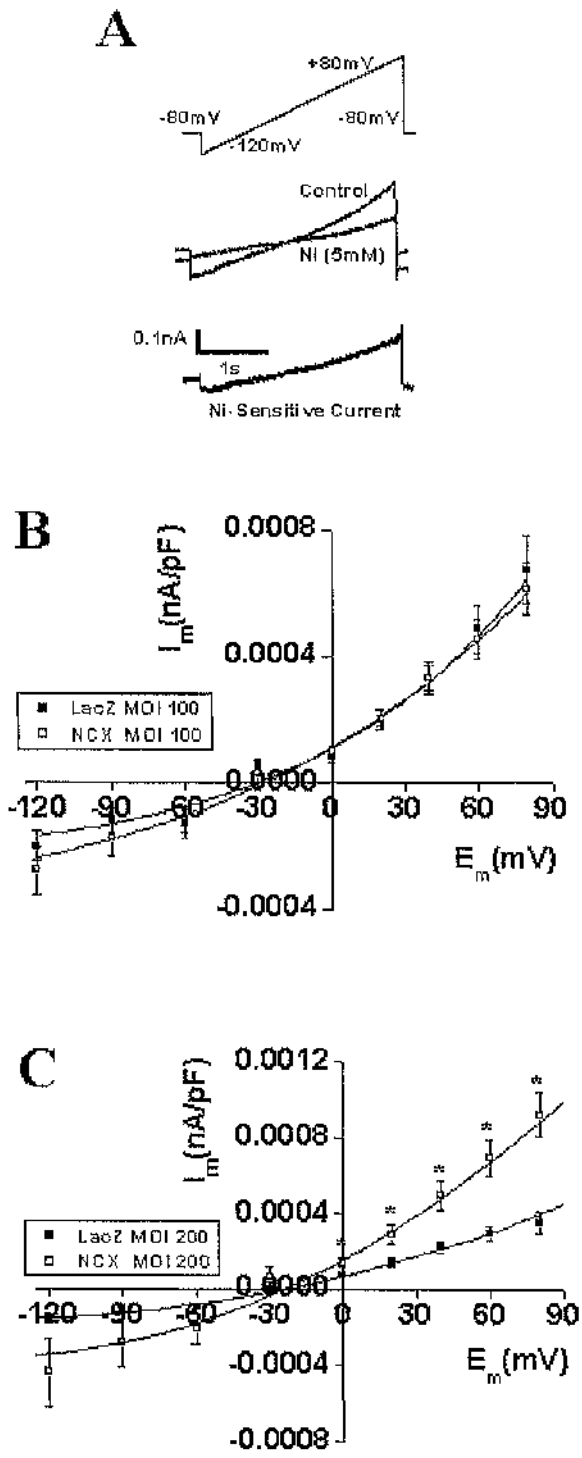

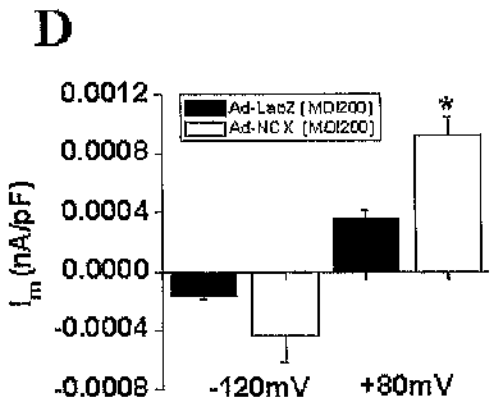


**Figure 6 - 1. NCX activity in Ad-NCX (MOI 100 & 200) transfected cardiomyocytes.**

**The I-V relationship for the $Ni^{2+}$-sensitive NCX current. A, Voltage clamp protocol used to determine the I-V relationship under control conditions and in the presence of 5mM $Ni^{2+}$ along with the difference current, attributable to NCX. B, Average I-V relationship in Ad-LacZ, n=14 (MOI 100) and Ad-NCX, n=13 (MOI 100) transfected cardiomyocytes. C, Average I-V relationship in Ad-LacZ, n=14 (MOI 200) and Ad-NCX, n=14 (MOI 200) transfected cardiomyocytes. D, Average currents measured at membrane potentials of -120mV and +80mV in both experimental groups (MOI 200).**

The effect of NCX overexpression at MOI100 & MOI200 on NCX activity was investigated by determining the $Ni^{2+}$-sensitive NCX current measured whilst slowly ramping the membrane potential from –120mV to +80mV (Figure 6-1, A). With $[Ca^{2+}]_i$ buffered at 250nM using 50mM EGTA in the patch pipette solution and $[Na^+]_i$ at 20mM, NCX currents were identical in Ad-NCX (MOI 100) transfected cardiomyocytes were compared to Ad-LacZ (MOI 100) control (Figure 6-1, B). However, NCX current were significantly increased at positive membrane potentials when Ad-NCX (MOI 200) transfected cardiomyocytes were compared to Ad-LacZ (MOI 200) control (Figure 6-1, C & D).

### 6.2.2 Effect of NCX overexpression on the L-type $Ca^{2+}$ current and intracellular $Ca^{2+}$ transient

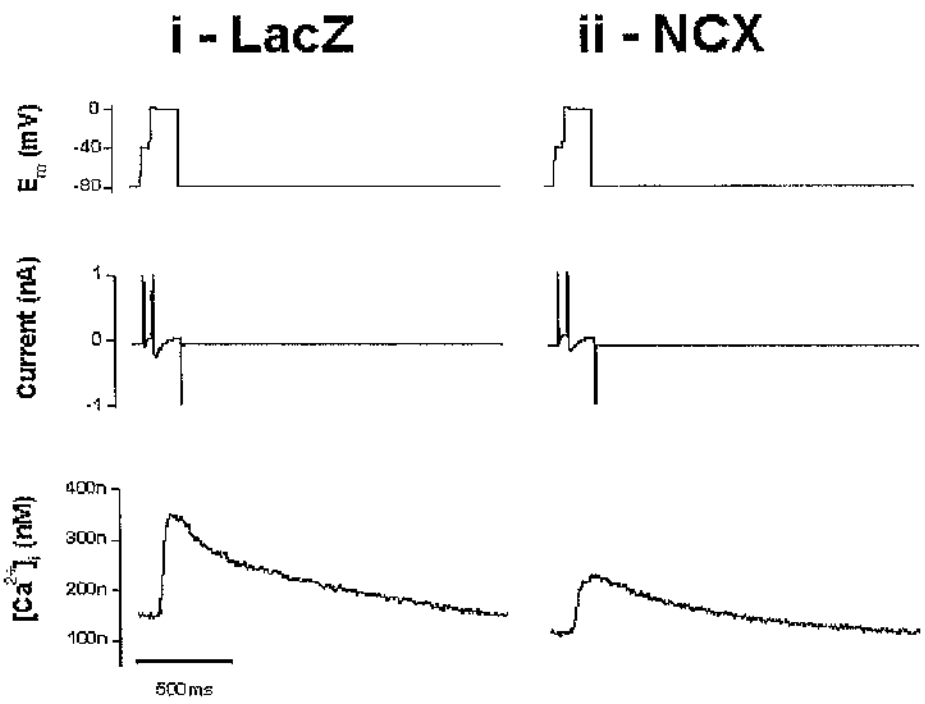


**Figure 6 - 2. NCX overexpression and EC-coupling.**

**Depolarisation-induced L-type $Ca^{2+}$ currents and intracellular $Ca^{2+}$ transients in voltage clamped Ad-LacZ (i) and Ad-NCX (ii) transfected cardiomyocytes. Typical traces of membrane potential ($E_m$), membrane current and $[Ca^{2+}]_i$ from single cardiomyocytes (average of 10 sweeps).**

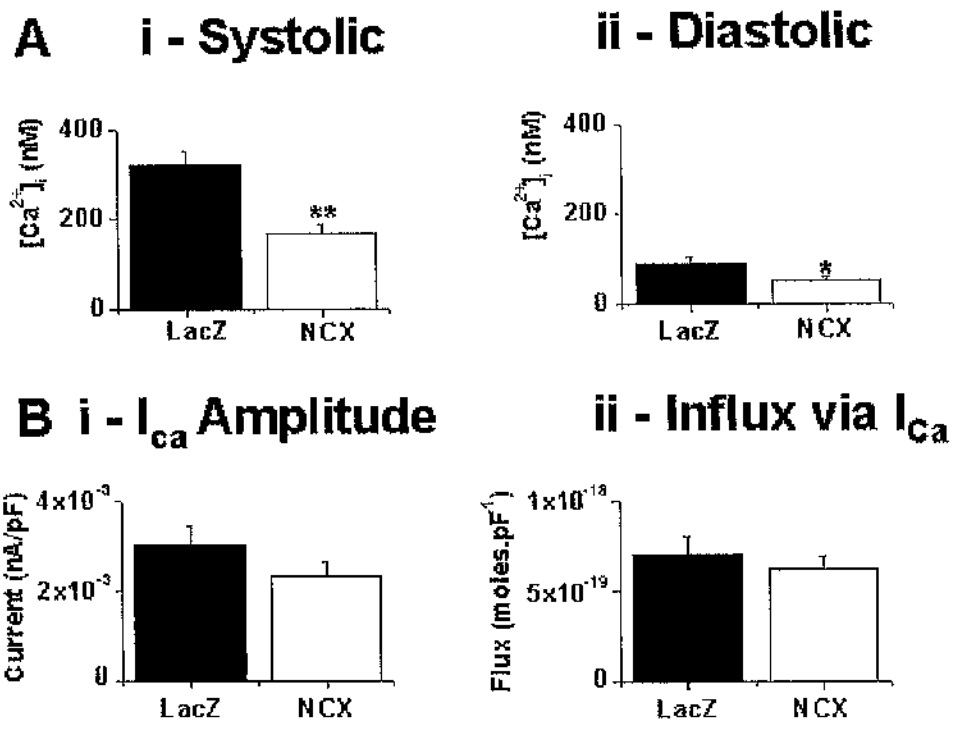


**Figure 6 - 3.** A, Mean ± SEM values of peak systolic (i) and end diastolic (ii) $[Ca^{2+}]_i$ and B, Mean ± SEM values of peak $I_{Ca}$ (i) and $Ca^{2+}$ influx via $I_{Ca}$ in Ad-LacZ (n=15) and Ad-NCX (n=14) transfected cardiomyocytes.

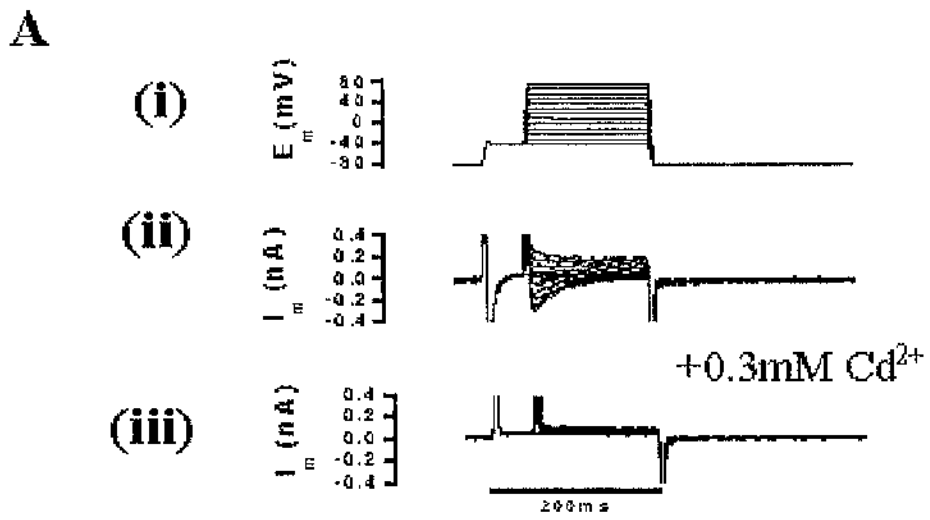


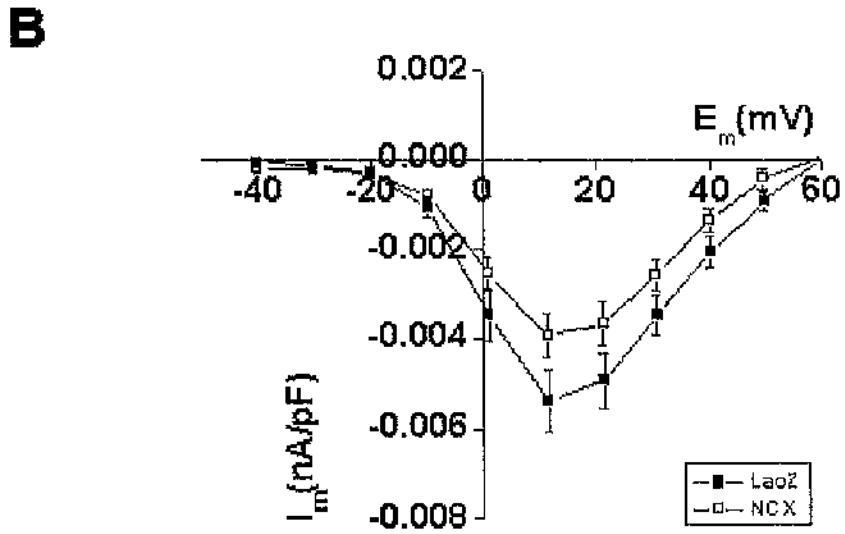


**Figure 6 - 4. I-V relationship for $I_{Ca}$ in Ad-LacZ and Ad-NCX transfected cardiomyocytes.**

**A, Voltage clamp protocol (i) used to investigate the I-V relationship for $I_{Ca}$ in Ad-LacZ (n=11) and Ad-NCX (n=10) transfected cardiomyocytes. Current traces obtained in the absence (ii) and in the presence of $Cd^{2+}$ (iii). B, I-V relationship for $I_{Ca}$ (points represent mean ± SEM values).**

Figure 6-3 demonstrates that Ad-NCX transfection significantly decreased both peak systolic and end diastolic $[Ca^{2+}]_i$ in voltage clamped rabbit cardiomyocytes. In addition it shows that both the amplitude and the time integral of $I_{Ca}$ (which can be converted to a $Ca^{2+}$ influx) were unaltered by NCX overexpression. This observation was confirmed via investigation of the I-V relationship for $I_{Ca}$. Figure 6-4 shows that Ad-NCX transfection did not significantly alter L-type $Ca^{2+}$ current amplitude over a range of membrane potentials. However, there was a trend towards a decreased $I_{Ca}$ at all voltages.

6.2.3 Effect of NCX overexpression on the rate of decay of the intracellular $Ca^{2+}$ transient

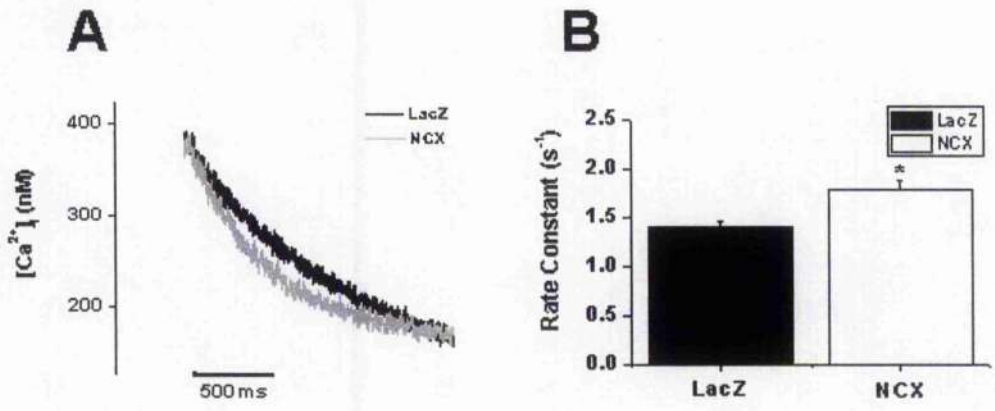


**Figure 6 - 5. Rate of decay of the intracellular $Ca^{2+}$ transient in Ad-NCX transfected cardiomyocytes.**

**A, Superimposed declines of $[Ca^{2+}]_i$ in Ad-LacZ and Ad-NCX transfected cardiomyocytes. B, Mean ± SEM values for rate constant of intracellular $Ca^{2+}$ transient decay in Ad-LacZ (n=12) and Ad-NCX (n=11) transfected cardiomyocytes.**

Figure 6-5 clearly demonstrates that the rate constant of decay of the intracellular $Ca^{2+}$ transient, calculated by fitting with a single exponential, is significantly increased in Ad–NCX transfected cardiomyocytes.

6.2.4 Effect of NCX overexpression on SR $Ca^{2+}$ content (assessed by rapid application of 10mM caffeine)

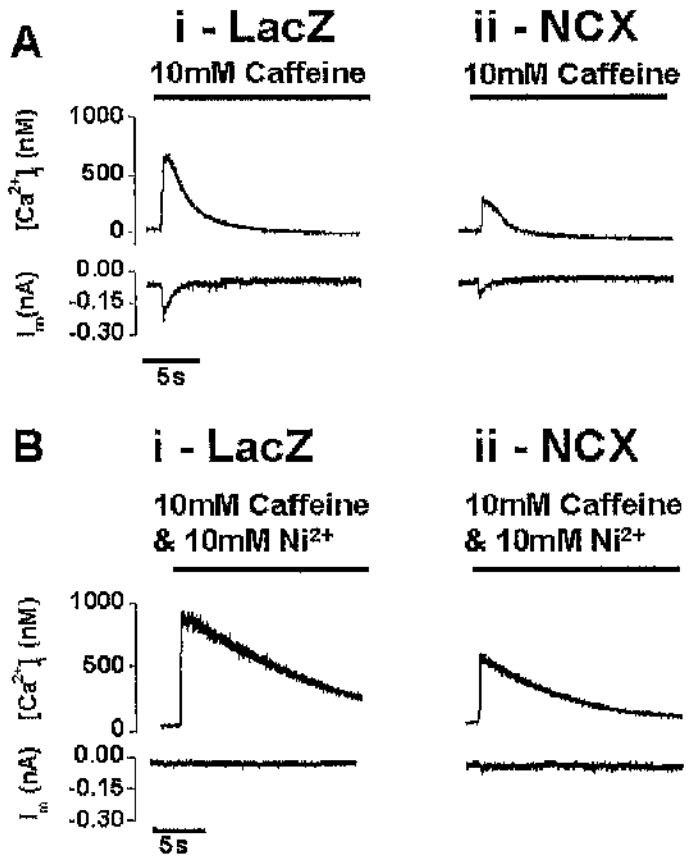


**Figure 6 - 6. NCX overexpression and the rapid application of 10mM caffeine.**

**A, SR $Ca^{2+}$ release and corresponding membrane currents recorded upon rapid application of 10mM caffeine in typical Ad-LacZ (i) and Ad-NCX (ii) transfected cardiomyocytes. B, SR $Ca^{2+}$ release and corresponding membrane currents recorded upon rapid application of 10mM caffeine & 10mM $Ni^{2+}$ in typical Ad-LacZ (i) and Ad-NCX (ii) transfected cardiomyocytes.**

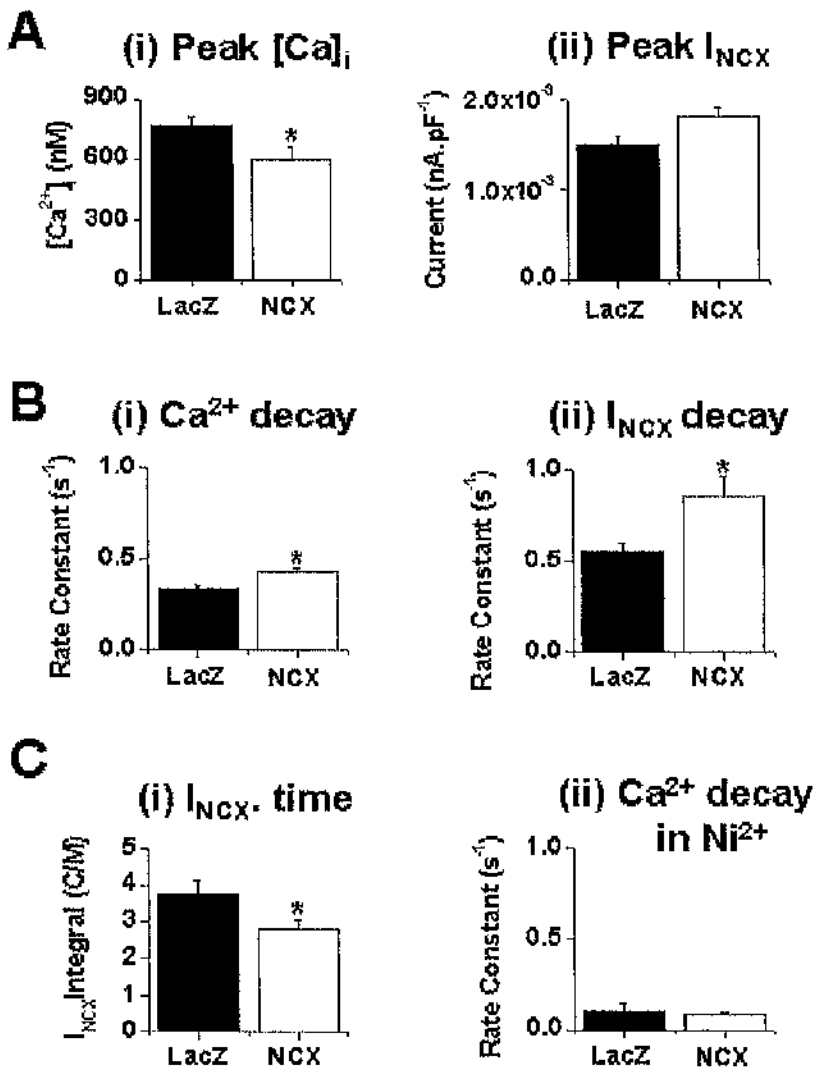


**Figure 6 - 7. NCX overexpression and SR $Ca^{2+}$ load.**

**A, Mean ± SEM values for (i) peak $[Ca^{2+}]_i$ (Ad-LacZ, n=15 vs. Ad-NCX, n=13) and (ii) and peak $I_{NCX}$ (Ad-LacZ, n=12 vs. Ad-NCX, n=12). B, Mean ± SEM values for (i) rate constant of $[Ca^{2+}]_i$ decay (Ad-LacZ, n=10 vs. Ad-NCX, n=13) and (ii) and rate constant of $I_{NCX}$ decay (Ad-LacZ, n=12 vs. Ad-NCX, n=11). C, Mean ± SEM values for (i) $I_{NCX}$.time integral (Ad-LacZ, n=12 vs. Ad-NCX, n=12) and (ii) rate constant of $[Ca^{2+}]_i$ decay in $Ni^{2+}$ (Ad-LacZ, n=6 vs. Ad-NCX, n=6).**

10mM caffeine was rapidly applied to cardiomyocytes contracting in the steady state in order to assess SR $Ca^{2+}$ load. Figures 6-7 A (i) and C (i) clearly demonstrate that both the caffeine-induced $Ca^{2+}$ transient and the integral of caffeine-induced transient inward current with respect to time are significantly decreased in the Ad-NCX transfected cardiomyocytes when compared to control. These results indicate that NCX overexpression significantly reduces SR $Ca^{2+}$ content.

Whilst figure 6-7 A (ii) shows that the peak of the transient inward current was not affected by NCX overexpression, figure 6-7 B (ii) shows that its rate constant of decay, calculated by fitting with a single exponential, was significantly increased when compared to Ad-LacZ control. Similarly, the rate constant for the decay of the caffeine-induced $Ca^{2+}$ transient (see figure 6-7 B (i)) was significantly increased in the Ad-NCX transfected myocytes. These larger rate constants suggest that the rate of extrusion of $Ca^{2+}$ from the cytosol at the sarcolemma via NCX has, perhaps predictably, been increased by NCX overexpression. Figure 6-7 C (ii) demonstrates that when caffeine was applied with $Ni^{2+}$, the rate constant for the decay of the corresponding $Ca^{2+}$ transient was similar in the Ad-NCX transfected myocytes when compared to control. This would suggest that NCX overexpression does not affect the activity of the sarcolemmal $Ca^{2+}$-ATPase.

6.2.5 Relationship between SR $Ca^{2+}$ content and $Ca^{2+}$ transient amplitude in Ad-LacZ and Ad-NCX transfected cardiomyocytes

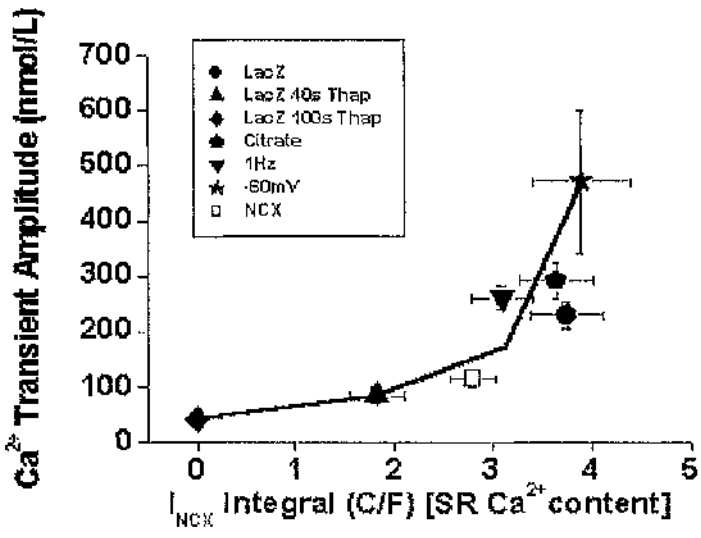


**Figure 6 - 8. NCX overexpression and the gain of EC-coupling.**

**Relationship between $I_{NCX}$ integral (an index of SR $Ca^{2+}$ content) and $Ca^{2+}$ transient amplitude for cardiomyocytes from Ad-LacZ (Control; Thapsigargin 40s exposure; Thapsigargin 100s exposure; Citrate; 1Hz stimulation ; Hold -60mV) and Ad-NCX groups. Measurements were obtained in the steady state; lower SR loads were achieved by exposure to 5μM Thapsigargin for various times, higher SR loads were obtained by adding 20mM Citrate to the pipette solution, by stimulating at a frequency of 1Hz or by holding membrane potential at -60mV between depolarisations.**

The SR $Ca^{2+}$ load of Ad-LacZ transfected cardiomyocytes was increased either by the addition of 20mmol/L citrate to the pipette solution (SR $Ca^{2+}$ load 3.64+/-0.37 C/F and $Ca^{2+}$ transient amplitude 294+/-32 nmol/L), by clamping at –60mV during diastole (SR $Ca^{2+}$ load 3.89 ± 0.49 C/F and $Ca^{2+}$ transient amplitude 471 ± 131 nmol/L) or by stimulating at a frequency of 1Hz (SR $Ca^{2+}$ load 3.10 ± 0.30 C/F and $Ca^{2+}$ transient amplitude 262 ± 21

nmol/L). SR $Ca^{2+}$ load was decreased by the addition of 5μM thapsigargin to the superfusate. After 40s, SR $Ca^{2+}$ load was reduced to 1.82+/-0.28 C/F and the $Ca^{2+}$ transient amplitude to 85+/-15 nmol/L. Exposure for 100s completely emptied the SR of $Ca^{2+}$ and the $Ca^{2+}$ transient amplitude was reduced to 61+/-16 nmol/L. These points allowed determination of the normal relationship between SR $Ca^{2+}$ content and $Ca^{2+}$ transient amplitude for 1-day cultured rabbit cardiomyocytes. As is evident from figure 6-8, the Ad-NCX group have a reduced SR $Ca^{2+}$ content (2.8 ± 0.23 C/F) and a reduced $Ca^{2+}$ transient amplitude (116 ± 16nmol/L) when compared to LacZ control (SR $Ca^{2+}$ content 3.75 ± 0.37 C/F, $Ca^{2+}$ transient amplitude 230 ± 25 nmol/L). The point which represents the relationship between SR $Ca^{2+}$ content and $Ca^{2+}$ transient amplitude for the Ad-NCX transfected cardiomyocytes lies very close to the curve which describes the same relationship for Ad-LacZ transfected cardiomyocytes over a range of SR $Ca^{2+}$ loads. Thus NCX overexpression does not appear to alter the gain of EC-coupling.

## 6.3 Discussion

The results presented in this chapter would suggest that adenoviral mediated NCX overexpression in cultured rabbit cardiomyocytes has a negative inotropic effect on EC-coupling.

### 6.3.1 The effect of NCX overexpression on sarcolemmal $Ca^{2+}$ entry and extrusion

This study reveals that NCX overexpression had no significant effect on $I_{Ca}$. Both the amplitude and the integral (a measure of the amount of $Ca^{2+}$ entering the cardiomyocyte via $I_{Ca}$) of this current were unaffected by NCX overexpression. In addition the I-V relationship for $I_{Ca}$ was similar in both Ad-LacZ and Ad-NCX transfected cardiomyocytes. It has recently been demonstrated that cardiomyocytes from double NCX1 knockout mice exhibit a 50% reduction in the size of the L-type $Ca^{2+}$ current (Philipson, 2004. The authors speculated that the myocytes adapted to the absence of NCX by limiting $Ca^{2+}$ influx into the cell via other routes. By this rationale, one might have expected NCX overexpression to increase the size of the L-type $Ca^{2+}$ current. Such an adaptation was not observed.

Somewhat predictably, NCX activity was significantly increased in Ad-NCX transfected cardiomyocytes. The rate constants of both $Ca^{2+}$ extrusion and $I_{NCX}$ decay in response to caffeine, along with the rate constant of decay of the intracellular $Ca^{2+}$ transient were all significantly increased by

overexpression of NCX. In addition, $Ni^{2+}$-sensitive NCX currents over the voltage range –120mV to +80mV were significantly increased at positive membrane potentials in Ad-NCX transfected cardiomyocytes when compared to control. Cardiomyocytes isolated from transgenic mice overexpressing NCX1 have previously been shown to exhibit enhanced rates of relaxation (Terracciano *et al.*, 1998) and an acceleration in the rate of decay of the intracellular $Ca^{2+}$ transient (Yao *et al.*, 1998).

Finally, the rate constant of $Ca^{2+}$ extrusion in response to caffeine and in the presence of $Ni^{2+}$, taken to represent sarcolemmal $Ca^{2+}$-ATPase activity, was unaltered by NCX overexpression.

### 6.3.2 Effects of NCX overexpression on E-C coupling and SR $Ca^{2+}$ content.

Voltage clamp studies show that both the intracellular $Ca^{2+}$ transient amplitude and the SR $Ca^{2+}$ content were significantly reduced in Ad-NCX transfected cardiomyocytes when compared to Ad-LacZ control. The L-type $Ca^{2+}$ current, generally accepted as the trigger for CICR, was unaltered in terms of peak amplitude and integral by NCX overexpression. Thus the reduction in SR $Ca^{2+}$ content could explain the reduction in the size of the intracellular $Ca^{2+}$ transient.

Figure 6-8 demonstrates the relationship between SR $Ca^{2+}$ load and intracellular calcium transient amplitude for Ad-LacZ transfected cardiomyocytes. When the SR $Ca^{2+}$ load of the Ad-LacZ transfected

cardiomyocytes was reduced to the level observed in the Ad-NCX transfected cells, the calcium transient amplitudes in both experimental groups did not differ significantly. Hence, these results indicate that the reduced SR $Ca^{2+}$ content in the Ad-NCX transfected cardiomyocytes can predominantly account for the reduction in the amplitude of the intracellular $Ca^{2+}$ transient observed and that NCX overexpression does not affect the gain of EC-coupling. Indeed a previous study by Schillinger *et al.*, 2000, used adenoviral mediated gene transfer to overexpress NCX in cultured rabbit cardiomyocytes and observed reduced fractional shortening and smaller caffeine contractures which would indicate a reduced SR $Ca^{2+}$ load. Ranu *et al.*, 2002, have also used the same technique to overexpress NCX in rabbit cardiomyocytes, observing reduced contraction amplitude, reduced diastolic and systolic $[Ca^{2+}]_i$ and a depleted SR $Ca^{2+}$ content. The results of both of these studies are consistent with the data presented here.

### 6.3.3 Comparing manipulation of NCX in the rabbit with manipulation of NCX in the rat/mouse

In stark contrast to the situation in the rabbit described above, overexpression of NCX in both the rat and the mouse has remarkably little effect on cardiomyocyte function under normal circumstances. Adenoviral mediated overexpression of NCX in rat cardiomyocytes had no significant effect on twitch amplitude (Zhang *et al.*, 2001). Likewise, $Ca^{2+}$ transient amplitude was found to be unaltered in transgenic mice overexpressing NCX (Terracciano *et al.*, 1998, Yao *et al.*, 1998 & Linck *et al.*, 2000).

To explain this dichotomy one must look for species differences between the rabbit and the rat/mouse. In the rabbit, NCX removes ~28% of $Ca^{2+}$ from the cytosol after contraction, compared to ~7-9% in the rat/mouse. This difference may be because intracellular $[Na^+]$ is much lower in the rabbit (3-5mM) compared to the rat/mouse (12mM). This difference would be enough to bias the mode of operation of NCX. In the rabbit, where $[Na^+]_i$ is relatively low, forward mode NCX function and thus $Ca^{2+}$ removal from the cardiomyocyte would be favoured. In the rat/mouse, a higher $[Na^+]_i$ would tend to inhibit forward mode NCX function and enhance reverse mode NCX function, thus the amount of $Ca^{2+}$ leaving the cardiomyocyte relative to the rabbit would be reduced. Thus NCX overexpression in the rabbit would be expected to enhance removal of $Ca^{2+}$ from the cell to a much greater extent than in the rat/mouse, compromising SR $Ca^{2+}$ load and ultimately the size of the intracellular $Ca^{2+}$ transient.

### 6.3.4 Conclusions.

In summary, the data presented here would suggest that overexpression of NCX and increased removal of $Ca^{2+}$ from the cytosol at the sarcolemma causes a reduction in SR $Ca^{2+}$ load that ultimately reduces the size of the intracellular $Ca^{2+}$ transient. Furthermore, these results bear striking resemblance to, and thus support the novel findings in Chapter-3, where adenoviral-mediated overexpression of sorcin was demonstrated to increase NCX activity and similarly reduce both SR $Ca^{2+}$ load and the size of the intracellular $Ca^{2+}$ transient.

# Chapter 7 – General Discussion and Conclusions:

# Relevance to the failing myocardium.

## 7.1 Relevance to Heart Failure

Heart Failure is a condition in which the heart is unable to maintain a sufficient cardiac output to meet the metabolic demands of the organism (Bers, 2001). Contractile function of the heart is reduced and is associated with a disturbed intracellular $Ca^{2+}$ homeostasis. In addition there is often a marked myocardial hypertrophy. Depending on the species studied and the etiology of the disease, changes in one or more of the following (twitch contraction, intracellular $Ca^{2+}$ transient, myofilament $Ca^{2+}$ sensitivity, $I_{Ca}$, $I_{to}$, $I_{K1}$, $G_I$, $G_s$, SR $Ca^{2+}$ ATPase, SR $Ca^{2+}$ content, phospholamban, RyR, Na/K-ATPase and action potential duration) have been implicated in the disease process. This general discussion examines each of the proteins studied in this thesis in the context of their contributions to the contractile dysfunction observed in heart failure.

### 7.1.1 Abnormal intracellular $Ca^{2+}$ homeostasis and heart failure

Altered $Ca^{2+}$ homeostasis, reduced cell contraction and thus reduced twitch force are common to almost all models of heart failure. Reduced contractility is generally coupled with a reduction in the size of the intracellular $Ca^{2+}$ transient amplitude. In addition, the rate of decline of the intracellular $Ca^{2+}$ transient and hence the rate of cardiomyocyte relaxation is generally reduced. In order to explain this altered $Ca^{2+}$ homeostasis, one must look closely at the various components that contribute towards the mechanism of cardiac EC-coupling.

The main trigger for CICR in EC-coupling is the L-type $Ca^{2+}$ current and thus a reduction in the size of this trigger may contribute towards the reduced intracellular $Ca^{2+}$ transient observed in heart failure. However, most reports find little change $I_{Ca}$ current density in heart failure (e.g. Beuckelmann & Erdmann, 1992, Pogwizd *et al.*, 1999). The possibility remains that a combination of cellular hypertrophy and loss of t-tubule density, as observed by Quinn *et al.*, 2003, affects the close opposition between the L-type $Ca^{2+}$ channels on the sarcolemma and the RyRs on the junctional SR. Hence the same $I_{Ca}$ may be less effective in triggering SR $Ca^{2+}$ release.

The more likely explanation for the reduced intracellular $Ca^{2+}$ transient in heart failure is a reduced SR $Ca^{2+}$ load, demonstrated both in failing human (Lindner *et al.*, 1998) and rabbit (Pogwizd *et al.*, 1999) cardiomyocytes. There are a number of possible explanations for this reduction in SR $Ca^{2+}$ load. Firstly the activity of the SR $Ca^{2+}$-ATPase (SERCA2a) is reduced in almost all models of heart failure, as reviewed by Hasenfuss, 1998. This may be partly due to a reduction in the phosphorylation status of phospholamban (Huang *et al.*, 1999). However, in other heart failure models, increases in the phosphorylation status of phospholamban have been observed (Currie & Smith, 1999). Regardless, any depression in re-uptake of $Ca^{2+}$ from the cytosol by SERCA2a would be expected to reduce SR $Ca^{2+}$ load and may also contribute to the reduced rate of decline of the intracellular $Ca^{2+}$ transient. Secondly, NCX expression is often increased in models of heart failure (e.g. Flesch *et al.*, 1996, Pogwizd *et al.*, 1999). It is thought that this compensates for the reduction in SERCA2a activity and

thus helps to maintain diastolic function. Increased NCX activity would mean increased competition with SERCA2a in removing $Ca^{2+}$ from the cytoplasm during relaxation/diastole, tending to reduce SR $Ca^{2+}$ content. Finally, regulation of the SR $Ca^{2+}$ release channel may be altered in heart failure. Marx *et al.*, 2000, have demonstrated that RyR2 can become hyper-phosphorylated by PKA in heart failure, resulting in displacement of FKBP 12.6 from the RyR and an increase in the resting $P_O$ of the channel. It was suggested that this might cause an increase in diastolic $Ca^{2+}$ leak from the SR and thus also reduce SR $Ca^{2+}$ load.

It is also noteworthy that action potential duration is generally prolonged in heart failure (Beuckelmann *et al.*, 1992). A reduction in the density of outward potassium currents such as $I_{to}$ and $I_{K1}$ (Beuckelmann *et al.*, 1993) combined with a reduction in $3Na^+/2K^+$-ATPase activity (Schwinger *et al.*, 1999) may underlie this prolongation. However, action potential prolongation in itself would be expected to have a beneficial effect on the size of the intracellular $Ca^{2+}$ transient, increasing $Ca^{2+}$ influx via $I_{Ca}$ and slowing $Ca^{2+}$ extrusion via NCX.

A more detailed discussion of how altered expression of sorcin, CSQ, FKBP 12.6 and NCX may be of relevance to the altered $Ca^{2+}$ handling observed in heart failure and can be found below.

### 7.1.2 Sorcin and Heart failure

The data presented in Chapter 3 of this thesis demonstrate for the first time that adenoviral overexpression of sorcin causes an increase in NCX activity. Overexpression of NCX, at least in the rabbit (see Chapter 6) (Schillinger *et al.*, 2000, Ranu *et al.*, 2002), causes a reduction in the size of the intracellular $Ca^{2+}$ transient. In addition, it has been demonstrated that sorcin is localised at or near to the t-tubules in adults mouse cardiomyocytes (Farrell *et al.*, 2003). These invaginations of the sarcolemma are also where NCX is thought to be most prevalent (Yang *et al.*, 2002). Therefore one might expect that any increase in sorcin expression in heart failure would be negatively inotropic.

However, Suarez *et al.*, 2004, have used adenovirus to mediate sorcin overexpression in both mouse hearts *in vivo* and isolated rat cardiomyocytes and demonstrated a positive inotropy. A 274% increase in sorcin expression caused a 40% increase in left ventricular pressure, a 54% increase in max dP/dt and a 72% increase in min dP/dt when compared with control. Similarly, 3-fold sorcin overexpression was reported to improve *in vivo* contractility in the failing hearts of diabetic mice. Interestingly, field stimulated rat cardiomyocytes overexpressing sorcin exhibited significantly larger $Ca^{2+}$ transients and an increased SR $Ca^{2+}$ content when compared to control. The SR rich fractions of the sorcin overexpressing myocytes revealed a 3-fold increase in SERCA2a expression and a 66% increase in PLB expression when compared to control. Increased expression of SERCA2a may explain the increased SR

$Ca^{2+}$ load and intracellular $Ca^{2+}$ transients in the sorcin overexpressing myocytes.

Zhu, 2003 have demonstrated that sorcin expression was increased 3-fold in a rat-aorta banding model of heart failure, characterised by defective $Ca^{2+}$ handling. To determine whether these increased levels of sorcin expression were detrimental or beneficial to the cardiomyocyte, it was over-expressed using Herpes Simplex Virus as a vehicle. 12hrs after transfection, $Ca^{2+}$ transient amplitude was reduced when compared to control, while after 36hrs $Ca^{2+}$ transient amplitude was increased with respect to control. These results suggest that depending on time, sorcin may have either a negative or a positive inotropic effect on cardiomyocyte contractility.

To conclude with, Quinn *et al.*, 2003, have demonstrated that NCX activity was markedly reduced in cardiomyocytes isolated from a rabbit model of LVD, despite the observation that both NCX mRNA and protein expression were increased. Elliott, 2004, have demonstrated that sorcin expression was reduced to ~75% of control in cardiomyocytes from the same failure model. Hence the reduction in sorcin expression may help to explain the paradox of reduced NCX activity, despite increased NCX expression. Frank, 2004 have demonstrated that sorcin expression is reduced by ~30% in the failing human myocardium, however the functional consequences of this down regulation remain unclear.

7.1.3 Calsequestrin and heart failure.

The data presented in Chapter 4 of this thesis show that adenoviral-mediated overexpression of CSQ paradoxically increased SR $Ca^{2+}$ load, but reduced both diastolic and systolic $[Ca^{2+}]_i$. The data are in agreement with results from previous studies which have transgenically overexpressed cardiac CSQ in mice (Sato *et al.*, 1998, Jones *et al.*, 1998 & Wang *et al.*, 2000). In addition to reducing diastolic and systolic $[Ca^{2+}]_i$, transgenic overexpression of CSQ is consistently associated with cardiac hypertrophy, also a common feature of heart failure. Thus one could speculate that increased CSQ expression in the failing heart may have a negative inotropic effect and contribute to reduced contractility.

Naqvi *et al.*, 2001, have studied a rabbit model of cardiac hypertrophy (aortic banding) and have shown that after 6 weeks, myocardial CSQ protein expression is significantly increased (approximately doubled) in hypertrophied hearts when compared to control. Counter-intuitively, there was no effect on either SR $Ca^{2+}$ load or peak systolic $[Ca^{2+}]_i$ and thus the increased expression of CSQ would appear to be of little functional significance. Indeed, reduced rates of rise and decline of the intracellular $Ca^{2+}$ transient were attributed to a prolongation of action potential duration. Duncan, 2001 have also demonstrated a significant increase in myocardial CSQ protein expression after 8 weeks in failing rabbit hearts (induced by coronary ligation), when compared to control. However Currie & Smith, 1999, demonstrated that SERCA2a expression was also significantly reduced in the same failure model. Thus it seems likely that the reduced

SR $Ca^{2+}$ load and reduced peak systolic $[Ca^{2+}]_i$ were a consequence of reduced SERCA activity. This may have masked any functional effects of increased CSQ expression.

It should be highlighted that 3 studies of end-stage human heart failure (Movsesian *et al.*, 1994, Meyer *et al.*, 1995 & Munch *et al.*, 1998) have demonstrated that there is no significant difference in myocardial CSQ protein expression in the disease state when compared to control. Similarly studies by Takahashi *et al.*, 1992, & Arai *et al.*, 1993, have demonstrated that myocardial CSQ RNA expression is also unaltered in end-stage human heart failure when compared to control. Hence it may be the case that changes in CSQ protein expression are most evident in the early stages of heart failure and this may help to explain why the human studies (dealing with end-stage heart failure) were not able to identify differences in expression of the protein.

### 7.1.4 FKBP 12.6 and heart failure

The data presented in chapter 5 of this thesis demonstrate that adenoviral-mediated overexpression of FKBP 12.6 in rabbit cardiomyocytes increases both SR $Ca^{2+}$ load and intracellular $Ca^{2+}$ transient amplitude. Thus any reduction in FKBP 12.6 expression or even its association with RyR2 in heart failure might be expected to have a negative inotropic effect.

Indeed, FKBP 12.6 has been strongly linked with heart failure. Marx *et al.*, 2000, demonstrated that PKA phosphorylation of RyR2 resulted in a 90% reduction in the amount of FKBP 12.6 co-immunoprecipitating with RyR2. This caused an increase in the open probability of the channel and induced subconductance states. Phosphorylation of RyR2 was elevated in failing hearts from both humans and dogs and there was a 65% reduction in the amount of FKBP 12.6 that co-immunoprecipitated with RyR2 from failing hearts when compared to control. When single RyR2 channels from failing hearts were studied they also exhibited an increased sensitivity to $Ca^{2+}$-dependent activation along with subconductance states. If the association between FKBP 12.6 and RyR2 is reduced in heart failure there may be an increased leak of $Ca^{2+}$ from the SR and hence a reduced SR $Ca^{2+}$ load. This would be expected to contribute to the reduced contractility associated with heart failure.

Research from the Matsuzaki group also implies that FKBP 12.6 may have a role in the pathophysiology of heart failure. Yano *et al.*, 2000, have shown that the stoichiometry of FKBP 12.6 per RyR2 was significantly reduced in isolated cardiac SR vesicles from dogs suffering from pacing induced heart failure. Additionally application of FK506 to normal SR caused a dose dependent $Ca^{2+}$ leak, whilst in failing SR a prominent $Ca^{2+}$ leak was observed even in the absence of FK506. Assuming that the reduced binding of FKBP 12.6 to RyR2 was due to hyper-phosphorylation of the calcium release channel, Doi *et al.*, 2002, went on to investigate whether administration of a β-blocker could protect against the increased SR $Ca^{2+}$ leak. SR was isolated from the left ventricular muscles of dogs

that had been exposed to 4 weeks of rapid right ventricular pacing, either with or without propanolol. The SR from dogs not treated with propanolol once again exhibited a marked SR $Ca^{2+}$ leak, whilst there was no appreciable SR $Ca^{2+}$ leak from dogs that had been treated with propanolol.

Xin *et al.*, 2002, have demonstrated that disruption of the FKBP 12.6 gene causes cardiac hypertrophy in male mice. Female hearts appeared normal despite the fact that cardiomyocytes isolated from both male and female FKBP 12.6 knockout mice displayed larger intracellular $Ca^{2+}$ transients with no change in the amplitude of $I_{Ca}$. The authors interpreted this as an increase in the gain of E-C coupling, but bearing in mind that SR $Ca^{2+}$ loads were not reported, it is not possible to be certain of this conclusion. Interestingly, when female FKBP 12.6 knockout mice were treated with the oestrogen receptor antagonist, tamoxifen, they developed a cardiac hypertrophy similar to that of male mice. It is paradoxical that Xin *et al.*, 2002, should disrupt the FKBP 12.6 gene in mice and observe an increase in the size of the intracellular $Ca^{2+}$ transient, while results presented here demonstrate that overexpression of FKBP 12.6 in rabbits has a similar functional effect.

The link between the phosphorylation of RyR2, the dissociation of FKBP 12.6 and heart failure is becoming increasingly controversial with recent studies contradicting Marx *et al.*, 2000. Jiang *et al.*, 2002, have studied cardiac SR from both failing human hearts and pacing-induced failing dog hearts. They have demonstrated that the open probability of RyR2 was the same for control and heart failure and that subconductance states (seen in

FKBP 12.6 stripped RyR2) were also equally frequent in control and heart failure channels. In addition that PKA phosphorylation of RyR2 did not affect the association of FKBP 12.6 with the channel. They attributed the contractile dysfunction observed in both the human and canine failing hearts to a reduction in the expression of SERCA2a, which would be expected to cause a reduction in the SR $Ca^{2+}$ load. Stange *et al.*, 2003, have created mutant RyR2's that mimic constitutively phosphorylated and dephosphorylated channels carrying Ser/Asp (S2809D) and Ser/Ala (S2809A) substitutions respectively. After transient expression in HEK cells, single channel activity was found to be unaltered in both mutants when compared to wild type. Additionally the pseudo-phosphorylated mutant was found to bind FKBP's to a similar extent to both the wild type and the pseudo-dephosphorylated channels. Finally Xiao *et al.*, 2004, have also shown that FKBP 12.6 can bind to both the serine-2808 phosphorylated and non-phosphorylated forms of RyR2. In addition an S2808D mutant, thought to mimic constitutive phosphorylation also retained the ability to bind FKBP 12.6.

### 7.1.5 NCX and heart failure

The data presented in chapter 6 of this thesis demonstrate that adenoviral-mediated overexpression of NCX in rabbit cardiomyocytes reduces both SR $Ca^{2+}$ load and the size of the intracellular $Ca^{2+}$ transient. Thus one would expect that if its expression were to be increased in heart failure, it would have a negative inotropic effect and serve to compound the type of

dysfunctional $Ca^{2+}$ homeostasis previously described. However, in many models of heart failure increased expression of NCX is thought to compensate for reduced expression SERCA2a in the preservation of diastolic function.

This is exactly what Hasenfuss *et al.*, 1999, observed when studying NCX and SERCA protein expression in failing human hearts. They were able to correlate decreased SERCA expression and unaltered NCX expression with disturbed diastolic function, which manifest as increased diastolic force and decreased maximal rate of force decline. However, when decreased SERCA expression was combined with increased NCX expression diastolic force and maximal rate of force decline did not change. Similarly, Studer *et al.*, 1994, studied NCX gene expression in end stage human heart failure. In patients presenting with coronary artery disease NCX mRNA levels were increased by 41% with respect to control whereas SERCA mRNA levels were reduced by 45%. Likewise, in patients presenting with dilated cardiomyopathy, NCX mRNA levels were increased by 55% when compared to control, with SERCA mRNA levels reduced by 50%.

In a rat model of heart failure caused by myocardial infarction, NCX protein expression was increased by 180%. Using whole cell voltage clamp and LSCM, flash photolysis was employed to release caged $Ca^{2+}$ and measure the $I_{NCX}$ currents associated with the changes in $[Ca^{2+}]_i$. $I_{NCX}$ density when normalised to the $[Ca^{2+}]_i$ jump was 2.6 fold higher in failing cardiomyocytes versus control (Gomez *et al.*, 2002). Interestingly, with $[Ca^{2+}]_i$ buffered at 200nM/L, cardiomyocytes isolated from a canine pacing induced model of heart failure exhibited unaltered NCX activity over the voltage range –100

to +100mV. However when $[Ca^{2+}]_i$ was only minimally buffered with 50μM/L indo, the rate of $Ca^{2+}$ extrusion via NCX during caffeine application was doubled in failing cardiomyocytes when compared to control (Hobai & O'Rourke, 2000). Hence any increase in NCX function in the failing heart may depend on $[Ca^{2+}]_i$.

It is noteworthy that not all models of heart failure are associated with increased NCX activity. Wang *et al.*, 2001, (murine aortic banding model of heart failure) and Quinn *et al.*, 2003, (rabbit coronary ligation model of heart failure) have both demonstrated increased NCX mRNA and protein expression but decreased NCX activity. However, in the case of Quinn *et al.*, failing cardiomyocytes also exhibited a reduced t-tubule density as evidenced by staining with DI-8-ANEPPS. Previous work suggests that NCX is almost exclusively located within the t-tubule network (Yang *et al.*, 2002) and it was suggested that disruption of this structure may occur in such a way as to prevent a significant amount of expressed NCX access to the extracellular space, effectively reducing NCX activity.

## 7.2 $Ca^{2+}$ sparks and intracellular $Ca^{2+}$ transients

### 7.2.1 $Ca^{2+}$ sparks and SR $Ca^{2+}$ load in permeabilised cardiomyocytes overexpressing either sorcin, CSQ or FKBP 12.6

Any experimental intervention that interacts with the RyR could potentially affect the amplitude, time course or frequency of a $Ca^{2+}$ spark. Reduction of the amplitude or frequency of $Ca^{2+}$ sparks would reduce $Ca^{2+}$ efflux from the SR. In the absence of any other changes, SR $Ca^{2+}$ content would be expected to increase. Cheng *et al.*, 1996, have demonstrated that a larger SR $Ca^{2+}$ content increased spark amplitude and frequency. Therefore interventions that act solely on the RyR might be expected to have only a transient effect on spark size/frequency before a new steady state SR $Ca^{2+}$ content is established.

Gyorke *et al.*, 1997, have investigated the effects of 0.5mM tetracaine on spontaneous $Ca^{2+}$ sparks in intact rat ventricular myocytes. They demonstrated that initially both the frequency and magnitude of $Ca^{2+}$ sparks were reduced, but as SR $Ca^{2+}$ load gradually increased, $Ca^{2+}$ sparks also increased in both frequency and magnitude. It seems strange that tetracaine, an agent that reduces the $Ca^{2+}$ sensitivity and hence the $P_O$ of the RyR, should cause an increase in the steady state frequency of $Ca^{2+}$ sparks. Tetracaine is thought to act cytoplasmically to reduce the RyR $P_O$. Thus an increased SR $Ca^{2+}$ load would be required to act luminally to overcome this inhibition and allow $Ca^{2+}$ sparks to occur. The occurrence of $Ca^{2+}$ sparks would empty the SR of $Ca^{2+}$ to some extent. For sparks to

occur again the SR would have to be re-filled with $Ca^{2+}$ (but to a greater extent than control to overcome the effects of tetracaine). Given that SERCA activity is unaffected it would take longer to reach this increased SR $Ca^{2+}$ load and thus be expected to cause a reduction in the frequency of $Ca^{2+}$ sparks. Finally, the steady state magnitude of the $Ca^{2+}$ sparks might be predicted to increase in the presence of tetracaine. In support of this possibility is a study that investigated the effects of tetracaine on spontaneous $Ca^{2+}$ waves in permeabilised rabbit cardiomyocytes (Smith & O'Neill, 2001). They demonstrated that 50μM tetracaine initially abolished $Ca^{2+}$ waves, but as SR load increased, $Ca^{2+}$ waves returned increased in magnitude but reduced in frequency. However thinking of a spontaneous $Ca^{2+}$ wave as "one big $Ca^{2+}$ spark" is an oversimplification.

Sorcin (Lokuta *et al.*, 1997) and CSQ (Gyorke *et al.*, 2004) have both been shown to reduce $P_O$ of RyR2 while dissociation of FKBP 12.6 from RyR2 increases $P_O$ (Kaftan *et al.*, 1996). Therefore adenoviral overexpression of these proteins would be expected to affect spontaneous $Ca^{2+}$ sparks in a manner similar to that predicted for tetracaine, i.e. increased spark size, reduced spark frequency and increased SR $Ca^{2+}$ load. However the data presented in chapters 3, 4 & 5 of this thesis indicate that overexpression of each of these proteins had unexpected effects on both $Ca^{2+}$ sparks and SR $Ca^{2+}$ load. Sorcin overexpression had no effect on SR $Ca^{2+}$ load, but reduced both the magnitude and frequency of $Ca^{2+}$ sparks. CSQ overexpression increased SR $Ca^{2+}$ load but had no effect on either $Ca^{2+}$ spark magnitude or frequency. FKBP 12.6 overexpression increased SR $Ca^{2+}$ load with both the magnitude and frequency of $Ca^{2+}$ sparks reduced.

At this stage it is not possible to explain why these observations do not meet with expectation. The results are consistent with each of the proteins exerting effects on the SR that are additional to their documented modes of action on RyR $P_O$.

### 7.2.3 Intracellular $Ca^{2+}$ transients and SR $Ca^{2+}$ load in whole cell voltage clamped cardiomyocytes

The spontaneous $Ca^{2+}$ sparks observed in resting cardiomyocytes are also thought to form the basic units of triggered SR $Ca^{2+}$ release (Cannell *et al.*, 1995). Hence, one would expect that interventions which affect $Ca^{2+}$ sparks in permeabilised cells would affect the intracellular $Ca^{2+}$ transient in voltage clamped intact cells in a similar way (providing the size of the L-type $Ca^{2+}$ current is unaffected). Additionally, the overexpression of sorcin, CSQ and FKBP 12.6 described in Chapters 3, 4 & 5 of this thesis, all of which reduce RYR2 $P_O$, should theoretically reduce the gain of E-C coupling.

The results presented in chapter 3 of this thesis demonstrate that adenoviral mediated sorcin overexpression reduces both SR $Ca^{2+}$ load and the size of the intracellular $Ca^{2+}$ transient. The reduced SR $Ca^{2+}$ load can be explained by the observation that sorcin increases the activity of NCX and hence the reduced $Ca^{2+}$ transient. In addition, when adenovirus was employed to overexpress NCX in rabbit cardiomyocytes (see Chapter 6), the results were similar to those observed for sorcin overexpression.

However, given that sorcin also reduces the $P_O$ of RyR2, one would expect it to reduce the gain of E-C coupling. From the data presented in chapter 3 this does not appear to be the case, with the relationship between SR $Ca^{2+}$ load and $Ca^{2+}$ transient amplitude for Ad-sorcin transfected cardiomyocytes similar to that described for Ad-LacZ transfected cells. It may be that at low SR $Ca^{2+}$ loads, our resolution of the relationship between SR $Ca^{2+}$ load and $Ca^{2+}$ transient amplitude is not good enough to detect changes in gain (see "red area" in figure 7-1 below). Future work might employ an experimental intervention to negate the effects of sorcin on NCX activity (e.g removing $Na^+$ from the bathing solution). Such a protocol may reveal that sorcin does infact reduce the gain of E-C coupling.

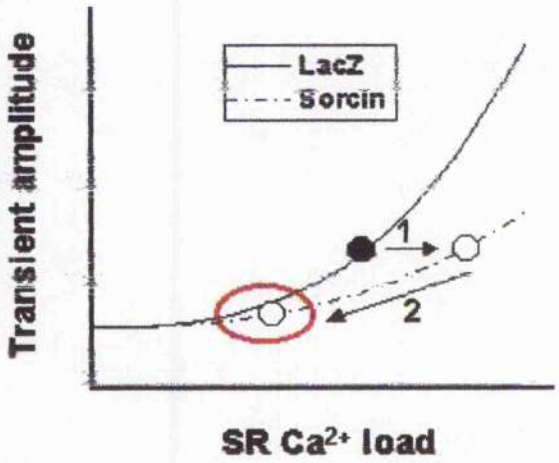


**Figure 7 - 1. Representation of how increased NCX (2) activity may reduce SR $Ca^{2+}$ load in sorcin transfected cardiomyocytes to an extent that one can longer resolve changes in gain due to reduced RYR2 $P_O$ (1).**

The reduced $Ca^{2+}$ spark size demonstrated in Ad-sorcin transfected permeabilised cardiomyocytes is consistent with the reduction in $Ca^{2+}$ transient size observed in the same group under conditions of whole cell

voltage clamp. Again further study might employ whole cell voltage clamp in combination with confocal microscopy to enable the study of both $Ca^{2+}$ sparks and intracellular $Ca^{2+}$ transients in the same cardiomyocyte. This experimental set up would help to confirm that reduced spark size contributes to the smaller intracellular $Ca^{2+}$ transients in Ad-sorcin transfected cardiomyocytes.

The results presented in Chapter 4 of this thesis demonstrate that adenoviral mediated overexpression of CSQ increased SR $Ca^{2+}$ load but had no effect on the size of the intracellular $Ca^{2+}$ transient. Thus it effectively reduced the gain of E-C coupling. This is precisely what would be predicted by Trafford *et al.*, 2000, who demonstrated that experimental interventions which alter only RyR2 $P_O$ have no effect on the size of the steady state intracellular $Ca^{2+}$ transient. The observation that CSQ did not affect the size of spontaneous $Ca^{2+}$ sparks in permeabilised cardiomyocytes is consistent with the findings in whole cell voltage clamp studies where the size of the intracellular $Ca^{2+}$ transient was also unaffected by CSQ overexpression.

The results presented in Chapter 5 show that adenoviral mediated overexpression of FKBP 12.6 increases both SR $Ca^{2+}$ load and $Ca^{2+}$ transient amplitude, but has no effect on the gain of E-C coupling. On first inspection the smaller $Ca^{2+}$ sparks observed in permeabilised cardiomyocytes over expressing FKBP 12.6 are not consistent with the larger intracellular $Ca^{2+}$ transients reported under conditions of whole cell voltage clamp. However, data included in chapter 5 reveals that FKBP 12.6

also increases the synchronicity of SR $Ca^{2+}$ release. Hence increased synchronicity may over-compensate for a reduction in spark size, ultimately enhancing the size of the intracellular $Ca^{2+}$ transient. Given that FKBP 12.6 overexpression should reduce the $P_O$ of RyR2, it might also be predicted to reduce the gain of E-C coupling. The data presented in chapter 5 do not support this hypothesis, with the relationship between SR $Ca^{2+}$ load and $Ca^{2+}$ transient amplitude for Ad-FKBP 12.6 transfected cardiomyocytes similar to that described for Ad-LacZ transfected cells. It is possible that a combination of reduced diastolic SR $Ca^{2+}$ leak and increased synchronicity of SR $Ca^{2+}$ release may effectively cancel each out the effects of reduced RyR2 $P_O$ on the gain of E-C coupling (see figure 7-2 below).

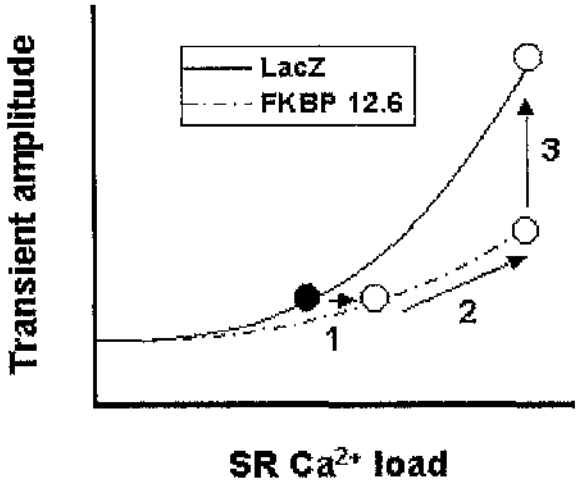


**Figure 7 - 2. Representation of how reduced diastolic SR $Ca^{2+}$ leak (2) and increased SR $Ca^{2+}$ release synchronicity may combine to mask the effect of reduced RYR2 $P_O$ (1) on the gain of E-C coupling.**

Finally, data presented in chapter 5 also reveal that voltage clamped cardiomyocytes transfected with Ad-FKBP 12.6 mutant (lacking calcineurin-binding site) have similar $Ca^{2+}$ transients to Ad-LacZ transfected

cardiomyocytes, despite exhibiting increased SR $Ca^{2+}$ loads. As such, it is tempting to speculate that the calcineurin-binding site is important for mediating the effects of FKBP 12.6 on SR $Ca^{2+}$ release synchronicity.

### 7.2.4 Conclusions

In conclusion it would appear that the cultured rabbit cardiomyocyte in combination with the adenoviral mediated overexpression system represents an extremely useful tool with which to study how specific proteins affect E-C coupling. The main strength of this approach is the acute overexpression of the protein of interest, allowing little time for compensatory changes in the expression of other proteins involved in E-C coupling. Such compensatory changes, as observed in many studies employing transgenic overexpression, would only serve to distort any changes in functionality and thus provide erroneous results. In the future it would be useful to consolidate the work presented in this thesis with a method that allowed for acute downregulation of proteins of interest.

Finally, it should be borne in mind that cultured cardiomyocytes differ significantly from their freshly dissociated counterparts. Similarly, one must be careful when extrapolating results obtained in single cell investigations to the functional syncytium that is the whole heart.

# References


Adams, W., Trafford, A. W., & Eisner, D. A. (1998). 2,3-Butanedione monoxime (BDM) decreases sarcoplasmic reticulum Ca content by stimulating Ca release in isolated rat ventricular myocytes. *Pflugers Arch.* **436**, 776-781.

Aggarwal, R., Shorofsky, S. R., Goldman, L., & Balke, C. W. (1997). Tetrodotoxin-blockable calcium currents in rat ventricular myocytes; a third type of cardiac cell sodium current. *J.Physiol* **505 ( Pt 2)**, 353-369.

Arai, M., Alpert, N. R., MacLennan, D. H., Barton, P., & Periasamy, M. (1993). Alterations in sarcoplasmic reticulum gene expression in human heart failure. A possible mechanism for alterations in systolic and diastolic properties of the failing myocardium. *Circ.Res.* **72**, 463-469.

Babcock, D. F. & Hille, B. (1998). Mitochondrial oversight of cellular Ca2+ signaling. *Curr.Opin.Neurobiol.* **8**, 398-404.

Baker, L. C., London, B., Choi, B. R., Koren, G., & Salama, G. (2000). Enhanced dispersion of repolarization and refractoriness in transgenic mouse hearts promotes reentrant ventricular tachycardia. *Circ.Res.* **86**, 396-407.

Bandyopadhyay, A., Shin, D. W., Ahn, J. O., & Kim, D. H. (2000). Calcineurin regulates ryanodine receptor/Ca(2+)-release channels in rat heart. *Biochem.J.* **352 Pt 1**, 61-70.

Banville, I. & Gray, R. A. (2002). Effect of action potential duration and conduction velocity restitution and their spatial dispersion on alternans and the stability of arrhythmias. *J.Cardiovasc.Electrophysiol.* **13**, 1141-1149.

Barg, S., Copello, J. A., & Fleischer, S. (1997). Different interactions of cardiac and skeletal muscle ryanodine receptors with FK-506 binding protein isoforms. *Am.J.Physiol* **272**, C1726-C1733.

Bassani, J. W., Bassani, R. A., & Bers, D. M. (1994). Relaxation in rabbit and rat cardiac cells: species-dependent differences in cellular mechanisms. *J.Physiol* **476**, 279-293.

Bassani, J. W., Yuan, W., & Bers, D. M. (1995). Fractional SR Ca release is regulated by trigger Ca and SR Ca content in cardiac myocytes. *Am.J.Physiol* **268**, C1313-C1319.

Bassani, R. A., Bassani, J. W., & Bers, D. M. (1992). Mitochondrial and sarcolemmal Ca2+ transport reduce [Ca2+]i during caffeine contractures in rabbit cardiac myocytes. *J.Physiol* **453**, 591-608.

Beard, N. A., Sakowska, M. M., Dulhunty, A. F., & Laver, D. R. (2002). Calsequestrin is an inhibitor of skeletal muscle ryanodine receptor calcium release channels. *Biophys.J.* **82**, 310-320.

Becker, K. G., Jedlicka, P., Templeton, N. S., Liotta, L., & Ozato, K. (1994). Characterization of hUCRBP (YY1, NF-E1, delta): a transcription factor that binds the regulatory regions of many viral and cellular genes. *Gene* **150**, 259-266.

Bers, D. M. Excitation-contraction coupling and cardiac contractile force. Kluwer Academic Publishers . 2001.
Ref Type: Generic

Bers, D. M., Philipson, K. D., & Peskoff, A. (1985). Calcium at the surface of cardiac plasma membrane vesicles: cation binding, surface charge screening, and Na-Ca exchange. *J.Membr.Biol.* **85**, 251-261.

Bers, D. M. & Stiffel, V. M. (1993). Ratio of ryanodine to dihydropyridine receptors in cardiac and skeletal muscle and implications for E-C coupling. *Am.J.Physiol* **264**, C1587-C1593.

Beuckelmann, D. J. & Erdmann, E. (1992). Ca(2+)-currents and intracellular [Ca2+]i-transients in single ventricular myocytes isolated from terminally failing human myocardium. *Basic Res.Cardiol.* **87 Suppl 1**, 235-243.

Beuckelmann, D. J., Nabauer, M., & Erdmann, E. (1992). Intracellular calcium handling in isolated ventricular myocytes from patients with terminal heart failure. *Circulation* **85**, 1046-1055.

Beuckelmann, D. J., Nabauer, M., & Erdmann, E. (1993). Alterations of K+ currents in isolated human ventricular myocytes from patients with terminal heart failure. *Circ.Res.* **73**, 379-385.

Beuckelmann, D. J. & Wier, W. G. (1988). Mechanism of release of calcium from sarcoplasmic reticulum of guinea-pig cardiac cells. *J.Physiol* **405**, 233-255.

Blanchard, E. M., Smith, G. L., Allen, D. G., & Alpert, N. R. (1990). The effects of 2,3-butanedione monoxime on initial heat, tension, and aequorin light output of ferret papillary muscles. *Pflugers Arch.* **416**, 219-221.

Brownawell, A. M. & Creutz, C. E. (1997). Calcium-dependent binding of sorcin to the N-terminal domain of synexin (annexin VII). *J.Biol.Chem.* **272**, 22182-22190.

Cachelin, A. B., de Peyer, J. E., Kokubun, S., & Reuter, H. (1983). Ca2+ channel modulation by 8-bromocyclic AMP in cultured heart cells. *Nature* **304**, 462-464.

Cameron, A. M., Steiner, J. P., Roskams, A. J., Ali, S. M., Ronnett, G. V., & Snyder, S. H. (1995). Calcineurin associated with the inositol 1,4,5-trisphosphate receptor-FKBP12 complex modulates Ca2+ flux. *Cell* **83**, 463-472.

Campbell, K. P., MacLennan, D. H., Jorgensen, A. O., & Mintzer, M. C. (1983). Purification and characterization of calsequestrin from canine cardiac sarcoplasmic reticulum and identification of the 53,000 dalton glycoprotein. *J.Biol.Chem.* **258**, 1197-1204.

Cannell, M. B., Berlin, J. R., & Lederer, W. J. (1987). Effect of membrane potential changes on the calcium transient in single rat cardiac muscle cells. *Science* **238**, 1419-1423.

Cannell, M. B., Cheng, H., & Lederer, W. J. (1995). The control of calcium release in heart muscle. *Science* **268**, 1045-1049.

Chandler, W. K., Rakowski, R. F., & Schneider, M. F. (1976a). A non-linear voltage dependent charge movement in frog skeletal muscle. *J.Physiol* **254**, 245-283.

Chandler, W. K., Rakowski, R. F., & Schneider, M. F. (1976b). Effects of glycerol treatment and maintained depolarization on charge movement in skeletal muscle. *J.Physiol* **254**, 285-316.

Cheng, H., Lederer, M. R., Lederer, W. J., & Cannell, M. B. (1996). Calcium sparks and [Ca2+]i waves in cardiac myocytes. *Am.J.Physiol* **270**, C148-C159.

Cheng, H., Lederer, W. J., & Cannell, M. B. (1993). Calcium sparks: elementary events underlying excitation-contraction coupling in heart muscle. *Science* **262**, 740-744.

Cheng, H., Song, L. S., Shirokova, N., Gonzalez, A., Lakatta, E. G., Rios, E., & Stern, M. D. (1999). Amplitude distribution of calcium sparks in confocal images: theory and studies with an automatic detection method. *Biophys.J.* **76**, 606-617.

Ching, L. L., Williams, A. J., & Sitsapesan, R. (2000). Evidence for Ca(2+) activation and inactivation sites on the luminal side of the cardiac ryanodine receptor complex. *Circ.Res.* **87**, 201-206.

Colyer, J. (1998). Phosphorylation states of phospholamban. *Ann.N.Y.Acad.Sci.* **853**, 79-91.

Convery, M. K. & Hancox, J. C. (1999). Comparison of Na+-Ca2+ exchange current elicited from isolated rabbit ventricular myocytes by voltage ramp and step protocols. *Pflugers Arch.* **437**, 944-954.

Currie, S. & Smith, G. L. (1999). Enhanced phosphorylation of phospholamban and downregulation of sarco/endoplasmic reticulum Ca2+ ATPase type 2 (SERCA 2) in cardiac sarcoplasmic reticulum from rabbits with heart failure. *Cardiovasc.Res.* **41**, 135-146.

de Leon, M., Wang, Y., Jones, L., Perez-Reyes, E., Wei, X., Soong, T. W., Snutch, T. P., & Yue, D. T. (1995). Essential Ca(2+)-binding motif for Ca(2+)-sensitive inactivation of L-type Ca2+ channels. *Science* **270**, 1502-1506.

Diaz, M. E., Trafford, A. W., O'Neill, S. C., & Eisner, D. A. (1997). Measurement of sarcoplasmic reticulum Ca2+ content and sarcolemmal Ca2+ fluxes in isolated rat ventricular myocytes during spontaneous Ca2+ release. *J.Physiol* **501 ( Pt 1)**, 3-16.

Dixon, D. A. & Haynes, D. H. (1989). Kinetic characterization of the Ca2+-pumping ATPase of cardia sarcoiemma in four states of activation. *J.Biol.Chem.* **264**, 13612-13622.

Doering, A. E. & Lederer, W. J. (1993). The mechanism by which cytoplasmic protons inhibit the sodium-calcium exchanger in guinea-pig heart cells. *J.Physiol* **466**, 481-499.

Doering, A. E. & Lederer, W. J. (1994). The action of Na+ as a cofactor in the inhibition by cytoplasmic protons of the cardiac Na(+)-Ca2+ exchanger in the guinea-pig. *J.Physiol* **480 ( Pt 1)**, 9-20.

Doi, M., Yano, M., Kobayashi, S., Kohno, M., Tokuhisa, T., Okuda, S., Suetsugu, M., Hisamatsu, Y., Ohkusa, T., Kohno, M., & Matsuzaki, M. (2002). Propranolol prevents the development of heart failure by restoring FKBP12.6-mediated stabilization of ryanodine receptor. *Circulation* **105**, 1374-1379.

duBell, W. H., Lederer, W. J., & Rogers, T. B. (1996). Dynamic modulation of excitation-contraction coupling by protein phosphatases in rat ventricular myocytes. *J.Physiol* **493 ( Pt 3)**, 793-800.

duBell, W. H., Wright, P. A., Lederer, W. J., & Rogers, T. B. (1997). Effect of the immunosupressant FK506 on excitation-contraction coupling and outward K+ currents in rat ventricular myocytes. *J.Physiol* **501 ( Pt 3)**, 509-516.

Duncan, A. M. Transmural differences in calcium handling proteins in normal rabbit hearts and hearts with left ventricular dysfunction. Currie, S. and Smith, G. L. J.Physiol 536P, S122. 2001.
Ref Type: Generic

Eisner, D. A., Choi, H. S., Diaz, M. E., O'Neill, S. C., & Trafford, A. W. (2000). Integrative analysis of calcium cycling in cardiac muscle. *Circ.Res.* **87**, 1087-1094.

Eisner, D. A., Nichols, C. G., O'Neill, S. C., Smith, G. L., & Valdeolmillos, M. (1989). The effects of metabolic inhibition on intracellular calcium and pH in isolated rat ventricular cells. *J.Physiol* **411**, 393-418.

Elliott, E. Decreased sorcin expression in a rabbit model of left ventricular dysfunction. Currie, S. and Smith, G. L. Physiological Society (Glasgow Meeting) Abstract, C2. 2004.
Ref Type: Generic

Fabiato, A. (1983). Calcium-induced release of calcium from the cardiac sarcoplasmic reticulum. *Am.J.Physiol* **245**, C1-14.

Fabiato, A. (1985a). Time and calcium dependence of activation and inactivation of calcium-induced release of calcium from the sarcoplasmic reticulum of a skinned canine cardiac Purkinje cell. *J.Gen.Physiol* **85**, 247-289.

Fabiato, A. (1985b). Use of aequorin for the appraisal of the hypothesis of the release of calcium from the sarcoplasmic reticulum induced by a change of pH in skinned cardiac cells. *Cell Calcium* **6**, 95-108.

Farrell, E. F. Sorcin modulates calcium spark characteristics and excitation contraction coupling in cardiac myocytes. Gomez, A. M., Antaramian, A., Benkusky, N., and Valdivia, H. Biophys.J. 82(1), 178a. 2002.
Ref Type: Generic

Farrell, E. F., Antaramian, A., Rueda, A., Gomez, A. M., & Vaidivia, H. H. (2003). Sorcin inhibits calcium release and modulates excitation-contraction coupling in the heart. *J.Biol.Chem.* **278**, 34660-34666.

Ferreira, G., Artigas, P., Pizarro, G., & Brum, G. (1997). Butanedione monoxime promotes voltage-dependent inactivation of L-type calcium channels in heart. Effects on gating currents. *J.Mol.Cell Cardiol.* **29**, 777-787.

Ferrier, G. R. & Howlett, S. E. (1995). Contractions in guinea-pig ventricular myocytes triggered by a calcium-release mechanism separate from Na+ and L-currents. *J.Physiol* **484 ( Pt 1)**, 107-122.

Ferrier, G. R., Zhu, J., Redondo, I. M., & Howlett, S. E. (1998). Role of cAMP-dependent protein kinase A in activation of a voltage-sensitive release mechanism for cardiac contraction in guinea-pig myocytes. *J.Physiol* **513 ( Pt 1)**, 185-201.

Flesch, M., Schwinger, R. H., Schiffer, F., Frank, K., Sudkamp, M., Kuhn-Regnier, F., Arnold, G., & Bohm, M. (1996). Evidence for functional relevance of an enhanced expression of the Na(+)-Ca2+ exchanger in failing human myocardium. *Circulation* **94**, 992-1002.

Frank, K. Decreased expression but increased binding of sorcin to the ryanodine receptor channel of the failing human myocardium. Boelck, B., Hattebuhr, N., Malik, A., and Schwinger, R. Z Kardiol Supplement, 93(3), V519. 2004.
Ref Type: Generic

Franzini-Armstrong, C., Kenney, L. J., & Varriano-Marston, E. (1987). The structure of calsequestrin in triads of vertebrate skeletal muscle: a deep-etch study. *J.Cell Biol.* **105**, 49-56.

Franzini-Armstrong, C., Protasi, F., & Ramesh, V. (1999). Shape, size, and distribution of Ca(2+) release units and couplons in skeletal and cardiac muscles. *Biophys.J.* **77**, 1528-1539.

Fujioka, Y., Komeda, M., & Matsuoka, S. (2000). Stoichiometry of Na+-Ca2+ exchange in inside-out patches excised from guinea-pig ventricular myocytes. *J.Physiol* **523 Pt 2**, 339-351.

George, C. H., Sorathia, R., Bertrand, B. M., & Lai, F. A. (2003). In situ modulation of the human cardiac ryanodine receptor (hRyR2) by FKBP12.6. *Biochem.J.* **370**, 579-589.

Ginsburg, K. S. Isoproterenol does not enhance Na/Ca exchange current in intact rabbit ventricular myocytes. Bers, D. M. Biophys.J. Supplement, 86(1), 26a. 2004.
Ref Type: Generic

Goeger, D. E., Riley, R. T., Dorner, J. W., & Cole, R. J. (1988). Cyclopiazonic acid inhibition of the Ca2+-transport ATPase in rat skeletal muscle sarcoplasmic reticulum vesicles. *Biochem.Pharmacol.* **37**, 978-981.

Gomez, A. M., Schwaller, B., Porzig, H., Vassort, G., Niggli, E., & Egger, M. (2002). Increased exchange current but normal Ca2+ transport via Na+-Ca2+ exchange during cardiac hypertrophy after myocardial infarction. *Circ.Res.* **91**, 323-330.

Gracy, K. N., Clarke, C. L., Meyers, M. B., & Pickel, V. M. (1999). N-methyl-D-aspartate receptor 1 in the caudate-putamen nucleus: ultrastructural localization and co-expression with sorcin, a 22,000 mol. wt calcium binding protein. *Neuroscience* **90**, 107-117.

Greenstein, J. L. & Winslow, R. L. (2002). An integrative model of the cardiac ventricular myocyte incorporating local control of Ca2+ release. *Biophys.J.* **83**, 2918-2945.

Gunter, T. E., Buntinas, L., Sparagna, G., Eliseev, R., & Gunter, K. (2000). Mitochondrial calcium transport: mechanisms and functions. *Cell Calcium* **28**, 285-296.

Gwathmey, J. K., Hajjar, R. J., & Solaro, R. J. (1991). Contractile deactivation and uncoupling of crossbridges. Effects of 2,3-butanedione monoxime on mammalian myocardium. *Circ.Res.* **69**, 1280-1292.

Gyorke, I. & Gyorke, S. (1998). Regulation of the cardiac ryanodine receptor channel by luminal Ca2+ involves luminal Ca2+ sensing sites. *Biophys.J.* **75**, 2801-2810.

Gyorke, I., Hester, N., Jones, L. R., & Gyorke, S. (2004). The role of calsequestrin, triadin, and junctin in conferring cardiac ryanodine receptor responsiveness to luminal calcium. *Biophys.J.* **86**, 2121-2128.

Gyorke, S., Lukyanenko, V., & Gyorke, I. (1997). Dual effects of tetracaine on spontaneous calcium release in rat ventricular myocytes. *J.Physiol* **500 ( Pt 2)**, 297-309.

Hadley, R. W. & Hume, J. R. (1987). An intrinsic potential-dependent inactivation mechanism associated with calcium channels in guinea-pig myocytes. *J.Physiol* **389**, 205-222.

Hasenfuss, G. (1998). Alterations of calcium-regulatory proteins in heart failure. *Cardiovasc.Res.* **37**, 279-289.

Hasenfuss, G., Schillinger, W., Lehnart, S. E., Preuss, M., Pieske, B., Maier, L. S., Prestle, J., Minami, K., & Just, H. (1999). Relationship between Na+-Ca2+-exchanger protein levels and diastolic function of failing human myocardium. *Circulation* **99**, 641-648.

Henderson, S. A., Goldhaber, J. I., So, J. M., Han, T., Motter, C., Ngo, A., Chantawansri, C., Ritter, M. R., Friedlander, M., Nicoll, D. A., Frank, J. S., Jordan, M. C., Roos, K. P., Ross, R. S., & Philipson, K. D. (2004). Functional Adult Myocardium in the Absence of Na+-Ca2+ Exchange. Cardiac-Specific Knockout of NCX1. *Circ.Res.*

Herr, C., Smyth, N., Ullrich, S., Yun, F., Sasse, P., Hescheier, J., Fleischmann, B., Lasek, K., Brixius, K., Schwinger, R. H., Fassler, R., Schroder, R., & Noegel, A. A. (2001). Loss of annexin A7 leads to alterations in frequency-induced shortening of isolated murine cardiomyocytes. *Mol.Cell Biol.* **21**, 4119-4128.

Hess, P., Lansman, J. B., & Tsien, R. W. (1984). Different modes of Ca channel gating behaviour favoured by dihydropyridine Ca agonists and antagonists. *Nature* **311**, 538-544.

Hille, B. Ionic Channels of Excitable Membranes. Sinauer Associates, Sunderland, MA. 1992.
Ref Type: Generic

Hobai, I. A. & O'Rourke, B. (2000). Enhanced Ca(2+)-activated Na(+)-Ca(2+) exchange activity in canine pacing-induced heart failure. *Circ.Res.* **87**, 690-698.

Huang, B., Wang, S., Qin, D., Boutjdir, M., & El Sherif, N. (1999). Diminished basal phosphorylation level of phospholamban in the postinfarction remodeled rat ventricle: role of beta-adrenergic pathway, G(i) protein, phosphodiesterase, and phosphatases. *Circ.Res.* **85**, 848-855.

Ikemoto, N., Ronjat, M., Meszaros, L. G., & Koshita, M. (1989). Postulated role of calsequestrin in the regulation of calcium release from sarcoplasmic reticuium. *Biochemistry* **28**, 6764-6771.

Jayaraman, T., Brillantes, A. M., Timerman, A. P., Fleischer, S., Erdjument-Bromage, H., Tempst, P., & Marks, A. R. (1992). FK506 binding protein associated with the calcium release channel (ryanodine receptor). *J.Biol.Chem.* **267**, 9474-9477.

Jeyakumar, L. H., Ballester, L., Cheng, D. S., McIntyre, J. O., Chang, P., Olivey, H. E., Rollins-Smith, L., Barnett, J. V., Murray, K., Xin, H. B., & Fleischer, S. (2001). FKBP binding characteristics of cardiac microsomes from diverse vertebrates. *Biochem.Biophys.Res.Commun.* **281**, 979-986.

Jiang, M. T., Lokuta, A. J., Farrell, E. F., Wolff, M. R., Haworth, R. A., & Valdivia, H. H. (2002). Abnormal Ca2+ release, but normal ryanodine receptors, in canine and human heart failure. *Circ.Res.* **91**, 1015-1022.

Jones, L. R., Suzuki, Y. J., Wang, W., Kobayashi, Y. M., Ramesh, V., Franzini-Armstrong, C., Cleemann, L., & Morad, M. (1998). Regulation of Ca2+ signaling in transgenic mouse cardiac myocytes overexpressing calsequestrin. *J.Clin.Invest* **101**, 1385-1393.

Kaftan, E., Marks, A. R., & Ehrlich, B. E. (1996). Effects of rapamycin on ryanodine receptor/Ca(2+)-release channels from cardiac muscle. *Circ.Res.* **78**, 990-997.

Kawasaki, T. & Kasai, M. (1994). Regulation of calcium channel in sarcoplasmic reticulum by calsequestrin. *Biochem.Biophys.Res.Commun.* **199**, 1120-1127.

Kimura, J., Miyamae, S., & Noma, A. (1987). Identification of sodium-calcium exchange current in single ventricular cells of guinea-pig. *J.Physiol* **384**, 199-222.

Knollmann, B. C., Knollmann-Ritschel, B. E., Weissman, N. J., Jones, L. R., & Morad, M. (2000). Remodelling of ionic currents in hypertrophied and failing hearts of transgenic mice overexpressing calsequestrin. *J.Physiol* **525 Pt 2**, 483-498.

Lam, E., Martin, M. M., Timerman, A. P., Sabers, C., Fleischer, S., Lukas, T., Abraham, R. T., O'Keefe, S. J., O'Neill, E. A., & Wiederrecht, G. J. (1995). A novel FK506 binding protein can mediate the immunosuppressive effects of FK506 and is associated with the cardiac ryanodine receptor. *J.Biol.Chem.* **270**, 26511-26522.

Leblanc, N. & Hume, J. R. (1990). Sodium current-induced release of calcium from cardiac sarcoplasmic reticulum. *Science* **248**, 372-376.

Lee, M. H., Lin, S. F., Ohara, T., Omichi, C., Okuyama, Y., Chudin, E., Garfinkel, A., Weiss, J. N., Karagueuzian, H. S., & Chen, P. S. (2001). Effects of diacetyl monoxime and cytochalasin D on ventricular fibrillation in swine right ventricles. *Am.J.Physiol Heart Circ.Physiol* **280**, H2689-H2696.

Levi, A. J., Spitzer, K. W., Kohmoto, O., & Bridge, J. H. (1994). Depolarization-induced Ca entry via Na-Ca exchange triggers SR release in guinea pig cardiac myocytes. *Am.J.Physiol* **266**, H1422-H1433.

Lew, W. Y., Hryshko, L. V., & Bers, D. M. (1991). Dihydropyridine receptors are primarily functional L-type calcium channels in rabbit ventricular myocytes. *Circ.Res.* **69**, 1139-1145.

Li, L., Chu, G., Kranias, E. G., & Bers, D. M. (1998). Cardiac myocyte calcium transport in phospholamban knockout mouse: relaxation and endogenous CaMKII effects. *Am.J.Physiol* **274**, H1335-H1347.

Linck, B., Boknik, P., Huke, S., Kirchhefer, U., Knapp, J., Luss, H., Muller, F. U., Neumann, J., Tanriseven, Z., Vahlensieck, U., Baba, H. A., Jones, L. R., Philipson, K. D., & Schmitz, W. (2000). Functional properties of transgenic mouse hearts overexpressing both calsequestrin and the Na(+)-Ca(2+) exchanger. *J.Pharmacol.Exp.Ther.* **294**, 648-657.

Lindner, M., Erdmann, E., & Beuckelmann, D. J. (1998). Calcium content of the sarcoplasmic reticulum in isolated ventricular myocytes from patients with terminal heart failure. *J.Mol.Cell Cardiol.* **30**, 743-749.

Lipp, P., Huser, J., Pott, L., & Niggli, E. (1996). Spatially non-uniform Ca2+ signals induced by the reduction of transverse tubules in citrate-loaded guinea-pig ventricular myocytes in culture. *J.Physiol* **497 ( Pt 3)**, 589-597.

Lipp, P. & Niggli, E. (1994). Sodium current-induced calcium signals in isolated guinea-pig ventricular myocytes. *J.Physiol* **474**, 439-446.

Litwin, S. E., Li, J., & Bridge, J. H. (1998). Na-Ca exchange and the trigger for sarcoplasmic reticulum Ca release: studies in adult rabbit ventricular myocytes. *Biophys.J.* **75**, 359-371.

Lokuta, A. J., Meyers, M. B., Sander, P. R., Fishman, G. I., & Valdivia, H. H. (1997). Modulation of cardiac ryanodine receptors by sorcin. *J.Biol.Chem.* **272**, 25333-25338.

Lokuta, A. J., Rogers, T. B., Lederer, W. J., & Valdivia, H. H. (1995). Modulation of cardiac ryanodine receptors of swine and rabbit by a phosphorylation-dephosphorylation mechanism. *J.Physiol* **487 ( Pt 3)**, 609-622.

Loughrey, C. M., Seidler, T., Miller, S. L., Prestle, J., MacEachern, K. E., Reynolds, D. F., Hasenfuss, G., & Smith, G. L. (2004). Over-expression of FK506-binding protein FKBP12.6 alters excitation-contraction coupling in adult rabbit cardiomyocytes. *J.Physiol* **556**, 919-934.

Lukyanenko, V., Gyorke, I., & Gyorke, S. (1996). Regulation of calcium release by calcium inside the sarcoplasmic reticulum in ventricular myocytes. *Pflugers Arch.* **432**, 1047-1054.

Lukyanenko, V. & Gyorke, S. (1999). Ca2+ sparks and Ca2+ waves in saponin-permeabilized rat ventricular myocytes. *J.Physiol* **521 Pt 3**, 575-585.

MacLennan, D. H., Clarke, D. M., Loo, T. W., & Skerjanc, I. S. (1992). Site-directed mutagenesis of the Ca2+ ATPase of sarcoplasmic reticulum. *Acta Physiol Scand.Suppl* **607**, 141-150.

MacLennan, D. H. & Wong, P. T. (1971). Isolation of a calcium-sequestering protein from sarcoplasmic reticulum. *Proc.Natl.Acad.Sci.U.S.A* **68**, 1231-1235.

Majlof, L. & Forsgren, P. O. (1993). Confocal microscopy: important considerations for accurate imaging. *Methods Cell Biol.* **38**, 79-95.

Marks, A. R. (1996). Cellular functions of immunophilins. *Physiol Rev.* **76**, 631-649.

Marx, S. O., Gaburjakova, J., Gaburjakova, M., Henrikson, C., Ondrias, K., & Marks, A. R. (2001). Coupled gating between cardiac calcium release channels (ryanodine receptors). *Circ.Res.* **88**, 1151-1158.

Marx, S. O., Reiken, S., Hisamatsu, Y., Jayaraman, T., Burkhoff, D., Rosemblit, N., & Marks, A. R. (2000). PKA phosphorylation dissociates FKBP12.6 from the calcium release channel (ryanodine receptor): defective regulation in failing hearts. *Cell* **101**, 365-376.

Matsuoka, S., Nicoll, D. A., Reilly, R. F., Hilgemann, D. W., & Philipson, K. D. (1993). Initial localization of regulatory regions of the cardiac sarcolemmal Na(+)-Ca2+ exchanger. *Proc.Natl.Acad.Sci.U.S.A* **90**, 3870-3874.

McCall, E., Li, L., Satoh, H., Shannon, T. R., Blatter, L. A., & Bers, D. M. (1996). Effects of FK-506 on contraction and Ca2+ transients in rat cardiac myocytes. *Circ.Res.* **79**, 1110-1121.

Meissner, G. & Henderson, J. S. (1987). Rapid calcium release from cardiac sarcoplasmic reticulum vesicles is dependent on Ca2+ and is modulated by Mg2+, adenine nucleotide, and calmodulin. *J.Biol.Chem.* **262**, 3065-3073.

Mejia-Alvarez, R., Kettlun, C., Rios, E., Stern, M., & Fill, M. (1999). Unitary Ca2+ current through cardiac ryanodine receptor channels under quasi-physiological ionic conditions. *J.Gen.Physiol* **113**, 177-186.

Mella, M., Colotti, G., Zamparelli, C., Verzili, D., Iiari, A., & Chiancone, E. (2003). Information transfer in the penta-EF-hand protein sorcin does not operate via the canonical structural/functional pairing. A study with site-specific mutants. *J.Biol.Chem.* **278**, 24921-24928.

Meyer, M., Schillinger, W., Pieske, B., Holubarsch, C., Heilmann, C., Posival, H., Kuwajima, G., Mikoshiba, K., Just, H., Hasenfuss, G., & . (1995). Alterations of sarcoplasmic reticulum proteins in failing human dilated cardiomyopathy. *Circulation* **92**, 778-784.

Meyers, M. B., Fischer, A., Sun, Y. J., Lopes, C. M., Rohacs, T., Nakamura, T. Y., Zhou, Y. Y., Lee, P. C., Altschuld, R. A., McCune, S. A., Coetzee, W. A., & Fishman, G. I. (2003). Sorcin regulates excitation-contraction coupling in the heart. *J.Biol.Chem.* **278**, 28865-28871.

Meyers, M. B., Pickel, V. M., Sheu, S. S., Sharma, V. K., Scotto, K. W., & Fishman, G. I. (1995a). Association of sorcin with the cardiac ryanodine receptor. *J.Biol.Chem.* **270**, 26411-26418.

Meyers, M. B., Puri, T. S., Chien, A. J., Gao, T., Hsu, P. H., Hosey, M. M., & Fishman, G. I. (1998). Sorcin associates with the pore-forming subunit of voltage-dependent L-type Ca2+ channels. *J.Biol.Chem.* **273**, 18930-18935.

Meyers, M. B., Spengler, B. A., Chang, T. D., Melera, P. W., & Biedler, J. L. (1985). Gene amplification-associated cytogenetic aberrations and protein changes in vincristine-resistant Chinese hamster, mouse, and human cells. *J.Cell Biol.* **100**, 588-597.

Meyers, M. B., Zamparelli, C., Verzili, D., Dicker, A. P., Bianck, T. J., & Chiancone, E. (1995b). Calcium-dependent translocation of sorcin to membranes: functional relevance in contractile tissue. *FEBS Lett.* **357**, 230-234.

Mitcheson, J. S., Hancox, J. C., & Levi, A. J. (1996). Action potentials, ion channel currents and transverse tubule density in adult rabbit ventricular myocytes maintained for 6 days in cell culture. *Pflugers Arch.* **431**, 814-827.

Movsesian, M. A., Karimi, M., Green, K., & Jones, L. R. (1994). Ca(2+)-transporting ATPase, phospholamban, and calsequestrin levels in nonfailing and failing human myocardium. *Circulation* **90**, 653-657.

Munch, G., Bolck, B., Hoischen, S., Brixius, K., Bloch, W., Reuter, H., & Schwinger, R. H. (1998). Unchanged protein expression of sarcoplasmic reticulum Ca2+-ATPase, phospholamban, and calsequestrin in terminally failing human myocardium. *J.Mol.Med.* **76**, 434-441.

Nabauer, M. & Morad, M. (1990). Ca2(+)-induced Ca2+ release as examined by photolysis of caged Ca2+ in single ventricular myocytes. *Am.J.Physiol* **258**, C189-C193.

Nakamura, H., Nakasaki, Y., Matsuda, N., & Shigekawa, M. (1992). Inhibition of sarcoplasmic reticulum Ca(2+)-ATPase by 2,5-di(tert-butyl)-1,4-benzohydroquinone. *J.Biochem.(Tokyo)* **112**, 750-755.

Naqvi, R. U., Tweedie, D., & MacLeod, K. T. (2001). Evidence for the action potential mediating the changes to contraction observed in cardiac hypertrophy in the rabbit. *Int.J.Cardiol.* **77**, 189-206.

Nicoll, D. A., Hryshko, L. V., Matsuoka, S., Frank, J. S., & Philipson, K. D. (1996). Mutation of amino acid residues in the putative transmembrane segments of the cardiac sarcolemmal Na+-Ca2+ exchanger. *J.Biol.Chem.* **271**, 13385-13391.

Nicoll, D. A., Longoni, S., & Philipson, K. D. (1990). Molecular cloning and functional expression of the cardiac sarcolemmal Na(+)-Ca2+ exchanger. *Science* **250**, 562-565.

Pack-Chung, E., Meyers, M. B., Pettingell, W. P., Moir, R. D., Brownawell, A. M., Cheng, I., Tanzi, R. E., & Kim, T. W. (2000). Presenilin 2 interacts with sorcin, a modulator of the ryanodine receptor. *J.Biol.Chem.* **275**, 14440-14445.

Pasumarthi, K. B. & Field, L. J. (2002). Cardiomyocyte cell cycle regulation. *Circ.Res.* **90**, 1044-1054.

Peskoff, A. & Langer, G. A. (1998). Calcium concentration and movement in the ventricular cardiac cell during an excitation-contraction cycle. *Biophys.J.* **74**, 153-174.

Philipson, K. D. Functional adult myocardium in the absence of sodium-calcium exchange: cardiac specific knockout of NCX1. Henderson, S. A., Jordan, M., Roos, K., Goldhaber, J., Motter, C., Han, T., Frank, J., Ross, R., Nicoll, D., Ritter, M., and Friedlander, M. Biophys.J. Supplement, 86(1), 224a. 2004.
Ref Type: Generic

Philipson, K. D., Bersohn, M. M., & Nishimoto, A. Y. (1982). Effects of pH on Na+-Ca2+ exchange in canine cardiac sarcolemmal vesicles. *Circ.Res.* **50**, 287-293.

Philipson, K. D. & Nicoll, D. A. (2000). Sodium-calcium exchange: a molecular perspective. *Annu.Rev.Physiol* **62**, 111-133.

Pignier, C., Ancey, C., Fares, N., Bescond, J., & Potreau, D. (2002). Reexpression of the nifedipine-resistant calcium channel during dedifferentiation of adult rat ventricular cardiomyocytes. *J.Cardiovasc.Electrophysiol.* **13**, 178-183.

Pogwizd, S. M., Qi, M., Yuan, W., Samarel, A. M., & Bers, D. M. (1999). Upregulation of Na(+)/Ca(2+) exchanger expression and function in an arrhythmogenic rabbit model of heart failure. *Circ.Res.* **85**, 1009-1019.

Prestle, J., Janssen, P. M., Janssen, A. P., Zeitz, O., Lehnart, S. E., Bruce, L., Smith, G. L., & Hasenfuss, G. (2001). Overexpression of FK506-binding protein FKBP12.6 in cardiomyocytes reduces ryanodine receptor-mediated Ca(2+) leak from the sarcoplasmic reticulum and increases contractility. *Circ.Res.* **88**, 188-194.

Quinn, F. R., Currie, S., Duncan, A. M., Miller, S., Sayeed, R., Cobbe, S. M., & Smith, G. L. (2003). Myocardial infarction causes increased expression but decreased activity of the myocardial Na+-Ca2+ exchanger in the rabbit. *J.Physiol* **553**, 229-242.

Ranu, H. K., Terracciano, C. M., Davia, K., Bernobich, E., Chaudhri, B., Robinson, S. E., Bin, K. Z., Hajjar, R. J., MacLeod, K. T., & Harding, S. E. (2002). Effects of Na(+)/Ca(2+)-exchanger overexpression on excitation-contraction coupling in adult rabbit ventricular myocytes. *J.Mol.Cell Cardiol.* **34**, 389-400.

Reeves, J. P. & Hale, C. C. (1984). The stoichiometry of the cardiac sodium-calcium exchange system. *J.Biol.Chem.* **259**, 7733-7739.

Reeves, J. P. & Sutko, J. L. (1980). Sodium-calcium exchange activity generates a current in cardiac membrane vesicles. *Science* **208**, 1461-1464.

Reuter, H. & Seitz, N. (1968). The dependence of calcium efflux from cardiac muscle on temperature and external ion composition. *J.Physiol* **195**, 451-470.

Riccio, M. L., Koller, M. L., & Gilmour, R. F., Jr. (1999). Electrical restitution and spatiotemporal organization during ventricular fibrillation. *Circ.Res.* **84**, 955-963.

Ringer, S. A further contribution regarding the influence of the different constituents of the blood on the contraction of the heart. J.Physiol 4, 29-42. 1883.
Ref Type: Generic

Rios, E. & Pizarro, G. (1991). Voltage sensor of excitation-contraction coupling in skeletal muscle. *Physiol Rev.* **71**, 849-908.

Rousseau, E. & Meissner, G. (1989). Single cardiac sarcoplasmic reticulum Ca2+-release channel: activation by caffeine. *Am.J.Physiol* **256**, H328-H333.

Rousseau, E., Smith, J. S., Henderson, J. S., & Meissner, G. (1986). Single channel and 45Ca2+ flux measurements of the cardiac sarcoplasmic reticulum calcium channel. *Biophys.J.* **50**, 1009-1014.

Sagara, Y. & Inesi, G. (1991). Inhibition of the sarcoplasmic reticulum Ca2+ transport ATPase by thapsigargin at subnanomolar concentrations. *J.Biol.Chem.* **266**, 13503-13506.

Saito, A., Inui, M., Radermacher, M., Frank, J., & Fleischer, S. (1988). Ultrastructure of the calcium release channel of sarcoplasmic reticulum. *J.Cell Biol.* **107**, 211-219.

Santana, L. F., Gomez, A. M., & Lederer, W. J. (1998). Ca2+ flux through promiscuous cardiac Na+ channels: slip-mode conductance. *Science* **279**, 1027-1033.

Sato, Y., Ferguson, D. G., Sako, H., Dorn, G. W., Kadambi, V. J., Yatani, A., Hoit, B. D., Walsh, R. A., & Kranias, E. G. (1998). Cardiac-specific overexpression of mouse cardiac calsequestrin is associated with depressed cardiovascular function and hypertrophy in transgenic mice. *J.Biol.Chem.* **273**, 28470-28477.

Satoh, H., Delbridge, L. M., Blatter, L. A., & Bers, D. M. (1996). Surface:volume relationship in cardiac myocytes studied with confocal microscopy and membrane capacitance measurements: species-dependence and developmental effects. *Biophys.J.* **70**, 1494-1504.

Schillinger, W., Janssen, P. M., Emami, S., Henderson, S. A., Ross, R. S., Teucher, N., Zeitz, O., Philipson, K. D., Prestle, J., & Hasenfuss, G. (2000). Impaired contractile performance of cultured rabbit ventricular myocytes after adenoviral gene transfer of Na(+)-Ca(2+) exchanger. *Circ.Res.* **87**, 581-587.

Schillinger, W., Ohler, A., Emami, S., Muller, F., Christians, C., Janssen, P. M., Kogler, H., Teucher, N., Pieske, B., Seidler, T., & Hasenfuss, G. (2003). The functional effect of adenoviral Na+/Ca2+ exchanger overexpression in rabbit myocytes depends on the activity of the Na+/K+-ATPase. *Cardiovasc.Res.* **57**, 996-1003.

Schulze, D. H., Muqhal, M., Lederer, W. J., & Ruknudin, A. M. (2003). Sodium/calcium exchanger (NCX1) macromolecular complex. *J.Biol.Chem.* **278**, 28849-28855.

Schwinger, R. H., Wang, J., Frank, K., Muller-Ehmsen, J., Brixius, K., McDonough, A. A., & Erdmann, E. (1999). Reduced sodium pump alpha1, alpha3, and beta1-isoform protein levels and Na+,K+-ATPase activity but unchanged Na+-Ca2+ exchanger protein levels in human heart failure. *Circulation* **99**, 2105-2112.

Shin, D. W., Pan, Z., Kim, E. K., Lee, J. M., Bhat, M. B., Parness, J., Kim, d. H., & Ma, J. (2003). A retrograde signal from calsequestrin for the regulation of store-operated Ca2+ entry in skeletal muscle. *J.Biol.Chem.* **278**, 3286-3292.

Shou, W., Aghdasi, B., Armstrong, D. L., Guo, Q., Bao, S., Charng, M. J., Mathews, L. M., Schneider, M. D., Hamilton, S. L., & Matzuk, M. M. (1998). Cardiac defects and altered ryanodine receptor function in mice lacking FKBP12. *Nature* **391**, 489-492.

Simmerman, H. K., Collins, J. H., Theibert, J. L., Wegener, A. D., & Jones, L. R. (1986). Sequence analysis of phospholamban. Identification of phosphorylation sites and two major structural domains. *J.Biol.Chem.* **261**, 13333-13341.

Sipido, K. R., Carmeliet, E., & Pappano, A. (1995). Na+ current and Ca2+ release from the sarcoplasmic reticulum during action potentials in guinea-pig ventricular myocytes. *J.Physiol* **489 ( Pt 1)**, 1-17.

Sipido, K. R., Carmeliet, E., & Van de, W. F. (1998). T-type Ca2+ current as a trigger for Ca2+ release from the sarcoplasmic reticulum in guinea-pig ventricular myocytes. *J.Physiol* **508 ( Pt 2)**, 439-451.

Sipido, K. R., Maes, M., & Van de, W. F. (1997). Low efficiency of Ca2+ entry through the Na(+)-Ca2+ exchanger as trigger for Ca2+ release from the sarcoplasmic reticulum. A comparison between L-type Ca2+ current and reverse-mode Na(+)-Ca2+ exchange. *Circ.Res.* **81**, 1034-1044.

Smith, G. L. & O'Neill, S. C. (2001). A comparison of the effects of ATP and tetracaine on spontaneous Ca(2+) release from rat permeabilised cardiac myocytes. *J.Physiol* **534**, 37-47.

Stange, M., Xu, L., Balshaw, D., Yamaguchi, N., & Meissner, G. (2003). Characterization of recombinant skeletal muscle (Ser-2843) and cardiac muscle (Ser-2809) ryanodine receptor phosphorylation mutants. *J.Biol.Chem.* **278**, 51693-51702.

Steele, D. S. & Smith, G. L. (1993). Effects of 2,3-butanedione monoxime on sarcoplasmic reticulum of saponin-treated rat cardiac muscle. *Am.J.Physiol* **265**, H1493-H1500.

Stern, M. D. (1992). Theory of excitation-contraction coupling in cardiac muscle. *Biophys.J.* **63**, 497-517.

Studer, R., Reinecke, H., Bilger, J., Eschenhagen, T., Bohm, M., Hasenfuss, G., Just, H., Holtz, J., & Drexler, H. (1994). Gene expression of the cardiac Na(+)-Ca2+ exchanger in end-stage human heart failure. *Circ.Res.* **75**, 443-453.

Su, Z., Sugishita, K., Li, F., Ritter, M., & Barry, W. H. (2003). Effects of FK506 on [Ca2+]i differ in mouse and rabbit ventricular myocytes. *J.Pharmacol.Exp.Ther.* **304**, 334-341.

Suarez, J., Belke, D. D., Gloss, B., Dieterle, T., McDonough, P. M., Kim, Y. K., Brunton, L. L., & Dillmann, W. H. (2004). In vivo adenoviral transfer of sorcin reverses cardiac contractile abnormalities of diabetic cardiomyopathy. *Am.J.Physiol Heart Circ.Physiol* **286**, H68-H75.

Szegedi, C., Sarkozi, S., Herzog, A., Jona, I., & Varsanyi, M. (1999). Calsequestrin: more than 'only' a luminal Ca2+ buffer inside the sarcoplasmic reticulum. *Biochem.J.* **337 ( Pt 1)**, 19-22.

Tadros, G. M., Zhang, X. Q., Song, J., Carl, L. L., Rothblum, L. I., Tian, Q., Dunn, J., Lytton, J., & Cheung, J. Y. (2002). Effects of Na(+)/Ca(2+) exchanger downregulation on contractility and [Ca(2+)](i) transients in adult rat myocytes. *Am.J.Physiol Heart Circ.Physiol* **283**, H1616-H1626.

Takahashi, T., Allen, P. D., Lacro, R. V., Marks, A. R., Dennis, A. R., Schoen, F. J., Grossman, W., Marsh, J. D., & Izumo, S. (1992). Expression of dihydropyridine receptor (Ca2+ channel) and calsequestrin genes in the myocardium of patients with end-stage heart failure. *J.Clin.Invest* **90**, 927-935.

Terentyev, D., Viatchenko-Karpinski, S., Gyorke, I., Terentyeva, R., & Gyorke, S. (2003a). Protein phosphatases decrease sarcoplasmic reticulum calcium content by stimulating calcium release in cardiac myocytes. *J.Physiol* **552**, 109-118.

Terentyev, D., Viatchenko-Karpinski, S., Gyorke, I., Volpe, P., Williams, S. C., & Gyorke, S. (2003b). Calsequestrin determines the functional size and stability of cardiac intracellular calcium stores: Mechanism for hereditary arrhythmia. *Proc.Natl.Acad.Sci.U.S.A* **100**, 11759-11764.

Terentyev, D., Viatchenko-Karpinski, S., Valdivia, H. H., Escobar, A. L., & Gyorke, S. (2002). Luminal Ca2+ controls termination and refractory behavior of Ca2+-induced Ca2+ release in cardiac myocytes. *Circ.Res.* **91**, 414-420.

Terracciano, C. M., Souza, A. I., Philipson, K. D., & MacLeod, K. T. (1998). Na+-Ca2+ exchange and sarcoplasmic reticular Ca2+ regulation in ventricular myocytes from transgenic mice overexpressing the Na+-Ca2+ exchanger. *J.Physiol* **512 ( Pt 3)**, 651-667.

Timerman, A. P., Jayaraman, T., Wiederrecht, G., Onoue, H., Marks, A. R., & Fleischer, S. (1994). The ryanodine receptor from canine heart sarcoplasmic reticulum is associated with a novel FK-506 binding protein. *Biochem.Biophys.Res.Commun.* **198**, 701-706.

Timerman, A. P., Onoue, H., Xin, H. B., Barg, S., Copello, J., Wiederrecht, G., & Fleischer, S. (1996). Selective binding of FKBP12.6 by the cardiac ryanodine receptor. *J.Biol.Chem.* **271**, 20385-20391.

Tinker, A. & Williams, A. J. (1993). Using large organic cations to probe the nature of ryanodine modification in the sheep cardiac sarcoplasmic reticulum calcium release channel. *Biophys.J.* **65**, 1678-1683.

Trafford, A. W., Diaz, M. E., & Eisner, D. A. (1999). A novel, rapid and reversible method to measure Ca buffering and time-course of total sarcoplasmic reticulum Ca content in cardiac ventricular myocytes. *Pflugers Arch.* **437**, 501-503.

Trafford, A. W., Diaz, M. E., Sibbring, G. C., & Eisner, D. A. (2000). Modulation of CICR has no maintained effect on systolic Ca2+: simultaneous measurements of sarcoplasmic reticulum and sarcolemmal Ca2+ fluxes in rat ventricular myocytes. *J.Physiol* **522 Pt 2**, 259-270.

Trafford, A. W. & Eisner, D. A. (2003). No role for a voltage sensitive release mechanism in cardiac muscle. *J.Mol.Cell Cardiol.* **35**, 145-151.

Tripathy, A. & Meissner, G. (1996). Sarcoplasmic reticulum lumenal Ca2+ has access to cytosolic activation and inactivation sites of skeletal muscle Ca2+ release channel. *Biophys.J.* **70**, 2600-2615.

Valdivia, H. H., Kaplan, J. H., Ellis-Davies, G. C., & Lederer, W. J. (1995). Rapid adaptation of cardiac ryanodine receptors: modulation by Mg2+ and phosphorylation. *Science* **267**, 1997-2000.

Varmus, H. (1988). Retroviruses. *Science* **240**, 1427-1435.

Verrecchia, F. & Herve, J. C. (1997). Reversible blockade of gap junctional communication by 2,3-butanedione monoxime in rat cardiac myocytes. *Am.J.Physiol* **272**, C875-C885.

Verzili, D., Zamparelli, C., Mattei, B., Noegel, A. A., & Chiancone, E. (2000). The sorcin-annexin VII calcium-dependent interaction requires the sorcin N-terminal domain. *FEBS Lett.* **471**, 197-200.

Viatchenko-Karpinski, S., Terentyev, D., Gyorke, I., Terentyeva, R., Volpe, P., Priori, S. G., Napolitano, C., Nori, A., Williams, S. C., & Gyorke, S. (2004). Abnormal calcium signaling and sudden cardiac death associated with mutation of calsequestrin. *Circ.Res.* **94**, 471-477.

Wang, W., Cleemann, L., Jones, L. R., & Morad, M. (2000). Modulation of focal and global Ca2+ release in calsequestrin-overexpressing mouse cardiomyocytes. *J.Physiol* **524 Pt 2**, 399-414.

Wang, Z., Nolan, B., Kutschke, W., & Hill, J. A. (2001). Na+-Ca2+ exchanger remodeling in pressure overload cardiac hypertrophy. *J.Biol.Chem.* **276**, 17706-17711.

Watanabe, Y., Iwamoto, T., Matsuoka, I., Ohkubo, S., Ono, T., Watano, T., Shigekawa, M., & Kimura, J. (2001). Inhibitory effect of 2,3-butanedione monoxime (BDM) on Na(+)/Ca(2+) exchange current in guinea-pig cardiac ventricular myocytes. *Br.J.Pharmacol.* **132**, 1317-1325.

Weber, C. R., Ginsburg, K. S., Philipson, K. D., Shannon, T. R., & Bers, D. M. (2001). Allosteric regulation of Na/Ca exchange current by cytosolic Ca in intact cardiac myocytes. *J.Gen.Physiol* **117**, 119-131.

Wei, S. K., Ruknudin, A., Hanlon, S. U., McCurley, J. M., Schulze, D. H., & Haigney, M. C. (2003). Protein kinase A hyperphosphorylation increases basal current but decreases beta-adrenergic responsiveness of the sarcolemmal Na+-Ca2+ exchanger in failing pig myocytes. *Circ.Res.* **92**, 897-903.

Witcher, D. R., Kovacs, R. J., Schulman, H., Cefali, D. C., & Jones, L. R. (1991). Unique phosphorylation site on the cardiac ryanodine receptor regulates calcium channel activity. *J.Biol.Chem.* **266**, 11144-11152.

Xiao, B., Sutherland, C., Walsh, M. P., & Chen, S. R. (2004). Protein kinase A phosphorylation at serine-2808 of the cardiac Ca2+-release channel (ryanodine receptor) does not dissociate 12.6-kDa FK506-binding protein (FKBP12.6). *Circ.Res.* **94**, 487-495.

Xiao, R. P., Valdivia, H. H., Bogdanov, K., Valdivia, C., Lakatta, E. G., & Cheng, H. (1997). The immunophilin FK506-binding protein modulates Ca2+ release channel closure in rat heart. *J.Physiol* **500 ( Pt 2)**, 343-354.

Xie, X., Dwyer, M. D., Swenson, L., Parker, M. H., & Botfield, M. C. (2001). Crystal structure of calcium-free human sorcin: a member of the penta-EF-hand protein family. *Protein Sci.* **10**, 2419-2425.

Xin, H. B., Rogers, K., Qi, Y., Kanematsu, T., & Fleischer, S. (1999). Three amino acid residues determine selective binding of FK506-binding protein 12.6 to the cardiac ryanodine receptor. *J.Biol.Chem.* **274**, 15315-15319.

Xin, H. B., Senbonmatsu, T., Cheng, D. S., Wang, Y. X., Copello, J. A., Ji, G. J., Collier, M. L., Deng, K. Y., Jeyakumar, L. H., Magnuson, M. A., Inagami, T., Kotlikoff, M. I., & Fleischer, S. (2002). Oestrogen protects FKBP12.6 null mice from cardiac hypertrophy. *Nature* **416**, 334-338.

Xu, L., Tripathy, A., Pasek, D. A., & Meissner, G. (1998). Potential for pharmacology of ryanodine receptor/calcium release channels. *Ann.N.Y.Acad.Sci.* **853**, 130-148.

Yang, Z., Pascarel, C., Steele, D. S., Komukai, K., Brette, F., & Orchard, C. H. (2002). Na+-Ca2+ exchange activity is localized in the T-tubules of rat ventricular myocytes. *Circ.Res.* **91**, 315-322.

Yano, K. & Zarain-Herzberg, A. (1994). Sarcoplasmic reticulum calsequestrins: structural and functional properties. *Mol.Cell Biochem.* **135**, 61-70.

Yano, M., Ono, K., Ohkusa, T., Suetsugu, M., Kohno, M., Hisaoka, T., Kobayashi, S., Hisamatsu, Y., Yamamoto, T., Kohno, M., Noguchi, N., Takasawa, S., Okamoto, H., & Matsuzaki, M. (2000). Altered stoichiometry of FKBP12.6 versus ryanodine receptor as a cause of abnormal Ca(2+) leak through ryanodine receptor in heart failure. *Circulation* **102**, 2131-2136.

Yao, A., Su, Z., Nonaka, A., Zubair, I., Lu, L., Philipson, K. D., Bridge, J. H., & Barry, W. H. (1998). Effects of overexpression of the Na+-Ca2+ exchanger on [Ca2+]i transients in murine ventricular myocytes. *Circ.Res.* **82**, 657-665.

Yuan, W. & Bers, D. M. (1995). Protein kinase inhibitor H-89 reverses forskolin stimulation of cardiac L-type calcium current. *Am.J.Physiol* **268**, C651-C659.

Zamparelli, C., Ilari, A., Verzili, D., Giangiacomo, L., Colotti, G., Pascarella, S., & Chiancone, E. (2000). Structure-function relationships in sorcin, a member of the penta EF-hand family. Interaction of sorcin fragments with the ryanodine receptor and an Escherichia coli model system. *Biochemistry* **39**, 658-666.

Zhang, L., Kelley, J., Schmeisser, G., Kobayashi, Y. M., & Jones, L. R. (1997). Complex formation between junctin, triadin, calsequestrin, and the ryanodine receptor. Proteins of the cardiac junctional sarcoplasmic reticulum membrane. *J.Biol.Chem.* **272**, 23389-23397.

Zhang, X. Q., Song, J., Rothblum, L. I., Lun, M., Wang, X., Ding, F., Dunn, J., Lytton, J., McDermott, P. J., & Cheung, J. Y. (2001). Overexpression of Na+/Ca2+ exchanger alters contractility and SR Ca2+ content in adult rat myocytes. *Am.J.Physiol Heart Circ.Physiol* **281**, H2079-H2088.

Zhu, X. Overexpression of sorcin improves cardiac excitation-contraction coupling in normal and failing ventricular cardiomyocytes. Farrell, E. F., Robu, V., Schmidt, U., Hajjar, R., Allen, P., and Valdivia, H. H. Journal of Cardiac Failure Supplement 1, 9(5), S3. 2003. Ref Type: Generic

Zuhlke, R. D., Pitt, G. S., Deisseroth, K., Tsien, R. W., & Reuter, H. (1999). Calmodulin supports both inactivation and facilitation of L-type calcium channels. *Nature* **399**, 159-162.